THÈSE

pour l'obtention du titre de

DOCTEUR

de

L'UNIVERSITE DES SCIENCES ET TECHNOLOGIES DE LILLE

Discipline : **GÉNIE CIVIL**

présentée par

RAFEH Faten

THREE DIMENSIONAL MODELLING FOR THE LONG TERM STABILITY ANALYSIS OF UNDERGROUND CAVITIES

---

soutenue le 14 décembre 2015 devant le jury composé de

Rapporteurs :	MERRIEN-SOUKATCHOFF Véronique	Professeur, Université de Loraine
	VINCENS Eric	MdC, Ecole Centrale de Lyon
Examinateurs :	BURLON Sébastien	Ingénieur de Recherche, Ifsttar
	PANTET Anne	Professeur, Université du Havre
	SHAHROUR Isam	Professeur, Université Lille 1
	SHAO Jianfu	Professeur, Ecole Centrale de Lille
Invité :	GALLET de SAINT AURIN Jean-Marc	Ingénieur, Sémofi
Directeur de thèse :	MROUEH Hussein	Professeur, Université Lille 1

ACKNOWLEDGEMENT

The work in this thesis has been carried out at the Laboratory of Civil and Geo-Environmental Engineering LGCgE at Polytech'Lille, University of Lille 1 under the supervision of Professor Hussein Mroueh and the assistance of Dr. Sébastien Burlon. This work, which provides a long term stability assessment of the shallow underground cavities identified in Lille and North France consists a part of the Plan of Prevention of Risks PPR and particularly the National Plan of Cavities PNC held in France. It is performed in collaboration with the City of Lille, Service of Urban and Health Risks, as well as the specialized engineering company for geotechnical research works Sémofi.

Foremost, I would like to thank my supervisor, Professor Hussein Mroueh, for the trust he had in me from the very beginning. Both, his continuous support and guidance all along those 3 years have been a key to this achievement. My thankfulness is also owed to Doctor Sébastien Burlon for believing in this work, and thereafter for the fruitful discussions we have been through during the last 2 years. His patience, despite the complaints that I am a bit stubborn, has been priceless too.

I am also grateful for the people who have contributed to this work by non-rewardable confidence and support. Thanks to the head of the Service of Urban and Sanitary Risks at the City of Lille, Mr. Gaëten Cheppe. Thanks to the head of Sémofi, Mr. Jean Marc Gallet de Saint Aurin. And my sincere thankfulness also goes to Madame Géraldine Berrehouc, representing both the City of Lille and Sémofi, for her serious engagement and enthusiasm towards this project.

I would like to thank my PhD committee for accepting to be a part of this achievement by reading, reporting, and examining my work at one hand, and for crossing distances to participate in and chair the jury on the day of my PhD defence. Thanks to Professors Anne Pantet, Véronique Merrien-Soukatchoff, Eric Vincens, Jianfu Shao, and Isam Shahrour.

Three years at Polytech'Lille were not only about making a PhD; they were also about making a new family of friends and colleagues with whom I've shared the ups and downs, in and out of the lab. I would like to express my gratitude to all my PhD fellows at LGCgE, those who are already done with their PhDs, and those who are on the way. Besides, I would like to thank my colleagues of lecturers and professors at Lille 1 University with whom I've

shared the hassles, as well as joyful moments of teaching at the department of civil and mechanical engineering.

I can't but express my heartfelt and profound thankfulness to all my friends in Lebanon, in France, and elsewhere for all the encouragement and enjoyment they've got into my life. This has been necessary and non-doubtfully treasured.

Last but not least, I am indebted to my family, my dad and mom and my 2 brothers; without you standing by me, without you believing in me, and without you giving me all, I couldn't have been me, I couldn't have struggled for further achievements, and I couldn't have succeeded on and on. This PhD is dedicated to you. Thank you!

ABSTRACT

The presence of hundreds of unexploited underground quarries in the region of North France regarding their close proximity to urbanized areas, poses serious problems in terms of the security of both people and constructions on one hand, and induces a strong constraint against the planning and urban development on the other hand. In this framework, this thesis presents a numerical analysis of the stability of underground cavities excavated decades ago in the chalk substratum of North France. It aims to provide a complementary understanding for the geological investigations and observations carried out. These latter have shown that two stratigraphic joints are present in the chalk layers. Besides, fractures developing due to the progressive degradation of chalk are observed. Hence, the first target in this thesis is to account for the anisotropic behaviour induced due to the presence of joints. Anisotropy, whether inherent or induced, intrinsically affects the strength, and the strain behaviour of the chalk mass especially at shallow depths (which represents our case study) where confining stresses are low. Hence, a constitutive law accounting for the anisotropic behaviour is studied by considering several mechanisms of plasticity. Next, a three dimensional numerical modelling of the excavation is performed and a stability analysis which depends on the conventional shear strength reduction procedure is integrated. The influence of joints is described in details and the strain and failure mechanisms are also analysed. This provides a better understanding of the mechanical behaviour of the jointed underground cavities under study. Time effects and degradation mechanisms induced in the presence of different aggravating factors have an important influence on the stability. A time-dependent-degradation model is developed. It is used to model the time-dependent deformation and failure mechanisms and to assess the long term stability of these cavities. A comparison between the stability analysis achieved using conventional shear reduction method, and that using the developed non-homogeneous time-dependent degradation model which depends on the accumulation of plastic strains in the continuum is done. At the end, for the direct preliminary assessment of the stability of identified cavities, a parametric stability study was

conducted and extrapolated formulae as well as abacuses were developed. This helps in the preliminary estimation of stability state of the investigated quarries.

KEY WORDS: UNDERGROUND CAVITIES, CHALK, JOINTS, STABILITY, DEGRADATION

RESUME

La présence de centaines de carrières souterraines abandonnées dans le nord de la France, à proximité de zones urbanisées, est à l'origine de problèmes importants touchant à la sécurité des personnes et des constructions, d'une part, et à l'élaboration de plans d'urbanisme d'autre part. Dans ce cadre, cette thèse présente l'analyse numérique de la stabilité de cavités souterraines creusées il y a des dizaines d'années dans la craie du nord de la France. Elle a pour objectif de proposer une approche complémentaire aux observations et investigations menées habituellement. Ces dernières permettent de savoir que la craie du nord de la France présente des familles de joints. Par ailleurs, la dégradation de la craie induit le développement d'autres plans de faiblesse. Ainsi, le premier objectif de la thèse est de rendre compte du comportement anisotrope induit par la présence de ces joints. Cette anisotropie, induite ou intrinsèque, affecte le comportement de la craie en termes de déformation et de résistance. En particulier, à faible profondeur (ce qui est le cas ici) où les contraintes de confinement sont faibles, le comportement de la craie est contrôlé par des phénomènes de glissement le long des joints et des déformations de cisaillement peuvent s'accumuler jusqu'à induire des ruptures et des effondrements. Une loi de comportement rendant compte de ce comportement anisotrope est étudiée en considérant différents mécanismes de plasticité. Une modélisation numérique tridimensionnelle d'une excavation est mise en œuvre et une analyse de la stabilité basée sur la procédure de réduction des paramètres de résistance au cisaillement est proposée. Le rôle de joints décrit en détail et les mécanismes de déformation et de rupture sont aussi analysés. Il ressort de cette analyse une meilleure compréhension du comportement des cavités souterraines et du rôle des joints. Les effets du temps et les mécanismes de dégradation induits par différents facteurs aggravants ont aussi un rôle important sur la stabilité. Une approche de dégradation dépendante du temps a été développée. Elle permet l'étude des mécanismes de déformation et de rupture en fonction du temps et l'estimation de la stabilité à long terme de la carrière. Une comparaison avec l'analyse de la stabilité mettant en œuvre la procédure conventionnelle de réduction des paramètres de cisaillement est

réalisée. Enfin, pour l'étude préliminaire de la stabilité des carrières, des abaques sont proposés aux gestionnaires, scientifiques et donneurs d'ordre, et constituent un précieux outil d'aide à la décision concernant l'action à mener pour prévenir les risques.

MOTS CLEFS: CARRIERES SOUTERRAINES, CRAIE, JOINTS, STABILITE, DEGRADATION

TABLE OF CONTENTS

LIST OF FIGURES

LIST OF TABLES

SYMBOLS

F_s	Factor of Safety
R_f	Reduction Factor
E	Young Modulus (Pa)
ν	Poisson Ratio
c	Matrix Cohesion (Pa)
φ	Matrix Friction Angle (°)
ψ	Dilation Angle (°)
c_j	Joint Cohesion (Pa)
φ_j	Joint Friction Angle (°)
ψ_j	Joint Dilation Angle (°)
K_0	Coofficient of Earth Pressure at Rest
f_j	Joint Failure Function
$f_j^{\deg}$	Relative to Degradation Approach
f_j^{red}	Relative to Reduction Approach
g_j	Joint Potential Function
σ	Full Stress Tensor
$\vec{n}$	Normal Vector to Joint Plane
σ_{n}	Normal Stress Tensor
τ	Tangential Stress Tensor

R_m	Plastic Hardening Function
B	Constant affecting the Hardening Rate
γ_p	Plastic Shear Strain
e_{ij}^p	Deviatoric Plastic Strain
de_{ij}^p	Deviatoric Plastic Strain Increment
ε_{ij}^p	Total Plastic Deformation
ε_{ij}^e	Total Elastic Deformation
δ_{ij}^p	Kronecker Tensor
$\overline{\overline{C}}$	Stiffness Tensor
λ	Plastic Multiplier
D	Degradation Factor
$D*$	Degradation Function
γ	Material Constant
α	Constant to limit Degradation

GENERAL INTRODUCTION

Underground cavities constitute a serious geological hazard due to the consequential collapses developed on the overlaying terrain. In urban areas, generally the sudden collapse causes damages to properties, infrastructure, and even lives. Hence, it is a real challenge for land use planners and engineers to provide adequate safeguards to reduce the consequences of this hazardous phenomenon and prevent the substantial risks. Yet, such provisions have to be based on a broad understanding of the nature of induced instabilities and the global mechanical behaviour of the underground cavities.

North France is one of the regions threatened by such risks due to the high presence of anthropogenic underground cavities. The exploitation of these cavities was accompanied with the economic and demographic development of this region that had to face in the nineteenth century the strong population growth by building large urbanized sets. The excessive demand of construction material in that period urged the extraction of huge amounts of rock and particularly chalk blocks. According to the City of Lille in North France (Ville de Lille 2012 and 2013), more than 4,500,000 cubic meters of voids have been identified in the underground layers of Lille Metropolis in a survey done in 2009. Large surfaces in this region are now under-mined by underground cavities which constitute a source of serious insecurity problems for the population, constructions and infrastructure, as well as the urban planning and impending development projects

For this reason, the City of Lille in North France and particularly the Service of Urban and Health Risks has launched a project endorsed under the Plan for Prevention of Risks (PPR) and concerned particularly in the study of the phenomenon of underground cavities. This project is known as the 'Plan National Cavité', where it includes several axes which come across. One is dedicated for the naturalistic surveys and observations at these cavities

performed based on regular geological investigations. This provides measures of displacements occurring at the cavities, inspection of new features developing such as induced fractures, and continuous alert against any sudden disorders. A second axe is devoted to the experimental work and testing done on chalk samples taken from the cavities. This is needed to illustrate the mechanical behaviour of the chalk under real conditions. Another axe is concerned in the numerical analysis of the behaviour of these cavities. Numerical tools could be efficient in such a study since it is possible to investigate different existing cases of cavities under varying external and internal conditions and at the same time consider an envelope of these cases and conditions too. Besides, it is possible to model the foreseeable deformation profiles with the associated failure mechanisms and investigate the stability state of the cavity. In this research, we deal with the third axe taking into account the outcomes obtained on the other two levels.

Our main intention throughout this work is to provide by means of numerical analysis a complementary understanding of the deformational behaviour and the stability state of these cavities under different circumstances. In this thesis, a numerical study is conducted to assess the stability of shallow underground cavities identified in the chalk layers of Lille and its region in North France. From a safety point of view, these cavities are not only required to prevent ultimate collapse, but also to avoid deformations due to encountered instabilities and thus satisfy limits of a displacement-based criterion.

Major topics of this work are illustrated within five chapters:

- **Chapter One**

An overview about the phenomenon of underground cavities in France and particularly in North France is advocated in the first chapter. An idea about the reasons behind excavating huge areas, the common methods of exploitation, and the encountered risks is provided. The particularity of the cavities in the zone of study is addressed showing the main highlights of this work. Cavities of Lille and its region in North France were excavated in the chalk layers at shallow depths and most frequently using the method of rooms-and-pillars. Frequent failure mechanisms in this type of exploitations are discussed. This is associated with a review on the research works done addressing this problematic in terms of numerical modelling basically. Afterwards, a description of the behaviour of chalk and the relevant yield mechanisms is done. A state of the art concerning the stress-strain behaviour including

the effects of material structure like anisotropy induced by the presence of joints, the water-dependent behaviour in accordance with the featured physical aspects, and the time dependent behaviour in the presence of various aggravating factors, is performed.
An outline of the provisions and the novelty of this thesis are stated at the end of this chapter.

- **Chapter Two**

In the study of underground instabilities originating from the quarries excavated in the jointed chalk bed, it is necessary to understand the behaviour of the jointed continuum. Discontinuities such as stratigraphic joints and induced fractures inherently affect the material strength and deformational behaviour especially at shallow depths where mean stresses are low and failure is rather driven by shear at the discontinuities.
In chapter two, an equivalent continuum constitutive model accounting for the critical effect of anisotropy induced by the presence of joints is proposed. In this model, two joint sets are defined implicitly in the chalk continuum and an oriented yield criterion is developed to simulate the stresses induced on these joints. Three yield envelopes are defined separately for the chalk matrix (representing the intact part of the continuum) and the two joint sets. Failure is tested and whenever it is detected, relevant plastic corrections are applied. Based on the theory of multi-mechanisms for plastic strain (Koiter 1953 and 1960), updated stresses are recuperated all over the chalk continuum. Triaxial tests are simulated on models with single and double joint sets. Comparisons with results based on existing models are illustrated to verify the applicability of the proposed model. Stress-strain responses and failure modes are investigated to describe the strength and deformational behaviour of the anisotropic chalk.

- **Chapter Three**

In this chapter, we use the joint model developed in chapter two to integrate the joint effect in the mechanical behaviour of the underground cavities excavated in jointed chalk layers. The major intention is to study the impact of joints, whatever its nature is whether stratified joints or induced fractures, on the strain and failure mechanisms as well as on the stability state of the cavities. A three dimensional numerical modelling of the excavation operation of these cavities is developed. Both geometric characteristics of the room-and-pillar quarries and the mechanical properties of the soil and chalk layers are inspired from site investigations and experimental tests done in the zone of study. The oriented criterion developed is assigned for

the behaviour of the joints as mentioned before. Strain profiles are simulated and the effect of joints is analysed considering different properties and orientations too.

In order to assess the effect of joints on the failure mechanisms and the stability state of these cavities, a stability criterion is implemented and assigned to the joints. Since in shallow excavations dominating failure is often realized by shear, the criterion used was based on the conventional shear strength reduction technique. The safety factor is calculated taking into account the presence of joints. Numerical analysis is carried out to provide a better understanding of the critical effect of joints or discontinuities on the global behaviour and stability of the cavities. In other words, it illustrates the influence of induced anisotropy on the stability and failure mechanisms of the underground galleries excavated in jointed chalk layers of North France and its region.

- **Chapter Four**

In the investigation of ancient unexploited cavities, it is of high importance to account for the effect of time on the resistance of the cavity and in the presence of various aggravating factors. This chapter addresses the time-dependent study conducted to analyse the long term stability of the underground cavities. Usually, the type of time-dependent deformation known as creep deformation is entirely related to the viscous effects of the material and is analysed using models of viscoelasticity and viscoplasticity (Perzyna, 1966, and Cristescu, 2009). In this work, a methodology based on the law of hardening and micro-structural evolution inspired by Shao et al. (2003) is used to generate both instantaneous and time dependent irreversible deformations of the degraded chalk. This is achieved in the presence of the joints defined previously in the continuum of the model. Unlike the conventional reduction methods that are used to simulate stability, the developed time-dependent-degradation approach implements a non-homogeneous kinetic reduction of the resistive shear properties of chalk producing a non-uniform evolution of shear plastic strains in the room-and-pillar model. Numerical analysis of the time dependent behaviour that accounts for the associated physical aspects is performed. The influence of varying joint orientations is also considered.

A comparison with results obtained using the conventional shear strength reduction method is also done. This provides a physical interpretation and a better understanding of the time dependent behaviour and the progressive failure associated in these quarries after a long time from excavation.

- **Chapter Five**

In chapter five, we intend to run a parametric study that accounts for the range of different geometries of the room-and-pillar quarries, including different width to height ratios of pillars (W:H) and spans of void rooms/galleries (L), aiming to achieve two purposes. The first one is illustrating the effect of confining pressure which is directly related to the dimensions of the supporting pillars and void rooms in the quarry on the nature of the rupture mechanisms, i.e, whether brittle or ductile. The next purpose is achieved by complementing the parametric study-based-numerical results with a third order regression analysis. Thereafter, extrapolated formulae for the preliminary estimation of the resistance of the pillar and the safety of the room-and-pillar quarry are developed. The same study is performed in the presence of one joint set at three different orientations and consequently three new corresponding formulae are proposed in the same context. In addition, an abacus is generated for the direct estimation of the critical width of the pillars and another one to determine the maximum permissible scaling of pillars with different dimensions such that they stay in the safety zone.
This might provide a feasible and helpful tool for geo-engineers involved in this project with the City of Lille since it is now possible, being only given its dimensions and the orientation of the detected discontinuities, to assess the stability of the underground cavity.

CHAPTER ONE
UNDERGROUND CAVITIES: A DESCRIPTIVE OVERVIEW – STATE OF THE ART

1.1 Introduction

The important concentration of unexploited underground cavities in close proximity to urbanized areas poses problems in terms of security of both people and constructions at one hand, and induces a constraint against planning and urban development at the other hand. Hence, it is of major interest to conduct a study about this phenomenon aiming to understand the behaviour of the underground cavities, estimate their stability state and provide insights about the shape and intensity of expected damage, and last but not least give some provisions on how to limit the substantial risks encountered due to consequential instabilities.

From this perspective, this thesis comes to suggest some sorts of a better understanding of this issue after raising a couple of questions such as: Why were these cavities formed? Where in France are they massively located? How were they excavated? What are the risks on both: land and constructions, and people? What are the regulations proposed by authorities of concerned cities such as the City of Lille in North France? What is the particularity of the cavities of North France? What achievements have been made in this domain, whether in terms of numerical study, empirical analysis, or constitutive modelling? What are the novel propositions in this thesis concerning the problematic of underground cavities or in other words where do the innovation and originality of this work lay?

1.2 Why were underground cavities formed and where are they concentrated throughout the French territory?

Since ancient times and until now, civil engineers have found in the extraction of intact rock masses from underground layers a nourishing source to support them permanently with construction materials needed in their building works for both structural and infrastructural development. Consequently, this type of exploitations has ended up in the formation of large areas of anthropogenic underground cavities known as quarries. Other motives stood behind excavations of underground cavities such as military ones where combatants used cavities as shelters and underground passages among villages. Some were excavated for agricultural uses after finding out that the environment inside the cavities is convenient for certain cultivations such as mushrooms cultivation for example.

Throughout the French territory, underground cavities cover tens of thousands hectares of the area. It is more frequent in layers of chalk, limestone, gypsum and marble materials that were extracted to be used in construction works. Figure 1.1 shows the distribution of different types of underground cavities in France including both natural (in yellow) and anthropogenic cavities excavated in different ground layers like chalk (in green) and others.

Most of these quarries are very ancient by which some belong to the seventh century (suburbs of Lille, North France), others to the eleventh, fourteenth and fifteenth century (Caen, Normandy and Paris, Picardy). The development of the operation of underground openings, however, reached its peak between the seventeenth and nineteenth century (Mikolajczak 1996, Ineris, 2007, 2012, Courbot et al. 2009, Ville de Lille 2012 and 2013). This was accompanied by the economic and demographic development of many regions and cities that have faced in the nineteenth century strong growth in population which in turn required building new large urbanized sets.

For many centuries, such operations were carried out without authorization or any type of supervision. These resulted in problems of instability at or beneath the location of these quarries which started to gain concern after a series of serious accidents that occurred in late eighteenth century in Paris region (see section 1.4.2). The concentration of such incidents in different regions of France is shown in Figure 1.2.

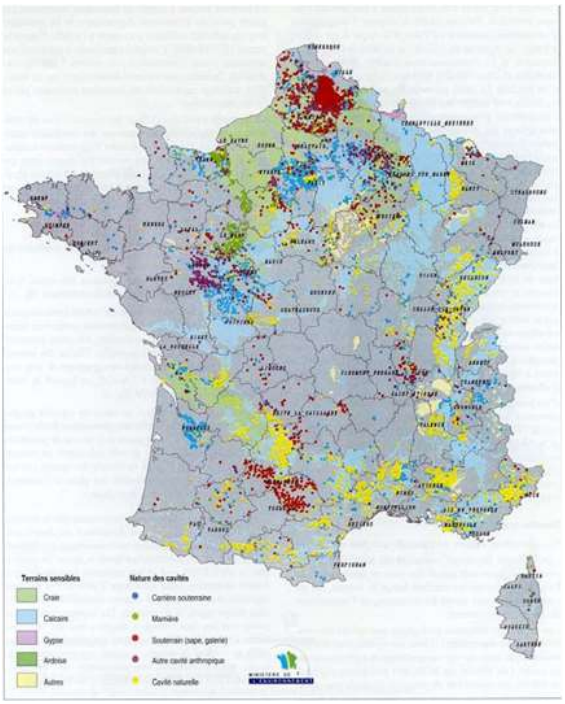

Figure 1.1. Distribution of underground cavities in France, 1994 - by BRGM

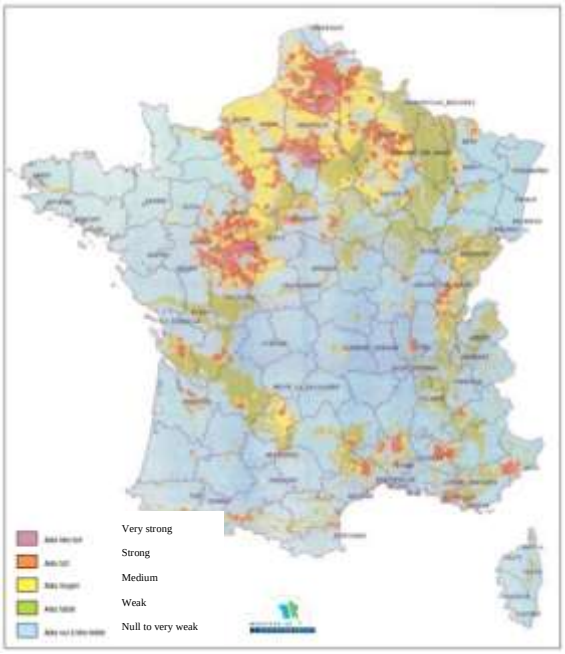

Figure 1.2. Hazard associated with underground cavities in France – by BRGM

1.3 How were the underground cavities excavated: Exploitation methods?

The typology of underground quarries is based on the diversity of the exploitation methods used. The most frequent exploitation methods used in the excavation of underground cavities in France are described below (Ineris, 2007):

1.3.1 Room-and-pillar exploitations

This method is the oldest and the most commonly used where it showed up after the nineteenth century. It is characterized by a regular, almost orthogonal distribution of pillars with different sections to ensure sufficient stability. Usually, it consists of a vertical well of 8 to 30 meters depth linked to a network of galleries with pillars supporting the overburden. The constituent materials were extracted sorted through the wells, and the waste was discarded forming a thick fill layer on the floor of the galleries. At the end of the operation the wells were backfilled from the surface to keep plane topography. This method has been largely used in the North France. In Lille Metropolis, 80% of the quarries were excavated by the 'room-and-pillar' method. For this reason, this study focuses on the study of this type cavities (Figure 1.3 and Figure 1.4).

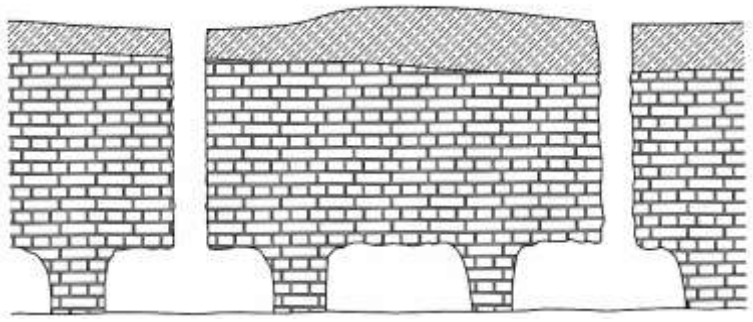

Figure 1.3. Rooms-and-pillars cavities - Document by City of Lille

Figure 1.4. Rooms-and-pillars cavities in Hellemes, North France

1.3.2 Exploitations by holts-and-bottles

This method has started by the end of the nineteenth century and is often regular in terms of geometry and organization. In this type of underground excavations, the wells are of regular reparation and made in the shape of a bottle attached to a small gallery. The waste is abandoned at the bottom forming hills of embankment. At the end of the operation, a closure was done at the head by blocks of chalk corbelled to maintain the stability (Figure 1.5 and Figure 1.6).

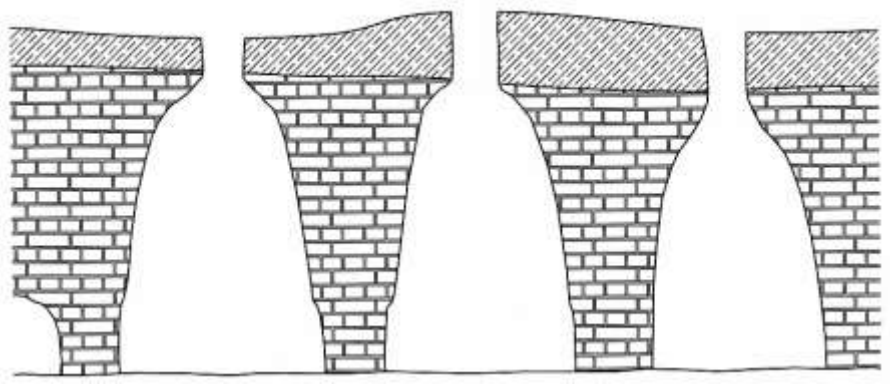

Figure 1.5. Exploitations by holts-and-bottles – by City of Lille

Figure 1.6. Holts-and-bottles cavity at Lezennes, North France

1.3.3 Mixed type exploitations

This is a combination between the rooms and pillars method and the method of holts and bottles within the same quarry. Here the pillars will be more regular than in the chambers and pillars method.

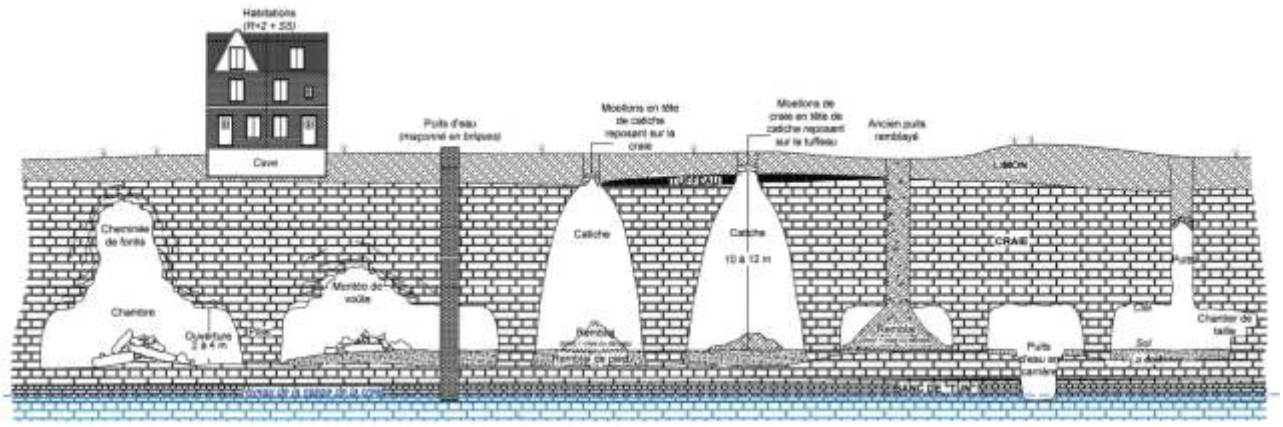

Figure 1.7. Type of underground cavities in North France – BRGM

1.4 Common Risks

1.4.1 Risks at the surface

The main risks arising from the presence of underground cavities correspond to the surface manifestation of disorders whose effects differ depending on the associated failure modes and the nature of the land forming the cover. Common surface accidents are described below (City of Lille, 2012).

Figure 1.8. Accident close to a house in Normandy, France, 2001 - Document by LCPC

1.4.1.1 The generalized collapse

This type of collapse is reflected by a violent and spontaneous lowering of the surface sometimes covering several hectares and reaching several meters in depth while the ground above the cavity collapses suddenly (Figure 1.9).

Failure mechanisms that trigger the spontaneous collapse are preceded by different and somehow complex instability processes like fractures in the pillars, roof collapse, punching of the walls, shear boards spacers or inconvenient superposition of pillars among different exploited levels, hydraulic loading of the roof, deviation of the stress field in case of inclined overburdens, human actions, etc. This type of phenomenon can cause huge damage to buildings and serious substantial losses like victims because of the remarkable speed and magnitude of this phenomenon (Figure 1.10).

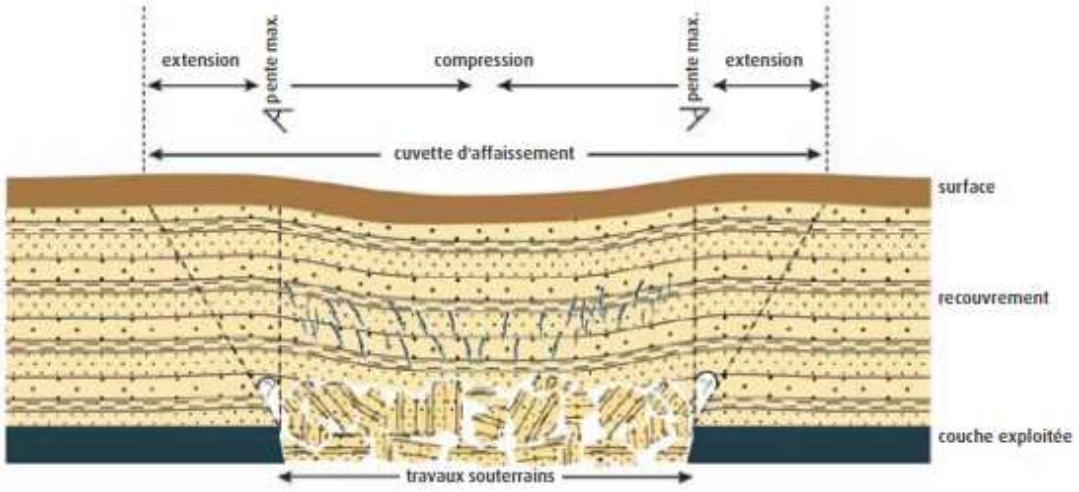

Figure 1.9. Sketch of the generalized collapse – Document by INERIS

Figure 1.10. Case of generalized collapse in Lille, North France

1.4.1.2 The collapse by localized rupture at pillars

This localized rupture occurs when one or more pillars are no more able to support the weight of the overburden and other existing loads. This might happen due to the small effective section and may thus lead to failure in this pillar. Consequently, the applied loads are redistributed among the adjacent supporting pillars which might become overstressed due to the additional loads. In this case, other pillars are subjected to fail gradually ending up with a total collapse of the whole gallery (Figure 1.11).

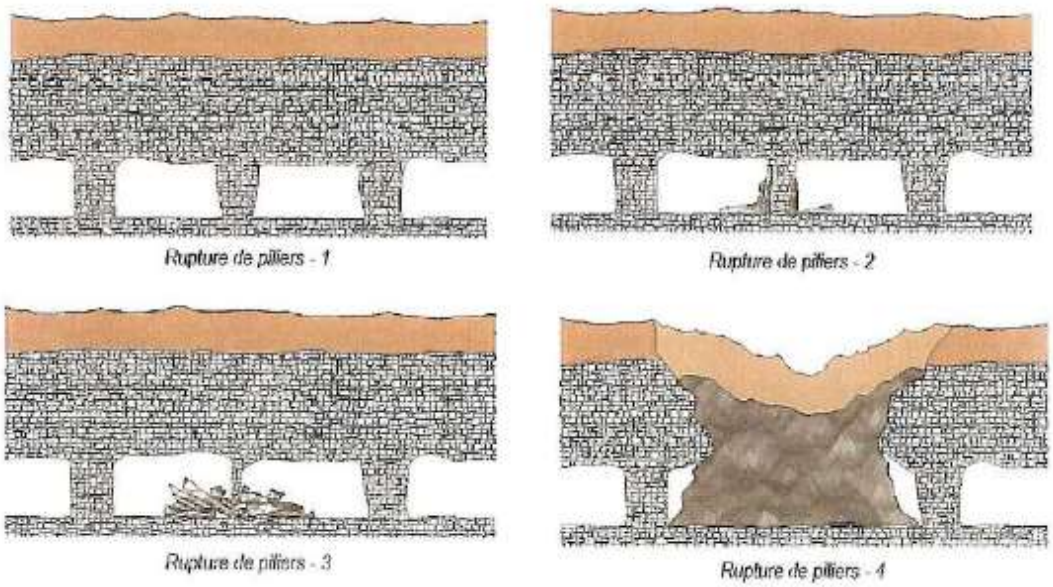

Figure 1.11. Scenario of the pillars rupture – by SEISM, 2008

1.4.1.3 The collapse localized by roof rupture/ sinkholes

In general, sinkholes (fontis) correspond to a sudden but localized collapse manifesting itself in the form of a funnel or crater from the bottom towards the top. It is most often caused by the progressive failure that extends gradually to the roof of a cavity, and leads abruptly to creating a circular funnel with a diameter that can vary from a few meters to several tens of meters on the surface. The sinkholes occur most often in the form of a cone whose slope angle is related to the slope angle of the natural land. For a 45° angle, the radius surface is equal to the depth of the cavity (Figure 1.12 and Figure 1.13).

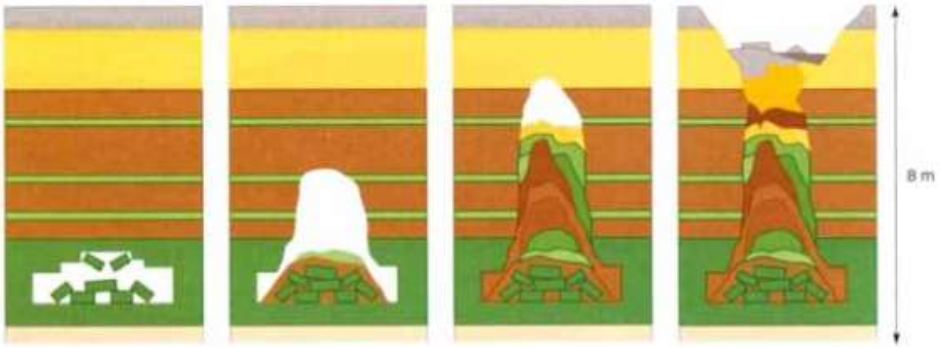

Figure 1.12. Sketch of the development of a sinkhole - (Ineris, 2007)

This type of instability takes place frequently since it can occur over any empty mid-average extension (abandoned galleries, wells, karst). Sinkholes can cause significant damage to close structures and this phenomenon is usually associated with a high risk of physical victims because of the speed and dimensions of the phenomenon.

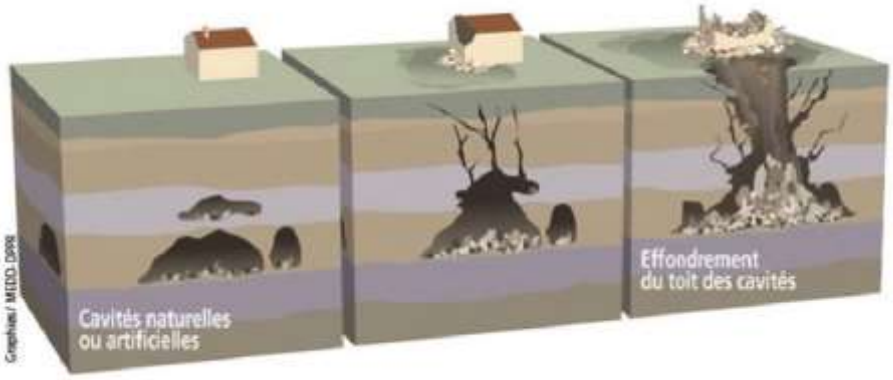

Figure 1.13. Sketch showing the sinkhole formation by upward progression - BRGM

1.4.1.4 Subsidence or sagging

Subsidence or sagging is a flexible deformation that does not really leave remarkable damage. It results in a topographic depression generally bowl-shaped with a flat bottom and bent edges (Figure 1.14). This type of disorder sometimes develops over several hectares at the place of large quarries or mines. Subsidence can cause disturbances in the adjacent buildings but without really causing physical victims due to the fact that this phenomenon occurs slowly (Figure 1.15).

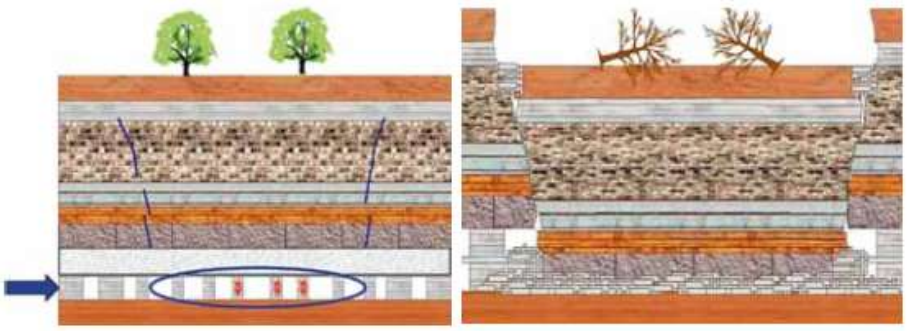

Figure .1.14. Descriptive sketch of sagging – Document by INERIS

Figure 1.15. Generalized subsidence on surface over a chalk quarry at Indre et Loire, France - Document by INERIS

1.4.1.5 Other types: Suffosions and Stripping

Two other types of surface accidents known as stripping and suffosions are directly related to the water circulation in case of rainfall in the area of the underground cavities. Stripping corresponds to the gravity drive, usually caused by massive water circulation, and material filling a cavity. This type of phenomenon can lead to the sudden onset of an empty surface, usually not more than a few square meters. This is the risky phenomenon that affects most natural networks developed in the limestone massifs. During heavy rainfall, the water circulation in depth can enforce the material which initially filled the large cracks, to strip and break and get to the surface leaving a gaping hole in the rock.

Suffosion is an internal erosion phenomenon which affects mainly sand and silt. It consists of a particle entrainment in the soil mass due to rapid pore water circulations. Later, a part of these fine particles is released, so, real hoses can develop. When the size of these gaps becomes excessive, brutal sinkholes might occur in local places causing disorders at the surface.

1.4.2 Risks on people

Underground cavities are known for the threatening hazards not only for the damage they append to the environment; land and constructions; but also because of the direct risk they

induce on the lives of the people living in the surrounding. They are considered to have both socio-economic and human consequences. Based on the Ineris reports, some incidents were recognized (Ineris, 2007):

- The majority of human accidents are caused by degradation of abandoned underground quarries that were exploited by the room-and-pillar method. The death toll recorded between 1778 and 1998, gave 62 dead and 73 wounded;
- The highest loss was observed in the Paris region, probably due to the extreme density of exploitations in urban areas;
- Most events of localized collapse listed are basically subsidence (more than 90% of cases). Fortunately, they cause the most often small number of victims (1 or 2 per accident);
- The widespread (generalized) collapse of one to several hectares are rare (1 only for the period 1950-1998), but very deadly.

In addition, some risks are related to the access to the abandoned underground cavities where many visitors who came to explore these cavities without any previous planning got lost. The risk is not only related to probable unawareness, but also to the inconvenient atmosphere in these cavities due to the loss of oxygen, presence of allergic organic material, release of dangerous gas from contaminants, pollution of the water table, and others.

1.5 What are the regulations taken by concerned authorities towards this problematic?

Today, studying the deformational behaviour and the failure mechanisms associated in underground quarries, predicting and preventing the consequential risks of generated aleas, as well as developing adequate safeguards for both people and properties, have become major objectives of the responsible authorities of the cities concerned by the hazardous phenomena generating from the underground cavities. In France, a high concentration of these cavities and the corresponding aleas was identified in the Northern region (Figure 1.1 and Figure 1.2). To date, several damages, whether minor or substantial, have been recorded in urbanized areas in this region whereas some zones are classified under permanent risk of abrupt

collapses due to the instabilities originating from underlain shallow cavities and their close proximity to urbanized areas. Figure 1.16 for example shows the access of a cavity in Hellemes, North France which is located in the garden of a nursery school where the cavity is few meters under this school and it extends over hectares by width to underlain streets and residences in the area. Figure 1.17 is taken during a site visit to this cavity in June 2012.

Figure 1.16. Access to the underground quarry in Hellemes, North France.

Figure 1.17. Undeground Quarry in Hellemes, North France.

As reported by the City of Lille, 15% of the population is nowadays exposed to this risk. More than 364 incidents of collapses, subsidence, and landslides have been recorded to date due to the presence of underground quarries (Ineris, 2007, 2012, Courbot et al. 2009, Ville de

Lille 2012 and 2013). An example of a recent incident that shows the volume of collapse in a district in Lille is provided (Figure 1.18). Being aware to the circumstances of this hazardous phenomenon, the Service of Urban and Health Risks of the City of Lille has launched a 'Plan for the Prevention of Risks' (PPR) including urgent regulations and prerequisites to avoid anticipated risks and control the encountered damage in threatened regions.

Figure 1.18. General view of the collapse above the Don Bosco cavity in Lille recorded in February 2012 (by City of Lille)

This plan is associated to the project enrolled on risks of underground quarries in collaboration with several parities by which different aspects based on naturalistic, instrumental, and numerical approaches are advocated. A combination of these latter leads to identify the zones of threatened areas, evaluate the volume and intensity of risk, understand the mechanical behaviour of the underground cavities, model the modes of deformation and failure, and last but not least establish stability state predictive tools and suggest appropriate protective measures.

1.6 Underground cavities of North France: Zones of concentration

The area of the underground quarries in Lille and its region in North France is estimated by120 hectares and risks cover about 300 hectares of the above surface (mainly in Lille Sud,

Moulins, and Faubourg de Bethune) (Mikolajczak, 1996, Ineris, 2007, Courbot et al. 2009, Ville de Lille 2012 and 2013). Maps provided on the website related to this issue: cavites.fr (Figure 1.19) and others from the City of Lille (Figure1.20 and Figure 1.21) show the repartition of quarries and zones of risk in North France and particularly in urbanized regions of the sectors of Lille and Hellemes in North France (Ville de Lille).

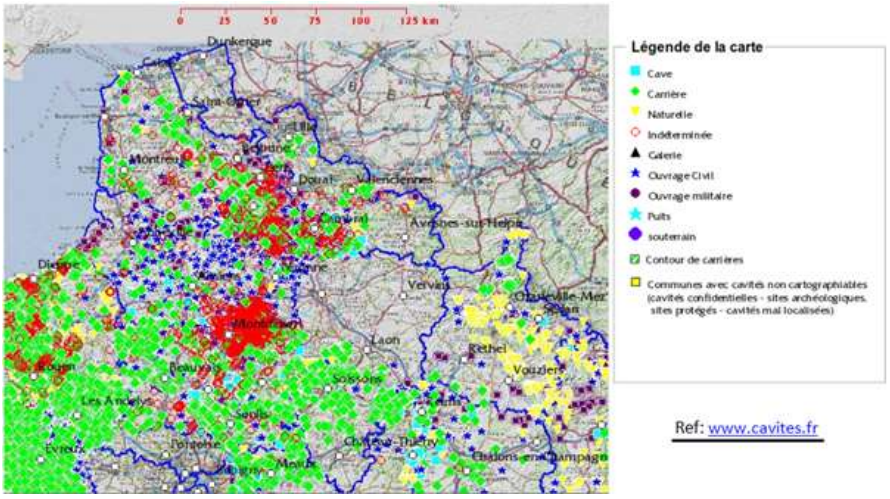

Figure 1.19. Types of underground cavities in North France - www.cavites.fr

Besides, a map showing the location of underground quarries in Lille Metropolis with the density of identified collapse incidents is provided the City of Lille (Ville de Lille 2012 and 2013).

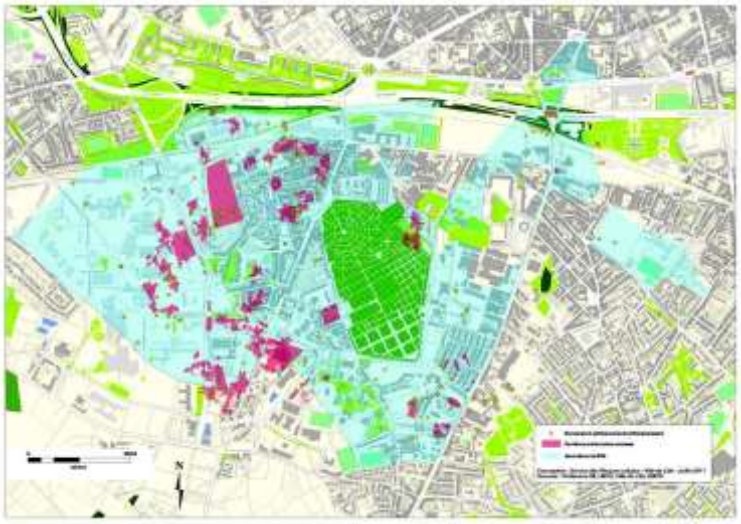

Figure 1.20. Distribution of identified cavities in Lille - by City of Lille

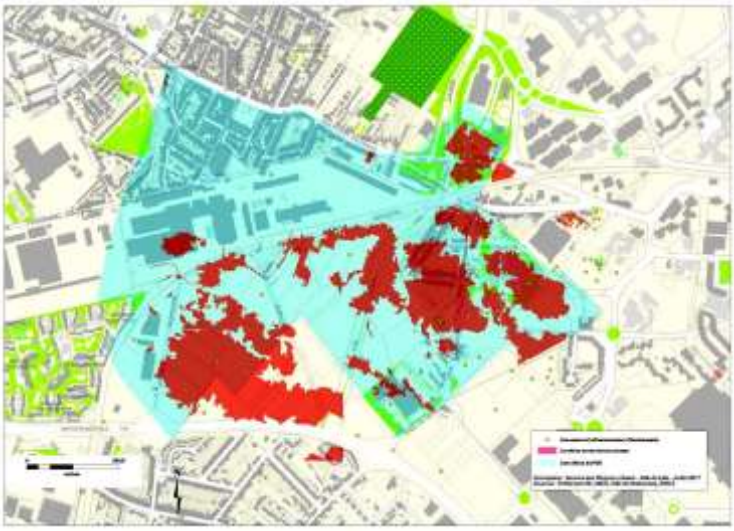

Figure 1.21. Repartition of Identified Cavities in Hellemmes - by City of Lille

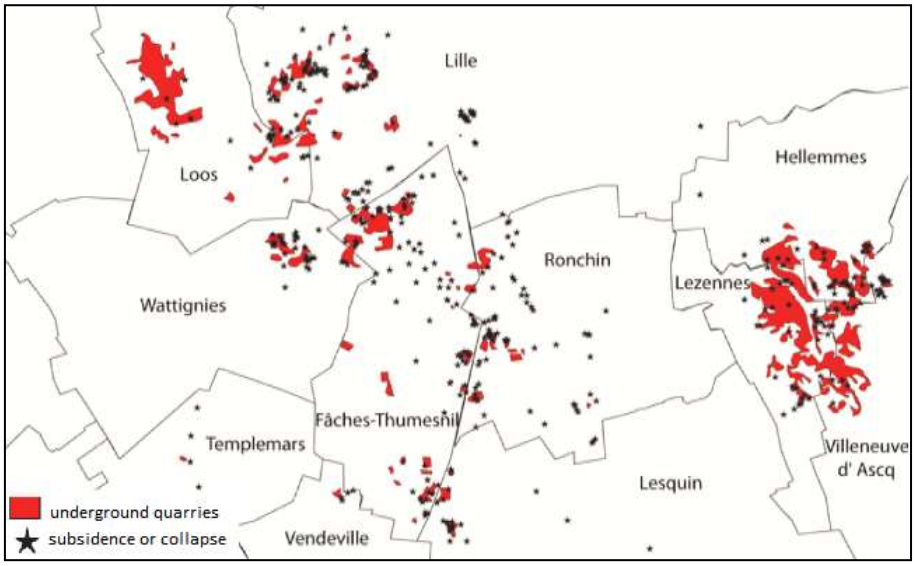

Figure 1.22. Repartition of underground quarries of Lille Metropolis and identified incidents until April 2010 (Document by City of Lille)

1.7 Common failure mechanisms in room-and-pillar quarries

The mechanisms of rupture furthermore depend on the characteristics of the exploitation methods and the environment. Eighty percent of the quarries in North France were excavated by the method of rooms-and-pillars. Usually several failure mechanisms might be associated

with this type of exploitation where instabilities can be often localized at either the pillars or the roof. A description of the frequent failure mechanisms based on a review by Watelet (1996) is provided to give a better understanding of the mechanical behaviour of these quarries.

1.7.1 Rupture of the Pillars/ Supports

1.7.1.1 Localized rupture of pillars

The localized ruptures are produced by the crushing of the pillars. Discontinuities or sometimes the heterogeneity existing in the pillars weaken them and make them incapable of supporting the exposed weight. Accordingly, this type of rupture leads to the damage of the roof and the appearance of the phenomena of widespread collapse or localized collapse as discussed before.

1.7.1.2 Crushing by uniaxial compression

The section of the pillar carrying the stress applied on the surface by the weight of the covering layer, originally is of an identified resistance. When this applied pressure exceeds the resistance of the pillar, this latter will gradually cross the elastic limit and tend to collapse. In this case, the rupture of one pillar will simultaneously exhibit an additional stress on the neighbouring pillars and encourage their rupture as well. This mechanism develops rapidly. The principle stages of this damage is often materialized by the visual indices of degradation, cracking, detaching , falls of the facing, falls of the blocks, etc.

1.7.1.3 Buckling of pillars after rupture of connecting/stabilizing bridges

This rupture mechanism appears due to the buckling of the pillars of almost high slenderness. Such a mechanism often takes place in the multilevel cavities where, initially the middle limestone connecting the bridge collapses, and hence pillars collapse after buckling due to the abruptly increased slenderness.

1.7.1.4 Rupture by shear and traction/ tension

Certain particular configurations of the site can modify the reparation of the state of the stress field and finally alter the mode of rupture. Consequently, if the field of the principal stresses is deviated, the rupture of the pillars by shear or tension can intervene with stress much lower than the compressive strength of the material.

1.7.2 Rupture of the Roof/ Slabs

1.7.2.1 Localized rupture of roof

One of the critical roof failure mechanisms is the local collapse that occurs when the existing cracks progressively open until it is assumed that a block falls from the roof. In this study we intend to model the cracks but without accounting for the kinetics of these cracks and their spatial propagation.

1.7.2.2 Rupture by flexure/ bending

Quarries are often favoured by the mode of exploitation with galleries of quadrangular sections. This exploitation mode is very practical but it is not the best one for stability where rupture is easily driven by the bending of the slabs constituting the roof. Usually, bending occurs in the case of excessive distance between the supports, or due to the insufficient thickness of the slab or other particular lithological conditions.

1.7.2.3 Rupture by shear

This classical mechanism often originates the phenomena of spontaneous collapse. The weight of the covering at the top of the roof imposes an important load on the pillars by the intermediate benches which are not thick, stiff and resistant enough to handle the localized rupture. Those benches or slabs will abruptly collapse and thus induce shear at the edges. Besides, this sudden rupture of the slab will cause the release of the previously stored elastic energy which will also generate an additional force on the pillars that are already near to reach their maximal resistance.

The shear rupture of the slabs is often intervened by certain configurations like the multilevel cavities and the sliding of the benches at the roof or sliding along the existing joints or discontinuities.

1.7.2.4 Rupture of wall/ Punching of walls

In fact the mechanism of rupture by walls punching is considered a particular case of the rupture of slab by pure shear. If the base of the cavity is not sufficiently resistant, or if this slab constituted at the bottom is of very small thickness, then, the pillars will not be capable of handling the bending of the roof anymore, and thus will punch progressively into the slab below.

1.8 Studies accounting for the frequent failure mechanisms

Researchers involved in the study of geo-engineering structures such as embankments, slopes, tunnels, underground cavities, mines and others have extensively relied on the numerical modelling in order to simulate approximate models of the real ones and try to analyse the mechanical behaviour of these models under different conditions. According to Starfield and Cundall in 1988, “we build models because the real world is too complex for our understanding; it does not help if we build models that are also too complex”. A lot of numerical modelling has been done to simulate the occurring failure mechanisms developing in underground cavities and thus try to understand the mechanical behaviour of these cavities and estimate their stability state.

Fayyad, (2004) have studied the stability of sinkhole formations at the surface above underground cavities in France. Two dimensional numerical models were simulated using the discrete element method where joints were defined as interfaces. In this 2D model, the roof above the galleries in the room-and-pillar cavity was modelled as a beam where the pillars and walls represented the supports. The aim was to study the behaviour of the beam at a certain point knowing that the rigidity of the overburden is critical in the study of sinkhole formations. It is the zone where the damage occurring at the galleries propagates upwards through it to reach the surface and become sometimes catastrophic. A development of techniques to predict and manage the impact of surface subsidence has been performed by

Canbulat et al. (2002). Gao (2013) has performed simulations of the failure mechanisms around underground coal mine openings using discrete element modelling. A discrete element framework model was developed to model rock mass behaviour, with a particular focus on the damage process including generation and propagation of fractures, and heavy dilation in the post-peak failure stage. Applications on road failure adjacent to unstable mines were performed.

Numerical modelling has been used in different applications for the assessment of stability conditions of ancient underground quarries. Ferrero and Segalini (2011) used numerical modelling and onsite monitoring to verify the actual structural predisposition to instability phenomena in the ancient ornamental stone quarries for a historical and cultural valorization as well as the recovery of the Danzi and Beltrami quarries in Italy. A similar study was performed to verify the feasibility of the underground ring road of Bressanone city in Bozen, Italy. The modeling has been finalized for the determination of the soil deformations around the digging and at the surface, during the execution of the gallery, in order to verify probable problems of subsidence.

1.9 Geological context

The geological context of the region of North France shows a variety of constituent materials such as clay, limestone, marl, gypsum, chalk, sandstone, sand, basalts, and rhyolites. However, chalk has the highest concentration and this is indicated in the lithographic map provided by the BRGM (Figure 1.23).

The majority of underground cavities identified in Lille and its region were dug in the first 30 meters of the underground substratum. During the Mesozoic era, the primary layer was covered with a large amount of marine sediments. This layer superimposes layers of Turonian and Senonian chalk. In the secondary layer, is the chalk used in construction and it is located over an average depth between 12 and 30 meters. In the tertiary layer, a cover of one to two meters of clay is found. In quaternary phase, a tan to brown layer covers all existing formations. This layer is also called the overburden favourable to agriculture because it is composed of silt sandy clay (Figure 1.24) (Dubois, 2008).

Due to tectonic movements and to erosion, the different layers mentioned above are not present everywhere in the underground sections. In quarries of Lille, chalk layer is closer to the ground surface. This is shown in a transversal section of the underground substratum in Lille Metropolis (Figure 1.25).

Figure 1.23. Lithographic map of North Region, France (not to scale) – by BRGM

The grey Senonian chalk and white chalk were extracted basically for construction aims. Among the identified quarries, 158 were recognized in chalk described as Senonian and Turonian chalk deposited 80 million years ago during the Cretaceous geological period (Ville de Lille 2012 and 2013). During eight centuries, the excavation of quarries has generated 4,500,000 cubic meters of void identified in the underground layers. The last chalk blocks extracted were used for the completion of the church of Saint Maurice Lille (Figure. 1.26). It is at the end of the nineteenth century that the exploitation of chalk ceased (Ville de Lille 2012 and 2013).

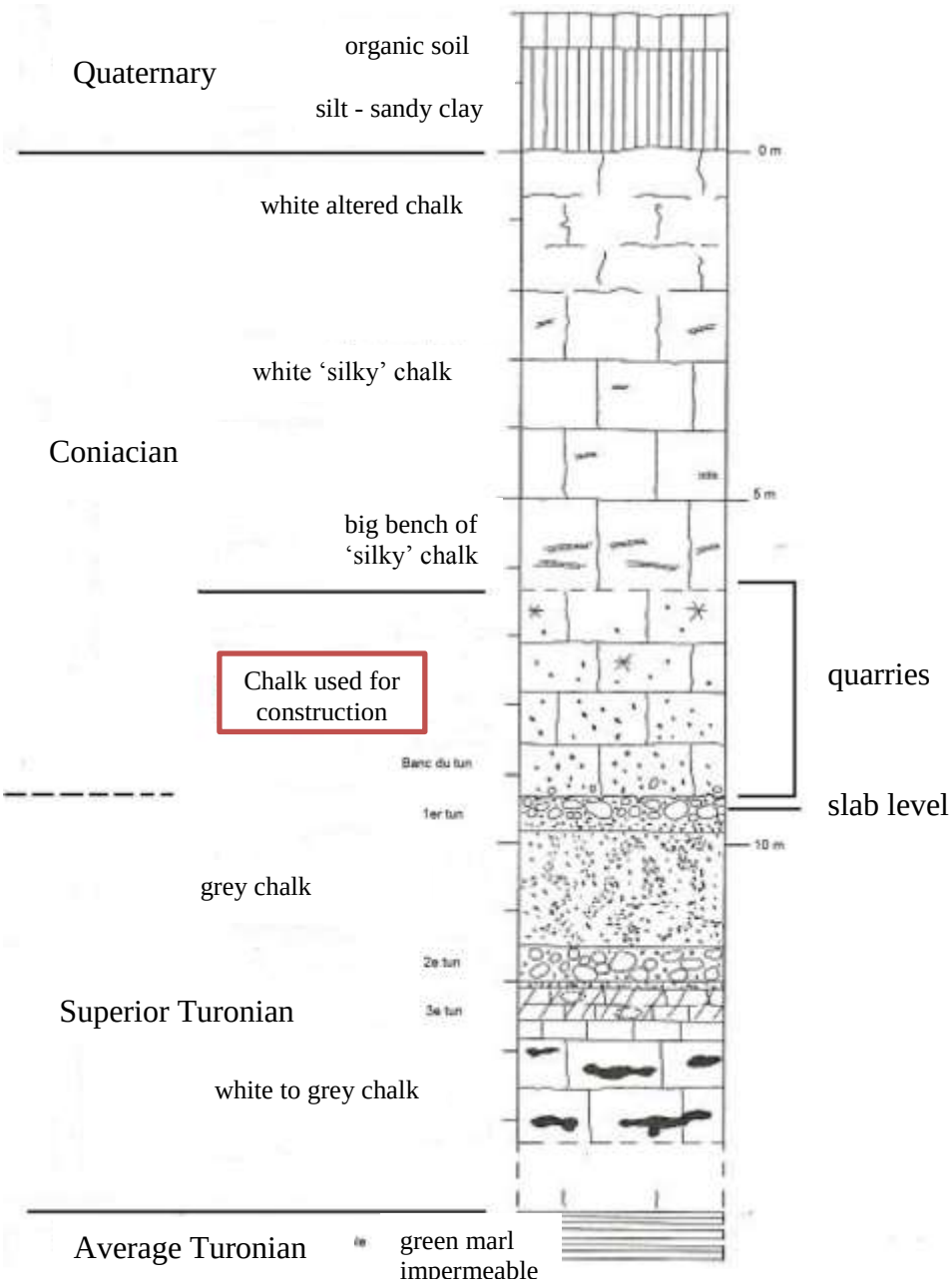

Figure 1.24. Geological section of the substratum at Lezennes, North France (M. Dubois, 2009)

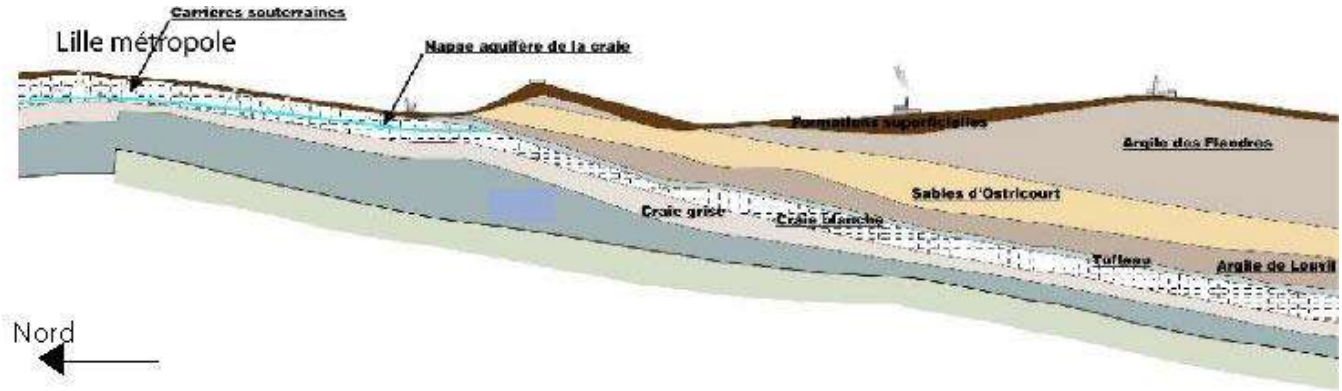

Figure 1.25. Transversal section of the substratum at a zone of study in Lille Metropolis – not to scale (Dubois, 2010)

Figure 1.26. Cathedral of Saint Maurice in Lille constructed using the chalk extracted from underground layers.

1.10 Behaviour of Chalk

According to the Emeritus Professor in Ground Engineering and Geotechnics Peter R. Vaughan: "Classical soil mechanics has evolved around a few simplified models which do not fit the properties of most real soils sufficiently for useful and safe predictions to be made... Since we cannot change the soil to fit the soil mechanics, perhaps we should change the soil mechanics to fit the soil. The theory which fails to fit their behaviour is problematic, not the soil."

Starting from this point of view, we intend to apply the best fitting model for the behaviour of chalk taking into consideration the particular conditions of our case study and accounting for diverse achievements done in this domain.

The mechanical behaviour of chalk is quite complex by which chalk can be modelled as either soil or rock at the same time. Chalk is known to exhibit nonlinear stress-strain relations, next to having both elastic and inelastic, or reversible and irreversible strains (Dahou, 1995). Moreover, deformations in chalk occur not only due to instantaneous applied stresses, but also due to the time dependent mechanisms favoured in the presence of various aggravating factors such as fractures, weathering effects and others. Multiple yielding and failure mechanisms have been observed experimentally in chalk masses (Shao, 1987, Bederiat, 1989, Schroeder, 1991, and Siwak, 1994). A number of constitutive models were developed to characterize the behaviour of chalk introducing the effect of induced stresses, material structure, water effects, time-dependent deformations like creep and weathering effects.

In general, the chalk behaviour can be characterized by: i) the stress-strain behaviour that is directly governed by the material structure which is usually known for the porous context or/and the discontinuous or jointed anisotropy-inducing medium, ii) the fluid dependent behaviour which is critical whenever the chalk-fluid contact is found, and iii) the time dependent behaviour featuring several aspects such as creep, fatigue, and aging or degradation where the influence of existent aggravating factors like weathering for example is elevated.

1.10.1.1 Stress-strain behaviour

Due to the complex arrangement of chalk which usually refers to its porous structure, the frequent occurrence of discontinuities and joints, and significant influence of aggravating factors contributing to their definition, stress-strain relations obtained from experimental tests show that an inelastic behaviour often dominates in chalk. Different plastic, elastoplastic, and elasto-viscoplastic models have been developed to simulate the behaviour featuring irreversible deformations. These models are mainly based on the classical theory of plasticity, with typical models using Von Mises, Mohr-Coulomb, Drucker-Praeger and Hoek-Brown failure criteria (Hoek, 1983).

1.10.1.2 Plastic yield mechanisms

Elasto-plastic material models consist of three main parts: (i) a yield condition, represented by a surface in the stress state defining the stress at which plastic deformation may occur, (ii) a hardening law, which describes the possible changes in shape, size and position of the yield surface and (iii) a flow rule, which governs the increment of the plastic strains. Besides, a generalized overview of experimental observations done on chalk (Shao 1987, and Homand and Shao, 2000) shows that the inelastic behaviour is associated with several independent yield mechanisms: (1) pore collapse, (2) shear failure, and (3) tensile failure. Pore collapse is a volumetric yielding mechanism in which the rock volume is reduced irreversibly due to a reduction in pore volume; experimentally, pore collapse occurs at relatively high mean stress and thus it is considerable at high depths like in the chalk reservoirs at the Northern Sea for example. Shear failure is a deviatoric yielding and brittle rupture failure mechanism in which solid rock grains rotate and/or slide past each other on internal surfaces. Shear failure occurs at relatively low mean stress and consequently it takes place more often at chalk outcrops and chalk at shallow depths. Tensile failure is a material failure mechanism in which rock grains pull apart from each other when one of the normal stress components in the rock becomes sufficiently small or tensile (Hickman 2006).

In our case of study, we are investigating the behaviour of chalk quarries at shallow depths, where joints were identified in the substratum. No high mean stresses are recognized and thus the porous characterization of chalk which is susceptible towards mean stresses is not influential at the level of failure mechanisms. However, deviatoric stresses are relatively important in our case study. Chalk in the zone of study behaves mechanically as a frictional material and thus the ultimate strength is described with respect to shear failure. The controlling failure mechanism is shear mechanism which is expected to be driven by sliding at the joints that have weaker resistance properties than those of the intact part of the chalk continuum.

1.10.1.3 Effect of confining pressure on the behaviour of chalk

Laboratory tests show that plastic strains generated during the inelastic behaviour is directly affected by the confining pressure where two distinct behaviours can take place in the stressed chalk (Xie 2005, Homand and Shao, 2000, Kageon and Loe cited by Andersen,

1995). Under high confining pressure, elastoplastic hardening in the stress-strain curves occurs and favours a ductile behaviour. Whereas, under weak confining pressure, elastoplastic softening with peak resistances takes place and thus a brittle behaviour dominates the failure process.

Triaxial tests performed on the chalk of Lezennes, North France (Siwak, 1994) show that the chalk presents two distinct behaviour types depending on the applied confining pressure. When this latter is low, softening elastoplastic behaviour is present. Otherwise, at high confining pressure, hardening elastoplastic behaviour dominates.

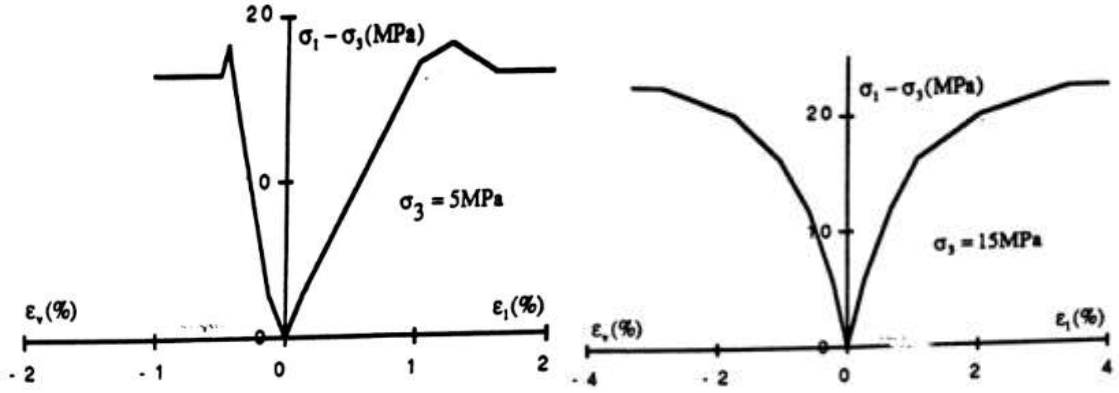

Figure 1.27. Behaviour of the chalk of Lezennes, North France at (a) low, and (b) high confining pressures (Bederiat, 1989 and Siwak, 1994).

Traditional continuum failure criteria (e.g. Mohr-Coulomb and Hoek-Brown) address regularly the assumption of shear failure. In these models cohesion and friction components are assigned and assumed to act simultaneously to define the maximum deviatoric stress limit or yield strength at any given confinement. However, at low or moderate confinement, the compressive damage in competent hard rocks occurs primarily as extensile cracking. The tensile nature of the damage process leads to a constitutive separation of cohesive and frictional strength components where stress-induced fractures grow and extend resulting in spalling and slabbing, which are a typical mechanism associated with brittle failure (Elmo, 2006).

In the same context addressing the effect of confining pressure on the behaviour of the constituent material, some approaches were developed in direct accordance to the application of underground quarries and particularly the room-and-pillar quarries. According to Alber, and Helland, (2001), removal of lateral confinement which implements rock relaxation leads

to the presence of horizontal tensile stresses and vertical compressive stresses on the pillar. When this stress exceeds the tensile strength of pillar, the pillar fails. In other words, rock relaxes due to removal of lateral constraint which results in the formation of strains. These strains across the pillar are oriented towards the void. Horizontally oriented stresses are tensile, but this does not necessarily mean the formation of new fractures. Nevertheless, when the pillar relaxes, it is subjected to the possibility of opening of the existing vertical joints. According to Cividini (1993), the softening behaviour is typically observed in hard, stiff rocks, in which a series of fractures develops and propagates when the load approaches its peak value. The softening behaviour is associated with a loss of continuity of the sample due to the formation of fractures or shear bands.

This again confirms the characterization of the chalk behaviour in the cavities under study where at relatively low confining pressure fractures develop, shear bands get formed and the discontinuous chalk continuum undergoes brittle failure.

1.10.1.4 Brittle Failure

Such type of failure is common in the domain of shallow underground cavities when confinement is moderate to low since cracks and induced fractures are urged to grow due to accumulated stresses. Brittle failure has been investigated using continuum models which considered traditional failure criteria and assumed that the mobilization of the cohesion and frictional strength components is instantaneous (Wagner (1987), Pelli et al. (1991), Castro et al. (1996), Martin (1997) and Grimstad and Bhasin (1997)). According to Elmo (2006), it has been stated by Martin et al. (2001) that this approach overlooks a fundamental observation of brittle failure; the formation of tensile cracks is the first step in the failure process. A new concept the brittle failure such that peak cohesion and friction are not mobilized together and most of the cohesion is lost before peak friction is mobilized (Martin and Chandler, 1994). A "cohesion weakening and friction strengthening" (CWFS) criterion was later on adopted by Martin et al. (2001) to numerically model the shape and extent of brittle failure for the AECL's Mine-by test tunnel constructed in Lac du Bonnet granite. In 2002, Hajiabdolmajid et al. (2002) used the same concept to predict the extent and depth of brittle failure of rocks. Nevertheless, it is important to mention in this domain the failure criterion defined by Stacey (1981), who changed the terminology from tensile strain to extension strain. According to Stacey (1981), if pillar failure is not caused by strength issue then it can be due to extension

strain criterion. At a certain depth where high compressive stresses result in high strains, and when these strains exceed the extension strain, formation of new fractures takes place. Present features like removal of lateral constraints may lead to extension of the fractures and thus failure of the bench. In this study, we intend to model the joints embedded in the chalk continuum in order to account for their critical effect on the mechanical behaviour of the chalk.

1.10.1.5 Discontinuities

Rock and chalk are distinguished from other engineering materials by the presence of inherent discontinuities such as joints, fractures, bedding planes and faults which constitute the weak planes in the rock or chalk mass. These discontinues can be naturally existing in the continuum or provoked due to the degradation mechanisms activated with time in the presence of aggravating factors (Figure 1.28). Whatever their origin is, an influence of these discontinuities on the constitutive behaviour of the rock or chalk is created. The prediction of the response of chalk and rock masses derives largely from their discontinuous and variable nature. In many situations, the deformational behaviour is much more dependent on the properties of joints than of intact rock. For instance, the strain and failure mechanisms of fractured rock masses are often governed by shear along discontinuities as mentioned before.

Figure 1.28. Mechanical fissures and faults at the pillars

Therefore, it is quite important to account for the effect of discontinuities in the analysis of the mechanical behaviour of chalk. This issue is a major focus of this work especially that at

shallow depths where these quarries are located, shear failure in joints is considered a principle controlling rupture mechanism. Details about the implementation of joints effect in the behaviour of chalk in addition to a review of the works achieved in this domain are provided in the coming chapter (chapter two).

1.10.1.6 Elastoplastic and elastoviscoplastic models

Back to the stress-strain relations integrated in the constitutive laws, several elastoplastic and elastoviscoplastic models were developed to characterize the chalk behaviour with three independent failure mechanisms defined: pore collapse, shear collapse, and tensile failure.
Based on a review performed by Hickman (2004), common achievements in this domain were classified into eight types of models (model 1: DeGennaro et al. (2003), Collin et al. (2002), Datcheva et al. (2001), Pasachalk (2004); model 2: Homand and Shao (2000); follows from Homand et al. (1998) and Schroeder and Shao (1996); model 3: Gutierrez (1998, 1999, 2000); model 4: Papamichos et al. (1997); model 5: Plischke (1994, 1996); model 6: Foged et al. (1995); model 7: Abdulraheem et al. (1993); and model 8: Shao and Henry (1991)).
All of these constitutive models except that of Papamichos et al. (1997) are multi-mechanism models which have separate yield surfaces one for the shear collapse yield mechanism and another for the pore collapse yield mechanism (usually modelled as straight line and elliptical cap surface respectively) while some models also include yield surfaces for tensile failure. In addition, all models are characterized by isotropic hardening for the hardening yield surfaces. They include hardening to the pore collapse yield surface which is mostly defined with associated plasticity; and concerning the shear yield surface, non-associated plastic flow is often defined where hardening is included in the recent models. For a better understanding, a categorization done by Hickman (2004) is provided (Table 1.1).

1.10.2 Water dependent behaviour

The presence of water activates various chemical and mechanical aspects like hydraulic loading, dissolution, saturation, suction, water flooding, porous effects and others. These aspects implement a direct influence on the constitutive behaviour of chalk itself.
The most frequent water-chalk degradation processes can be divided into two categories mechanical and chemical. A descriptive overview of these processes is given below.

Table 1.1. Summary of Elasto(visco)plastic Constitutive Models for Chalk

Model 1: DeGennaro et al. (2003), Collin et al. (2002), Datcheva et al.(2001), and PASACHALK (2004)	↓ Pore collapse mechanism and shear collapse mechanism both with isotropic hardening and tensile failure without hardening ↓ Overstress viscosity included in all exccept Collin et al. ↓ Size of shear and pore collapse yield surfaces change depending on suction. Datcheva et al. do not account for pore fluid effect
Model 2: Homand and Shao (2000), Homand et al. (1998) and Schroeder and Shao (1996)	↓ Pore collapse mechanism and shear collapse mechanism both with isotropic hardening ↓ No integration of time-dependent deformations ↓ Two yield surfaces corresponding for "oil-like", and for "water-like" saturating fluid are defined
Model 3: Gutierrez (1998, 1999, 2000)	↓ Pore collapse mechanism with isotropic hardening and shear and tensile failure mechanisms without hardening ↓ Rate-type model based on a volumetric creep model ↓ Creep parameter varies as a function of saturating fluid ↓ Time-dependent behavior through pore pressure change
Model 4: Papamichos et al. (1997)	↓ Pore collapse mechanism and shear collapse mechanism both with isotropic hardening ↓ No integration of time-dependent deformations ↓ Size of initial yield surface depends on water saturation

Model 5: Plischke (1994, 1996)	✚ Pore collapse mechanism with isotropic hardening and shear collapse mechanism without hardening ✚ Time-dependent deformations related to water injection ✚ Size of initial yield surface depends on water saturation
Model 6: Foged et al. (1995)	✚ Pore collapse mechanism with isotropic hardening and shear collapse mechanism without hardening ✚ No integration of time-dependent deformations ✚ No accounting for the effect of saturating fluid
Model 7: Abdelraheem et al. (1993)	✚ Pore collapse mechanism with isotropic hardening and shear collapse mechanism without hardening ✚ No integration of time-dependent deformations ✚ No accounting for the effect of saturating fluid
Model 8: Shao and Henry (1981)	✚ Pore collapse mechanism and shear collapse mechanism both with isotropic hardening ✚ No integration of time-dependent deformations ✚ No accounting for the effect of saturating fluid

1.10.2.1 Mechanical Processes

- Hydraulic, impact, and cyclic loads:

Rain involves either temporary or permanent presence of the water at the permeable or impermeable surface of the roof, respectively. The infiltration of the water depends on the permeability and the porous media in the overburden. At least, an instantaneous hydraulic load is created before gradual infiltration. Consequently, this load is added to the existing

loads that are to be supported by the roof of the galleries like the dry ground weight and the external acting loads.

Besides, if the aim is to increase the level of accuracy in this analysis, an impact live load which might be created in case of a heavy rainfall at the upper surface is to be considered.

In addition, the variation of water level at the ground of the galleries along the different seasons can be described by a cyclic load which is induced at the lower levels of the gallery walls. This has also to be taken into account in the calculation of water effects on the performance of the underground cavity.

In 2007, Tremblay and co-workers (2007) implemented a constitutive model CSDS (Complete Stress-Displacement Surface) to predict the hydro-mechanical behaviour rock by investigating the mechanical and hydraulic behaviour represented by water pressure and water flow respectively, in the rock joints. As claimed by Simon (1999), Simon and co-workers (1999 and 2003), Deng et al.(2004), the CSDS model is good for normal stiffness conditions, for determining the post-peak behaviour of intact rock, for well-considering scale effects, and for treating the effect of water pressure.

- Saturation:

Saturation degree of rock masses increase when rain water is infiltrated in the substratum. This leads to an inverse decrease of the strength properties of the massive. Related tests show that the increase in the saturation of the rock causes a reduction in its compressive and tensile strengths, as well as a reduction in its elasticity modulus.

Dessene (1971) and Masson (1973) have showed by experimental investigations that the influence of water on the mechanical behaviour of chalk is important. This was also demonstrated in tests done on the chalk of Lezennes at North France where the variation of internal chalk mechanical properties with respect to the degree of saturation are observed (cited by Dahoa, 1996). Figures 1.29 to 1.31 show that the Young modulus, elastic limit, and resistance to uniaxial compression are inversely proportional to the degree of saturation (Dahoa, 1996).

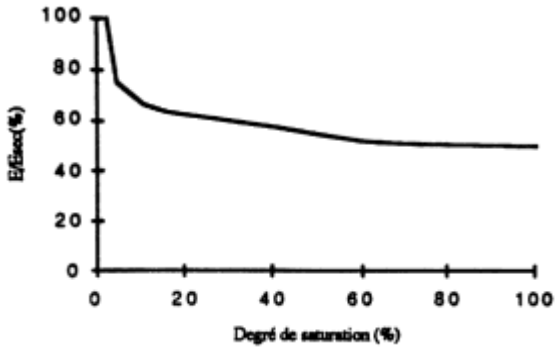

Figure 1.29. Variation of the Young modulus in terms of the degree of saturation.

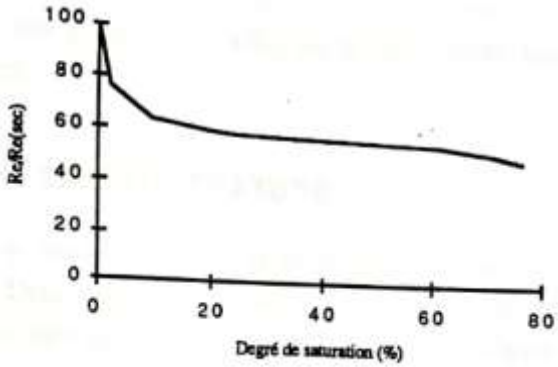

Figure 1.30. Variation of the elastic limit in terms of the degree of saturation.

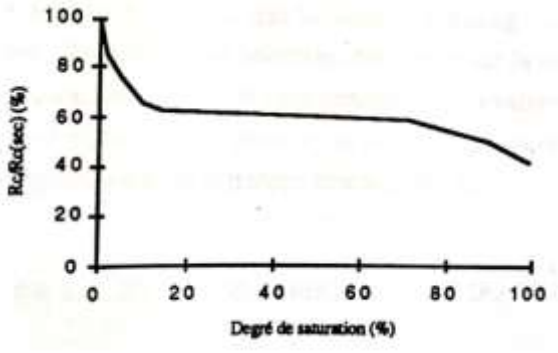

Figure 1.31. Variation of the resistance to uniaxial compression in terms of the degree of saturation.

Some authors have integrated the effect of water in constitutive behaviour laws of chalk and developed numerical models to study the effect of water on the deformational behaviour of existing geoengineering structures such as quarries. Piau et al. (1998), Maury et al. (1996), and Piau and Maury (1994 and 1995) studied the effect of water saturation on the yield

surface and the mechanical properties such as friction angle, critical shear stress ratio, and pre-consolidation stress.

Plischke (1994, 1996) simulates the effects of water flooding. Under these conditions, the pre-consolidation stress decreases gradually as water saturation increases. Papamichos et al. (1997) stated that both the tension cut-off and the pre-consolidation stress vary as a function of water saturation. The elastic modulus also decreases as water saturation increases, while Poisson's ratio is not affected. According to Papamichos et al. (1997), the weakening mechanism is attributed to changes in capillary forces, and thus the model is formulated in terms of suction.

- Suction

Suction is the difference between the air pressure and the water pressure in the chalk material. This phenomenon is activated in humid areas when there is difference in the degree of saturation of adjacent chalk media which occurs after rain. The consequential degrading process usually governs in porous media and can be explained by the following steps:

i. Chalk is in contact with a less humid environment
ii. Capillary Forces oppose removal of water from chalk
iii. This leads to extension of the elastic field (elastic limit increases)
iv. Hardening of the entire surface is generated
v. Progressive Water Logging
vi. Absence of Less Humid Zone
vii. Suction Diminishes
viii. Decay in Structure Strength

In their works to study the effects of suction in partially saturated soils, DeGennaro et al. (2003) and Collin et al. (2002) have used the Barcelona Basic Model (BBM) which was previously proposed by Alonso et al. (1990) for unsaturated soils. BBM defines suction in chalk based on the difference between oil and water pressures in this chalk. It separates irreversible strains into mechanical and suction-based components. Concerning the mechanical properties, results showed that cohesion and pre-consolidation stress vary with suction, but friction angle is independent of it.

- Pore Pressure:

Another effect of water is activated in porous media where water pressure drives the capillary forces to act on the chalk surfaces. A description of this process is given below:

i. Water gradually invades porous chalk
ii. High Pore Pressure (compared to acting normal stress)
iii. Force Resisting Sliding b/w Blocks is Reduced
iv. Tension at the interface decreases
v. Disturbing Forces Separating Blocks Intensively Activated

Homand et al. (1998) and Homand and Shao (2000) discussed the phenomenon of water/chalk interaction and developed constitutive relations to study the mechanical behaviour of porous chalk in the presence of water. This approach assumed that there are two chalk material states, dried or oil saturated and water saturated, superposed on the same material point. When the water saturation is less than the critical value, the "oil" chalk behaviour is active. On the other hand, the "water" chalk behaviour is activated when the water saturation is higher than the critical value. Water injection causes a jump of yield surfaces from the "oil state" to "water state" and the plastic equilibrium is disturbed. The way to re-establish this plastic equilibrium is to produce an instantaneous plastic deformation. Thus by integrating the water induced plastic strains in the strain relations, the effect of water on the constitutive behaviour is being accounted for.

1.10.2.2 Chemical Processes

More recently, Nguyen (2009) has studied the influence of water-rock interaction on the long term behaviour of chalk underground cavities. Experimental works on the cavity of Estreux in France were done using MEBE (Microscope Electronique à Balayage Environnemental) which is equipped by Ineris in order to study the hydro-mechanical behaviour of chalk. MEBE considers the Morphological and Mineralogical modifications induced in chalk by the hydration-dehydration process and therefore the variable behaviour mechanisms of chalk could be tracked. In order to account for the effect of suction, oedometric tests are simulated by the model of Barcelona-BBM (Barcelona Basic Model) by Alonso et al (1990). Then an extension of the visco-hydromechanical model developed from the model RASTRA (RAte of strain model) proposed by De Gennaro and Pereira (2008) is provided.

- Condensation:

Due to water saturation after the rain season, water penetrates the porous rock and reaches the cavity. Then, and after a raise in the temperature inside the gallery, water at the floor evaporates and then condenses at the roof of the gallery. A degradation process occurs repetitively in the following sequence:

i. Condensation of the pure water on the roof of the gallery.
ii. Dissolution of the CO_2 in the air.
iii. Water that becomes acidic infiltrates in the porous rock.
iv. Migration of the air CO_2 molecules in the rock pore water by convection and molecular diffusion.
v. Concentration of Ca^{2+} ions in the rock pore water increases.
vi. Limestone dissolves in its acidic pore water.
vii. Porosity increases and saturation increases.
viii. The mechanical degradation continues even without additional water infiltration.
ix. Failure of the roof.

The quantity of CO_2 dissolved in unit volume of water depends on the partial pressure in the cavity air and the temperature. The time needed for the completion of this process depends on the thickness and properties of the roof layer.

- Dissolution/Crystallization (Karstic Effect):

This process is a typical alteration of limestone rich in calcite like chalk. Dissolution is the process by which the solid chalk forms a solution after being dissolved in water. When water attacks the chalk, it invades the cracks and due to dissolution, these cracks get enlarged. Crystallization occurs in chalk when chalk solute transfers from the liquid solution to a pure solid crystalline. These processes may denote the karstic effect that frequently invades chalk (Figure 1.32). This phenomenon is well promoted by the mechanism of creep where time is an important factor in activating the chemical effect.

Figure 1.32. Karstic effect in the cavity of Cavagniac, Lille.

In the investigation of underground cavities in Lille and its region in North France, water was observed in few cavities located in the southern sector of Lille (Lille Sud) rather than other zones (Ville de Lille, 2012 and Dubois, 2010). However, it is still of high importance to study the effect of water on the behaviour of these chalk cavities including all the discussed physical features; both chemical and mechanical. Nevertheless, in this work the effect of water was integrated non-separately from the effects of other aggravating factors within a degradation model which is also time-dependent. This allows the investigation of the long term behaviour of chalk and therefore the cavities due to the encountered degradation.

1.10.3 Time dependent behaviour and effect of aggravating factors

Time is an important factor in the stability study of unexploited underground cavities which have been excavated decades ago like those in North France. The influence of time on the constitutive behaviour of stressed chalk is critical especially in the presence of various aggravating factors as it is the case of abandoned underground cavities. Time dependent deformations can be represented by several aspects despite the fact that there is still no clear distinction in the time dependent mechanisms that might occur.

1.10.3.1 Creep

Deformations can develop under constant loading upon time. This is known as creep where the corresponding typical relation of time dependent deformation exhibits three phases (Figure 1.33). The first phase is known as Primary or Transient Creep. In this phase, the rapid decrease of deformation rate is clear. Once the stress is removed the material retains its initial state. Hence, the deformation is reversible. The secondary phase is also known as Stationary or Steady State Creep. In this phase, the deformation rate is almost stable. Third phase known as Tertiary or Accelerating Creep undergoes rapid failure under high shear or deviatoric stresses occurs. In fact, this phenomenon is rarely encountered in chalk.

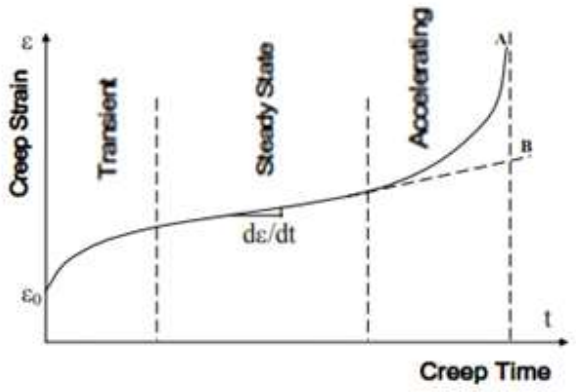

Figure 1.33. Typical Creep Curve

Triaxial creep tests done on the chalk of Lezennes by Dahou (1995) showed that this chalk at different confining pressures and under various applied deviatoric stresses exhibits only transient creep (Figure 1.34). No accelerating creep is advocated for this range of stresses. Uniaxial creep tests done by Monjoie and Schroeder (1990) show that for stresses greater than 0.7Rc (compression resistance), the creep is no more stable and the viscoplastic deformation will rapidly increase leading to rupture. In the creep analysis of Northern chalk performed by Dahou (1995), creep triaxial tests at different deformation rates were executed. This was introduced in the formulation of an elastoviscoplastic model for chalk behaviour (Dahou, 1995).

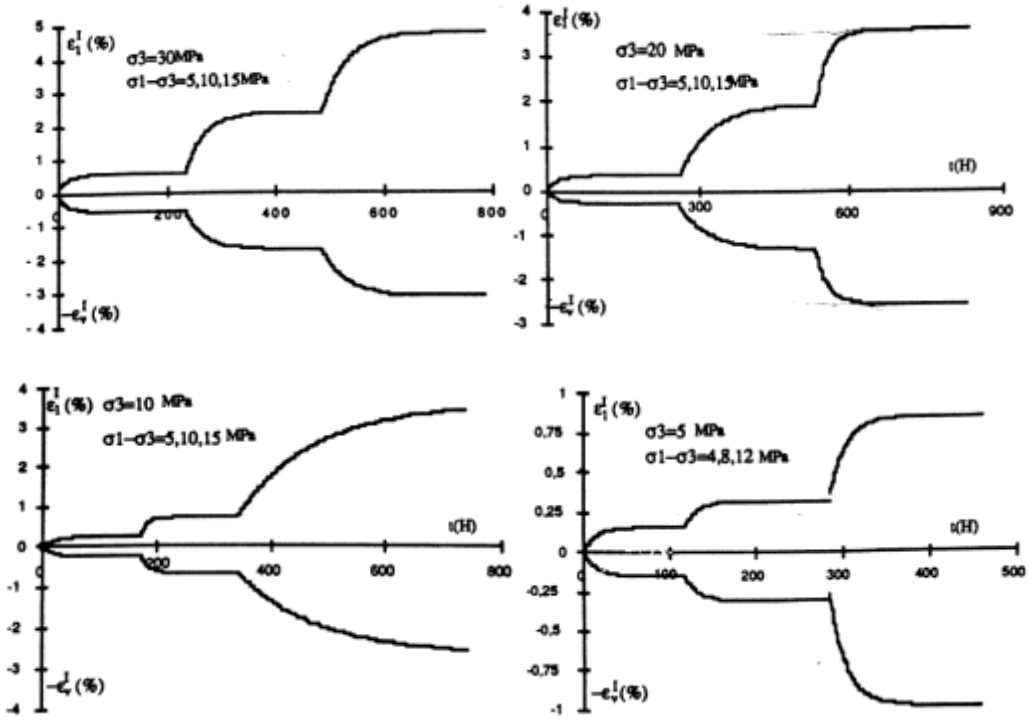

Figure 1.34. Creep triaxial tests performed on the chalk of Lezennes, North France under different confining pressures (σ_3) (by Dahou, 1995)

Transient creep constitutive model is formulated step by step from experimental data for hydrostatic and conventional triaxial tests and using the general Cristescu's procedure. The model takes into account different chalk failure behaviour under compressional and extensional conditions (Figure 1.35).

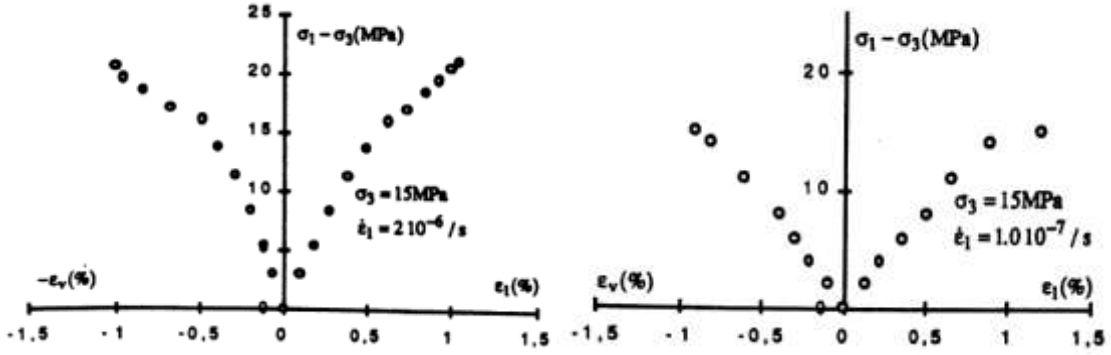

Figure 1.35. Creep triaxial tests performed on the chalk of Lezennes, North France at different deformation rates ($\dot{\varepsilon}_1$) (by Dahou, 1995)

Other models were developed to account for the effect of time on the mechanical behavior of rock masses in general, and chalk in particular (Datcheva, 2001).

Andersen et al. (1992) modeled the creep behaviour using the logarithmic rate-type model of Waal (1986) using lines on which stress rate is equal rather than time-lines on which age and viscoplastic strain rate are equal. Rhett (1994) proposed an approach to simulate creep using a linear relation between (1/time) and (1/strain). This type of model produces a hyperbolic relation between creep duration and creep strain. The Unified Chalk Model (UCM) of Gutierrez (1999, 2000) is formulated as a rate-type model. UCM uses the logarithmic model of Bjerrum (1967) and it exhibits the following principles: Viscoplastic volumetric strain rate is inversely proportional to the volumetric age of the material, and the volumetric age is proportional to the distance in stress space between the stress point and the pore collapse yield surface. According to Shao et al. (1993, 2003), Pietruszczak et al. (2004), and Amitrano and Helmstetter (2006), classical models attribute the creep deformation to the viscous properties and the time-dependent deformation is thus entirely described by viscoelastic and viscoplastic theories (Perzyna, 1966, Cristescu, 1989, and Cristescu and Hunsche, 1998). However, creep can be described in terms of microstructural evolution that integrates a progressive degradation in the material and thus accounts for the internal physical mechanisms (Shao et al., 2003). More details are provided in chapter four.

On the other hand, time effects can be represented by time dependent deformations resulting from the material degradation which is activated with time in the presence of the unavoidable aggravating factors and permanent stress conditions. Time analysis of unexploited underground cavities can be achieved by defining a time dependent degradation scheme and introducing it in the constitutive behaviour of chalk. Some works were developed in this domain and mostly under the title of weathering effects on rock masses.

1.10.3.2 Weathering effect

Seasonal variations reveal different aspects that might affect the internal properties of the chalk and thus increase the deteriorating mechanism known as weathering. Seasonal variations lead to temperature variations that can induce a phenomenon of cyclic deformation, called respiration, which causes fatigue and renders the resistance reduction of the material. Besides, this phenomenon provokes the occurrence of repetitive saturation-desaturation cycles, which come upon the variations of relative humidity inside the cavity.

This is basically related to the rainfall in the rain seasons and can impose various mechanical and chemical processes which were discussed before. In addition, all these aspects provide a new environment inside the cavity which might be favourable for the microbial activity that also influences the resistive properties of the chalk. Weathering is considered a serious degrading phenomenon that greatly affects the mechanical properties of the exposed chalk. Several workers in the domain have studied the induced degradation due to weathering and similar degrading factors. A common hypothesis was based on substituting the time effect implicitly by defining a degradation function to be imposed to the resistive properties of the chalk. In 2003, Nova et al., 2003 demonstrated the observed behaviour of bonded geomaterials subject to mechanical and/or chemical degradation. They found that it can be reproduced by simple elastoplastic strain hardening model, in which the internal variables depend on a scalar quantity related to the degree of weathering. The implemented model is capable of capturing a fairly large variety of physical phenomena with reasonable accuracy. Ghabezloo and Pouya (2006) discussed the gradual weathering of the rock mass accompanied with progressive failure and collapse of underground limestone quarries. The numerical model developed to simulate the cavity failure integrates a kinetic model defined including the temporal aspect through four phenomena: water transfer which characterizes the initial phase; diffusion-advection where mechanisms for the transport of the solids dissolved in rock pore water are activated; limestone dissolution which comes as a chemical result due to the preceding actions; and finally the mechanical degradation originating from the increase in degree of saturation and the porous matrix dissolution accumulating due to increased porosity.

1.10.3.3 Other external factors that motivate rupture

Whatever its nature is, the disorders occurring in underground chalk cavities often result due to a combination of one or more failure mechanisms (discussed before). These mechanisms are usually activated in the presence of aggravating factors that might either reduce the internal resistive properties of chalk (degrading weathering phenomenon for instance), or increase the acting loads. This latter can be attained by external factors such as anthropogenic activities and seismic loads which are capable of threatening the overall stability of the quarry and its surrounding.

- Anthropogenic Activities

Anthropogenic factors like certain engineering activities, civil works, machinery or traffic works vibrations, external loading (surcharge), discharging, modification of hydro-geologic network and others might have a substantial influence on the stability of the covering and surrounding layers of the quarries and can be transmitted to affect the overall stability of the quarry itself (Figure 1.36). Such effects can be easily involved in the stability study of the quarries after evaluating the applied loads and imposing them into the analysis. However, what really counts in this context is that these factors are case dependent. In other words, if we normalize all these factors to account for their envelope effect, we will be overestimating the consequences in the behaviour analysis. For this reason, none of these case-particular effects was inserted in the current study.

Figure 1.36. Surface damage at Boisselle, Lille – Journal : La Voix du Nord, 2015

- Seismic Effect

Seismic effects must be taken into consideration in the investigation of the stability of underground cavities. This can be achieved by carrying out a dynamic analysis to track the behaviour of the structure under these seismic effects separately, and in combination with the static loads and other aggravating factors. Nevertheless, Lille and its region in North France are classified seismic zone 2 ($0.7 m/s^2$) which is considered not critical (Pecker, 2013). For this reason, this factor is neglected in the current study.

In this study, we account for the degradation activated with time in the presence of aggravating factors by developing a time-dependant-degradation model and integrating it in the numerical analysis of the long term behaviour and stability of the underground cavity. This is described in chapter four of this thesis.

1.11 What do we propose in this thesis?

A brief overview on the propositions offered in this thesis in terms of the study of the behaviour and stability of the room-and-pillar chalk underground cavities is given below:

- Developing a three-dimensional numerical model of the cavities excavated at shallow depth using a continuum approach where:
    - The numerical analysis permits a better understanding of the failure mechanisms associated under different conditions and provides a complementary approach for the geological observations and measurements;
    - A three-dimensional model allows lessening the limitations on the boundaries and thus gives a more realistic representation of the case study;
- Developing an oriented yield criterion to model embedded joints implicitly and express different corresponding features such as:
    - Anisotropic behaviour due to presence of either stratigraphic joints or induced fractures;
    - Weakening effect due to induced fractures defined as weak planes with reduced strength properties;
    - Presence of geometric discontinuities (faults) by assigning the weak planes behaviour to specific zones in the continuum which correspond to the location of the faults;
- Studying the effect of joints on the strain and failure mechanisms as well as on the stability of the underground cavity;
- Developing a time-dependent-degradation model to account for the accumulated effect of aggravating factors on chalk with time at one hand, and to consider the impact of stress evolution with time on the mechanical behaviour of chalk at the other hand.

- Studying the long term stability of the underground cavity by incorporating the associated physical time dependent mechanisms instead of applying a uniform (geometrically homogeneous) and steady (constant incremental process) reduction technique of the strength properties as it is the case in traditional methods.
- The developed models can be used in different geotechnical applications and not only in the current study:
    - The criterion developed to model the joints can be used to model interfaces in different soil-structure interaction applications;
    - The time-dependent-degradation model can be considered a non-complicated approach that can be used to account for time effects in any other applications that require a time analysis;
    - A coupling of both models together, i.e. the joints model and the time-dependent-degradation model, allows us to carry out a non-homogeneous kinetic stability analysis which integrates the physical aspects unlike traditional stability analysis methods;
- Developing extrapolated formulae and abacuses for the direct preliminary assessment of the stability state of the underground cavities under study:
    - These tools can be helpful for geo-engineers investigating the risks in the cavities of the region under study; it gives them an idea about the stability state after just visual inspections;
    - Same procedure which is detailed in chapter five can be used for cavities having different characteristics to perform a likewise preliminary approach for the estimation of the stability state.

1.12 Conclusions

Based on this descriptive overview about the phenomenon of underground cavities in general, and the characterization of cavities identified in North France in particular, we define the focus of the work in this thesis as follows:

1) First, the aim is to study the behaviour and stability of underground quarries exploited by the method of rooms-and-pillars since this latter presents the majority of the cases in the zone of study, Lille and its region in North France;
2) Second, our concern is quarries excavated in the chalk layers since the lithographic maps of the region show high concentration of chalk in the zone of study;
3) Third, the fundamentals of this study will be based on the integration of a major property of the identified chalk: the discontinuities known as joints or fractures, which is at the same time considered as an aggravating factor responsible of activating certain failure mechanisms and controlling the scenarios of rupture. Besides, and as it was explained before, the controlling collapse mechanism in the shallow cavities under study is the shear collapse initiated at the joints;
4) Fourth, the associated strain and failure mechanisms are modelled and the effect of joints on these mechanisms and on the overall stability is analysed;
5) Fifth, the factor of time where the degrading effect of all other aggravating factors is accumulated is taken into account in this study by developing a time-dependent-degradation model, a long term stability analysis is performed using this model, results are compared to those obtained from the stability analysis using the traditional methods;
6) At last, a parametric stability study accounting for the range of different geometries of the room-and-pillar cavities is conducted. A regression analysis is then performed and tools for the preliminary estimation of stability state are provided.

In order to highlight to focus of this thesis and correlate the major intentions of this work via the coming chapters, a flow diagram is provided at the end of this chapter (Figure 1.37)

In the coming chapter, we describe and analyse the criterion developed to account for the presence of joints in the chalk continuum.

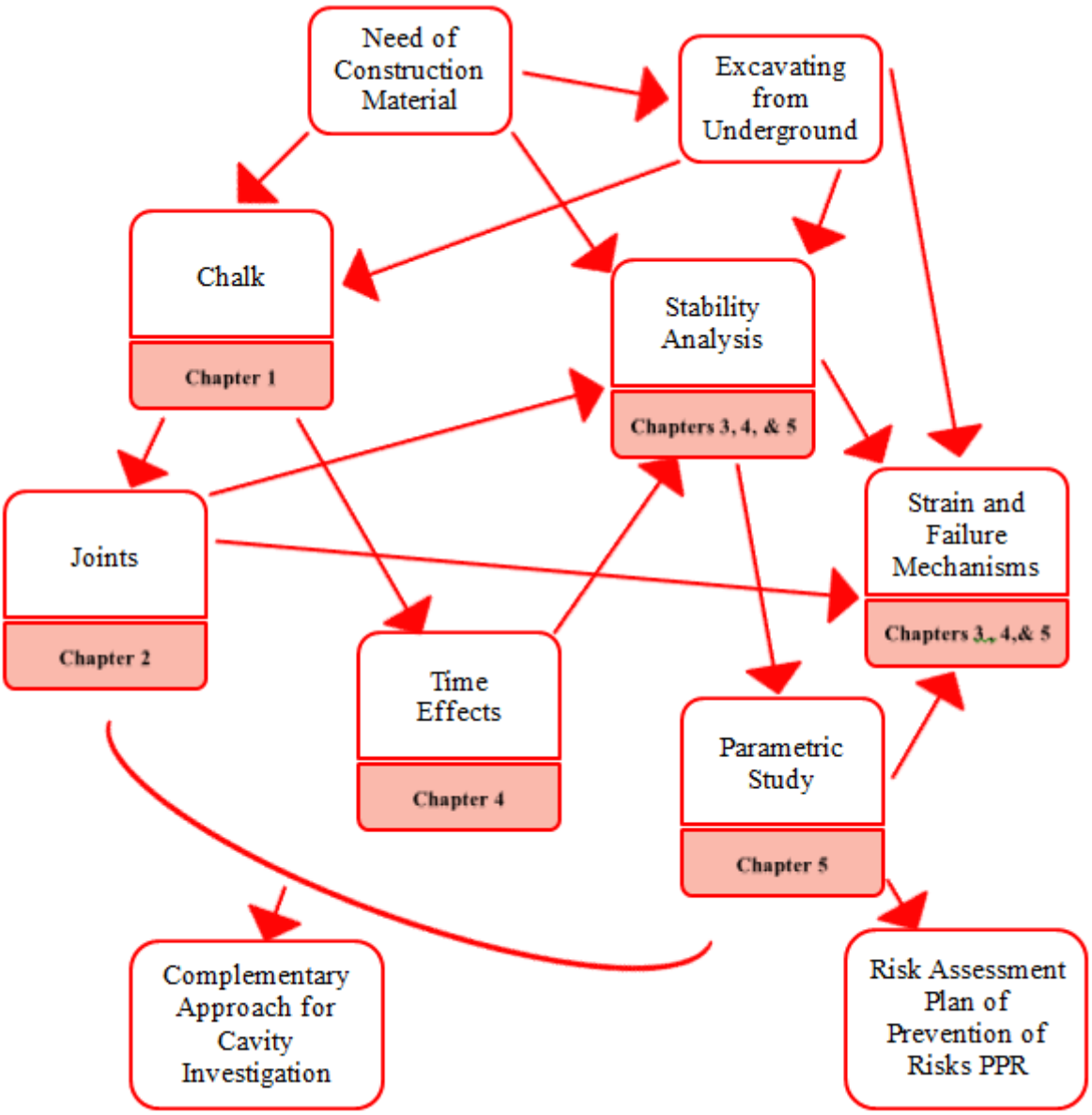

Figure 1.37. Flow diagram highlighting the major topics of the thesis.

CHAPTER TWO
BEHAVIOUR OF CHALK: ACCOUNTING FOR THE EFFECT OF JOINTS

2.1 Introduction

In the assessment of underground instabilities, originating from the quarries excavated in the jointed chalk bed decades ago in North France, it is necessary to comprehend the behaviour of the constituent chalk which in turn directly affects the global stability of the underground structure and its surrounding. Knowing that the chalk layers are originally embedded with joints and discontinuities (Mikolajczak 1996, Ineris, 2007, Courbot et al. 2009, Ville de Lille 2012 and 2013), an anisotropic behaviour is induced. Anisotropy, whether inherent presented by the embedded joints or provoked by generated fractures, intrinsically affects the strength, and the strain behaviour of the chalk mass. Especially at shallow depths where stresses are low, the behaviour of the chalk rock mass is controlled by sliding along the joints and accumulated shear strains in the discontinuities. Anisotropy may affect the failure mechanisms and thus modify the stability state of underground openings and their surroundings and induce collapses.

Different continuum and discontinuum approaches and numerical models were developed to account for the behaviour of jointed rock masses by either implicit or explicit presentation of fractures. For instance, the concept of homogenization of fractured rock media with explicit macroscopic fractures into equivalent continuous media (generally transverse isotropy for one network of joints, orthotropic two networks of joints, etc.) was proposed (Gerrard, 1982; and Singh, 2000) has presented continuum characterization methods for jointed rock masses and developed expressions to estimate the elastic moduli of the equivalent continuum anisotropic

rock mass. Gerrard (1982) used an equivalent continuum approach based on the idea of expressing the compliance of an element as the sum of the compliances of the intact rock and that of the individual joint sets. Zienkiewicz et al. (1975) have also used the equivalent continuum approach, referred to as a multi-laminate model to simulate a discontinuous rock mass. Moreover, Sitharam and Latha (2002), and Sitharam (2009), advocated a numerical approach treating the rock mass with equivalent material properties. Another approach based on the explicit consideration of the mechanical behaviour of both the matrix and the fractures was proposed by Cai et al. (1993). This was achieved through a constitutive model that accounts for the effects of density, orientation and connectivity of joints, as well as the properties of the joints themselves. In addition, anisotropic models and/or strength criteria for structurally anisotropic rocks were developed by Duveau et al. (1998). This latter has provided an assessment of representative failure criteria in the framework of modelling the failure behaviour of strongly anisotropic geomaterials. Another category of numerical modelling of anisotropic behaviour and/or strength of anisotropic rocks is achieved by assuming implicit representation of joint sets (Itasca, 2009). In this case, the rock mass consists of intact material with isotropic linear or nonlinear behaviour and weak planes presenting the joints based on the extension of Griffith theory (Griffiths, 1980; and Griffiths and Lane, 1999). This technique can be considered appropriate for the modelling and analysis of joints effect in fractured rock masses where joints or discontinuities cannot be precisely located. In chalk, this technique can be considered appropriate.

This chapter aims to study the effect of joints on the behaviour of underground cavities excavated at shallow depths in jointed chalk layers. A nonlinear constitutive law used to account for the effect of joints on the chalk behaviour by means of embedded joint sets with different orientations is developed based on the theory of multi-mechanisms for plastic strains by Koiter (1953 and 1960).

In this model, general failure at the level of intact chalk is initially checked, and relevant plastic corrections are applied when failure is detected. Triaxial tests are simulated after assigning the properties of the proposed joint model with single mechanism and that with double mechanism to the chalk behaviour. Comparisons with results using existing models are performed to validate the applicability of the proposed model. Stress-strain responses are presented and failure modes are analysed to describe the strength, deformability and displacement behaviour of the anisotropic chalk.

2.2 Constitutive law accounting for the presence of joints

2.2.1 Principles

In order to account for the effect of anisotropy on the behaviour of the stressed chalk, a model based on an implicit technique for representing the embedded joints, is proposed. This is used because the position of the joints is not exactly known. They can develop everywhere according to stress state. In this model, the joints known as weak planes are not defined separately from the intact chalk known as the matrix. They do not act as geometric interfaces or faults existing in the chalk rock mass. However, the weak planes are represented implicitly in the chalk continuum. They are defined uniformly over the zones of the model with varying orientations and reduced strength properties. Consequently, the anisotropic effect is advocated at the level of the mechanical behaviour of the chalk. This technique is considered appropriate for the fractured chalk where weak planes cannot be precisely located (Griffths, 1980 and Griffiths and Lane, 1999). The equivalent continuum model accounting for anisotropy is implemented and a flow chart describing the procedure is provided (Figure 2.1).

General failure at the level of the intact chalk is initially checked, and relevant plastic corrections are applied when failure is detected. The corrected stresses are then analysed for failure on different joint sets. A new yield function based on simulating the oriented stresses is developed for each joint set and denoted as the oriented yield criterion. Then, based on the theory of multi-mechanisms for plastic strains (Koiter, 1953), and using a combination of plastic indicators, plastic corrections are applied to the stresses so that they do not surpass the superposition of yield envelopes.

2.2.2 Formulation

The mechanism for each joint set or weak plane, considered as an individual source of plasticity, is defined by a loading surface f_i, and a plastic potential g_i where $\overrightarrow{\sigma_n}$ is the corresponding acting stress vector defined on a plane with a normal $\overrightarrow{n_i}$. The tangential component of the vector $\overrightarrow{\sigma_n}$ is denoted by τ.

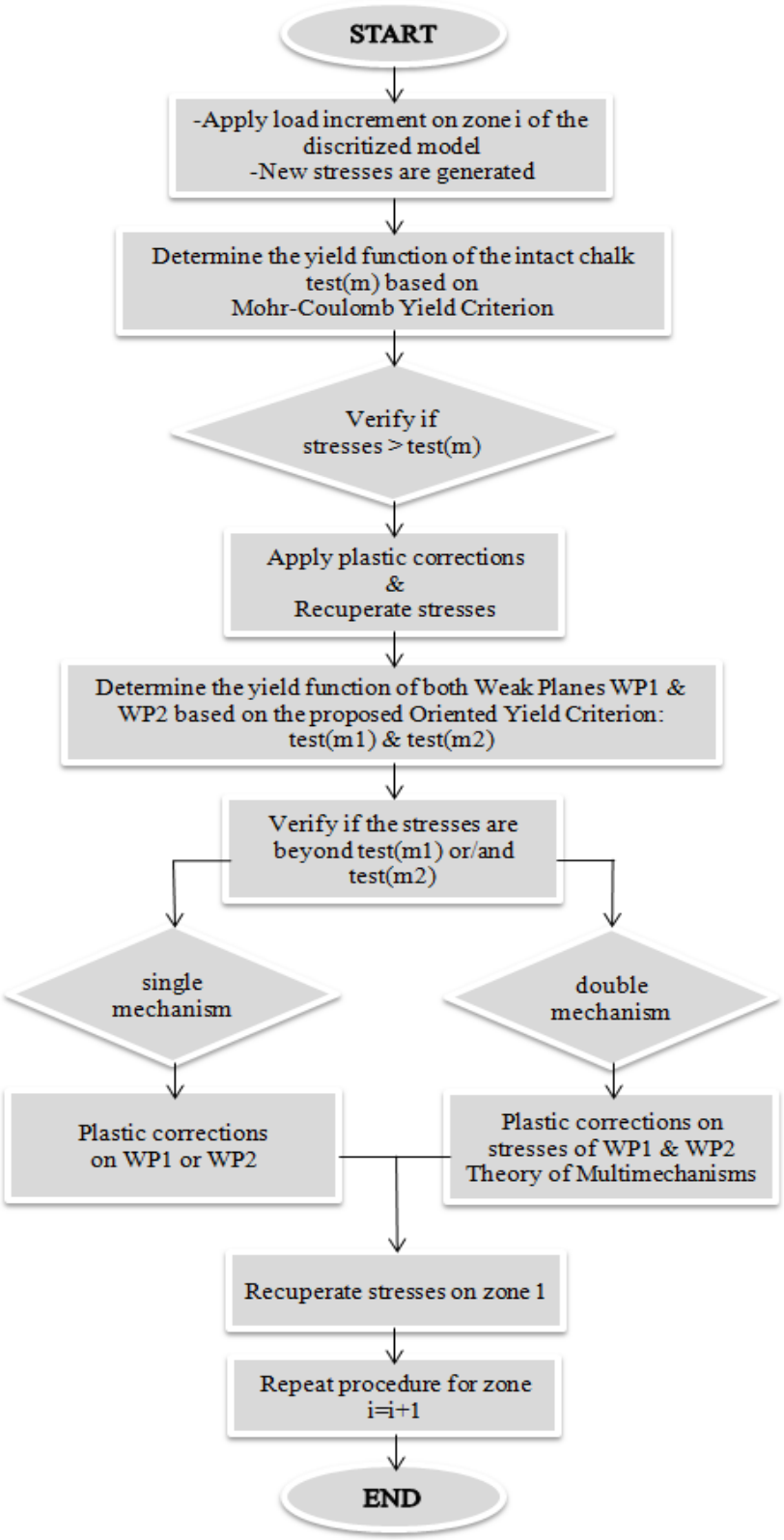

Figure 2.1. Flow Chart representing the numerical approach of the constitutive law with two embedded joint sets.

The notion of activation of one or more mechanisms takes the place of the notion of plastic loading in the classical plastic theory:

$$f_i\left(\overrightarrow{\sigma_n}\right) > 0 \qquad [2.1]$$

In our case of study, geological investigations showed that the chalk continuum is embedded by two symmetric joint sets. Hence, two weak planes are defined such that the joint set is illustrated by a weak plane in each zone of the model in an identical manner (Figure 2.3). Therefore, three yield criteria corresponding to the matrix which represents the intact chalk and each of the two weak planes are defined to control the plastic behaviour of the jointed chalk continuum. It is assumed that the plastic behaviour of the intact chalk acts upon a Mohr-Coulomb criterion. However, for the weak planes, the oriented yield criterion is assigned. This latter defines both, yield and potential functions, based on oriented stresses which are recuperated according to the orientation vectors of each of the weak planes $\overrightarrow{n_1}$ and $\overrightarrow{n_2}$. Since two weak planes are defined, then two corresponding mechanisms of plastic deformation are considered and thus two failure surfaces f_1 and f_2, potential functions g_1 and g_2, and plastic indicators λ_1 and λ_2 are associated for the two weak planes respectively. Knowing that $\overline{d\sigma}$ is the plastic stress correction and $\overline{\sigma_f}$ is the trial stress tensor (i.e., the stress tensor which surpasses the yield stress), the following equations are integrated:

$$f_i\left(\overline{\sigma_f}\right) = \tau - \left(\overrightarrow{\sigma_n}.\overrightarrow{n_i}\right)\tan\left(\varphi_i\right) - c_i \qquad [2.2]$$

$$f_1\left(\overline{\sigma_f} - \overline{d\sigma}\right) = 0 \Rightarrow f_1\left(\overline{\sigma_f}\right) - \frac{\overline{\partial f_1}}{\partial\sigma}.\overline{d\sigma} = 0 \qquad [2.3]$$

$$f_2\left(\overline{\sigma_f} - \overline{d\sigma}\right) = 0 \Rightarrow f_2\left(\overline{\sigma_f}\right) - \frac{\overline{\partial f_2}}{\partial\sigma}.\overline{d\sigma} = 0 \qquad [2.4]$$

Then, based on the theory used in this framework for elastic- plastic materials with singular yield surface (Koiter, 1953) and the general theories for elastic-plastic solids (Koiter, 1960), the theory

of multi mechanisms is used where the plastic strain increment $d\varepsilon_p$ is estimated to n sources of plasticity knowing that $\overline{\overline{C}}$ is the stiffness tensor.

$$d\varepsilon^p = \lambda_1.\overline{\frac{\partial g_1}{\partial \sigma}} + \lambda_2.\overline{\frac{\partial g_2}{\partial \sigma}} \qquad [2.5]$$

$$\overline{d\sigma} = \overline{\overline{C}}\left(\lambda_1.\overline{\frac{\partial g_1}{\partial \sigma}} + \lambda_2.\overline{\frac{\partial g_2}{\partial \sigma}}\right) \qquad [2.6]$$

Substituting in Eq. [2.5] and Eq. [2.6] where $\overline{\overline{C}}$ is the stiffness tensor, we get:

$$\lambda_1\overline{\frac{\partial f_1}{\partial \sigma}}\overline{\overline{C}}\overline{\frac{\partial g_1}{\partial \sigma}} + \lambda_2\overline{\frac{\partial f_1}{\partial \sigma}}\overline{\overline{C}}\overline{\frac{\partial g_2}{\partial \sigma}} = f_1\left(\overline{\sigma_f}\right) \qquad [2.7]$$

$$\lambda_1\overline{\frac{\partial f_2}{\partial \sigma}}\overline{\overline{C}}\overline{\frac{\partial g_1}{\partial \sigma}} + \lambda_2\overline{\frac{\partial f_2}{\partial \sigma}}\overline{\overline{C}}\overline{\frac{\partial g_2}{\partial \sigma}} = f_2\left(\overline{\sigma_f}\right) \qquad [2.8]$$

Let $[A] = \{a_{ij}\}_{2*2}$ be the matrix, defined component wise, as follows:

$$a_{ij} = \overline{\frac{\partial f_i}{\partial \sigma}}\overline{\overline{C}}\overline{\frac{\partial g_i}{\partial \sigma}} \qquad [2.9]$$

According to Eq. [2.7], Eq. [2.8] and Eq. [2.9]

$$\begin{pmatrix} a_{11} & a_{12} \\ a_{21} & a_{22} \end{pmatrix}\begin{pmatrix} \lambda_1 \\ \lambda_2 \end{pmatrix} = \begin{pmatrix} f_1\left(\overline{\sigma_f}\right) \\ f_2\left(\overline{\sigma_f}\right) \end{pmatrix} \qquad [2.10]$$

The plastic multipliers are then calculated:

$$\begin{pmatrix} \lambda_1 \\ \lambda_2 \end{pmatrix} = \frac{1}{\det A}\begin{pmatrix} a_{22} & -a_{12} \\ -a_{21} & a_{11} \end{pmatrix}\begin{pmatrix} f_1\left(\overline{\sigma_f}\right) \\ f_2\left(\overline{\sigma_f}\right) \end{pmatrix} \qquad [2.11]$$

If det(A) = 0, then in this case the solution proposed is as follows:

$$\begin{pmatrix}\lambda_1\\ \lambda_2\end{pmatrix}=\frac{1}{2}\begin{pmatrix}f_1\left(\overline{\sigma_f}\right)/a_{11}\\ f_2\left(\overline{\sigma_f}\right)/a_{22}\end{pmatrix} \quad [2.12]$$

Finally, depending on the obtained values of the plastic multipliers, plastic corrections are applied for the trial stresses on the chalk continuum.

2.2.3 Triaxial tests

In order to study the response of the proposed model, numerical tests are conducted on a homogeneous cubic chalk sample using the explicit finite difference code FLAC^{3D} (Itasca 2009) where the constitutive law presented above is implemented and integrated in this analysis. Boundary conditions are defined such that prescribed confining stresses are assigned on either sides and additional vertical displacements are applied for the top boundary. Base of the model is restrained and no displacements are allowed. The load definition and test conditions are similar to the triaxial test conditions with an initial confining stress equal to 1MPa. The material domain is discretized into a multiple zoned grid fitting the object being modelled. In order to increase the accuracy of this investigation, a refined mesh is used for all the simulations run for this study (Figure 2.2).

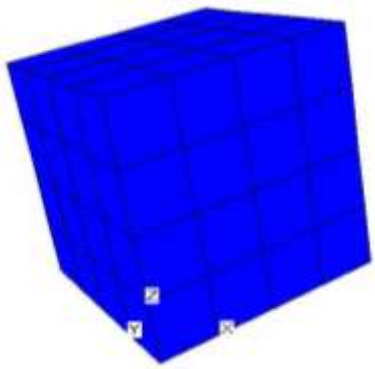

Figure 2.2. Geometry of the modelled chalk specimen

Likewise, elastic and plastic properties are assigned to every element, knowing that the joints are defined by similar shear strength properties which are weaker than those of the intact chalk (see

Table 2.1). An elastic model with perfectly plastic Mohr Coulomb criterion and non-associated flow rules is assigned to all zones of the model, whereas an oriented yield criterion is assigned for the joints. A sketch showing the weak planes in either single or double mechanism is provided (Figure 2.3).

Table 2.1. Mechanical properties of chalk including matrix and joints

		Young modulus (MPa)	Poisson ratio	Cohesion (kPa)	Friction angle (°)	Dilation angle (°)
Chalk	**matrix**	250	0.3	200	30	5
	joints			20	30	5

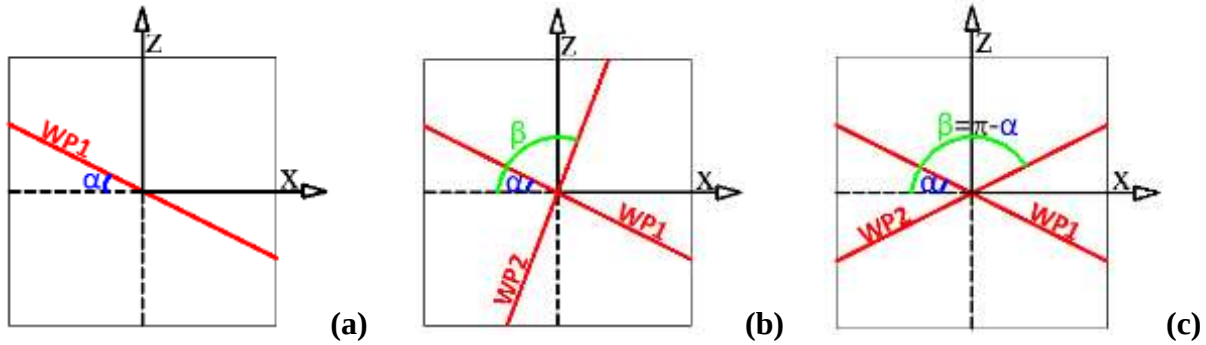

Figure 2.3. Sketch showing a vertical section of a zone of the chalk continuum with joints. (a) single joint set, (b) double joint sets, (c) symmetric joint sets.

2.3 Comparison between the proposed joint model and another existing joint model

To show its applicability, another set of triaxial tests is carried out using the ubiquitous joint model built in FLAC^{3D} which is able to account for the presence of a single weak plane of specific orientation embedded in a Mohr-Coulomb matrix (Itasca, 2009). A comparison between the obtained results is demonstrated.

But before presenting these results corresponding to the existing ubiquitous joint model, and our developed joint model, we would like to provide a brief analysis on the behaviour of rock masses

assigned with the ubiquitous joint models. This aims to give an idea about the model selected for the coming comparison and hence to make this latter more reasonable.

2.3.1 Ubiquitous joint model

A set of triaxial tests are modelled separately on rock specimens with same triaxial conditions, geometric characteristics, and mechanical properties (except for the cohesion; since in this analysis there is no need to restrict to the chalk properties and the aim is to present the effect of the joint in the continuum, so the cohesion of the chalk matrix and the joint is taken as 100 kPa and 0 kPa respectively).

2.3.1.1 Mesh refinement

The principle of ubiquitous joint model which is based on a Mohr Coulomb Model, is defining one and only one weak embedded in the studied body. Having a refined mesh of the solid mass under study will lead to the creation of multi zones. Hence, it is required to assign the properties of the ubiquitous model to every zone of this rock mass. So automatically, the single weak plane will be defined in each zone of the mesh of the rock mass. Normally, testing the same material under same properties and conditions but with a refined mesh does not affect the behaviour of the material except probably at the level of accuracy. To validate this hypothesis, the same test was applied on 2 different mesh refinements of the rock mass, 1 zone and 64 zones. The table below (Table 2.2.) shows a comparison at the level of resistance and deformability of rock mass modelled using Ubiquitous-Joint Model in 2 different manners. First, the whole specimen was defined as 1 zone and the other manner was achieved by refining the mesh into 64 zones.

Table 2.2. Stresses and strains values

Mesh	Stress (MPa)			Strain (m/m)			Shear	Volumetric
	SXX	SYY	SZZ	XX	YY	ZZ	Strain (m)	Strain (m)
1	-1.00	-1.00	-3.35	8.41E-02	8.41E-02	-1.50E-01	1.35E-01	1.82E-02
64	-1.00	-1.00	-3.35	8.37E-02	8.45E-02	-1.50E-01	1.38E-01	1.82E-02

Axial strain versus axial stress and volumetric strain versus deviatoric stress are plotted in the cases of a one-zone mesh and a refined mesh with 64 zones for a ubiquitous-joint model (Figures

2.4 and 2.5). The representation of the weak plane in ubiquitous-joint model is not geometric by creating a discontinuity in the solid mass. The weak plane as defined by this model is presented at the level of strength and behaviour of the material. Identical values of stresses and strains obtained from 2 different tests in terms of the mesh refinement assure this hypothesis.

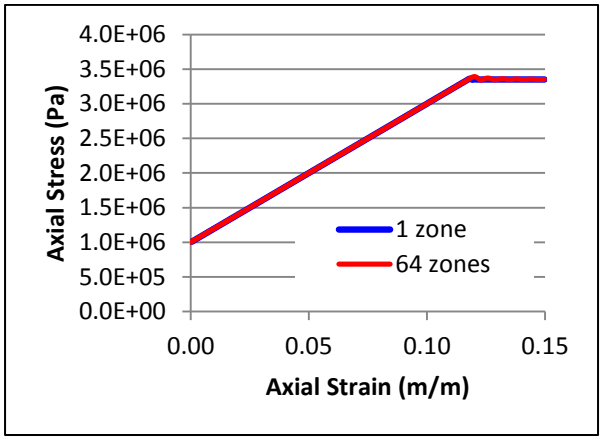

Figure 2.4. Axial Stress vs. Axial Strain

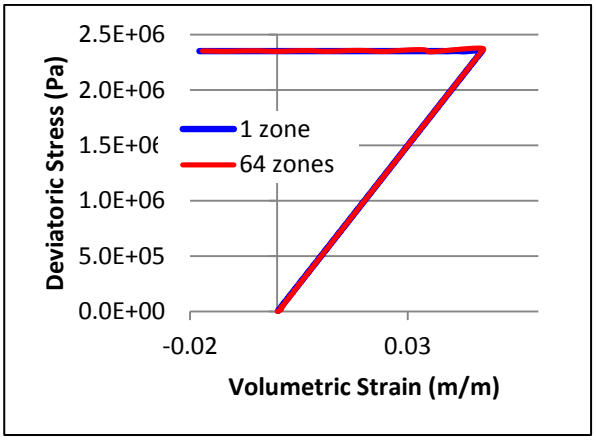

Figure 2.5. Deviatoric Stress vs. Volumetric Strain

2.3.1.2 Joint orientation: Joint dip direction (jdd) and joint dip angle (jdip)

The ubiquitous joint model defines the orientation of the weak plane by two angles: dip direction (jdd) and dip angle (jdip). A sketch is offered to clarify these notations (Figure 2.6).

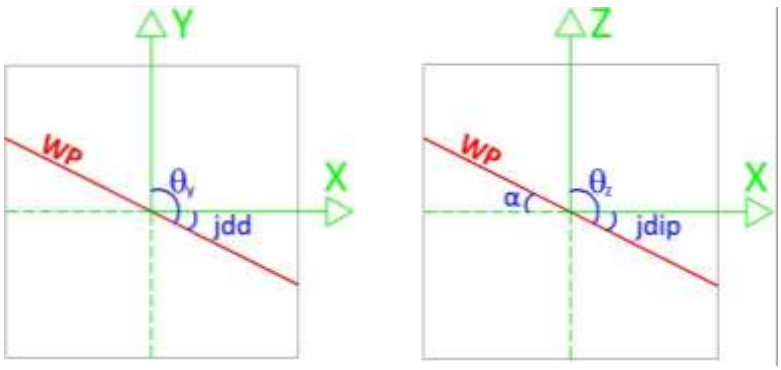

Figure 2.6. Sketch showing the dip direction (jdd) and the dip angle (jdip).

Simulations on the specimen undergoing triaxial test with vertical loading imposed in the z-axis direction show that when the weak plane is oriented in the same direction like that of the load, it will have no effect on the strength of the rock mass. In our case, the external load or velocity is

applied vertically downwards, so no matter how the weak plane is positioned or even rotated but kept in the vertical plane, this will induce no effect on the strength of the rock mass and it will stay identical to that in the case of rock mass without any joints. This is illustrated in the figure below (Figure 2.7).

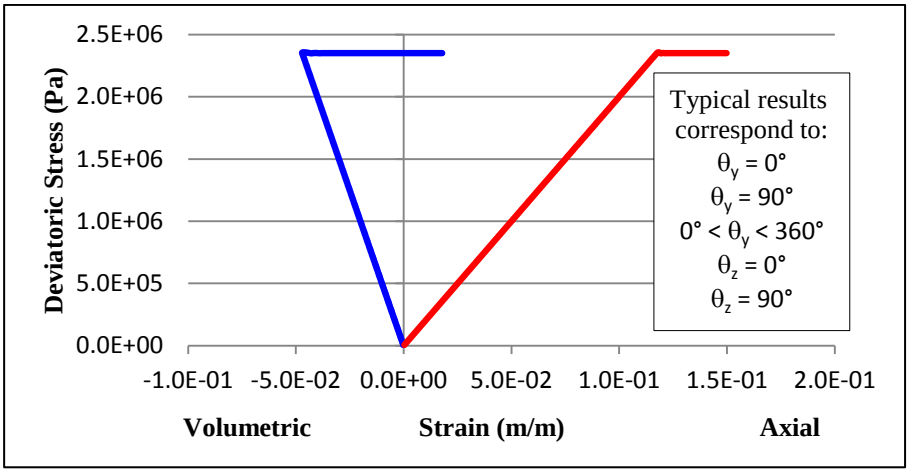

Figure 2.7. Volumetric Strain and Axial Strain vs. Deviatoric Stress for different jdd and jdip.

Similar results are observed when the weak plane is perpendicular to the load orientation; i.e. the weak plane is horizontal. The presence of a weak plane in a rock mass of weak strength properties with respect to those of the rock mass itself have no effect at all when this weak plane is located always parallel or perpendicular to the load direction where the specimen is uniformly confined at the lateral faces. This can be justified by the fact that under uniform geometric and confinement conditions, these cases of joint orientations will not induce any non-homogeneity in the material behaviour. However, this is not the case when the weak plane is inclined from the direction of the applied load (Figure 2.8).

A weak plane which is not parallel to the direction of the load applied on the specimen, meaning that the dip angle of the joint is varying, will have a remarkable effect in terms of the diminution of the ultimate resistance of this specimen. In this case of triaxial tests, the presence of a vertical weak plane located perpendicular to the x-y plane or a horizontal weak plane located parallel to the x-y plane has no effect on the strength of the rock mass. Otherwise, a weak plane of a non-0° and non-90° dip angle leads to decreasing the resistance of the rock mass. The change of the inclination of the weak plane from the vertical plane towards the horizontal plane, affects the behaviour of the rock in a random manner (Figure 2.9).

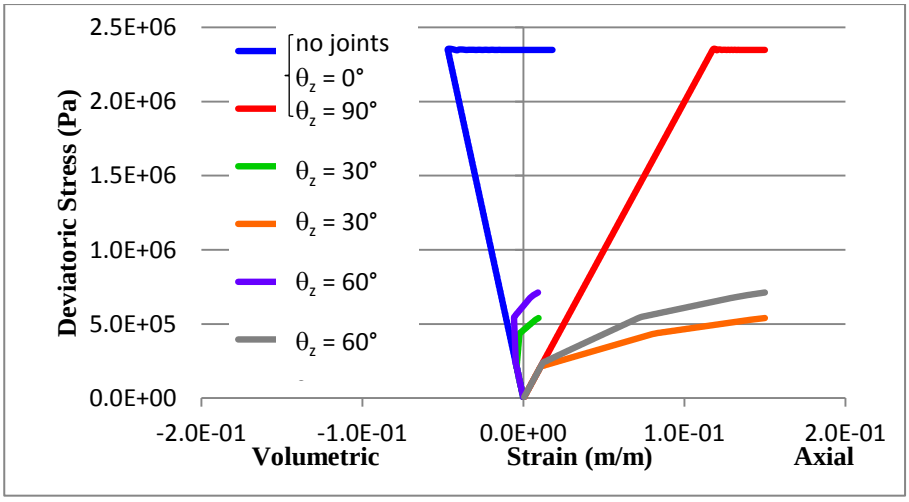

Figure 2.8. Volumetric Strain and Axial Strain vs. Deviatoric Stress at different dip angles or θ_z.

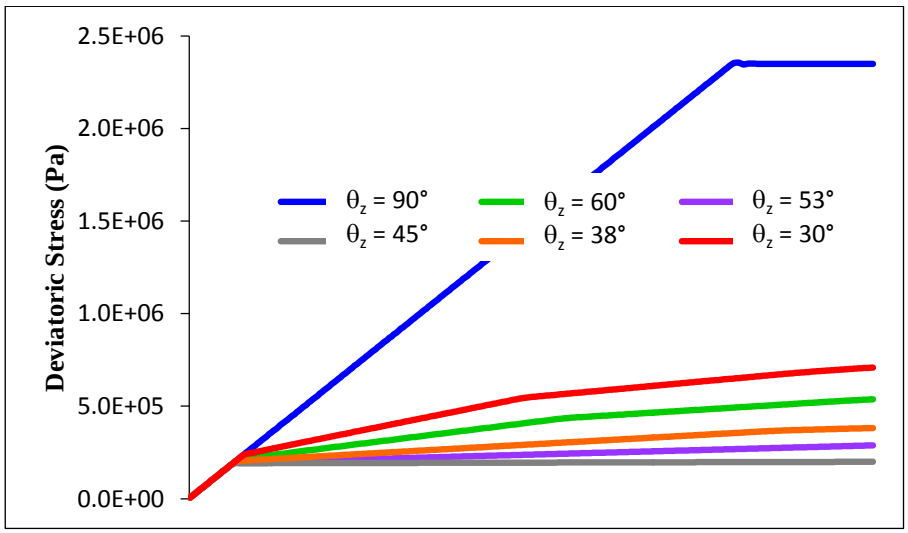

Figure 2.9. Variation of ultimate resistance with the variation of the weak plane inclination θ_z.

The time steps represent the increment of the applied load adjusted in the numerical simulations. In our case, the load is a velocity added in vertical downwards direction at the top face of the specimen. At each time step, an increment of the velocity is added. The graphs of the evolution of the deviatoric stress at different time steps are shown for four different inclinations of the weak plane θ_z (Figure 2.10). This shows the evolution of the deviatoric stresses and how it is affected by the joint orientation. It is clear again that horizontal and vertical weak planes, unlike inclined weak planes, induce no effect on the resistance.

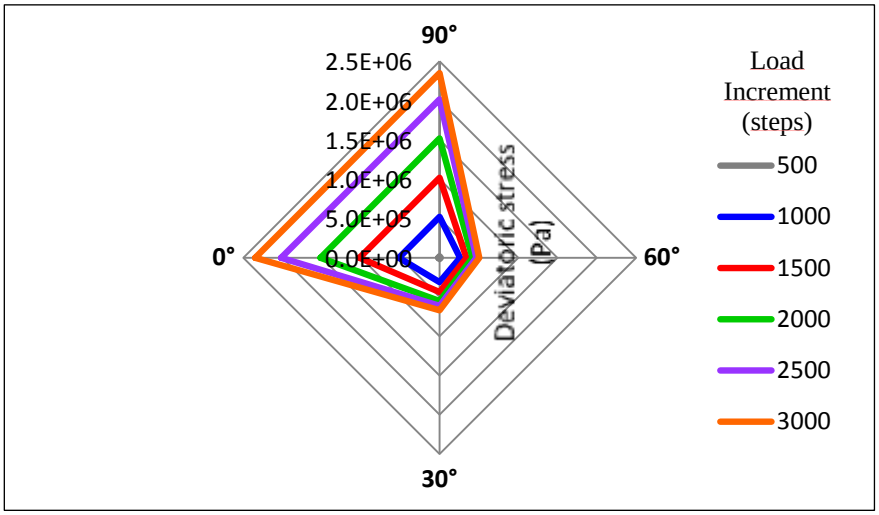

Figure 2.10. Evolution of deviatoric stress at different inclinations of weak plane θ_z.

2.3.1.3 Influence of the strength properties of the weak plane

First, a procedure of decreasing the cohesion of the weak plane by a percentage of the cohesion of the rock mass is maintained (Figure 2.11).

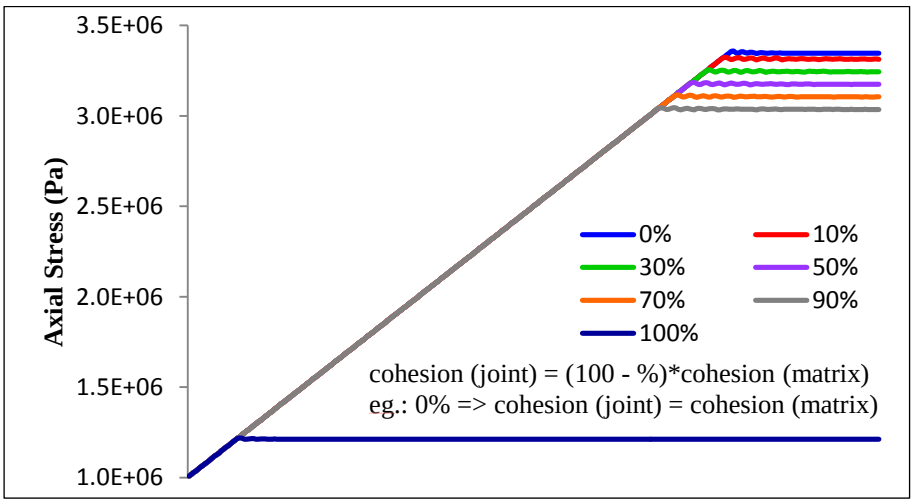

Figure 2.11. Variation of the axial stress with the variation of the weak plane cohesion.

The evolution of axial stresses is plotted at different cohesion cases to illustrate the effect of weakening the cohesion of the weak plane embedded in the rock mass, on the overall behaviour of the rock mass (Figure 2.11). The axial resistance of the rock mass subjected to axial load decreases gradually with the decrease of cohesion of the weak plane. Next, a procedure of

decreasing the friction of the weak plane by 5 degrees at each simulation from the value of the matrix friction is proposed. The axial resistance of the rock mass subjected to axial load decreases gradually with the decrease of friction of the weak plane (Figure 2.12).

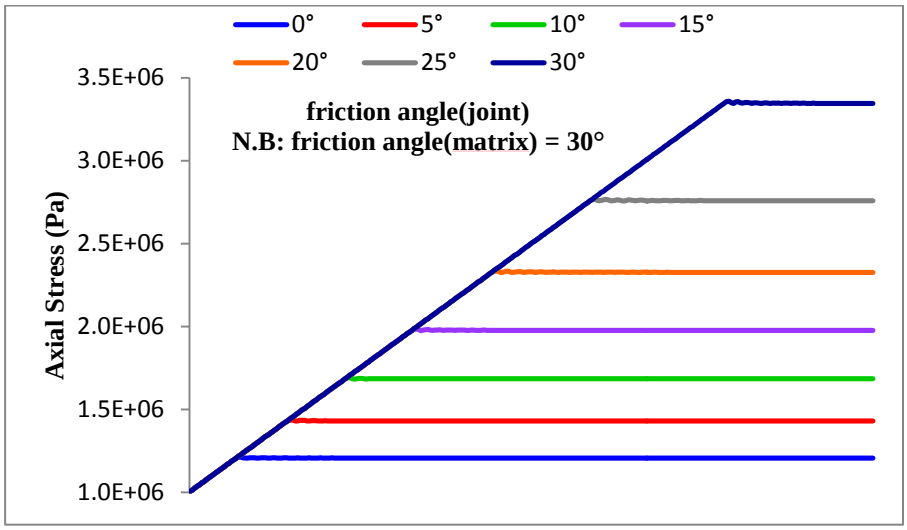

Figure 2.12. Variation of the axial stress with the variation of the weak plane friction.

2.4 Comparison between existing and developed joint models

2.4.1 Ultimate resistance

The Mohr-Coulomb criterion has been successfully used to simulate the failure of rock samples under uniaxial and triaxial compression (Fang and Harrison, 2002). In order to show the effect of joints in the chalk continuum adjusted by assigning the behaviour of the proposed jointed model, corresponding results are compared with those of a triaxial test of a Mohr-Coulomb criterion. Growth of axial deformation with respect to the increase of axial stress is plotted (Figure 2.13).The maximum strength of a non-fractured model where no weak planes with reduced strength properties are defined is greater than that of a model with joints. Besides, the elastic deformation in a non-jointed model lasts more, whereas plastic deformation initiates earlier and at lower stresses in the jointed model.

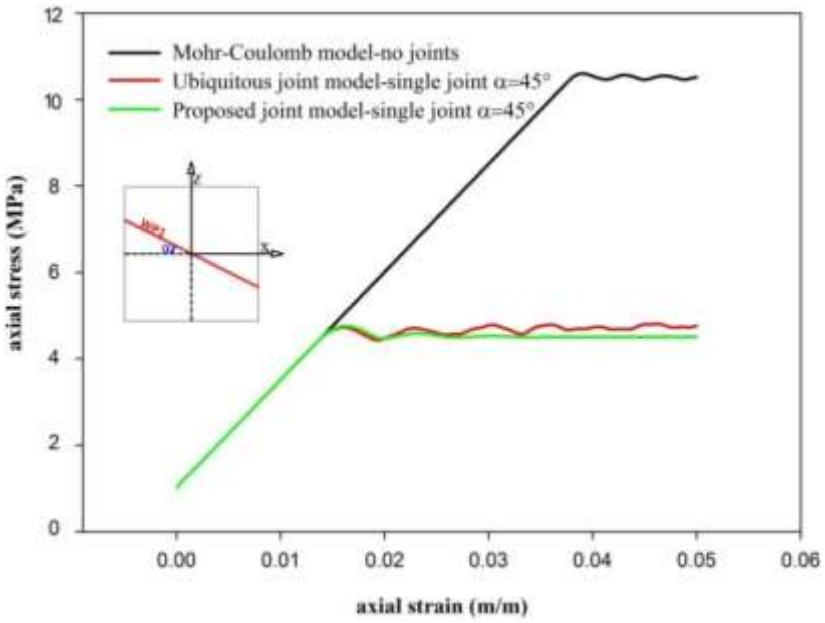

Figure 2.13. Stress-strain graphs for triaxial test of chalk continuum with different constitutive models.

2.4.2 Influence of the joint set orientation

The variation of the ultimate resistance with respect to the joint set orientation is illustrated in both cases (Figure 2.14). Consistent results show that the approach employed in the implementation of the proposed model is fitting. In the analysis of the triaxial tests outcome, where load is being applied vertically, the ultimate strength is maximal when the weak plane is embedded vertically, i.e. parallel to loading direction, or horizontally, i.e. perpendicular to the loading direction. Based on previous simulations performed on the chalk rock mass without any joints, the ultimate strength was found to be identical to that in case of single horizontal or vertical joint, which is proved to be at maximum. This shows that the effect of weak plane embedded in the chalk in direction parallel or perpendicular to the loading direction is negligible. Theoretically, for this example joints with inclination angle of 0° or 90° have no influence on the strength of the sample. Under triaxial conditions, results also show that a weak plane with inclination α where $0° < \alpha < \varphi+5 = 35°$ has negligible influence on the global resistance of the chalk continuum (Figure 2.14). Whereas, when $\alpha = 60°$, the weak plane has the greatest weakening effect on the specimen resistance. The most critical weak plane depending on the

most critical inclination angle is related to the fiction angle of the chalk continuum. This is explained more in a separate paragraph.

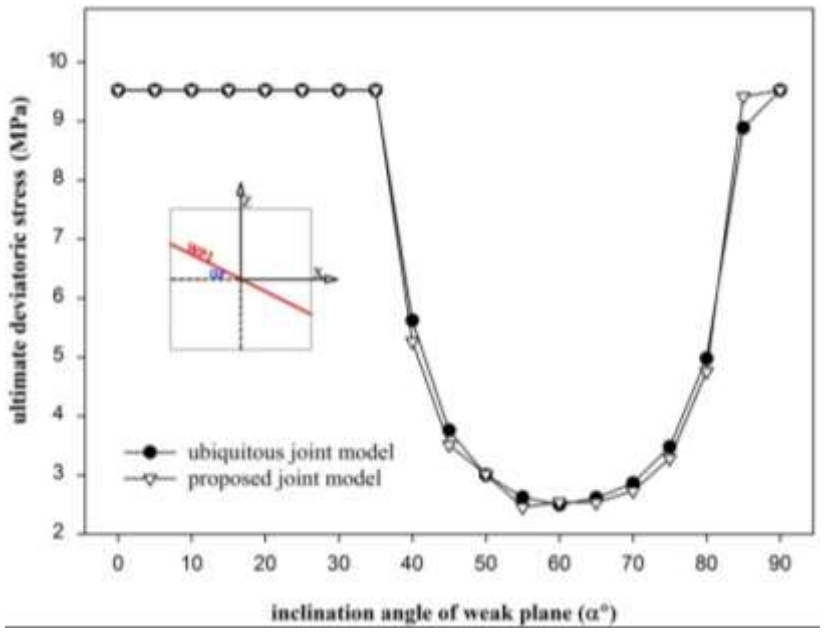

Figure 2.14. Comparison of the strength of the chalk examined by existing ubiquitous joint model [10] and the proposed jointed model.

2.5 Results for chalk with the proposed joint model - Case 1: single joint set

2.5.1 Joint orientation

2.5.1.1 Ultimate resistance

Stress-strain graphs from triaxial tests for chalk models with single joint sets of different orientations are presented (Figure 2.15). This illustrates the effect of the joints behaviour on the strength of the chalk model. Note that stress-strain graphs in both figures 5 and 6 do not pass by the origin. The initial value of the axial stress corresponds to the confining pressure which was taken equal to 1 MPa. Only the part of the axial strain due to the deviatoric stress is represented.

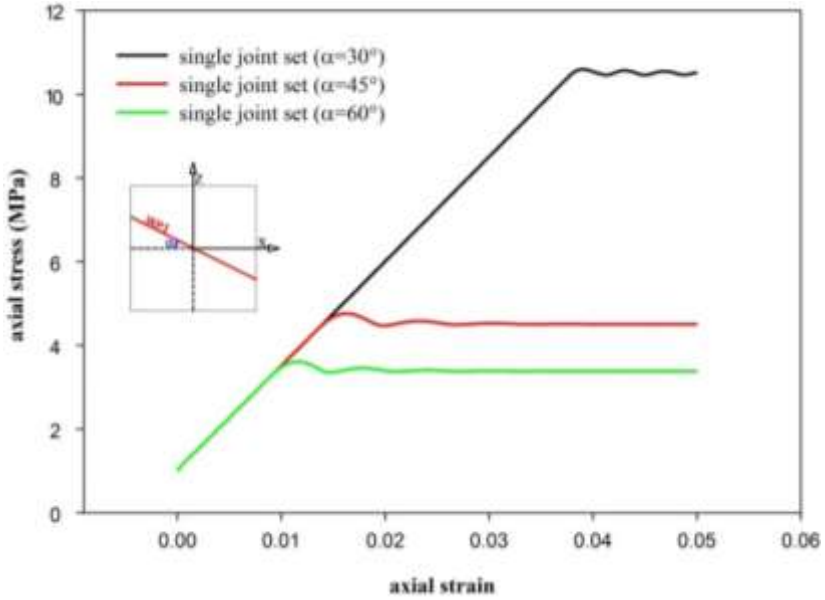

Figure 2.15. Stress-strain graphs for triaxial test of chalk continuum with proposed yield criterion at different joint set inclinations

2.5.1.2 Displacement distribution

In order to confirm the influence of joints orientation on the distribution of displacement in a jointed continuum, new simulations are performed considering horizontal, vertical joints orientations, and inclined joints. The sample is firstly confined with vertical displacements fixed at the base. A concentrated load is applied at the centre of the top surface of the chalk sample to provide a better emphasis of the displacement distribution (Figure 2.16).

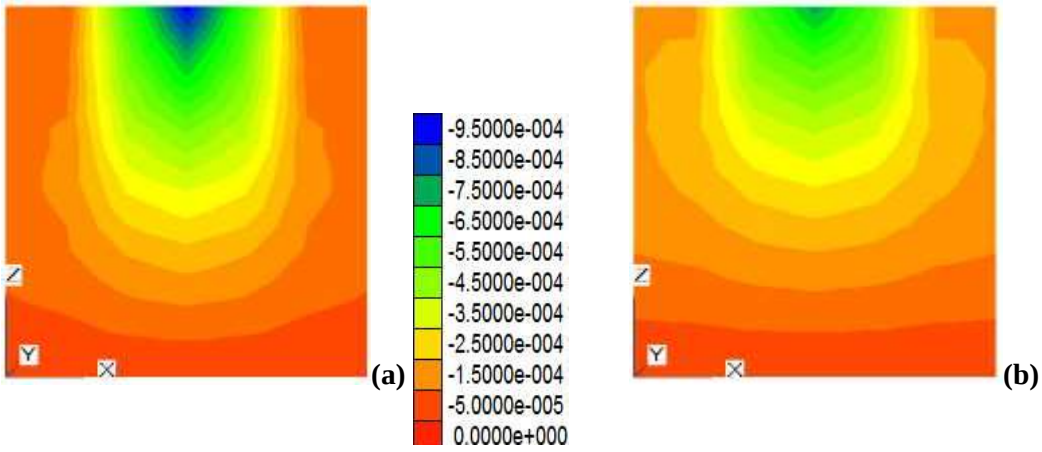

(a) **(b)**

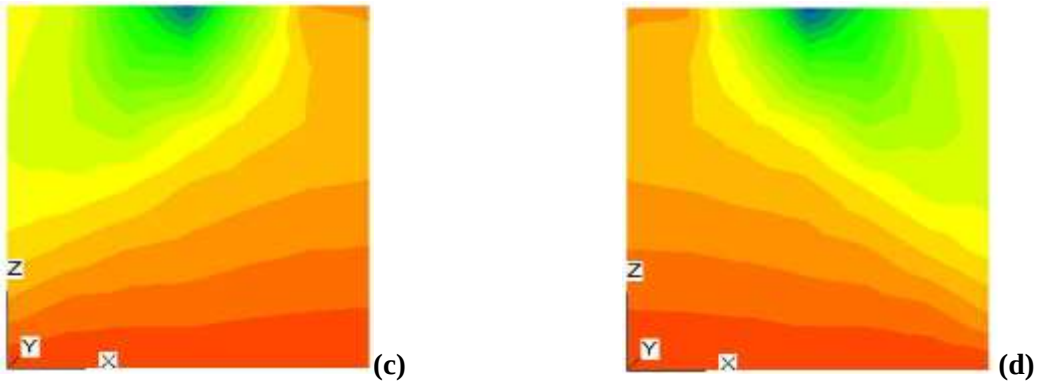

(c) **(d)**

Figure 2.16. Displacement distribution with joints inclined at **(a)** θ_z = 0° (vertical joint set) **(b)** θ_z = 90° (horizontal joint set) **(c)** θ_z = 120° **(d)** θ_z = 150°.

Vertical weak planes allow the displacement to spread vertically downwards. Whereas, presence of horizontal joints decreases the intensity of the displacement spread vertically downwards. The displacement in this case is being dissipated horizontally and stacked in the horizontal layers created by the horizontal joints. Consequently, in the case of vertical joints, displacements which are initially concentrated at the point of application of the load are then distributed vertically downwards. However, in the case of horizontal joints, the displacement resulted at the point of application of the load are directly distributed horizontally and partially stacked within the first layer (Figure 2.16). That's why; in case of horizontal joints, displacements at the centre are lower whereas at the extremities they are higher than those observed in the case of vertical joints. These results confirm similar works done in this domain. And this compatibility is also shown in the case where joints are inclined at 30° and 60° or 120° and 150° (Agharazi and Martin, 2011).

2.5.2 Relation between friction angle and the strength

In order to account for the effect of the friction angle of both the intact chalk as well as the joint sets on the strength of the chalk continuum, several triaxial tests of samples with different fiction angles are carried out. Plots of the ultimate stress corresponding to these tests with single joint sets inclined from 0° to 90° showed the effect of the friction angle on the continuum strength which is also dependent on the joint inclination (Figure 2.17).

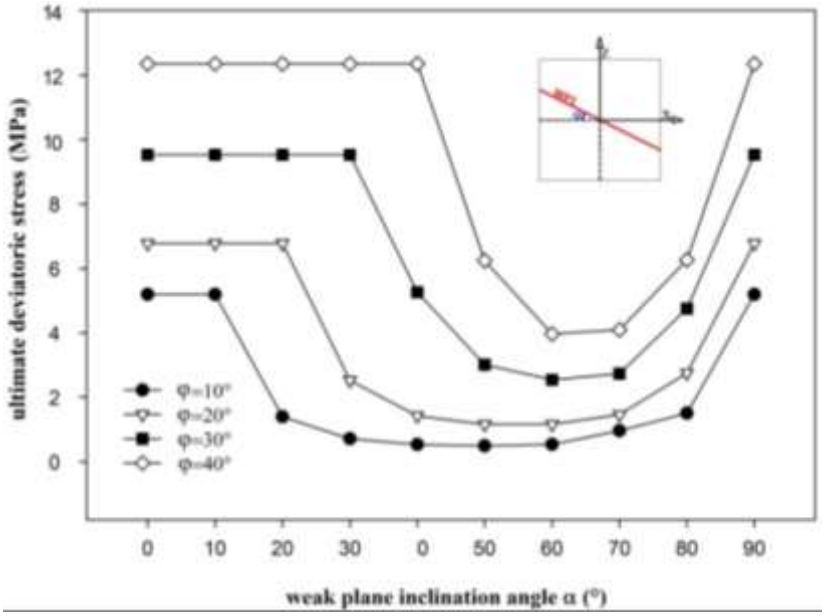

Figure 2.17. Variation of deviatoric stress with respect to joint set inclination at different joint friction angles.

The concept is to identify the joint that will have the most influence on the strength of the sample in each case of friction angle. Results show that for each case of friction angle φ, the lowest resistance is detected in the case of weak plane inclined at angle $\alpha = \pi/4 + \varphi/2$ (Figure 2.17). For example, lowest stress values for φ = 10°, 20°, 30°, 40°, and 50° correspond to weak plane inclined at approximately α = 50°, 55°, 60°, 65°, and 70° respectively. These values almost satisfy the previous hypothesis which matches with the specifications of a Mohr-Coulomb failure criterion.

2.6 Results for chalk with the proposed joint model - Case 2: two joint sets

Triaxial tests of chalk samples behaving according to the proposed model with double mechanism are carried out. Results in terms of strength, deformability, and displacement with respect to different inclinations of the weak planes are demonstrated.

2.6.1 Ultimate resistance

Knowing that the first weak plane is fixed with an inclination angle α, and the second weak plane has a varying inclination angle β, three cases with three different values of α are examined (Figure 2.3). The variations of the deviatoric stress at different inclinations of the weak planes are plotted (Figure 2.18).

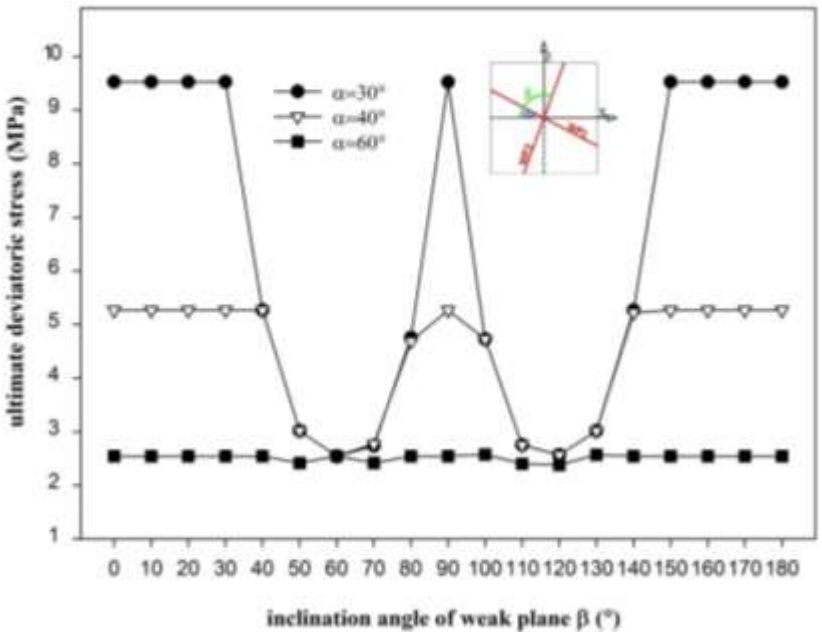

Figure 2.18. Variation of the deviatoric stress with the inclination of the weak planes.

It is shown that the strength of the chalk rock mass significantly varies with the inclination of the weak planes and thus the model exhibits anisotropy. It is worth noting the following outcomes:

- For $\alpha = 60^{\circ}$ (equal to $\pi/4+\varphi/2$), whatever the value of β is, at least one weak plane will have the greatest strength reducing effect on the specimen. This influence will dominate the resistance behaviour of the material and reduce it to the minimal.

- For $\alpha \neq 60^{\circ}$, maximum strength of the jointed model is achieved when:

- The weak planes are identical, i.e. $\alpha = \beta$
- The weak planes are symmetric, i.e. $\beta = \pi - \alpha$
- The second weak plane is parallel to loading direction (vertical), i.e $\beta = 90^{\circ}$ or $\beta = 270^{\circ}$
- The second weak plane is perpendicular to loading direction (horizontal), i.e $\beta = 0^{\circ}$ or $\beta = 180^{\circ}$

- The second weak plane is inclined with an angle between 0˚ and φ /2+5˚ = 35˚, i.e 0˚< β <35˚

2.6.2 Deformational behaviour

To study the deformational behaviour of the chalk specimen, variation of the volumetric strain with respect to the axial strain is plotted (Figure 2.19). Dilation of chalk in the plastic regime corresponding to the spread of irreversible strains is not the same in all cases where symmetric weak planes (β = π–α) are considered. This difference shows that the deformation of the chalk rock mass is also anisotropic (Wang, 2002, and Wang and Huang, 2009).

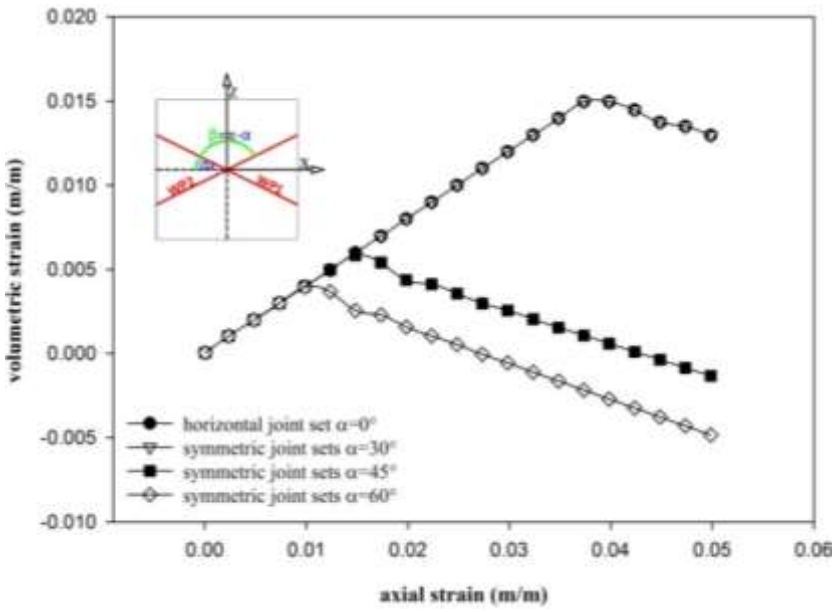

Figure 2.19. Variation of the volumetric strain with respect to the variation of inclination angle α of the symmetric weak planes.

In the case of α = 60˚, which represents the case of weak planes with highest influence, the dilative behaviour relevant to the plastic deformation is initiated the fastest, before that in the case of α = 45˚, and that in the case of α = 30˚ which represents the case of weak planes with least or negligible influence. At this value of the axial strain, the specimen with weak planes at α = 45˚ or α = 30˚ is still contracting in an elastic medium.

2.6.3 Displacement distribution

As shown in the previous results, chalk having a single weak plane with inclination α, will behave identically at the level of strength, as the chalk having two symmetric weak planes with same inclination angle α. However, with symmetric joints, the anisotropy is further exhibited at the level of displacement (Figure 2.20).

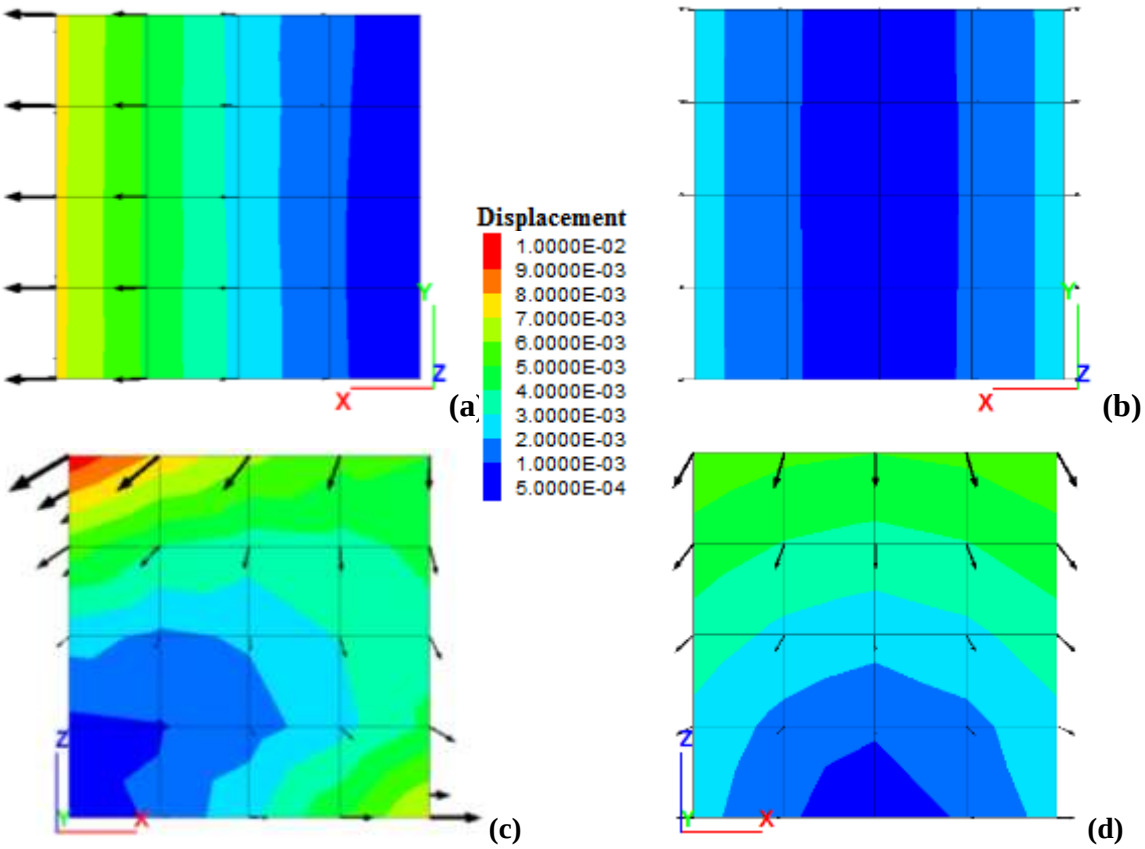

Figure 2.20. Displacement distribution about z-axis (a and b) or y-axis (c and d) of models with single joint (a and c) or models with two symmetric joints (b and d).

The figures plotted demonstrate the displacement distribution in the chalk specimen with single weak plane of $\alpha = 60^{\circ}$ and with double symmetric weak planes with $\alpha = 60^{\circ}$ and $\beta = \pi - \alpha$. The displacement distribution in y-plane and the displacement distribution in the z-plane in each of the two cases are presented (Figure 2.20). The difference obtained shows that although in the case of symmetric weak planes, the ultimate strength and the volumetric deformation are similar

to that in the case of single weak plane, but the displacement behaviour is greatly different and significantly anisotropic.

2.7 Conclusions

According to geological investigations, double symmetric joint sets are identified in the chalk substratum of North France and its region where the underground quarries were excavated decades ago. Hence, it is quite important to study the effect of these joints on the resistance, stability and failure mechanisms of these quarries which are at the same time affected by various degradation factors. In fact, the stability study of chalk quarries has been always a concern for geological and geotechnical researchers (Smith and Rosenbaum, 1993, and Gu and Ozbay, 2015). However, considering certain complexities (Yang et al. 2014, and Suchowerska et al. 2015), in a global scale numerical modelling allows to obtain complementary information to lead a more precise and reliable analysis. In this chapter, a constitutive model that accounts for anisotropic behaviour induced due to the presence of embedded joints is developed based on the theory of multi-mechanisms. This model is assigned to the chalk behaviour and the strength resistance of the jointed continuum is then analysed. This model has been successfully tested in some simple configurations of stress path after being implemented in the numerical software FLAC^{3D}.

It is now possible to develop a numerical model of the underground cavities and study its performance after assigning the properties of the developed joint model to the chalk continuum. In the same framework, it will be evident to analyse the anisotropic mechanical behaviour of the quarries and compare the strength resistance and the deformational behaviour under different joint configurations. A stability analysis of the underground cavities in the presence of joints is conducted using the developed oriented criterion in the coming chapter.

CHAPTER THREE
3D NUMERICAL MODELLING OF STRAIN AND FAILURE MECHANISMS IN THE CHALK UNDERGROUND CAVITIES

3.1 Introduction

Urban expansion requires building new constructions and infrastructure in places where geological risks might be high. In North France and its region, the major risk comes out from the presence of shallow underground chalk quarries. Because of the high density of cavities and natural and anthropogenic degradation of chalk, the risk of instabilities and collapses is continuously increasing with time. This, in fact, implements a real danger on both people and constructions at one hand, and induces a strong constraint in terms of planning and urban development on the other hand as stated by Lille Municipality (Ville de Lille 2013). Consequently, it is always of major interest to urge the study on these underground cavities.

From a safety point of view, these cavities are not only required to avoid ultimate collapse, but also to satisfy limits of a displacement-based criterion. Hence, in order to control the expected circumstances, understanding of instabilities induced by these cavities is quite important. In this aim, observations and measurements of the cavity displacements are necessary to predict the eventual collapses. Nevertheless, numerical modelling of strain and failure mechanisms can provide a complementary approach to understand these phenomena.

Knowing that the chalk layers are originally embedded with joints and discontinuities (Ineris 2007), an anisotropic behaviour is induced. In order to account for the presence of the joints, an oriented yield criterion was developed in the previous chapter. The non-negligible anisotropic

effect induced was verified after being numerically tested on chalk samples. It is now possible to use the developed criterion to represent the anisotropic behaviour induced at the level of the cavity due to the presence of discontinuities. Anisotropy may affect the failure mechanisms and thus modify the stability state of underground openings and their surroundings and induce collapses. To account for this former, the developed joint model with oriented criterion detailed in the previous chapter is integrated in the numerical analysis of the quarry model. A stability study is then achieved in the presence of joints and fractures in the chalk continuum.

For this stability study, a technique based on the Shear Strength Reduction (SSR) approach that permits the calculation of factor of safety using different numerical procedures is used. Zienkiewicz et al. (1975) showed that the factor of safety could be established by assisting numerical models that apply the strength reduction scheme. Griffths and Lane (1999) extended this work over a wide range of soil properties and geometries and presented reliable results for slope stability. Shear strength reduction technique employed in different practices by numerical stability study (Chenga et al. 2006) was later improved to consider nonlinear failure criteria by Dawson et al. (2000). The effect of joints was also integrated in the computation of factor of safety (York et al. 2000, Hammah et al. 2005, and Helmut and Schweiger 2002) in order to provide more reliable tools to be encountered in stability engineering problems.

This chapter addresses the algorithm developed to compute a strength reduction factor based on the conventional shear strength reduction (SSR) method (Zienkiewicz et al. 1975) which is afterwards implemented in the numerical analysis of the underground excavation. Strain and failure mechanisms are simulated and the influence of joints on the ultimate resistance and deformational behaviour of the underground cavities is analysed.

3.2 Algorithm for the joints shear strength reduction approach: Implementation in FLAC^{3D}

In shallow excavations where confining pressures can be considered low, dominant failure is controlled by shear mechanism into joints. Thus, the stability state of the excavation is affected by the shear strength parameters of the joints. Consequently, based on the conventional shear strength reduction (SSR) method, an approach to calculate the reduction factor is implemented. Integrating the proposed joint model in the reduction analysis allows us to examine different

aspects knowing that it becomes possible to reduce the strength parameters of each of the matrix representing the intact chalk or/and the weak planes. In other words, yield may occur in either intact rock or the joint planes, or both, depending on the stress state, orientation of the joint planes and the material properties of the intact rock and joint planes. If the aim is to study the stability by computing a factor of safety, shear strength reduction must be applied to both, the matrix and the weak planes. Moreover, the study of the stability requires considering the resistance of the soil at the surface above the chalk overburden as well as the expansion coefficient of the chalk itself which control the upper progression of collapses to the surface However, in this work, we intend to show, the significant effect of the joints on the stability rather than the stability itself. Hence, reduction is limited to the shear properties of the joints. Given an identified tolerance, a reduction factor R_f is systematically incremented starting from a value equal to 1.0 such that strength properties c, cohesion of the weak plane(s), and φ, friction angle of the weak plane(s), are reduced. Different parameters can be assigned to each joint set. For simplicity, both joint sets are given same shear strength parameters and reduction is done to both in same manner where c* and φ* are the reduced shear strength properties of the joints:

$$c^* = \frac{1}{R_f}.c \qquad [3.1]$$

$$\varphi^* = \arctan\left(\frac{1}{R_f}.\tan\varphi\right) \qquad [3.2]$$

At every step, calculations are performed until the unbalanced forces and the displacement increments can be neglected. As shear strength parameters of the weak planes are progressively reduced, the corresponding yield surfaces shrink. This procedure is repeated until the model no more converges to a solution, meaning that instability occurs in the model and the excavation fails. The final reduction factor, denoted by FRF, is reached when the model converges to its highest limit. This factor reflects the stability state of the excavation limited to reducing shear strength properties of the joint sets.

The conventional shear strength reduction method which is built in FLAC can be only used in the stability studies of materials assigned with specific constitutive models like Mohr-Coulomb. However in our case, we need to apply this method on our defined oriented model. In other words, we aim to use the developed oriented criteria to account for the presence of joints. Then, we intend to study the effect of these joints on the stability and failure mechanisms of the cavity

under study. Therefore, in our numerical models, we firstly integrate the developed oriented yield criterion in the numerical software FLAC^{3D}. Next, we implement the developed shear strength reduction approach in this software so that we apply it afterwards on the defined joints and thus we attain the suggested stability analysis of the jointed chalk quarry.

3.3 Case of study: numerical modelling of a room-and-pillar jointed chalk quarry

The geometry of underground quarries depends on the diversity of exploitation methods used. The most frequent discovered in North France and its region, are known by holts-and-bottles and room-and-pillar. This latter represents the majority of the cases (Ineris, 2012, and Anteagroup and Ville de Lille, 2012), and is the concern in this study (Figure 3.1).

(a)

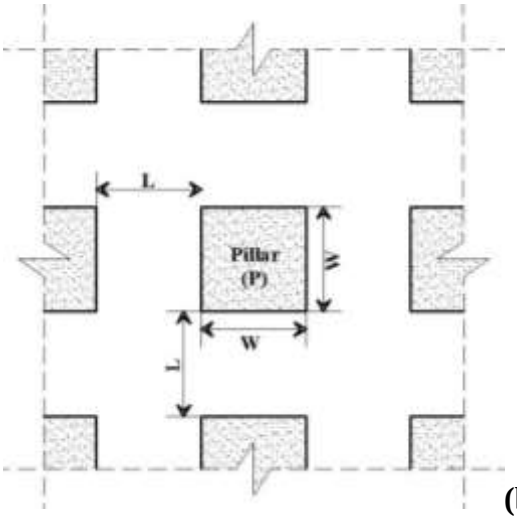

(b)

Figure 3.1. (a) Underground quarry in Hellemes- North France (Lille Municipality, 2013), (b) Top section of the room and pillar quarry

Consequently, dealing with cavities excavated by the method of rooms and pillars, a wide range of geometric parameters can be incorporated. Variation in dimensions of both pillar and roof is expected to produce a considerable influence on their deformability and strength. Nevertheless, the aim in this work is to focus merely on the effect of joints. Therefore, a particular case of geometry chosen from cases in North France (Ineris, 2012, and Anteagroup and Ville de Lille, 2012), is considered in the numerical modelling of the excavation which is detailed later. The pillar of jointed chalk is of width W=6m and height h=3m, the void room is of clear span L=6m, covered by H(chalk)=7m of jointed chalk at the roof and above them silt with H(silt)=3m (Figure 3.2). Ground properties are inspired from experiments carried out on chalk samples taken from the quarries excavated in North France and its region (Duwicquet and Hulo 1990, and Mikolajczak, 1996). A summary of these properties used in the numerical modelling is provided (Table 3.1).

Table 3.1. Mechanical properties of chalk including matrix and joints, and silt.

		Young modulus (MPa)	Poisson ratio	Cohesion (kPa)	Friction angle (°)	Dilation angle (°)
Chalk	**matrix**	250	0.3	200	30	5
	joints			20	30	5
Silt		10	0.3	10	30	5

The chalk continuum constitutes of intact chalk represented by the matrix and two symmetric embedded joint sets defined as weak planes (Ineris, 2012, and Anteagroup and Ville de Lille, 2012). Same elastic properties are defined to assess the stress state in the element including the matrix and the joints. The irreversible strains in the matrix and in the joint sets are simulated by considering several failure criteria in the framework. In our case, as the confining pressure is low and the stress varies in a small range due to the low depth of excavation, Mohr Coulomb criteria can be used to characterize the behaviour of the chalk. This assumption requires few parameters: two for the elastic domain (E, υ), and three (c_i, φ_i, ψ_i) for each yield function (one for the matrix and two for the joints). Normally, joints or weak planes where the sliding is localized are of shear strength properties lower than those of the matrix.

In order to account for the effect of anisotropy in the behaviour of the stressed chalk, the developed model based on an implicit technique for representing the embedded joints, is used. We recall that in our case, the position of the joints is not exactly known. They can develop everywhere according to stress state. For this reason, the joints known as weak planes are not defined separately from the intact chalk known as the matrix. They do not act as geometric interfaces or faults existing in the chalk rock mass. However, the weak planes are represented implicitly in the chalk continuum. They are defined uniformly over the zones of the model with varying orientations and reduced strength properties. Consequently, the anisotropic effect is advocated at the level of the mechanical behaviour of the chalk. This technique can be considered appropriate for the fractured chalk where the weak planes cannot be precisely located (Griffths, 1980 and Griffiths and Lane, 1999).

3.4 Analysis of the behaviour of the chalk cavity

3.4.1 Resistance in terms of the *FRF*

Different parameters of the joint sets produce different impact. This section demonstrates particularly the effect of joint sets orientation on the stability state of the underground excavation expressed by *FRF*. At first, effect of single joint set is discussed while the next paragraph illustrates the case of double joints. Before applying the SSR method, the excavation of the chalk cavity is modelled to define a first equilibrium state. The mesh and the boundary conditions in terms of displacements used for the calculation are presented in (Figure 3.2). The initial stress state is generated by applying gravity forces. For this condition, the value of the initial earth pressure coefficient at rest is close to $\nu/(1-\nu)$. Concerning the evaluation of the final reduction factor (*FRF*), the earth pressure coefficient at rest has no effect as previously mentioned by several authors (Potts and Zdravkovic, 2012). The excavation is performed in four steps with de-confining forces on the free edges of the mesh. In each phase, a layer of width 1.5 m and height 1.5 m is extracted. The excavation process occurs upon four phases by order from outside to inside and from top to bottom.

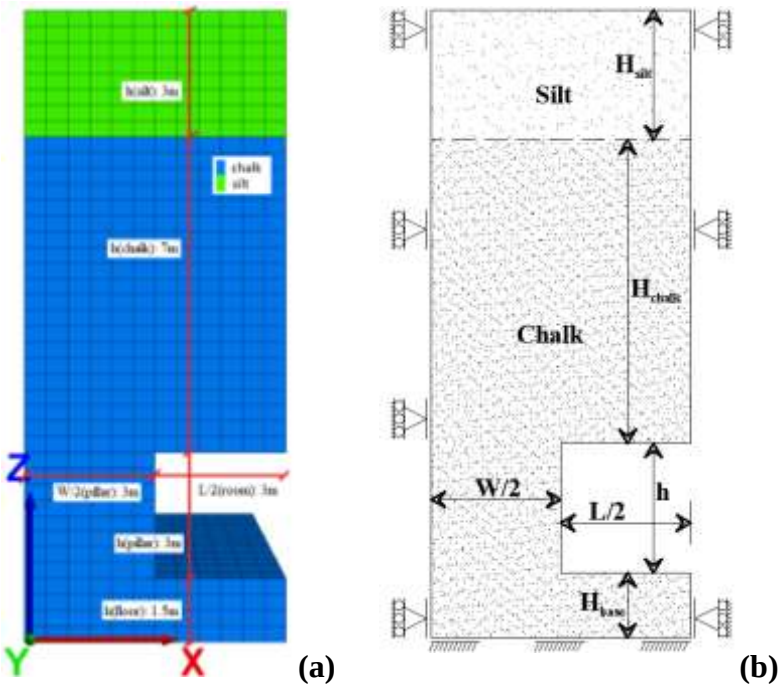

Figure 3.2. (a) Section of the excavation model showing the mesh, (b) Section of the excavation model showing the boundary conditions.

3.4.1.1 Single joint set

Joint set is demonstrated by a weak plane uniformly defined in each zone of the model. Weak plane orientations from 0° (horizontal) to 90° (vertical) are considered. *FRF* is established and shown to vary with the angle of the weak plane. Results show that the effect of joint orientation is not negligible. This proves again the influence of anisotropy on the behaviour of the underground structure (Figure 3.3). Lowest *FRF* values are obtained when the weak plane tends to be horizontal with inclination angle at 10° and 0°, where *FRF* values are 2.12 and 2.58 respectively. On the other hand, greatest *FRF*, 3.68, is achieved while the weak planes are almost vertical at angle 80° or vertical at 90° where *FRF* is 3.16. Higher *FRF* in the case of vertical joints is due to stabilizing effect exerted from the arching mechanism which might be created at the roof of the confined pillar-roof frame. However, horizontal joints drive the augmented stresses in the roof to the abutments and form weak points at the pillar roof connections. Thus a lower *FRF* is attained in the case of galleries with horizontal joints.

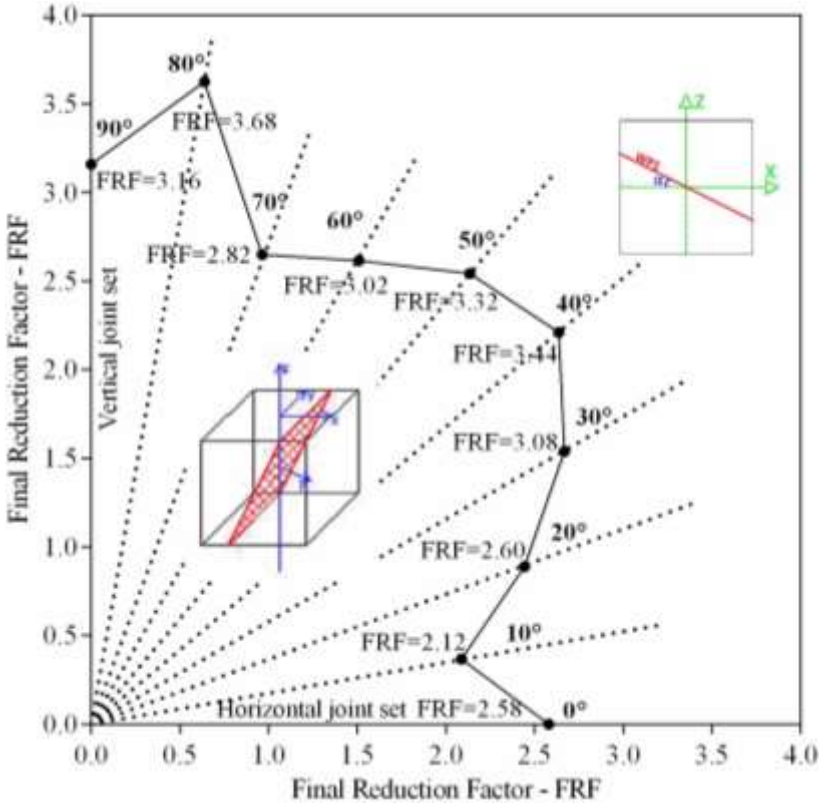

Figure 3.3. Variation of *FRF* with respect to angle of weak plane α.

By comparing the iso-values of the horizontal stresses, these results are confirmed. For example, at same level of *FRF*, horizontal stresses in case of vertical joints are higher at the lateral face of the pillar (Figure 3.4(a)) than in case of horizontal joints where a concentration of horizontal stresses is observed at mid span (Figure 3.4(b)).

At other inclinations of the joint set, *FRF* values vary irregularly. This can be better explained when failure mechanism reflected by the displacement distribution and stress localization through zones of structural elements of the excavation is analysed. During the reduction procedure of the strength properties of the weak planes, the evolution of the reduction factor 'F' can be linked to the development of the failure mechanism. Besides, the failure mechanism which is joint-controlled depends not only on joints orientation, but also on the geometry of galleries which affects the resistance of each of the roof and pillars. Failure modes with respect to different joint orientations are illustrated in a coming paragraph and further analysis is provided.

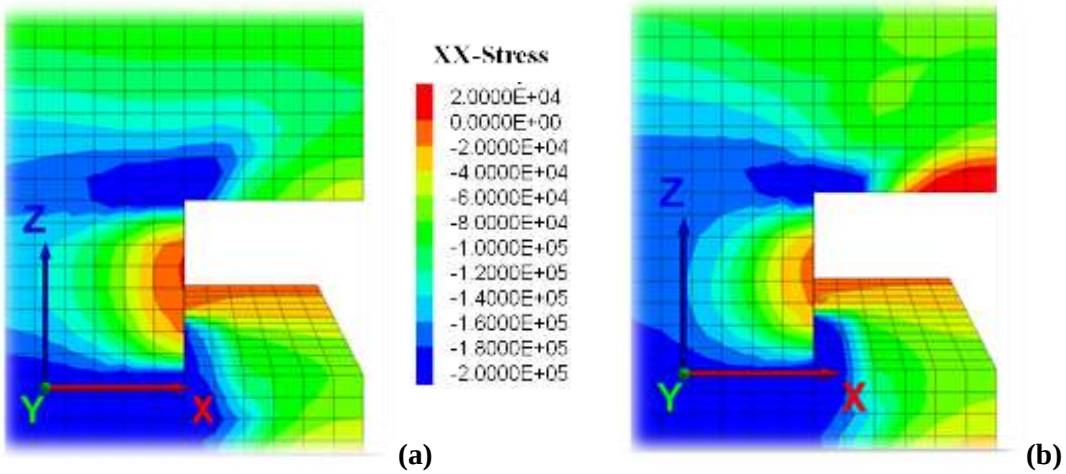

(a) **(b)**

Figure 3.4. Zoom on the void zone of the cavity model: Horizontal stress distribution on a section of the cavity model. (a) vertical joints, (b) horizontal joints.

3.4.1.2 Double joint sets

Chalk layers in North France, where these quarries were excavated, are originally embedded with double symmetric joints due to the geological conditions of the region (Ineris, 2012, and Anteagroup and Ville de Lille, 2012).

For this reason, symmetric weak planes are considered in the chalk models and corresponding *FRF* values are obtained and compared to those in case of single joint set (Figure 3.5). Having more than one joint set with reduced strength properties expands the weak zones which are favourable to degradation and hence drives the chalk continuum to be under risk of earlier failure which results in further decrease in *FRF*. This is illustrated in the graphs presented where *FRF* values in the case of double joint sets are almost always lower than in the case with single joint set. Consistency is confirmed in the case of vertical and horizontal planes where double symmetric joints will act as single joints and thus same *FRF* is obtained. Negligible difference is due to numerical error.

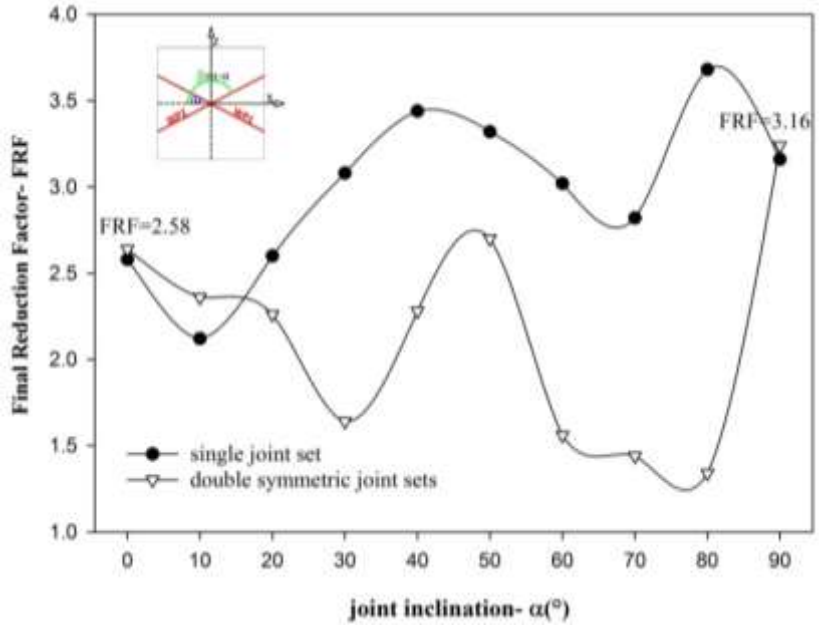

Figure 3.5. Comparison of *FRF* versus joint set inclination angle α in case of single joint set and double symmetric joint sets.

3.5 Failure mechanisms

3.5.1 Deformation profiles

The analysis of a fractured structure of pillars and rooms is complicated by the fact that there is no unambiguous analytical solution for the interaction among the abutments, roof and floor on one hand, and among the chalk layers on the other hand. Terzaghi (1946) had formulated the first method to study the stability of roofs of unsupported tunnels excavated in horizontally or vertically jointed rock by estimating the maximum over-brake height at the roof depending on the depth and span of the tunnel and on the orientation of inherent joints. Applications on tunnel excavations (Fortsakis et al. 2012) as well as on underground quarries (Fasani et al. 2012) were performed to study the influence of joint stratifications and fractures on the failure mechanisms However, the previous formulation that depends on two factors, geometry of the excavation and orientation of the joints was developed based on extensive numerical modelling (York et al. 2000) integrated in the analysis of underground quarries. For the excavation model described before, the displacement distribution at final reduction phase of strength properties of the weak planes are demonstrated to analyse the failure mechanisms of the excavations under the influence

of existing joints. The displacement values can be analysed since they correspond to a phase where the numerical convergence is still obtained and the equilibrium equations are verified. Strain profiles are affected by the orientation of the weak planes (Figure 3.6). For instance, the model with vertical joint set parallel to xz plane and perpendicular to yz and xy planes, forces the displacements to be oriented in the xz plane where they are highly concentrated at the weakest point of the structure according to its geometry conditions. Unlike vertical joint sets, horizontal joint sets implement symmetry in the joints distribution with respect to the critical section of the model. This explains the symmetric distribution of displacement contours in case of horizontal joint set which is probably more clearly demonstrated in the plot of the contours of the maximum shear strain (Figure 3.7). However, the concentration of the displacements in the roof is explained by the behaviour of these horizontal joint sets which might act as separating layers that stack the imposed vertical weight of layers above the galleries in the roof instead of transferring it to the pillars. In this case, shear stresses are highly concentrated at the abutments. In case of vertical joint sets, lower displacements and higher stability is observed. This is due to the arching effect exhibited at roof of the gallery due to lateral confinement which is not disturbed by the presence of vertical discontinuities. At specific geometries, the shear resistance at the abutments might not be sufficient to induce the stabilizing effect by arching mechanism. This shows again the important role of geometry that influences confinement and resistance of pillar and/or roof and thus activates the combined geometry-joint effect on the performance of the excavation. Eventually, horizontal joints (Figure 3.6(b)) might represent underground strata where each layer can act as a separated beam imposing its own weight to the underneath beam. The behaviour of the roof in this case will seem as a stack of beams imposing vertical load on the underlying beams (Fayol. 1885). Thus, high displacements are figured out in the roof. However, vertical joints (Figure 3.6(a)) impose a different behaviour. Due to lateral confinement and in the presence of vertical joints, the system roof pillar exhibit a stabilizing arching mechanism which induces excessive stresses at roof mid span and thus implements higher strength at this point (Esterhuizen and Iannacchione, 2004). Consequently, displacements are discovered at the roof pillar connections instead of being stacked at the mid span of roof. On the other hand, displacement contours of the model with inclined joints show up at the level of the pillar (Figure 3.6(c), 3.6(d)). This can be explained by the fact that inclined weak planes drive the excessive stresses that reach the pillar to attack its opposite faces at one hand, and be blocked there and create the shear bands where no continuity is available so that the excessive stresses are tracked

to a different and more supportive point in the structure. So, having weak planes at 45° implements a direct effect on strength of the vertical elements of the structure. As shown, the displacement contours appear to be at 45° along the orientation of the weak plane. Coherent results are observed in the case of double symmetric joint sets (Figure 3.6(c), 3.6(d)) where the profile of displacement is shaped in accordance with the symmetric weak planes inclined at 45°. Another comment on the displacement profiles can be given. Concerning the value of displacement achieved, it is not necessarily higher in case of double joint sets than in case of single joint set. This is explained by the fact that the figures shown display the displacement just before failure, i.e when *FRF* is calculated. Consequently, if we consider the case of joints inclined at 45° (Figure 3.6(c), 3.6(d)) *FRF* with single joint is found equal to 3.26 (Figure 3.6(c)) whereas with double joints it is equal to 2.6 (Figure 3.6(d)). Thus, cumulative displacements in case of single joint set have been calculated for longer phase than in case of two joint sets and hence it is possible to have overall displacements in case of single joint set greater than those in case of double joint sets. This was also the case with joints inclined at 30° (Figure 3.8(a), 3.8(b)). Also, strain profiles in case of single and double joint sets inclined at 30° and 60° are presented. This describes the previous deduction concerning single and double mechanism where the deformation is concentrated in the pillar and inclined with the angle of orientation of the weak planes (Figure 3.8). Nevertheless, for a more resisting pillar with a higher width to height ratio, the effect of joints might not be of same importance.

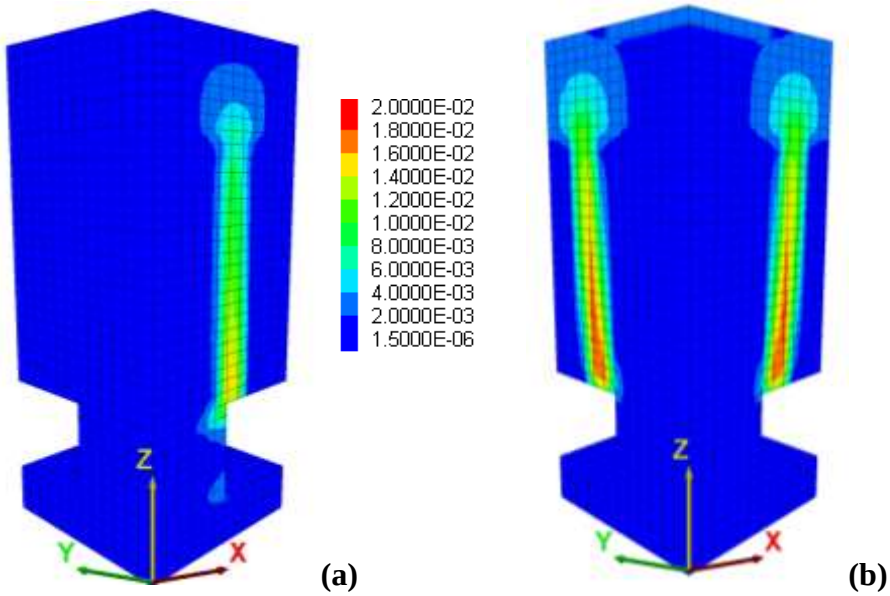

(a) **(b)**

Figure 3.7. Contour of maximum shear strain in the excavation model. (a) Vertical joint sets, (b) Horizontal joint sets.

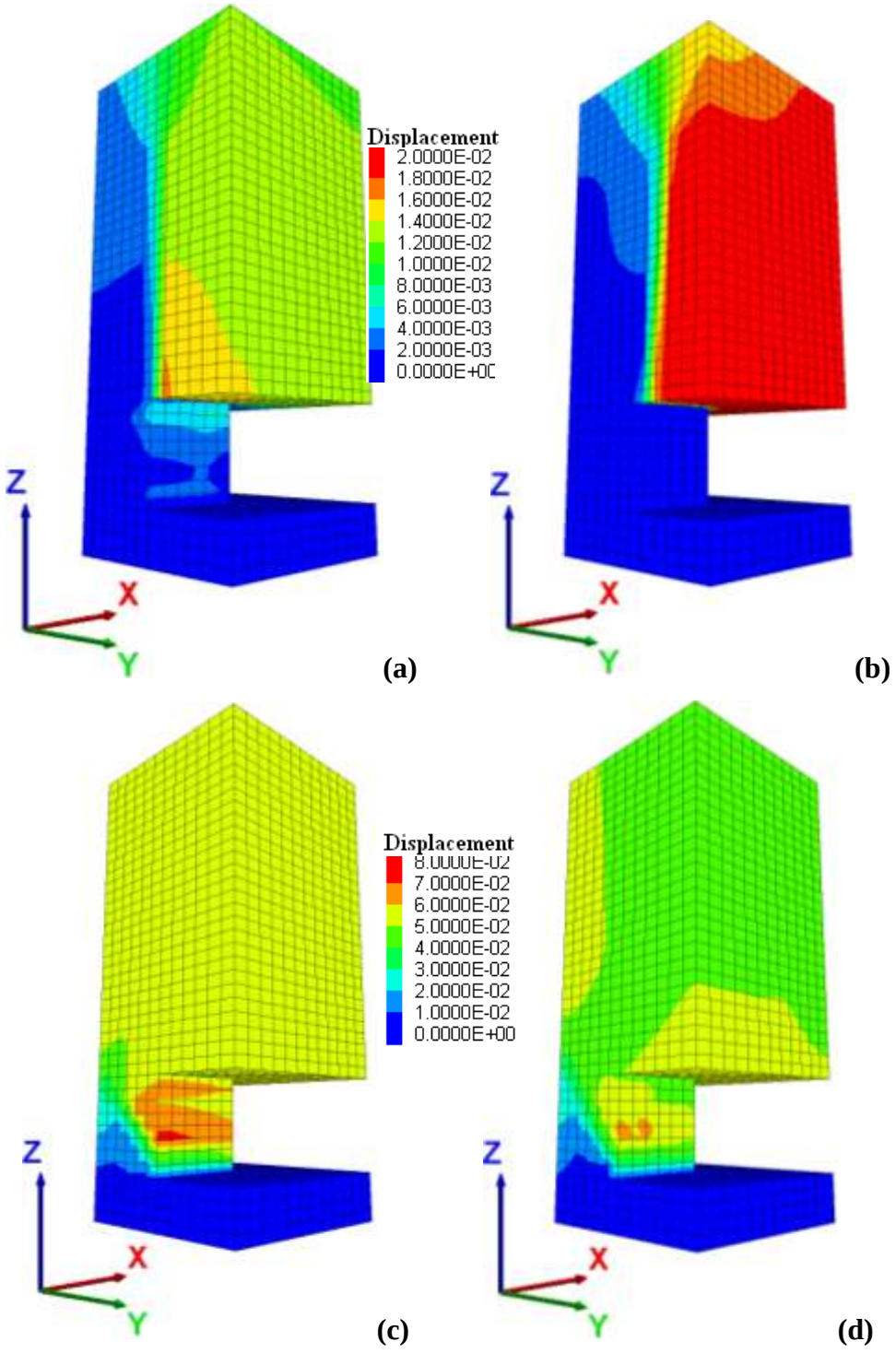

Figure 3.6. Displacement profile of the excavation model in different joint sets conditions. (a) single vertical joint set parallel to xz-plane, (b) single horizontal joint set parallel to xy-plane, (c) single non-vertical joint set inclined at 45°, (d) double symmetric non-vertical joint set inclined at 45°.

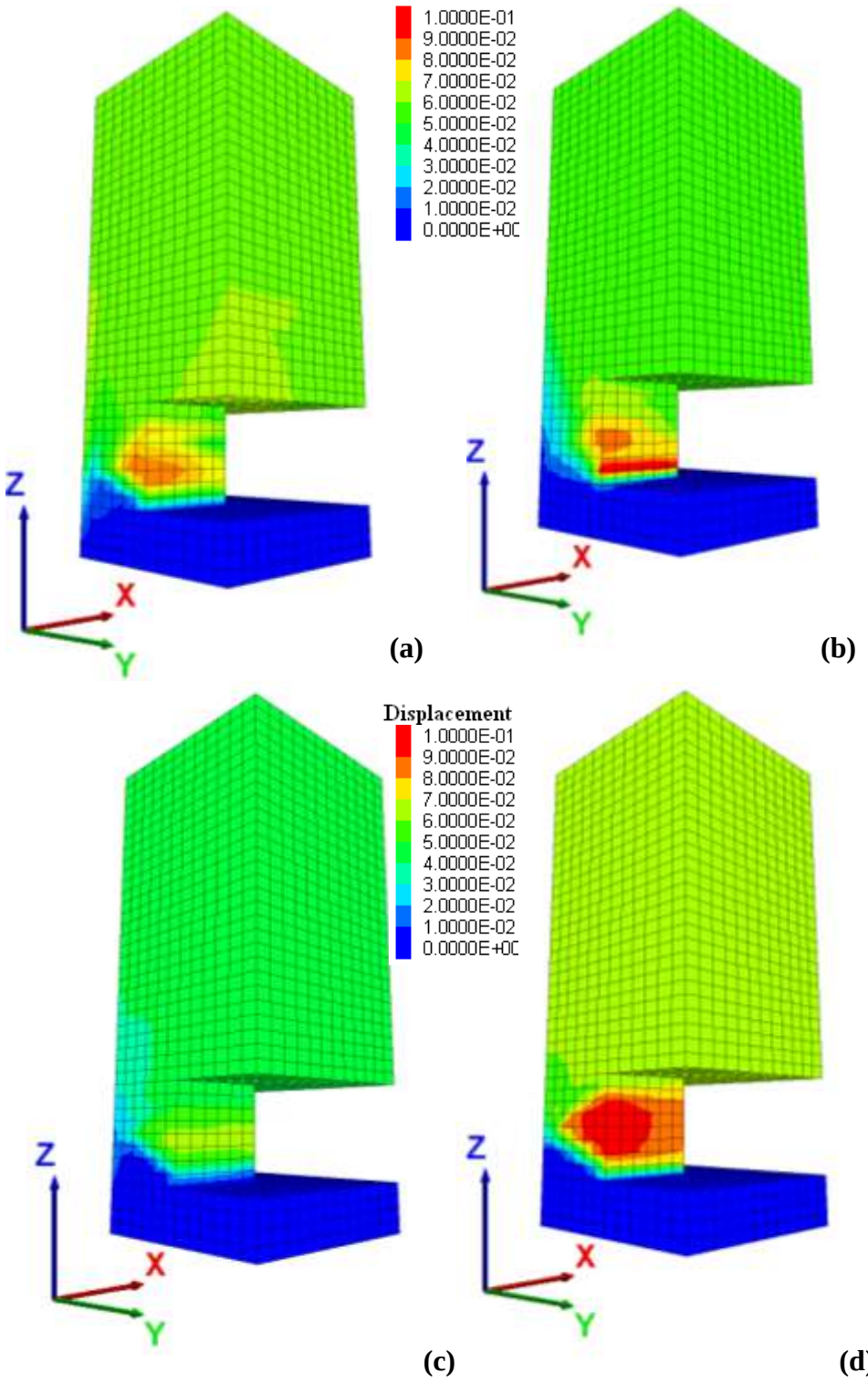

Figure 3.8. Displacement Contours of the excavation model in different joint sets conditions. (a) single non-vertical joint set inclined at 30°, (b) double symmetric non-vertical joint set inclined at 30°, (c) single non-vertical joint set inclined at 60°, (d) double symmetric non-vertical joint set inclined at 60°.

3.5.2 Displacements at the roof, pillar and surface

To complement the comprehension of the mechanisms of rupture expressed above by the strain modes, it is evident to investigate the displacements at every element of the excavation. So, settlement at the surface along x-direction (Figure 3.9), deflection at the roof along x-direction (Figure 3.10), and buckling of the pillar along z-direction (Figure 3.11) are plotted.

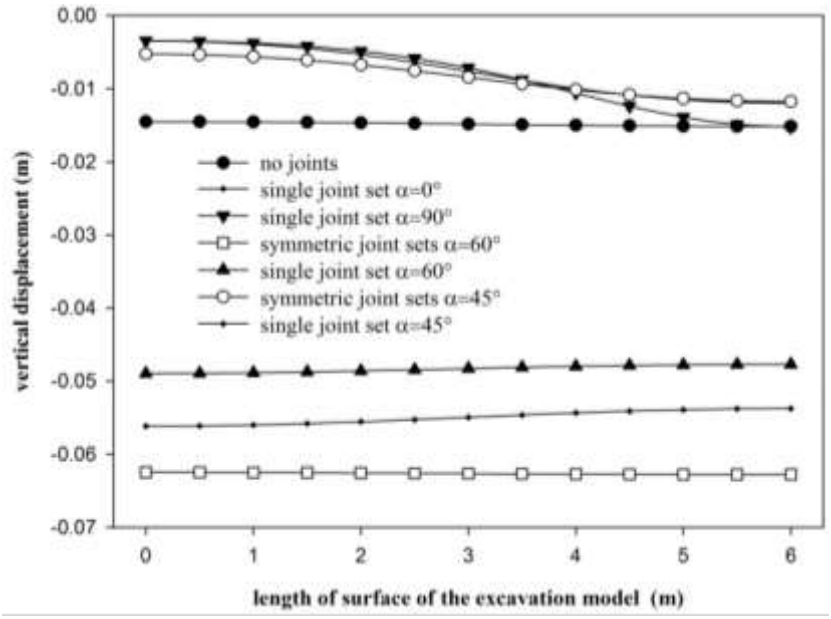

Figure 3.9. Settlement at the surface of the excavation model at different joint cases.

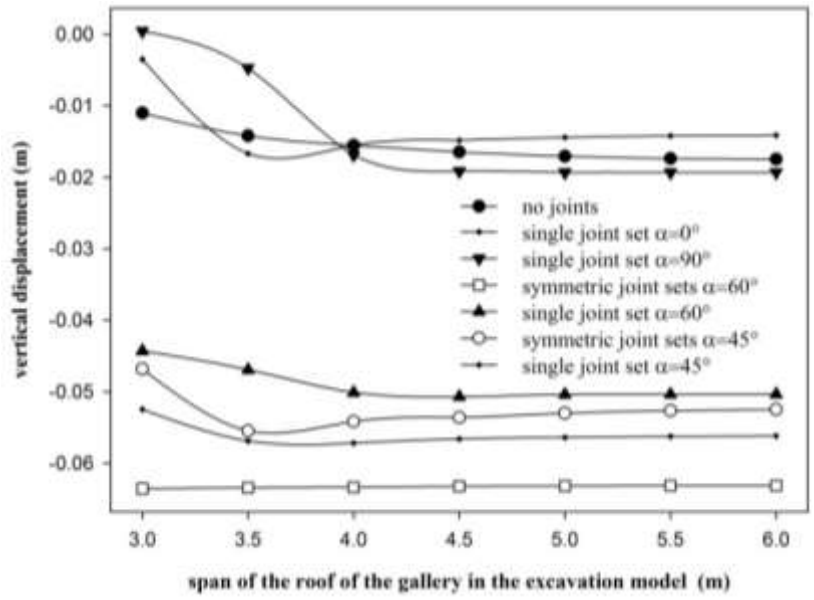

Figure 3.10. Deflection of the roof of the gallery of the excavation model at different joint cases.

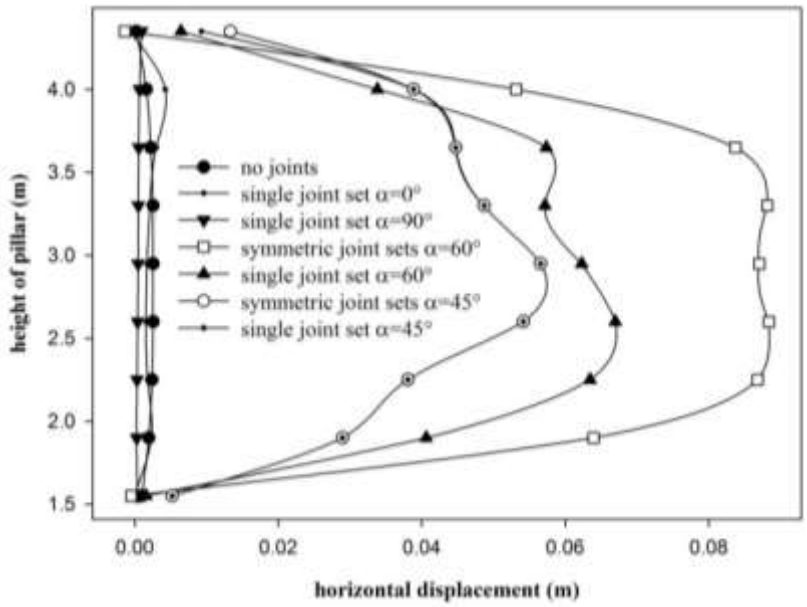

Figure 3.11. The lateral expansion of the pillar of the excavation model at different joint cases.

Results again show that higher displacements always appear when the joints are inclined. However, in case of vertical or horizontal joints, displacements are null in the pillar and negligible all elsewhere. Despite of the fact that the deflection of the roof in case of vertical or horizontal joints is close and small, its growth with respect to the strength reduction mechanism applied to the joints is not similar.

A better understanding is given by tracing the deflection at mid-span of the roof of the gallery versus *FRF* for both joint cases (Figure 3.12). Both graphs show that beyond a certain limit of deflection, *FRF* is almost constant. In the case of horizontal joints, roof settlement exceeds 0.14 cm reaching approximately 0.64 cm while maintaining the same *FRF* close to 2.55. Similar observation is obtained in the case of vertical weak planes where *FRF* after 0.26 cm of roof settlement is estimated not to exceed the value of 3.1. This stabilization may be related to the rapid deformation just before instability which results in augmented normal stresses and additional confinement that prevents the system from collapsing. Deformations increase significantly directly before instability occurs. Another point can be concluded from this tracing. A higher *FRF* in case of vertical joint set reflects the ductile behaviour of the model where in case of horizontal joint set where *FRF* is lower, the failure is less ductile or more brittle. This illustrates again the effect of joints orientation on stability and on failure mechanisms.

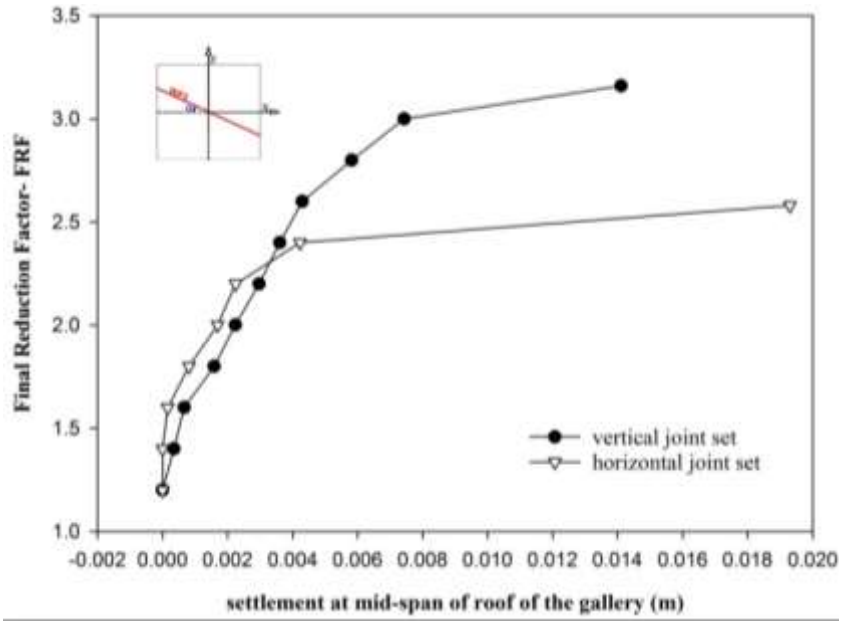

Figure 3.12. Plot of *FRF* against the settlement at the mid-span of the roof of the gallery.

3.6 Synthesis

Numerical modeling of the strain and failure mechanisms povide a better understanding of the impact of joints on the global behaviour of the underground structure. Nevertheless, it is important to keep in mind that the effect of joints is not independent from the geometry of the quarries. This latter can be considered by a parametric study which implements different confinement conditions and provides different weak and strong structural elements. Concerning our case of study, the following points are interpreted:

- Final reduction factor *FRF* representing the failure mechanisms is affected by the orientation of the existing joint sets.
- Symmetric joints at certain inclinations may induce an effect close to that of single joints. In our case this was obtained at angle 45° from the z-axis. In other geometry cases symmetric joints may produce a stabilizing act.
- The effect of joint orientation is always in accordance with the friction angle. This observation is coherent with the principles of the yield criteria used.

- Joint orientation provokes different failure mechnisms in roof and/or pillar for the same case of geometry of the cavity. Accordingly, rupture may be localized either in the roof or in the pillar and with different intensities.
- Inclined joints have a greater effect on the pillar than on the roof. This is shown up by shear bands crossing the pillar at almost coherent inclination with those of the joints.
- Because of null displacements observed in the pillar in case of vertical or horizontal joints, and even if those in the roof are low, shear bands appear in the roof.
- Plotting displacements with respect to the increase of *FRF* gives an indication about the stabilizing behaviour of the underground structure as well as the ductility of the rupture mechanisms.
- This provides a complementaryapproach for a better understanding of the visual inspections, onsite observations and measurements.

3.7 Conclusions

In this chapter, a numerical technique based on the shear strength reduction method was implemented to study the stability of the underground cavities due to failure in joints. Final reduction factors reflecting the stability of the quarries at maximum weakening of joints are computed. Different orientations and number of the joint sets are considered. Ultimate resistance and failure mechanisms are then analyzed.

By considering a numerical modelling of a chamber and pillar excavation, this study provides an idea about the stability state and the scenarios of rupture that might take place in the chalk quarries depending on the joints characterization. Moreover, since the weak planes are defined implicitly, then they can be representing the joint sets embedded in the chalk layers, as well as the emerging fractures that show up due to natural or anthropogenic degradation of the intact material. Eventually, this phenomenon has shown to create a non-negligible impact on the global behaviour of such underground structures.

This numerical study is extended to cover a wide range of the investigated room-and-pillar cavities in terms of the different dimensions identified. A parametric stability study that accounts for different dimensions of the pillars and/or roof is performed and discussed in chapter five.

Failure mechanisms are directly affected by the presence of joints and fractures. However, in the study of abandoned underground quarries which have been excavated decades ago, fractures develop and increase due to the accumulation of aggravating factors with time. Consequently, it would be of high importance being able to account for the effect of time on the stability of these unexploited quarries. In other words, processing a time dependent degradation, which can be applied either on the whole jointed chalk continuum or in a separate wise manner, i.e. only on the predefined joints, allows us to carry out a more realistic performance and stability study of the underground quarries in their current state.

CHAPTER FOUR
A TIME-DEPENDENT-DEGRADATION APPROACH FOR THE LONG TERM STABILITY ASSESSMENT OF UNEXPLOITED CAVITIES

4.1 Introduction

Stability of geotechnical structures such as slopes, excavations, and underground cavities or quarries, is an important topic for geotechnical engineering where time effects are generally not taken into account explicitly. In most cases, safety factors are used to justify the stability of these structures and, in order to ensure a sufficient level of safety or the development of small deformations and displacements, high values are considered for these factors.

Using numerical methods such as finite element method or finite difference method, the most common approach for a stability analysis is based on the conventional shear strength reduction technique. This technique was used in the stability analysis of the underground cavities in the presence of joints. It was discussed in chapter three. It is based on reducing the shear strength properties of the ground incrementally using a cumulatively increasing factor R_f until the failure is detected. The final value of the factor R_f corresponds to the safety factor F_s that reflects the stability state: F_s >1 means stable. Nevertheless, it is admitted that this value is not sufficient to ensure low displacements and greater values in this case have to be obtained (F_s >1.5 at least). The shear strength reduction technique has been successfully used in the analysis of geotechnical structures with the combination of analysis based on the limit equilibrium method in some applications (Zienkiewicz et al., 1975, Naylor, 1982, Matsui and San, 1992, Lane et al., 1997, Dawson et al., 1999, Rachez et al., 2002 and Roosta et al., 2005). Nevertheless, this technique

leads to a uniform decrease of the shear resistance properties which is applied without considering physical mechanisms such as time effects. Consequently, this method might not always seem ideal and thus other approaches could be tested.

Accounting for time effects in the study of stability problems may provide some elements to have a better understanding of the strain and failure mechanisms. It may also help for the analysis of the observations and measurements of accumulated displacements which are obviously necessary to predict the eventual collapses. Nevertheless, a time dependent stability analysis remains difficult and it is necessary to develop specific procedures. The effect of time can be studied by several approaches such as ageing or creep and includes various phenomena responsible for the evolution of strains and displacements: hydro-mechanical effects that are induced by seasonal cyclic loading, for example, suction and saturation, fatigue which rises from cyclic loading mechanisms, degradation of the internal mechanical properties of the constituent rock by means of physico–chemical actions like weathering that leads to ground alteration increasing with time.

For soils and rocks, a variety of constitutive approaches have been used to model the time-dependent behaviour, including ageing and creep effects associated to the stress-strain evolution and the internal material degradation with time. According to Shao et al. (1993, 2003), Pietruszczak et al. (2004), and Amitrano and Helmstetter (2006), classical models attribute the creep deformation to the viscous properties and the time-dependent deformation is thus entirely described by viscoelastic and viscoplastic theories (Perzyna, 1966, Cristescu, 1989, and Cristescu and Hunsche, 1998). However, creep can be described in terms of microstructural evolution that integrates a progressive degradation in the material and thus accounts for the internal physical mechanisms (Shao et al., 2003). From a different point of view, Gens and Nova (1993), Nova (2000), Nova et al (2001, 2003), Castellenza (2002), and Tamagnini et al. (2002), develop some approaches where time-dependant effects are directly related to the material degradation mainly induced by weathering being a major agent behind its deterioration. Hence, a model capable of capturing both mechanical and chemical degradation in bonded soils is developed in the frame of a reasonable agreement with experimental observations.

A synthesis table that summarizes major works done to account for the time-dependent behaviour whether by integrating viscous effects or degradation effects is provided (Table 4.1).

Table 4.1. Synthesis table of the works accounting for time-dependent behaviour. Some of time independent stability analyses are highlighted.

✚ Stability analysis using the conventional shear strength reduction method independently of time effects;	Zienkiewicz et al., (1975), Naylor, (1982), Matsui and San, (1992) Lane et al., (1997), Vinkler and Piguet (1999), Dawson et al., (1999), Rachez et al., (2002), and Roosta et al., (2005)
✚ Experimental creep analysis performed to assess the effect of time on chalk which influences long-term stability;	Monjoie and co-workers, (1990, 1991), Dahou et al., (1995), Gutierrez, (1999, 1998), De Gennaro and coworkers, (2003, 2004), and Auvray et al., (2004)
✚ Creep deformation attributed to the viscous properties; ✚ Time-dependent deformation entirely described by viscoelastic and viscoplastic theories;	Perzyna, (1966), Cristescu, (1989), and Cristescu and Hunsche, (1998)
✚ Time-dependant effects are directly related to the material degradation; ✚ Weathering is a major agent that encourages degradation of material strength properties upon time;	Gens and Nova, (1993), Nova, (2000), Nova et al., (2001, 2003), Castellenza, (2002), Tamagnini et al., (2002), Calvetti, (2004), and Miscevic and Vlastelica, (2014)
✚ Degradation by an elastoplastic strain hardening model; ✚ Hardening law depends on plastic strains and appropriate degradation function;	Shao et al., (2003), and Calvetti, (2004)
✚ Creep is independent of viscous properties; ✚ Creep involves a progressive evolution of micro-cracks;	Shao et al. (1993, 2003), Pietruszczak et al., (2004), and Amitrano and Helmstetter, (2006)

On the other hand, other works have been devoted to integrating the time analysis in direct geo-engineering applications such as mines, tunnels, and slopes. Shao et al. (1993) worked on a typical manifestation of creep that involves a progressive evolution of micro-cracks, as observed, around a tunnel in Lac du Bonnet granite, Canada. Also considering the collapses in region of

Lorraine iron basin, Castellanza (2002) and Calvetti (2004) have presented some studies. The former has showed that it is possible to simulate the progressive failure of geo-structures subjected to chemically induced bond degradation where failure had taken place due to progressive degradation of the pillars of abandoned iron mines (Castellanza, 2002), while Calvetti (2004) has described the behaviour of rocks exposed to weathering by an elastoplastic strain hardening model in which the hardening law depends on experienced plastic strains and an appropriately defined degradation parameter of chemical origin.

A variety of constitutive approaches have been used to model the time-dependent behaviour, including ageing and creep effects associated to the stress-strain evolution and the internal material degradation with time. Some works have addressed significant ageing and creep effects in soils (Yin et al. 1999), marl (Alonso and coworkers, 2009, 2010), soft clays and hard clays (Shao, 1998), salt rocks (Hunsche and Hampel 1999), hard rocks and other brittle rocks (Nawrocki and Mroz 1998). Extensive experimental analysis was also performed to assess the effect of time on chalk, Dahou et al. (1995), Gutierrez (1999, 1998), De Gennaro and coworkers (2003, 2004).

Other works have been performed considering ageing and creep and are devoted to applications on mines, tunnels, and slopes. Shao et al. (1993) worked on a typical manifestation of creep that involves a progressive evolution of micro-cracks, as observed, for example, around a tunnel in Lac du Bonnet granite, Canada. Vinkler and Piguet (1999) have studied the stability of two-level mine in the surrounding of the iron basin in Lorraine, France based on a strength reduction technique and predicted the short and long-term extent of failure zones. Also considering the collapses in region of Lorraine iron basin, Castellanza (2002) and Calvetti (2004) have presented some studies. The former has showed that it is possible to simulate the progressive failure of geo-structures subjected to chemically induced bond degradation where failure took place due to the progressive degradation of the pillars of abandoned iron mines (Castellanza, 2002), while Calvetti (2004) has described the behaviour of rocks exposed to weathering by an elastoplastic strain hardening model in which the hardening law depends on plastic strains experienced and an appropriately defined degradation parameter of chemical origin. The ageing properties of gypsum extracted from two underground mines in France (Livry –Gargan and Grozon) have been observed by Auvray et al. (2004) using scanning electron microscopy. The ageing process was investigated and assessed by determining various physical and mechanical parameters of the samples. More recently, Miscevic and Vlastelica (2014) have identified the main influences of

weathering on slope stability in marl formation, presenting some cases of engineering observations about slopes in this soil type, and proposing convenient solutions.

In this chapter, another technique is proposed to take into consideration the time effects. The developed model accounts for the time behaviour by defining a stress dependant degradation function based on a hardening function depending on deviatoric plastic strains inspired from the works of Shao et al. (2003). The degradation of the resistance properties and the strain evolution dependency are considered. The degradation function, which is applied uniformly on the massive at initial state, involves the geometric, in-situ and time dependent stress conditions in the process of reduction of the ground strength properties.

This technique is applied for shallow chalk quarries in the region of North France where several collapses caused by the progressive degradation of the pillars of unexploited chalk quarries have been observed. Knowing that joints were identified in the chalk substratum of this region, which are also expected to increase with degradation and time, the oriented failure criterion was developed in chapter two to account for the presence of these joints and the induced anisotropy (Rafeh et al., 2015). The degradation approach is then applied on these joints knowing that normally, the joints represent the weak planes of the continuum, and are prior favourable to degradation. Although joints are defined in a uniform manner, degradation is generated non-homogeneously through these joints with time due to the non-uniform evolution of stresses and the principle of stress dependency integrated in the degradation approach.

A numerical analysis of the time dependant behaviour of these quarries is then conducted using FLAC^{3D} (Itasca, 2009) where both, the oriented yield criterion for joints and the time degradation approach were implemented. The evolution of degradation is analysed according to time, and a parametric study of several parameters concerned in the degradation function is performed to explain their influence on the degradation process. The evolution of displacements and strain mechanisms with time, considering different joint orientations is demonstrated. At last, a comparison between the non-homogeneous degradation approach and the uniform shear strength reduction approach is elaborated and discussed.

4.2 Time degradation approach

4.2.1 Principles

Various processes occurring over time may induce degradation of the ground mass and reduction of its mechanical properties accompanied with time-dependent deformations. This may lead to development of fractures which will in turn accumulate the deteriorating influence of degradation and failure in some zones.

Usually, the type of time-dependent deformation known as creep deformation is entirely related to the viscous effects of the material and is analysed using models of viscoelasticity and viscoplasticity (Perzyna, 1966, and Cristescu, 2009). In this work, a methodology based on the law of hardening and micro-structural evolution inspired by Pietruszczak et al. (2004) is used to generate both instantaneous and time dependent irreversible deformations of the degraded rock mass.

The time-dependent deformation is considered as a consequence of progressive degradation of the material structure. Consequently, the evolution of this structure which happens at a micro-scale is a time dependent progressive damage process. This evolution is assessed by an internal variable, which is function of plastic deformation that in turn evolves in time (Shao et al. 2003). This concept is used to describe the long term degradation process of chalk of unexploited underground cavities. The strength properties of the rock mass are affected by the degradation phenomenon by means of degradation function (1-αD), denoted by D*, which depends on the degradation factor *D* varying between 0 and 1.2 and a constant α less than 1 used to limit the maximum degradation of the ground.

The degradation factor *D* is related to the accumulation of plastic shear strain γ_p and also depends on time, which requires using a formulation of the equilibrium equation including time t. Hence, *D* can also be written as a time-dependent function under the following form:

$$D(t) = D\left(\gamma_p(t)\right) \qquad [4.1]$$

The kinetics of microstructure evolution can be described in terms of the deviation from equilibrium state defined by elastic limit of the continuum that exhibits hardening (Pietruszczak et al. 2004). The following equation can be applied (see Annex I):

$$\dot{D}(t) = \gamma\left(R_m(t) - D(t)\right) \quad [4.2]$$

The plastic hardening is related to the evolution of the accumulated plastic shear strains with a function depending on the soil or the rock type: It is described by the increasing function R_m which is function h of the deviatoric plastic shear strain γ_p:

$$R_m = h(\gamma_p) \quad [4.3]$$

$$\gamma_p = \int \sqrt{\frac{2}{3} de_{ij}^p de_{ij}^p} \quad [4.4]$$

$$e_{ij}^p = \varepsilon_{ij}^p - \frac{1}{3} tr\left(\varepsilon_{ij}^p\right)\delta_{ij} \quad [4.5]$$

In equation [4.2], γ is a material constant with a positive value. This insures that the degradation rate is always positive knowing that $R_m(t) \geq D(t)$. The value of γ which depends on the soil itself has a considerable influence on the degradation rate (Equation [4.2]). Back to the relation between the hardening function R_m and the degradation parameter D, the differential equation is solved (Annex I) assuming that the degradation process is activated at a time t = 0 as an initial condition, i.e. $D(0) = 0$. As a result, the general form of the time dependant degradation function is obtained:

$$D(t) = \int_0^t \gamma R_m(u) e^{-\gamma(t-u)} du \quad [4.6a]$$

According to the Equation [4.6a], the degradation factor D varies between 0 for a time t=0 and R_{mf}, the value of R_m which is achieved when time t tends to infinity. Another expression for Equation [4.6a] is the following:

$$D(t) = R_m(t) - e^{-\gamma t}\left[R_m(0) + \int_0^t \gamma R'_m(u) e^{\gamma u} du \right] \quad [4.6b]$$

4.2.2 Implementation of the time degradation approach

Time degradation approach can be used with either constitutive law including an isotropic hardening mechanism. A failure criterion f with a hardening variable R_m and a non-associated flow rule g are considered. Concerning the failure criterion, Mohr Coulomb criterion can be considered as an example:

$$f\left(\sigma_{ij}, R_m\right) = \left(\sigma_1 - \sigma_3\right) - \left[\left(\sigma_1 + \sigma_3\right)\sin\left(\varphi\right) + 2c\cos\left(\varphi\right)\right]R_m \qquad [4.7]$$

where σ_1 and σ_2 are the principle stresses, φ is the internal friction angle, and c is the cohesion.

The plastic multiplier is obtained as following:

$$f\left(\sigma_{ij}^{f} - d\sigma_{ij}, R_m + dR_m\right) = 0 \qquad [4.8]$$

$$f\left(\sigma_{ij}^{f}, R_m\right) - \lambda \frac{\partial f}{\partial \sigma_{ij}} \overline{\overline{C}} \frac{\partial g}{\partial \sigma_{ij}} + \lambda \frac{\partial f}{\partial R_m} \frac{\partial R_m}{\partial \gamma_p} dX_p = 0 \qquad [4.9]$$

with: $d\gamma_p = \lambda dX_p$ and $dX_p = \sqrt{\frac{2}{3}} \sqrt{\frac{\partial g}{\partial \sigma_{ij}} . \frac{\partial g}{\partial \sigma_{ij}} - \frac{1}{3}\left(tr\left(\frac{\partial g}{\partial \sigma_{ij}}\right)\right)^2}$ according to equations [4.4] & [4.5]

$$\lambda = \frac{f\left(\sigma_{ij}^{f}, R_m\right)}{\frac{\partial f}{\partial \sigma_{ij}} \overline{\overline{C}} \frac{\partial g}{\partial \sigma_{ij}} - \frac{\partial f}{\partial R_m} \frac{\partial R_m}{\partial \gamma_p} dX_p} \qquad [4.10]$$

where σ_{ij}^{f} designates the trial stress tensor obtained considering only an elastic strain increment, $d\sigma_{ij}$ designates the plastic stress correction and $\overline{\overline{C}}$ is the stiffness matrix.

Taking into account the degradation factor *D* in the previous equation, the following can be obtained (see for example Shao et al. 2003):

$$f\left(\sigma_{ij}, R_m, D\right) = \left(\sigma_1 - \sigma_3\right) - \left[\left(\sigma_1 + \sigma_3\right)\sin\left(\varphi\right) - 2c\cos\left(\varphi\right)\right]R_m\left(1 - \alpha D\right) \quad [4.11]$$

The resolution of the consistency equation gives the following results:

$$f\left(\sigma_{ij}^f - d\sigma_{ij}, R_m + dR_m, D + dD\right) = 0 \quad [4.12]$$

$$f\left(\sigma_{ij}^f, R_m\right) - \lambda \frac{\partial f}{\partial \sigma_{ij}} \overline{\overline{C}} \frac{\partial g}{\partial \sigma_{ij}} + \lambda \frac{\partial f}{\partial R_m} \frac{\partial R_m}{\partial \gamma_p} dX_p + \frac{\partial f}{\partial D} dD = 0 \quad [4.13]$$

$$\lambda = \frac{f\left(\sigma_{ij}^f, R_m\right) + \dfrac{\partial f}{\partial D} dD}{\dfrac{\partial f}{\partial \sigma_{ij}} \overline{\overline{C}} \dfrac{\partial g}{\partial \sigma_{ij}} - \dfrac{\partial f}{\partial R_m} \dfrac{\partial R_m}{\partial \gamma_p} dX_p} \text{ with } dD = \dot{D}(t) = \gamma\left(R_m(t) - D(t)\right) \quad [4.14]$$

In the absence of degradation ($dD = 0$), this last equation becomes similar to the Equation [4.10]. It shows that the plastic strains $\varepsilon_{ij}^p = \lambda \dfrac{\partial g}{\partial \sigma_{ij}}$ can be split into two parts: one part corresponds to the instantaneous behaviour (designated by the index ‘sh’) and the other part corresponds to time-dependent behaviour (designated by the index ‘lo’):

$$\varepsilon_{ij}^p = \varepsilon_{ij,sh}^p + \varepsilon_{ij,lo}^p \text{ and } \lambda \frac{\partial g}{\partial \sigma_{ij}} = \left(\lambda_{sh} + \lambda_{lo}\right) \frac{\partial g}{\partial \sigma_{ij}} \quad [4.15]$$

$$\text{with: } \lambda_{sh} = \frac{f\left(\sigma_{ij}^f, R_m\right)}{\dfrac{\partial f}{\partial \sigma_{ij}} \overline{\overline{C}} \dfrac{\partial g}{\partial \sigma_{ij}} - \dfrac{\partial f}{\partial R_m} \dfrac{\partial R_m}{\partial \gamma_p} dX_p} \text{ and } \lambda_{lo} = \frac{\dfrac{\partial f}{\partial D} dD}{\dfrac{\partial f}{\partial \sigma_{ij}} \overline{\overline{C}} \dfrac{\partial g}{\partial \sigma_{ij}} - \dfrac{\partial f}{\partial R_m} \dfrac{\partial R_m}{\partial \gamma_p} dX_p}$$

4.3 Application to shallow chalk underground cavities

4.3.1 Geometric characteristics

Based on geological investigations of the underground quarries of North France, it was shown that eighty percent of the excavations in this region were performed by the method of rooms and

pillars (Ineris, 2007, and Ville de Lille 2013). In such type of exploitations, a wide range of geometric parameters can be integrated in the numerical study (Figure 4.1a). However, the focus of this chapter lies on demonstrating the effect of joint degradation on the time dependent behaviour of quarries rather than presenting the effect of geometry. Therefore, a case of study with certain geometric characteristics inspired from the quarries of North France is modelled:

– width of pillar W=4 m,
– height of pillar H=3 m,
– spacing between adjacent pillars L= 3 m,
– height of overburden: h(chalk) = 7 m + h(silt) = 3 m (Figure 4.1b).

Concerning the joints orientation, a sketch is offered to make the notations (angles) used in this study clear (Figure 4.1c). Assuming that the lower substratum is stiff and contributes to have low influence on these values, the depth of the model is taken 1.5 m. In a multi-pillar quarry where identical dimensions of pillars are assumed, a symmetric model can be generated where one half of the room-and-pillar cavity is to be modelled with appropriately assigned boundary conditions (Figure 4.1b). The normal displacements on lateral faces of the model are blocked. For bottom plane at the base, displacements in 3 directions (x, y, and z) are blocked.

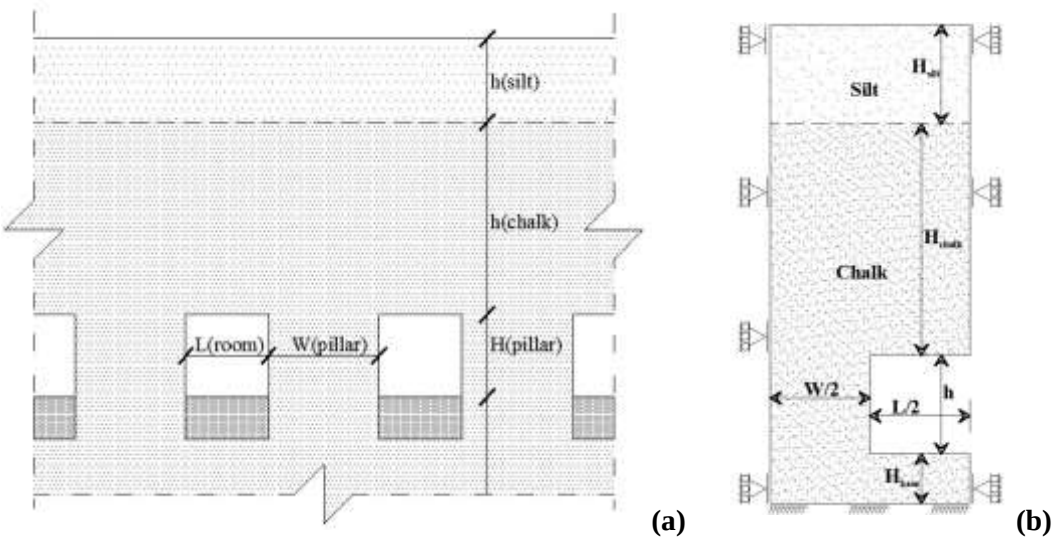

Figure 4.1. Sketch of the **(a)** multi-pillar system, **(b)** cavity symmetric model with assigned boundary conditions.

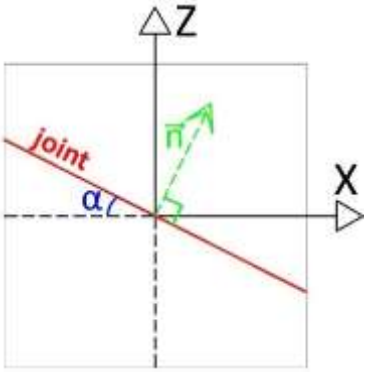

Figure 4.1c. Sketch showing the joint inclination angle α in a zone of the jointed chalk continuum.

4.3.2 Ground properties and constitutive models

4.3.2.1 Soil properties

In this framework, initially same elastic properties are used for the matrix and the joint set (E = 250 MPa, ν = 0.3). Then, irreversible strains in the matrix and in the joint are simulated by considering two different failure criteria. They are both associated to the strength properties of the matrix (c_m, φ_m, ψ_m) (designating the cohesion, friction angle, and dilation angle respectively) or the joint (c_j, φ_j, ψ_j). Normally, joints or weak planes where the sliding is localized are of shear strength properties lower than those of the matrix. The matrix is described by an elastic perfectly plastic model with a Mohr Coulomb failure criterion f_m and a non-associated flow rule g_m:

$$f_m(\sigma_{ij}) = (\sigma_1 - \sigma_3) - (\sigma_1 + \sigma_3)\sin(\varphi_m) - 2c_m\cos(\varphi_m) \quad [4.16]$$

$$g_m(\sigma_{ij}) = (\sigma_1 - \sigma_3) - (\sigma_1 + \sigma_3)\sin(\psi_m) \quad [4.17]$$

The joint set is described by an elastic perfectly plastic model with an oriented yield criterion that accounts for their spatial orientation into the chalk matrix (Rafeh et al. 2015):

$$f_j(\sigma_{ij}, R_m) = \tau - \sigma_n \tan(\varphi_j) - c_j \quad [4.18]$$

$$g_j(\sigma_{ij}, R_m) = \tau - \sigma_n \tan(\psi_j) \quad [4.19]$$

where f_j and g_j are the failure and potential surfaces respectively, of the defined joint set j. The tangential and normal stresses, τ and σ_n respectively, are obtained from the full stress tensor σ_{ij} by considering the vector $\vec{n}$ defining the orientation of the joint known as weakness plane:

$$\sigma_n = \left\| \left(\sigma_{ij}.\vec{n}\right)\vec{n} \right\| \text{ and } \tau = \left\| \sigma_{ij}.\vec{n} - \sigma_n.\vec{n} \right\| \quad [4.20]$$

This constitutive model using the Mohr Coulomb criterion for the chalk matrix and the oriented yield criterion for the joints is implemented in the finite difference code FLAC^{3D} (Rafeh et al. 2015). It is then assigned to the chalk continuum of the quarry where numerical models are simulated. The stress state related to the matrix criterion is checked and plastic corrections are done if the stress state exceeds the failure surface. This new stress state is then verified upon the joint criterion and plastic corrections are done if necessary. In this part of the work we intend to set similar properties for matrix and joints (c = 200 kPa, φ = 30°, ψ= 5°) in order to show clearly the effect of degradation revealed later with time after it is being applied only to the joints. These values, as well as the previous ones corresponding to the elastic part of the constitutive law, are supposed to represent the average behaviour of the chalk in North France (see for example Mikolajczak, 1996). In order to account for time degradation effects into the joints, an isotropic hardening function R_m is considered and the failure criterion is modified as follows:

$$R_m = R_{mi} + \left(R_{mf} - R_{mi}\right)\frac{\gamma_p}{B + \gamma_p} \quad [4.21]$$

$$f_j\left(\sigma_{ij}, R_m\right) = \tau - \left(\sigma_n \tan\left(\varphi_j\right) + c_j\right)R_m \quad [4.22]$$

where R_{mi} and R_{mf} are the initial and final values of R_m.

For the current analysis, the parameter B that is related to the plastic hardening rate is taken equal to 0.0027 which is in accordance with the value proposed by Shao et al. (2003) which is based on experimental findings. Besides, this value permits to obtain relevant results in comparison to observations in the quarries. Due to the relation between B and γ_p, as B decreases, then R_m reaches the maximum faster. The values corresponding to initial yield and failure are chosen as R_{mi} = 0.9 and R_{mf} = 1.2 respectively by which the strength properties in plastic domain are permitted to vary within a certain range. By this assumption, and if we substitute the values of

R_{mi} and R_{mf} in the previous equation [4.22], the apparent friction angle which is basically taken equal to 30° is permitted to vary from 27.5° at initial yield state reaching a maximum value of 35° at maximum hardening when R_m is above 1 already ($R_m = R_{mf} = 1.2$).
The degradation factor D is taken into account as presented in the previous section (section 2):

$$f_j(\sigma_{ij}, R_m) = \tau - (\sigma_n \tan(\varphi_j) + c_j) R_m (1 - \alpha D) \quad [4.23]$$

Table 4.2 includes the values of the mechanical properties of the two different soil layers considered in this study: chalk and silt.

4.3.2.2 Calculation steps

The calculation is performed into three main steps:

– (i): initial stress state by applying gravity volumetric forces, the initial earth pressure coefficient at rest K_0 is equal to $\nu/(1-\nu)$;

– (ii): underground excavation by applying de-confining forces on the free edges of the mesh and considering the matrix and the joints with the constitutive law described above. During this step, the hardening function R_m increases but the degradation rate dD is supposed to be equal to zero. At the end of this step, at each integration point, the hardening parameter is different according to the stress and strain paths followed in each integration point during the excavation.

– (iii): simulation of the time degradation approach. As the hardening parameter differs from one integration point to another, the evolution of the degradation factor D will be specific at each integration point taking into account the stress and strain paths. This point is very specific to the time-dependent degradation approach in comparison with the reduction strength approach where the decrease of shear properties is the same for all integration points. The time increment is equal to 1 day = 86400 seconds.

Table 4.2. Values of mechanical soil properties

Soil		Elastic properties	Plastic properties		
Chalk	Matrix	E = 250 MPa ν = 0.3	c_m = 200 kPa φ_m = 30° ψ_m = 5°		
	Joint		c_j= 200 kPa φ_j = 30° ψ_j = 5°	R_{mi} = 0.9 R_{mf} = 1.2 B = 0.0027	1.1574e-9 s^{-1} ≤ γ ≤ 1.1574e-5 s^{-1}
Silt		E = 10 MPa ν = 0.3	c =10 kPa φ = 30° ψ = 5°		

4.4 Analysis of the time-dependent behaviour of the cavity

4.4.1 Evolution of displacements and strains law

4.4.1.1 First results

The time analysis is being performed using the numerical software FLAC^{3D} (Itasca, 2009) where the oriented yield criteria and the time-dependent approach have been developed and implemented.

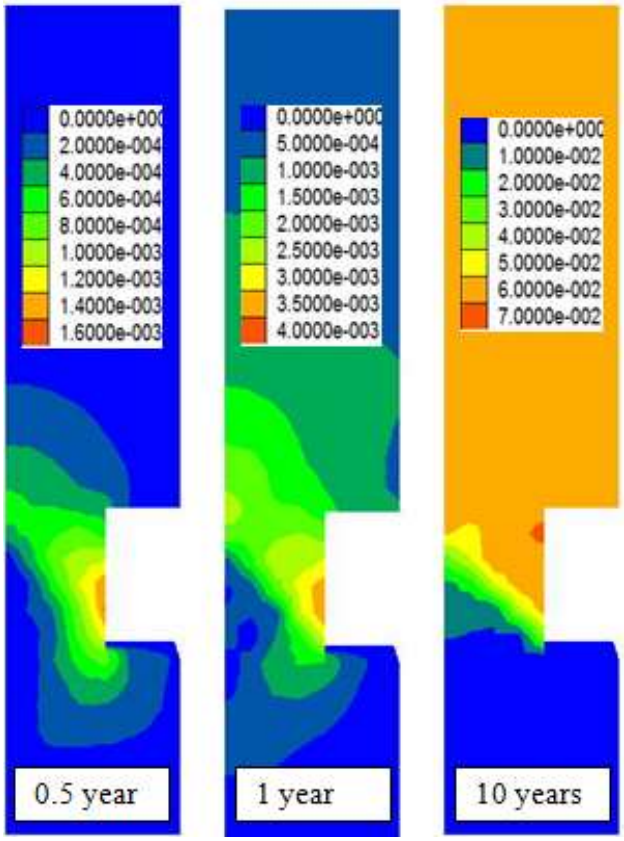

Figure 4.2. Evolution of the displacement (m) contours with time. Case of joint set inclined at $\alpha = 45°$ and $\gamma = 10^{-1}(1/\Delta t)$.

This provides an insight about the location of the weakness zones in the cavity model and the foreseeable failure mechanisms involved with time. The displacement distribution in the underground cavity when joints are inclined at 45° is presented at different time lags after excavation. As observed (Figure 4.2), higher displacements are concentrated at the pillar when the joints are inclined. As time passes, displacements increase and become localized forming clear shear band in the direction of the inclined joint set.

4.4.1.2 Influence of joints orientation

Displacement distribution

The joint set orientation has an influence on the extension of failure zones with time and thus on the displacement distribution. This latter is illustrated in the room-and-pillar cavity model after 10 years of degradation considering 5 cases of joints inclinations: 0˚, 30˚, 45˚, 60˚, and 90˚ (Figure 4.3).

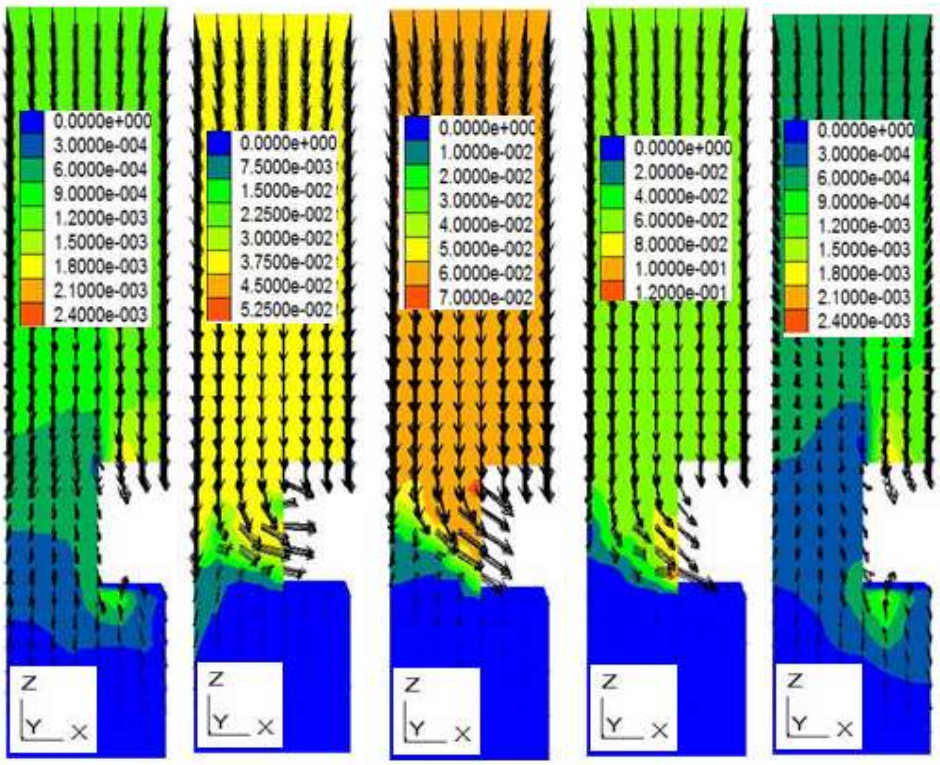

Figure 4.3. Displacements at 10 years after excavation. Joint set inclined at α = 0°, 30°, 45°, 60°, and 90°(from left to right).

In case of inclined joints, the displacement values are concentrated and localized at the pillar. Shear bands take the orientation of the joints defined. In the case of horizontal or vertical joints, higher displacements are obtained in the roof than in the pillar. These displacements however are still considered very low with respect to those created in the pillar in case of inclined joints. These results give the same trend as the previous analysis done using the shear strength reduction approach to understand the effect of joint inclinations on the deformational behaviour of similar quarries (Rafeh et al. 2015). The localization of displacements is affected by the orientation of the joints. In the case of vertical or horizontal joints, low displacements are stacked in the roof (Figure 4.3). This can be explained by the fact that horizontal joints seem to act as separating layers that stack the imposed vertical weight of layers above the galleries in the roof instead of transferring it to the pillars. In this case, shear stresses are distributed before being directly transferred to the pillar. In case of vertical joint sets, this is due to the arching effect exhibited at roof of the gallery due to lateral confinement which is not disturbed by the presence of vertical

discontinuities. On contrary, in the presence of inclined joints, the pillar is expected to feature high displacements. Inclined weak planes drive the excessive stresses that reach the pillar to attack its opposite faces at one hand, and be blocked there on the other hand. This creates shear bands since no continuity is available at lateral faces of the pillar so that the excessive stresses can be transferred to a more supportive zone in the structure. As shown, the displacement contours appear to be at same inclination α of the joint set (Figure 4.3).

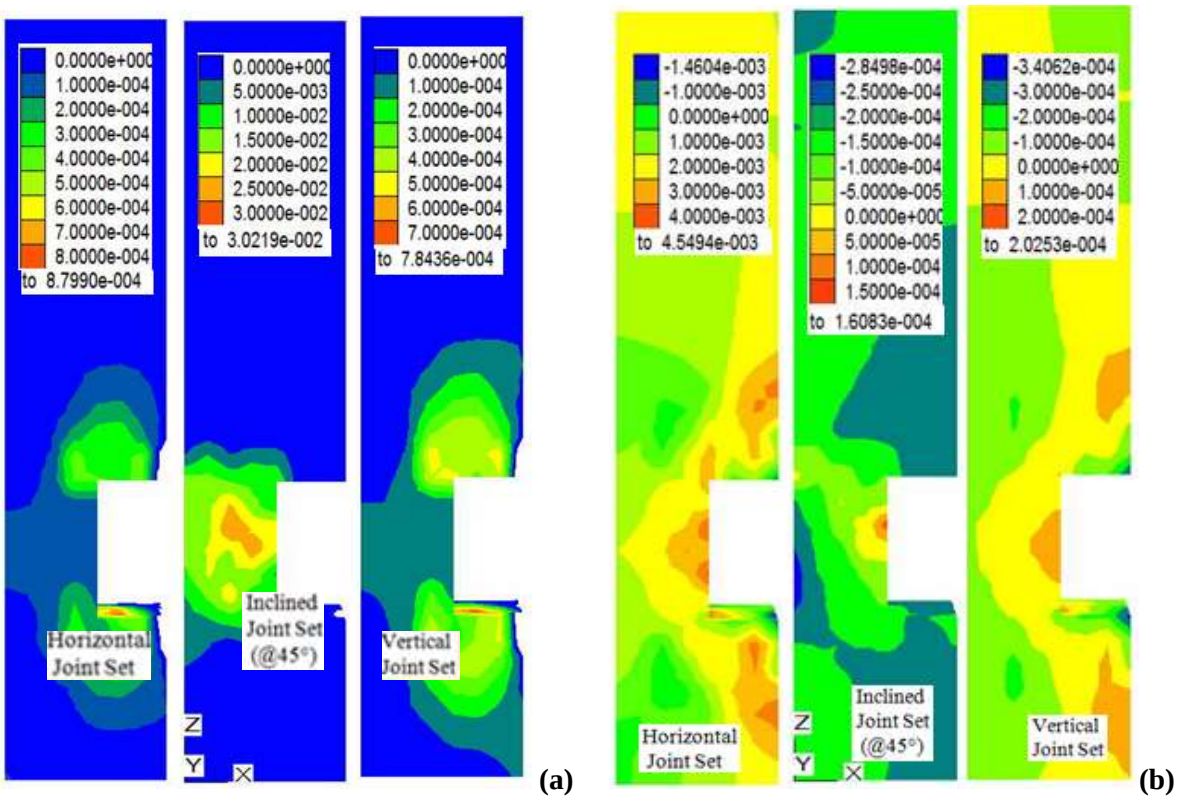

Figure 4.4. (a) Shear and **(b)** volumetric strain distribution after 10 years from excavation for different joint set inclinations.

Shear strain and volumetric strain distribution

After 10 years from excavation, the distribution of shear strains and volumetric strains is simulated for 3 different cases of joint set orientations: horizontal joint set, inclined joint set (α = 45°), and vertical joint set. As shown for both sets of figures (Figure 4.4), strains are observed at the pillar when the joints are inclined. Different mechanisms are associated when the joints are horizontal or vertical, i.e. perpendicular or parallel to the load direction which is vertically downwards. In either of these cases, non-zero positive strains are observed in the roof and the

floor. In the case of vertical or horizontal joints, shear strains are concentrated in the roof and floor whereas in case of inclined jointed, shear strains appear in the pillar (Figure 4.4a). This matches the previous observations concerning the distribution of displacements. Positive volumetric strain values accumulated particularly at the pillar indicate the dilative behaviour at this zone (Figure 4.4b). This is due to the degradation of the pillar exhibited with time.

4.4.2 Evolution of internal parameters R_m and D

4.4.2.1 Evolution of the degradation factor D

According to the degradation approach developed before, the degradation generated in the quarry upon time is represented by a degradation factor D (Figure 4.5).

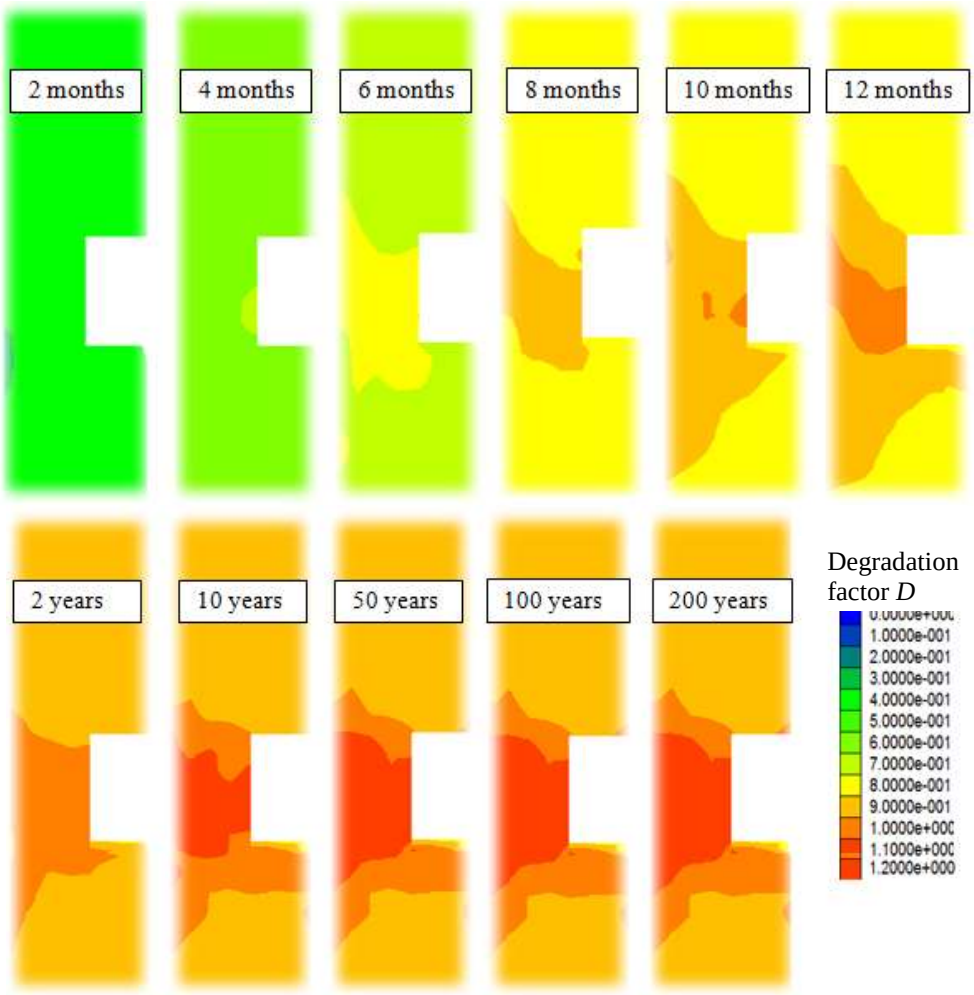

Figure 4.5. Evolution of the degradation factor D in the cavity model with joint set inclined at 45°.

The evolution of *D* depends on the evolution of the plastic deviatoric strains in the zones of the chalk continuum and thus it is directly related to the stress distribution in these zones. Hence, even though at the initial state, i.e. after the excavation (at time t = 0), the degradation is generated uniformly on all zones of the continuum, with time, unequal degradation factors are generated. This is due to the non-identical evolution of stresses in the zones which leads to a non-homogeneous distribution of plastic strains. In order to provide a better understanding of this concept, the distribution of the degradation based on the values of degradation factor obtained in each zone of the quarry under study is provided for different time lags (Figure 4.5).

The results presented show the distribution of the degradation factor *D* after 2, 4, 6, 8, 10, and 12 months and then after 2, 10, 50, 100, and 200 years from the time of excavation (at t = 0) (Figure 4.5). Note that in the study case presented, joints are inclined at an angle equal to 45° from the normal axis (z-axis). The degradation factor values are greater at the pillar which means that having fractures at 45° of inclination will affect the pillar zone rather than the roof. Different joint inclinations might lead to different degradation mechanisms. The influence of joint inclination is discussed afterwards.

4.4.2.2 Variation *D*: evolution with respect to R_m

According to the definition of the degradation function (Equation [4.6]), *D(t)* which is activated directly after excavation (t = 0), and depends on the evolution of the plastic hardening R_m of the chalk. In order to illustrate this concept, the average of the evolution of the hardening parameter R_m and the degradation factor *D* over all zones of the massive are plotted ($R_m(av)$ and *D(av)*) for the same time lags mentioned before during the first 200 years after excavation) (Figure 4.6). The evolution of degradation increases steeply in almost the first 2 years, where it starts to become steady afterwards. At this stage, the graph of *D* forms a horizontal asymptote with R_m where the maximum degradation factor achieved does not exceed R_{mf}. Numerical results are coherent with the assumptions considered for this approach. Initial value of R_m (at t = 0) is taken 0.9, R_{mi} = 0.9, and both functions, R_m and *D* are increasing. Since the evolution of both R_m and *D* is not homogeneous among the zones, i.e. some zones degrade to the maximum (*D* = 1.2) while others do not, then *D(av)* and $R_m(av)$ are always less than 1.2. The maximum values of R_m and *D* ($R_m(max)$ and *D(max)*) obtained at each time step are also plotted. After decades of degradation, *D* that corresponds to the mostly degraded zone tends to reach the maximum which is equal to

the max of R_m, R_{mf} = 1.2 (Figure 4.6). Note that the presented case refers to a value of $\gamma = 10^{-1}(1/\Delta t)$ where the time step taken is 1 day. The effect of γ is studied in the next paragraph.

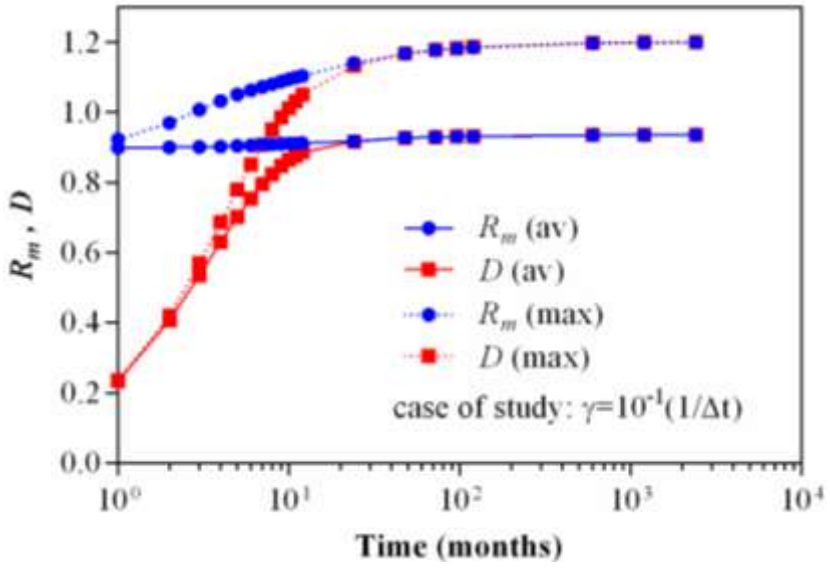

Figure 4.6. Evolution of the hardening parameter R_m and the degradation factor D with time

4.4.3 Evolution of degradation at different admissible degradation amounts

Aiming to give a descriptive explanation of the non-homogeneous degradation phenomenon taking place in the cavity model, a criterion to eliminate the massive zones with degradation factors beyond a certain limit is developed and integrated in the numerical analysis. This permits to view the kinematics of the degradation process and how would it develop with time in the room-and-pillar quarry. The case presented is with joints inclined at 45° where the pillar is the structural element which is subjected to greatest degradation as shown before. Hence, the rupture reaches this part of the quarry at first and most degraded blocks in the pillar start to fall with time. If the percentage of admissible degradation is greater, then the range of the increase of degradation without occurrence of failure is wider and the falling of the blocks for the same case of study start later. This is shown by comparing the 3 sets of figures representing 3 different amounts of admissible degradation (Figure 4.7).

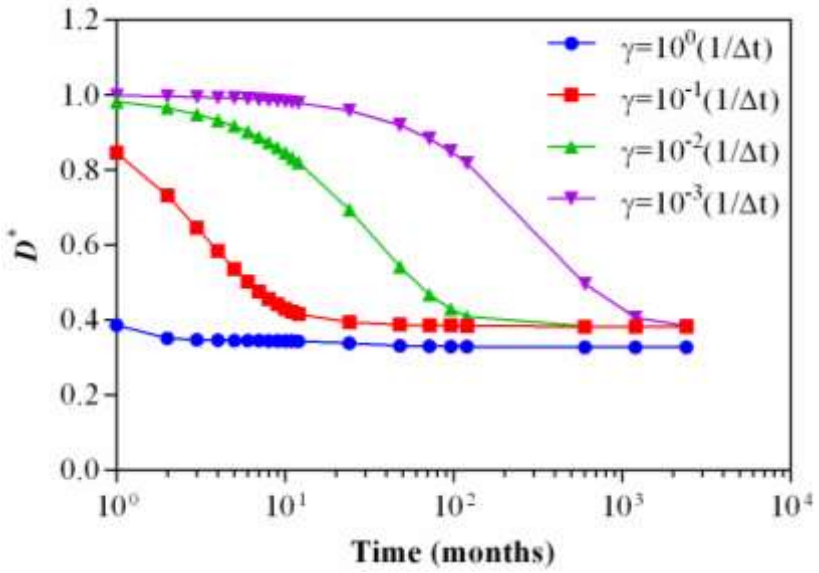

Figure 4.8. Degradation rate (average in massive) for different cases of γ (joint set inclined at 45°).

The percentage of admissible degradation is calculated after selecting a limit for the degradation factor *D*. For example, in order to have all zones with *D* greater than 0.909 eliminated, it means that the admissible degradation in this case is 60% (α x *D* x 100 = 0.66 x 0.909 x 100 ≈ 60). Recall that in all the simulations run for this study, the maximum admissible degradation allowed is ≈ 80% (where *D* = 1.2 and D* = (1-*αD*) = 0.2 with α = 0.66). The results presented in figure 4.8 show that the form of the degraded pillar achieved after 1 year of degradation with the limit of 60% admissible degradation is somehow similar to that achieved after 6 years with 70% as limit of admissible degradation and after 30 years when the admissible degradation is 78%.

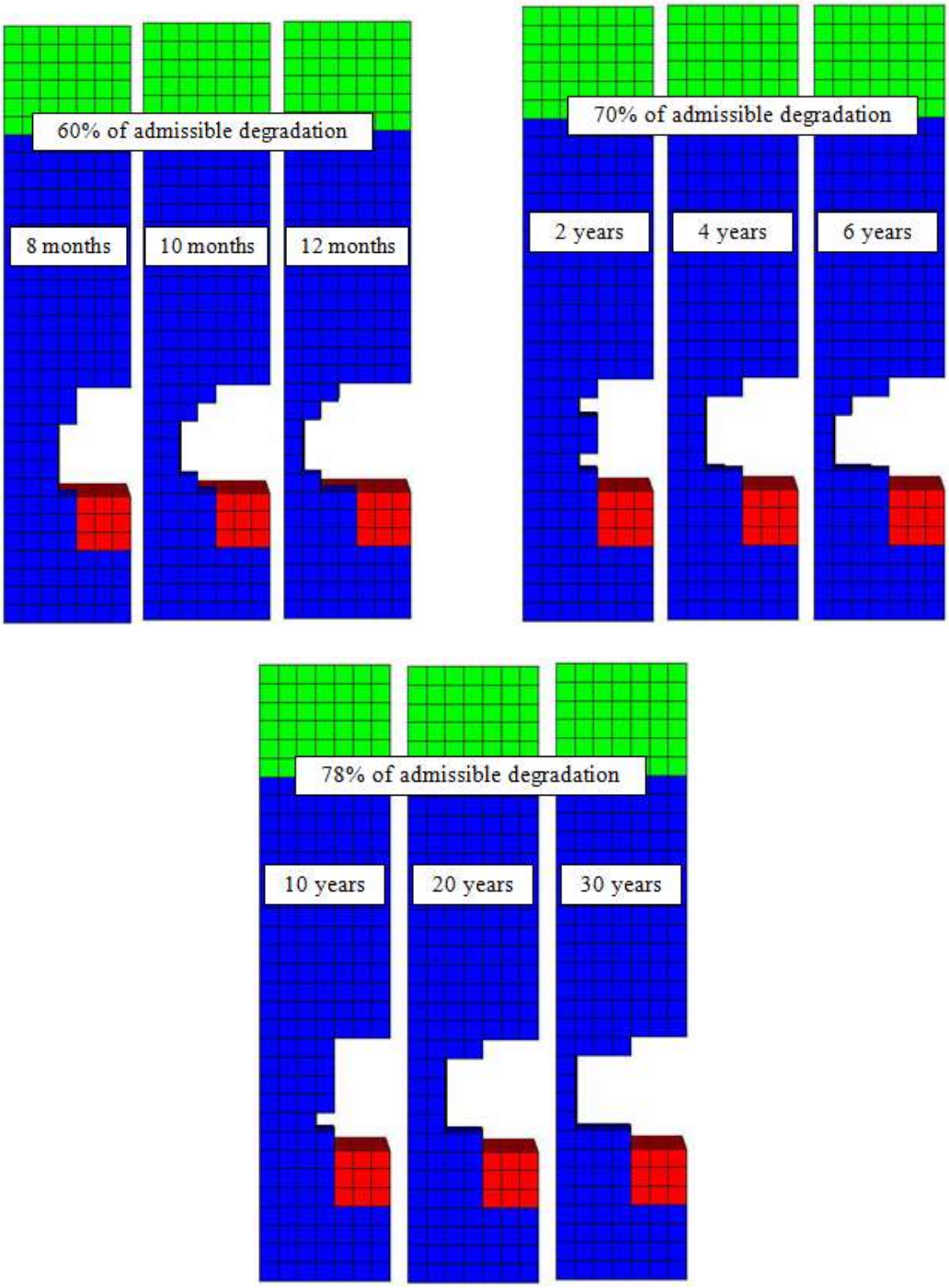

Figure 4.7. Degradation evolution at different admissible degradation amounts.

4.4.4 Effect of the material constant γ on the evolution of R_m and D

By definition (Equation [4.2]), the derivative of the degradation factor with respect to time $\dot{D}(t)$ is proportionally related to the material constant γ. Therefore, the degradation rate and hence the degradation evolution are affected by the value of γ. This latter, γ, is a positive constant less than 1. Greater values of γ mean that the degradation of the quarry goes faster. Besides, the plastic multiplier λ depends on *dD* (Equation [4.14]) and thus the accumulated plastic strains are influenced by its variation. For a better emphasis of the role of γ on the degradation process, a parametric study considering five different values γ is conducted. In the numerical approach developed for the integration of degradation, the material constant γ is defined in terms of the time step (γ = k*(1/Δt)) where k is a positive constant. In all the numerical simulations run for this study, the time step is fixed to 1 day which is equivalent to 86400 seconds. Five values *k* are considered (10^0, 10^{-1}, 10^{-2}, 10^{-3}, and 10^{-4}) and consequently the parametric study is based on five different values γ. The results are demonstrated in terms of average and maximum values for R_m (Figure 4.9) and *D* (Figure 4.10). Two basic outcomes can be drawn out from the obtained graphs. First, during the same time interval, if γ is greater, then the plastic hardening represented by R_m increases and degradation factor *D* also increases.

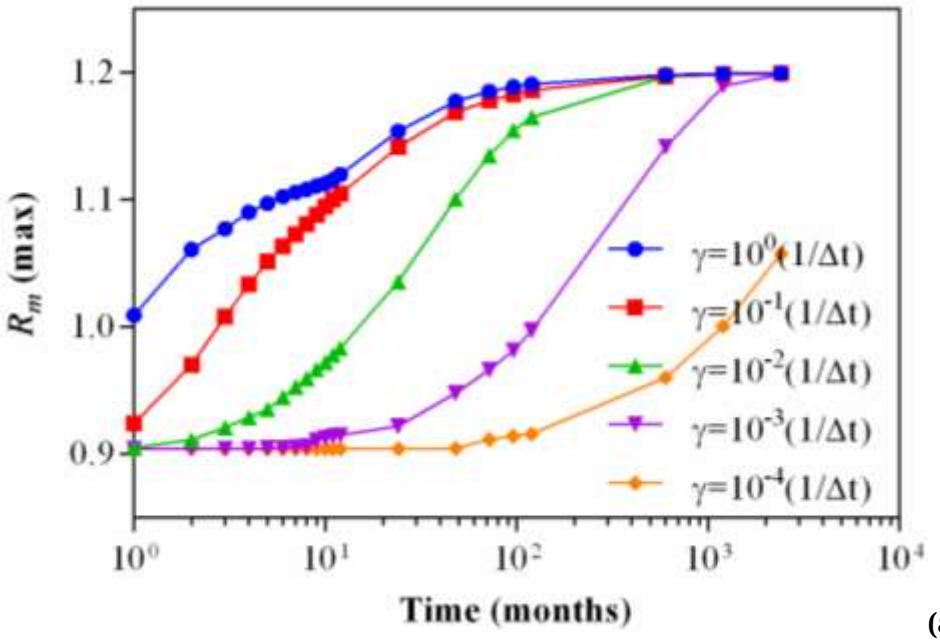

(a)

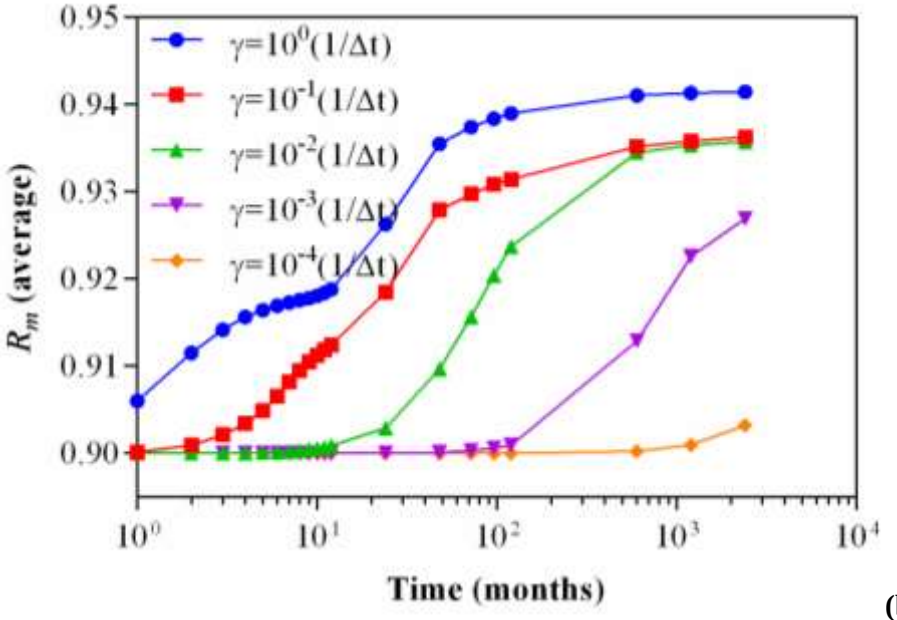

(b)

Figure 4.9. Evolution of **(a)** R_m, maximum and **(b)** average values, for different cases of γ.

This is clear in the early time intervals (first year or even first ten years) just after excavation where the evolution of the values R_m and D is supposed to be greatly exhibited as shown before (Figure 4.6). For example, at one year, there is a remarkable difference in $R_m(max)$ achieved at cases of k = 10^{-1}, 10^{-2}, and 10^{-3}. This also applies for the degradation factor D.

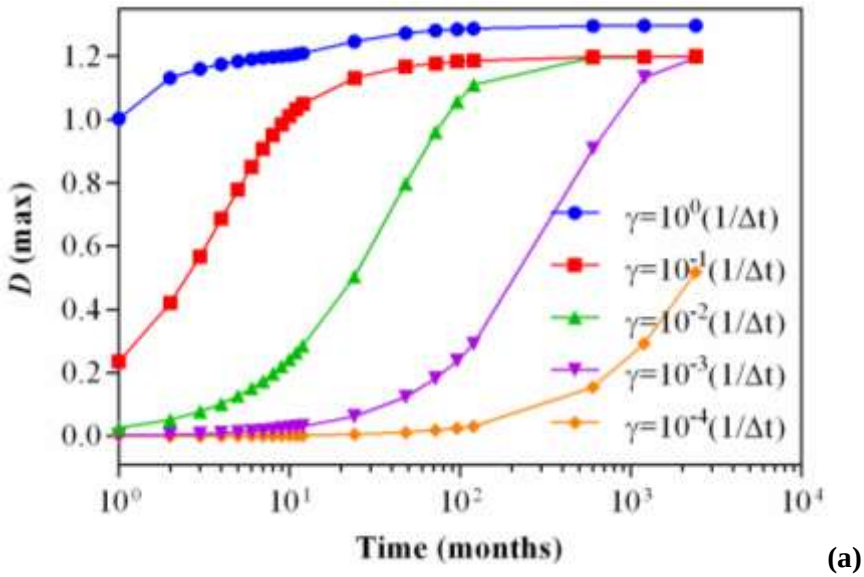

(a)

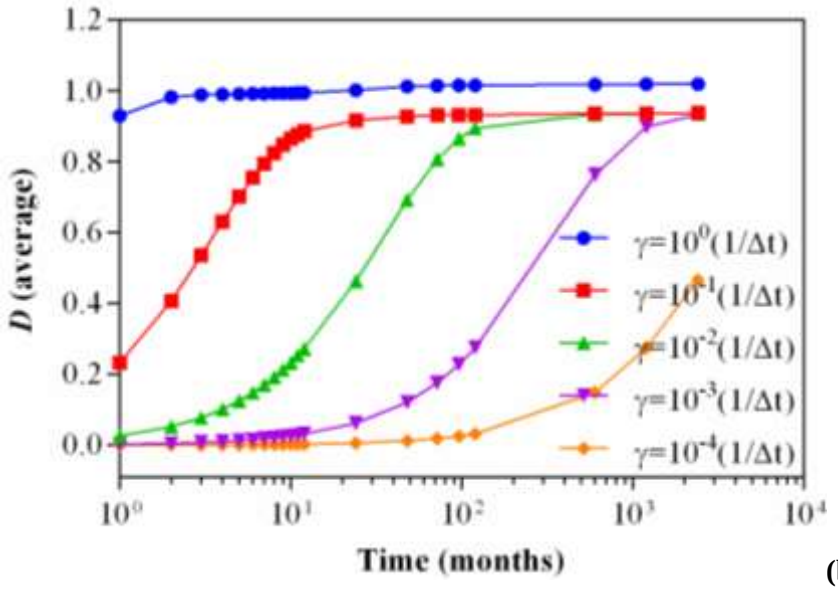

Figure 4.10. Evolution of **(a)** D, maximum and **(b)** average values, for different cases of γ.

Next, the evolution of both R_m and *D* varies for different values γ. The degradation rate is affected by the choice of the material constant γ and this verifies the hypothesis of the approach (Equation [4.2]). An extended discussion on this issue is provided in the coming paragraph. On the other hand, a very low value of γ (with k = 10^{-4} for example) imposes a very slow degradation evolution which turns to be negligible in the presented case of study, especially during the first 50 years. Also, a high value of γ (with k = 10^{0} for example) implements a rapid degradation process which might lead to early instability in the quarry structure. This justifies the values of *D* observed exceeding the value of R_{mf} = 1.2 (Figure 4.10b, γ = $10^{0}(1/\Delta t)$).

Knowing that in case of inclined joints, the pillar is subjected to degradation more than the roof and thus the degradation factor is obtained higher at the pillar than in other parts of the cavity model (Figure 4.5), then the average of *D* values corresponding to the pillar zones merely is plotted (Figure 4.11).

In comparison with the average of *D* corresponding to all the massive '*D*(average)', '*D* of Pillar (average)' shows greater values during the same time interval. This justifies again the previous hypothesis. At the end, in order to show the deviation of the degradation factors in the massive from their average, the coefficient of variation of *D*, i.e. the ratio of the standard deviation to the average of *D*, is demonstrated (Figure 4.12).

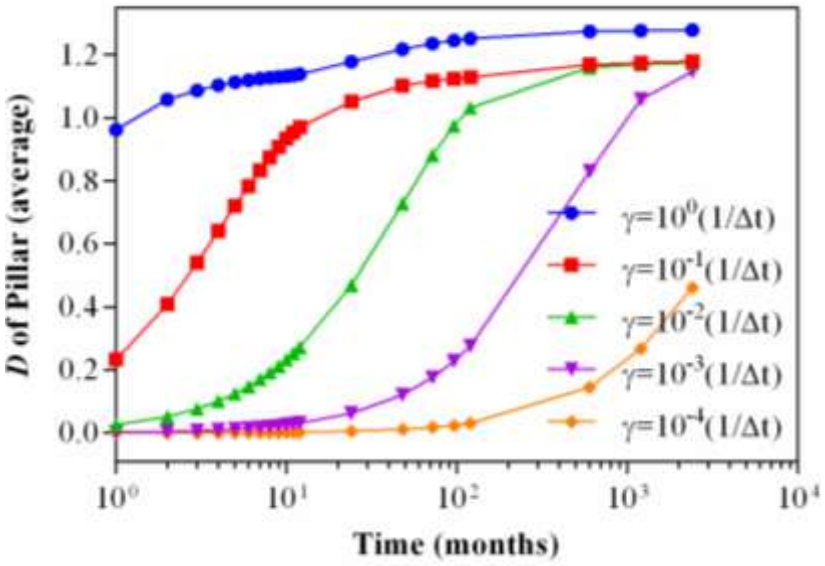

Figure 4.11. Evolution of degradation in the pillar considering the 5 different cases of γ:

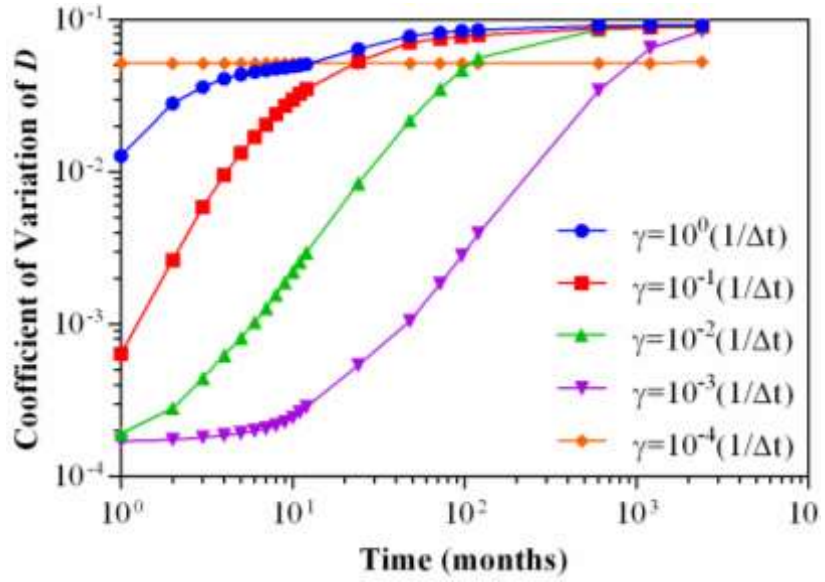

Figure 4.12. Evolution of the coefficient of variation of *D* considering the 5 different cases of γ:

Results show that the coefficient of variation increases with time. This is due to the fact that with time, the non-homogeneous evolution of degradation is activated and the degradation factor in some zones is increasing while in others it might be increasing very slightly. Low values of the coefficient of variation mean that the degradation is little whereas high values mean that the degradation is higher and more considerable. Concerning the different values of γ, and knowing

that *D* increases as γ increase (Figures 4.10 and 4.11), then so it is the case for the coefficient of variation of *D* (Figure 4.12). The graph corresponding to the low γ (with k = 10^{-4}) shows that this case does not properly undergo the degradation phenomenon (Figure 4.12). This can be due to the negligible degradation achieved in this case where the proposed approach might be no more fitting (Figure 4.11).

4.4.5 Effect of joint inclination on R_m and *D*

Different zones of the cavity model undergo different degradation amounts and thus show different degradation factors. Since the applied hypothesis activates the degradation merely on the identified joints, then degradation factors obtained are directly influenced by the joints characterization.

Particularly, the joint inclination which is supposed to have a considerable effect on the deformation profiles and hence the failure mechanisms, is as well expected to have an influence on the degradation intensity and distribution. For this reason, different cases of joint set orientations are modelled. To compare the progression of corresponding degradation factors, the arithmetic means of R_m and *D* all over the zones are plotted with respect to time at different joint inclinations (α) (Figures 4.13 and 4.14a).

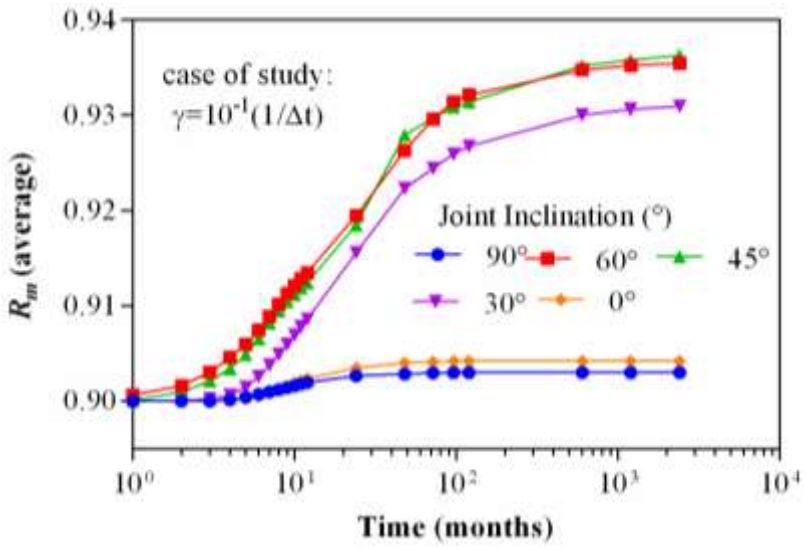

(a)

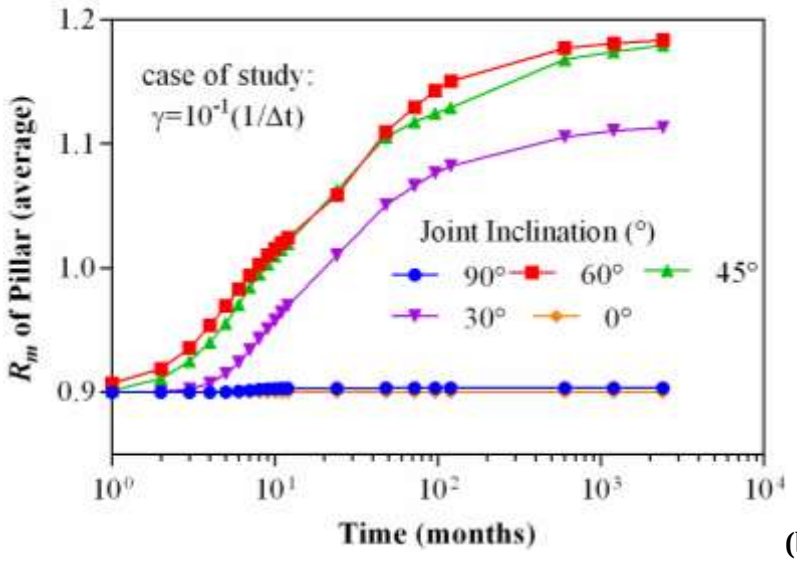

(b)

Figure 4.13. Evolution of **(a)** R_m(average) and **(b)** R_m of Pillar (average) with time, for different cases of joint inclination (α).

Results show that the degradation factor is low when the degradation is imposed to joints which are vertical or horizontal. However, inducing degradation to inclined joints will generate a greater degrading effect on the chalk continuum and thus the underground cavity. In this case, the degradation will be concentrated in the pillar (Figure 4.5) whereas horizontal or vertical joints lead to a degradation distribution which is more homogeneous.

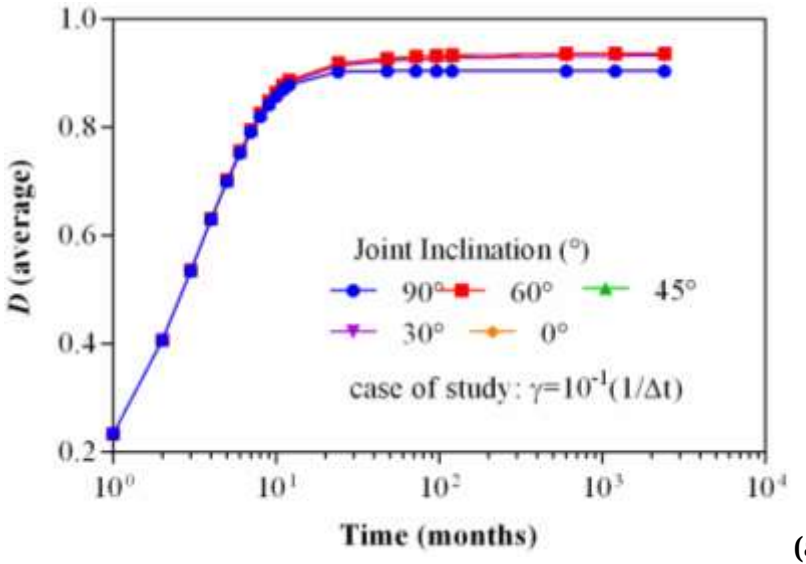

(a)

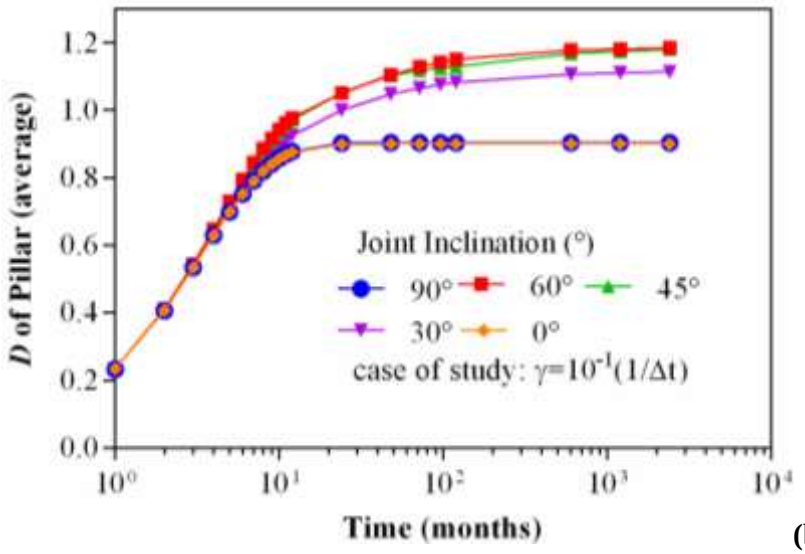

Figure 4.14. Evolution of **(a)** D(average) and **(b)** *D* of Pillar (average) with time, for different cases of joint inclination (α).

The choice of joint orientations has an influence on the extension of failure zones with time. Numerical analysis shows that the effect of vertical and horizontal joints (0° and 90° respectively) is small in comparison with that of inclined joints (30°, 45°, and 60°). Since the greater effect of degradation is observed in the case of inclined joints (Figures 4.13 and 4.14 on left), and since inclined joints affect the pillar rather than the roof as described before, an average of the degradation factors relative to the zones of the pillar is plotted (Figures 4.13 and 4.14 on right). Knowing that the developed approach applies the degradation on the joints, the results show that the degradation in the pillar is activated more when the joints are inclined. Otherwise, the average degradation of the pillar slightly exceeds the initial value of R_m which is $R_{mi} = 0.9$.

4.4.6 Degradation rate

According to the definition of the degradation approach, the degradation rate $\dot{D}(t)$ can be evaluated in terms of γ, R_m and D (Equation [4.2]). Plotting the variation of the degradation rate with respect to time for different cases of γ, gives an idea about the evolution of degradation in the quarry at different time phases after excavation. It also shows the dependency of $\dot{D}(t)$ on γ. Degradation rates are simulated at each zone of the chalk quarry. An average of the obtained value is traced and presented (Figure 4.15). Results show that the degradation rate is always

higher at earlier period directly after excavation. As the creep time increases, the degradation evolution becomes slower and the degradation rate decreases until it becomes null and no additional degradation takes place. Besides, at higher γ, the degradation rate is greater which is evident according to the proportional relation between $\dot{D}(t)$ and γ (Equation [4.2]). An exception is recognized in the case of high γ (with k = 10^0). In this case, the degradation is very fast and from the first month, the degradation factor D exceeds R_m (D = 0.9739 where R_m = 0.9035). For this reason, (R_m – D) is negative, and thus $\dot{D}(t)$ is negative too. In such a case, the degradation approach does not apply. By definition, the degradation factor obtained is always less than R_m and thus the degradation rate, $\dot{D}(t)$, is maintained positive knowing that γ is also positive. However, the double derivative of the degradation factor, $\ddot{D}(t)$, is negative meaning that the degradation rate, which is positive, decreases with time (D > 0, $\dot{D}(t) > 0$, $\ddot{D}(t) < 0$). Hereby, the material constant γ plays a basic role in the activation process of the degradation approach defined. For the rest of the integrated numerical simulations, γ is taken equal to $10^{-1}(1/\Delta t)$. This is based on the data in literature containing in situ experimental results related to similar material types (Shao et al. 2003).

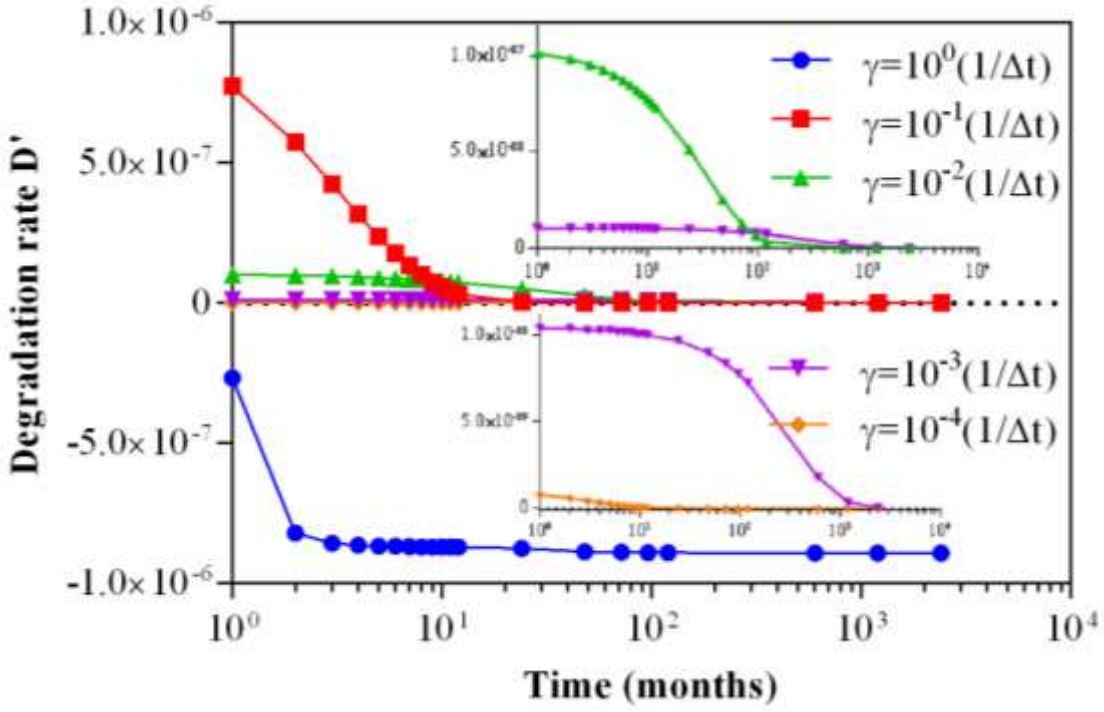

Figure 4.15. Degradation rate (average in massive) for different cases of γ (joint set inclined at 45°).

4.5 Comparison between degradation and c/phi reduction approach

4.5.1 Principles

In the analysis of the strain and failure mechanisms of unexploited quarries, it is of quite interest to demonstrate the time dependent degradation behaviour and study the influence of its evolution on the deformation profiles. This could provide a better understanding of the physical aspects associated with the mechanical behaviour of the abandoned quarry upon time. From a different point of view, investigating the stability of such quarries can be directly achieved by a shear strength reduction approach. A shear strength reduction approach is also applied on the joint set and integrated in the mechanical analysis of the chalk quarry under study. At each increment which represents an increased reduction in the joint shear properties c_j and φ_j, where c_j and φ_j refer to the cohesion and friction angle of the joint respectively, a reduction factor R_f, that corresponds to the ratio of the original joint shear properties to the current reduced joint shear properties, is calculated. This approach, noted here as c_j/φ_j reduction, is previously performed and discussed before by the authors (Rafeh et al. 2015). However, the aim for the meantime is to elaborate a comparison between the outcomes of the two approaches, the time-dependent degradation approach, and the c_j/φ_j reduction approach.

4.5.2 Comparison between the degradation and the reduction approaches

In order to compare the two considered approaches, a unified method must be selected as a reference for this comparison. In this case, the percentage of either degradation or reduction is used. Concerning the time-dependent degradation approach, and according to the definition of the joint failure function for long term behaviour (Equation [4.11]), the shear properties integrated in the failure function are factored by the degradation function $D^* = (1-\alpha D)$. In the case of joint strength reduction approach, and starting from the same original joint failure function (Equation [4.4]), the joint shear properties are factored by the reduction function $1/R_f$. Transforming these two factorizing functions (degradation and reduction) into percentage values

allows the comparison between the analyses relative to both mentioned approaches. A comparison chart is suggested to provide a better understanding of the utilized sequence in each approach (Table 4.3).

Table 4.3. Comparison between the degradation and the c/phi reduction approaches.

	Degradation Approach	Reduction Approach
1	$f_j(\sigma,R_m)=\tau-\left(\sigma_n\tan(\varphi_j)+c_j\right)R_m$	$f_j(\sigma,R_m)=\tau-\left(\sigma_n\tan(\varphi_j)+c_j\right)R_m$
2	$f_j^{deg}(\sigma,R_m)=\tau-\left(\sigma_n\tan(\varphi_j)+c_j\right)R_m(1-\alpha.D)$	$f_j^{red}(\sigma,R_m)=\tau-\left(\sigma_n\frac{\tan(\varphi_j)}{R_f}+\frac{c_j}{R_f}\right)R_m$
3	$f_j^{deg}(\sigma,R_m)=(D^*)\left[f_j(\sigma,R_m)\right]$	$f_j^{red}(\sigma,R_m)=\left(\frac{1}{R_f}\right)\left[f_j(\sigma,R_m)\right]$
4	$\frac{1}{nbz}\left[\sum_1^{nbz}(D^*)\right]\Leftrightarrow\frac{\Sigma(D^*)}{nbz}$	$\frac{1}{nbz}\left[\sum_1^{nbz}\left(\frac{1}{R_f}\right)\right]\Leftrightarrow\frac{1}{R_f}$
5	$\%=100*\left(1-\frac{\Sigma(D^*)}{nbz}\right)$	$\%=100*\left(1-\frac{1}{R_f}\right)$

Note that the equivalence in step 4 is explained by the non-homogeneous evolution of degradation on the joints of different zones of the massive (D and thus D^* is not the same in all zones) and the homogeneous evolution of the shear reduction of the joints of different zones of the massive (1/ R_f are not the same in all zones). Results referring to similar percentages between the two approaches are selected and analysed (Table 4.3). In case of the degradation approach, the degradation percentages refer to the degradation achieved after certain time intervals: 15.41%, 26.83%, 41.62%, 49.81%, 54.41%, 57%, 58.46%, 60.52%, 61.54%, and 61.81% refer to degradation after excavation by 1, 2, 4, 6, 8, 10 and 12 month(s), and then 2, 10, and 100 years respectively. In case of the reduction approach, the reduction percentages refer to the incremental reduction factor R_f values: 16.67%, 28.57%, 37.5%, 44.44%, 50%, 54.55%, 58.33%, 61.54%, 64.29%, and 66.67% refer to R_f equal to 1.2, 1.4, 1.6, 1.8, 2, 2.2, 2.4, 2.6, 2.8, and 3 respectively where 3 is the greatest values of R_f achieved before failure (Figure 4.15).

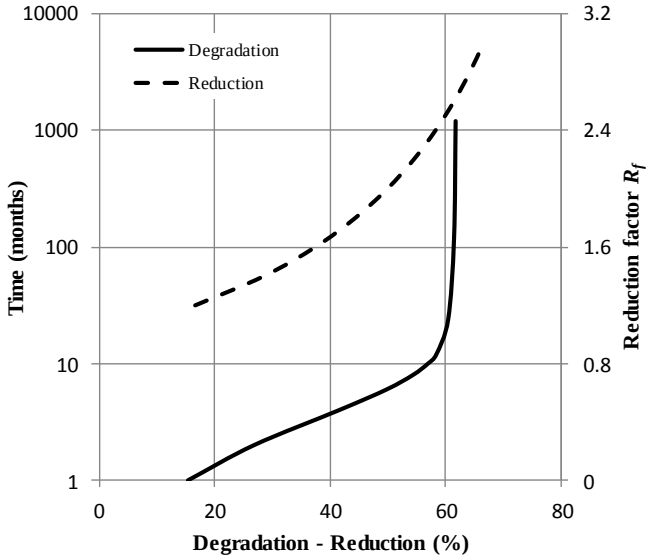

Figure 4.15. Reference base which is the percentage of either degradation or reduction used to represent either time or the reduction factor respectively.

4.5.2.1 Numerical results

In the stability study of underground cavities, numerical methods are considered helpful since it is possible to model the strain profiles and thus get an idea about the deformational behaviour of the cavity and the foreseeable failure mechanisms. In this work, two methods based on the reduction of the joint strength properties (cohesion and friction) are presented to assess the stability: the time-dependent degradation approach which implies a nonhomogeneous reduction (referenced as joints degradation), and the conventional shear strength reduction approach which implies homogeneous reduction (referenced as c_j/φ_j reduction). In order to illustrate the difference between these two approaches a set of results corresponding to models integrating both approaches are demonstrated.

Lateral strains at pillar

Since the joint set considered for this study is inclined at $\alpha = 45°$ (see Figure 4.1c), the shear bands are formed at the pillar. Lateral strains obtained on the pillar corresponding to both

approaches, joints degradation and c_j/φ_j reduction, are plotted with respect to the increasing percentage of degradation or reduction of the strength properties (Figure 4.17).

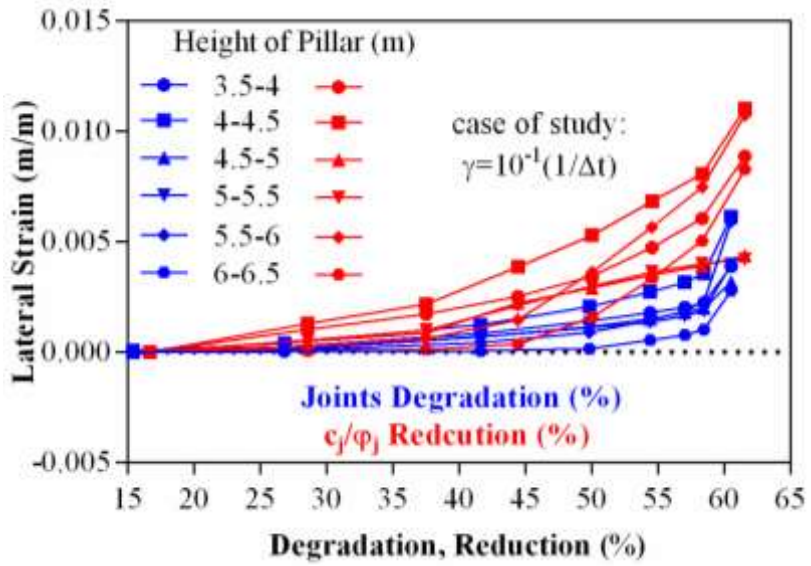

Figure 4.16. Evolution of the lateral stain at the pillar section applying both approaches.

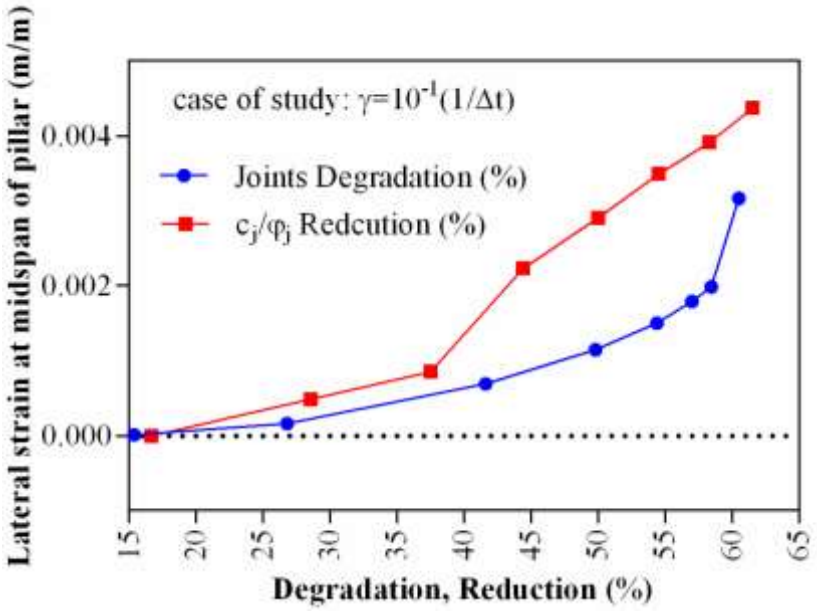

Figure 4.17. Evolution at the pillar centre applying both approaches.

As observed, both approaches lead to the increase of the lateral strain with the increase of the either degradation or reduction. However, a discrepancy is observed in the kinetics of the strain evolution. The non-homogeneous degradation approach implements a slower progression of the strains than the homogeneous reduction approach. For the same percentage of decrease in the strength properties, strains obtained in the case of time-dependent degradation approach are lower than those obtained in case of applying the c/phi reduction approach (Figure 4.17). Nevertheless, the results are quite close and show that the time-dependent approach could be used for the stability analysis of other geotechnical structures since it provides same trends as the reduction strength approach.

Horizontal displacements at the pillar (inclined joint set)

To provide a better emphasis of the difference between the two approaches presented before, the corresponding horizontal displacements obtained at the pillar for the case of joint set inclined at 45° are plotted. This shows the evolution of the displacement at the pillar with the increase of degradation or reduction of the joint friction and cohesion in terms of percentage. As the percentage of either degradation or reduction increases, the resistance of the pillar decreases and thus displacement increase. It is obvious that the displacements are higher at the centre of the pillar than at the connections (with roof and base) and this is demonstrated in both approaches (Figure 4.18). However, the difference in the displacement behaviour imposed between these two approaches is shown at the level of comparison of displacement values obtained at similar degradation or reduction percentages.

For example, at a joint degradation of 58 %, the horizontal displacement at the centre of the pillar is about 4 mm whereas at a c_j/φ_j reduction of 58 %, the displacement at the same location reaches about 12 cm. This high value of displacement is not realistic; it is just indicative since it is calculated based on an independent reduction mechanism which does not integrate any conditions of the model itself. This does not constitute a problem however because the aim in the traditional reduction approach is to calculate F_s the safety factor which is the parameter that indicates the stability state. On the other hand, the stability according to the degradation approach is related to the values of displacements achieved and whether they are admissible or not in the case of structure under study. These displacements are accumulated with time

according to a stress dependent degradation mechanism that accounts for the conditions of the model and thus can be the reference for the stability assessment.

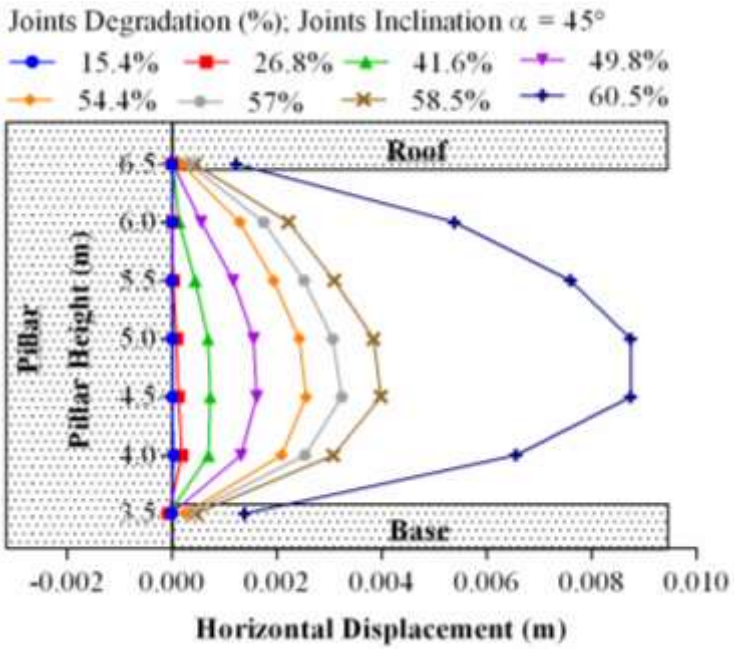

Figure 4.18a. Evolution of horizontal displacement at the pillar (degradation approach).

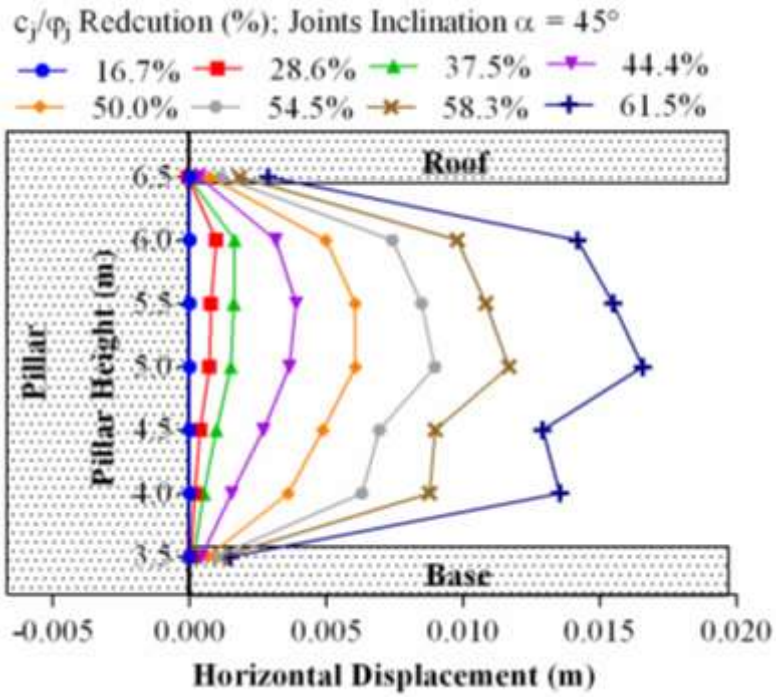

Figure 4.18b. Evolution of horizontal displacement at the pillar (reduction approach).

Vertical displacements at the roof (horizontal joint set)

In order to compare the evolution of vertical displacements at the roof, the case of horizontal joint set is considered (Figure 4.19). This is due to the previous analysis achieved on the effect of joint orientation on the displacement distribution which showed that negligible displacements are obtained in the roof with respect to those obtained in the pillar in case of inclined joints, where the contrary applies in the case of horizontal and vertical joints. In both approaches, the vertical displacement increases with the increase of either degradation or reduction. Besides, the values of these displacements according to both approaches are close. This can be justified by the fact that these displacements are very low in case of horizontal joints and may not be very indicative. Nevertheless, two differences can be drawn out. The first is in the rate of progression of the accumulated displacements, and the second is in the non-identical behaviour at the connections of pillar-roof. However, these differences stay not important due to the low values of the obtained displacements (Figure 4.19).

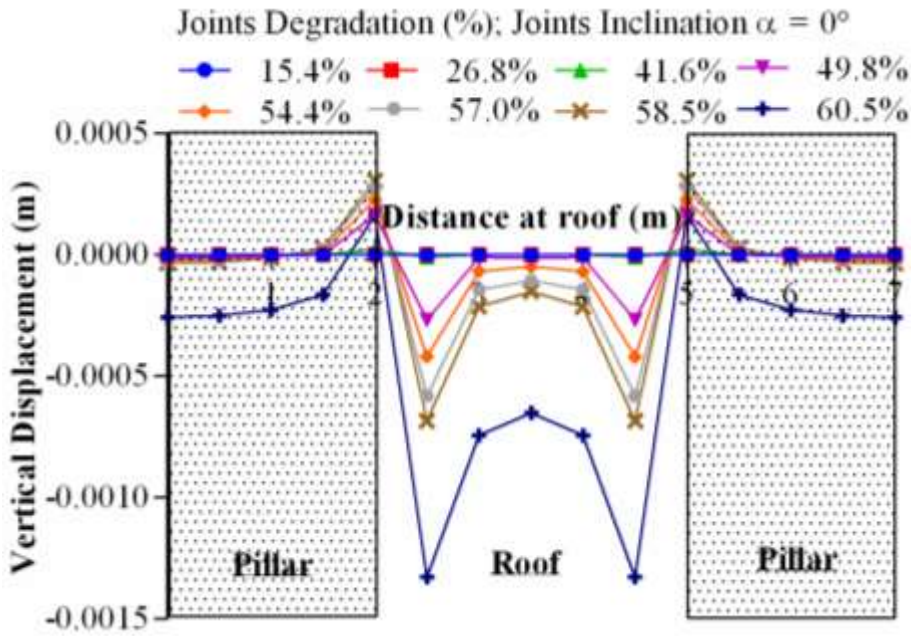

Figure 4.19a. Evolution of vertical displacement at the roof. Results corresponding to degradation approach.

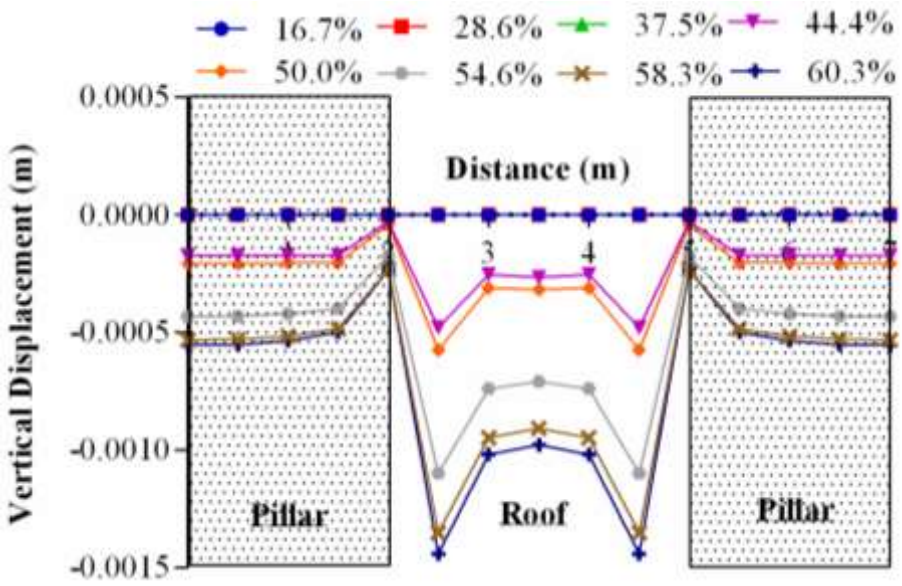

Figure 4.19b. Evolution of vertical displacement at the roof. Results corresponding to reduction approach.

4.6 Conclusion

Underground quarries in North France and its region have been excavated in the chalk layers decades ago without being exploited. Evidently, the various aggravating factors which are activated with time have caused degradation of the constituent chalk properties and the development of fractures. Consequently, the deformational behaviour as well as the overall stability of theses quarries is greatly affected. Therefore, in the stability study of unexploited quarries, it is essential to account for the time dependant behaviour assessed by the degradation phenomenon and the presence of fractures or joints. In this study, a time dependent degradation phenomenon based on the non-uniform evolution of shear plastic strains is developed. This latter is coupled with the nonlinear constitutive law that accounts for the presence of joints based on an oriented yield criterion. This is integrated in the numerical analysis of the underground quarries. Results show the evolution of degradation at different zones of the cavity and in different cases of joint set inclinations. Unlike existing works, the developed phenomenon permits a nonhomogeneous degradation distribution at the different elements of the cavity model. This is directly related to the progression of stresses in these elements with time and hence the obtained

results like displacements for example will have a physical meaning. Strain profiles and failure mechanisms are illustrated and analysed at different joint inclinations. In addition to visual inspections which remain important in the risk assessment of underground quarries, numerical analyses based on such a degradation approach provide additional elements for a better understanding of the time dependent behaviour and the progressive failure associated in these quarries. Note that additional results related to the time-dependent analysis are provided in ANNEX II.

CHAPTER FIVE
PRELIMINARY ESTIMATION OF THE STABILITY STATE OF UNDERGROUND CAVITIES IN NORTH FRANCE

5.1 Introduction

In North France, and basically in Lille Metropolis, 300 hectares of the above surface are classified under risk while the area of underground quarries is estimated by 120 hectares (Mikolajczak 1996, Ineris, 2007, Courbot et al. 2009, Ville de Lille 2012 and 2013). Among these, the majority were excavated in the chalk layers using the method of rooms and pillars (Figure. 1). In the domain of underground quarries different studies were performed to anticipate the stability behaviour (Mikolajczak 1996, El Shayeb et al. 2001, Auvray et al. 2004, Castellenza et al. 2010). In this chapter, a numerical based mechanical approach is conducted to provide a straightforward engineering tool for the preliminary estimation of the stability of identified cavities. This is based on the numerical analysis conducted in chapter three. In other words, it presents a generalization of the results obtained in chapter three since a wide range of the existing case studies is considered. A parametric stability study that considers different geometry cases of room-and-pillar quarries, inspired from the naturalistic inspections and measures, is conducted. A series of 3D nonlinear numerical models of the excavation in chalk layers, with or without joints, is simulated from initial state until failure. This allows understanding the effect of geometric characteristics on the stability state and failure mechanisms of these quarries. Upon this parametric study, a regression analysis is affected and numerical based empirical formulae that calculate the pillar strength R_p and the factor of safety F_s are proposed. This provides a

simplified risk assessment tool capable of estimating the stability state of room-and-pillar quarries given only few parameters.

Figure 5.1. Room-and-pillar quarry in Lille.

In the stability study of room-and-pillar quarries where pillar failure by compression is frequent, one of the basic provisions is to preserve the pillars as effective supporting members of the underground structure. This can be conventionally achieved by assessing the factor of safety F_s of individual pillars which gives insight of the stability state of such structures. The computation can be performed by using empirical formulations based on survey data from actual mining investigations (Salamon et al. 1967, Cook et al. 1978, Wagner, 1980, Bunting, 1991, Bieniawski, 1992, Salamon et al. 1998, Kortnik, 2009). However, experimental based empirical methods might not account for specific failure mechanisms; besides it is not always feasible to obtain sufficient survey data. On the other hand, numerical methods can avoid such restrictions in such type of work (Iannacchione 1992, Martin and Maybee 2000, York et al. 2000, Canbulat et al. 2002, Ferrero et al. 2010, Ferrero and Segalini 2011). It is possible to introduce special conditions to a numerical model like considering the presence of joints for example or accounting for different geometric characteristics and mechanical properties elsewhere. At the end, a correlation between the two approaches can lead for better results. This might be expressed in a simplified numerical based empirical formula capable of estimating a somehow realistic safety factor of quarries sharing similar conditions.

5.2 Numerical results

5.2.1 Factor of safety F_s

Using the 3D nonlinear finite difference code FLAC^{3D} (Itasca 2009), a series of excavation models accounting for a range of geometric characteristics is executed. This is in the same framework of the numerical modelling achieved chapter three. A list of geometric characteristics (Table 5.1) and mechanical properties (Table 5.2) used in the numerical models is provided based on geological investigations and observations in this field (Mikolajczak, 1996, Ineris, 2007, Courbot et al. 2009, Ville de Lille 2012 and 2013). The notations W, H, L, and h mentioned in the table refer to the width of pillar, height of pillar, length of the void or span between adjacent pillars, and height of the roof or overburden respectively (Figures 5.4).

Table 5.1. Summary of geometric characteristics used in the numerical study.

	Width (m)	Height (m)
Pillar	$2 \leq W \leq 8$	$3 \leq H \leq 5$
Room	$2 \leq L \leq 5$	$3 \leq H \leq 5$
Overburden Chalk	--	$h_{chalk} = 7$
Overburden Silt	--	$h_{silt} = 3$

Table 5.2. Summary of mechanical properties used in the numerical study.

	Density (t/m^3)	Young Modulus (MPa)	Poisson Ratio (-)	Cohesion (kPa)	Friction Angle (°)	Dilation Angle (°)
Chalk	2.1	250	0.3	1000	30	5
Silt	1.8	10	0.3	50	30	5

For each case of study, failure is tested and a computation of the factor of safety F_s at ultimate conditions is assessed based on the conventional shear strength reduction method which tends to

reduce the shear strength properties of chalk to the minimum such that no failure is yet attained. F_s values obtained from the numerical simulations are plotted with respect to different W:H (pillar width to height) ratios and L (spacing between pillars or room span) values (Figure 5.2). It is noticed that F_s increases as the width to height ratio of the pillar increases. This is evident since larger widths implement greater pillar strength. This also is consistent with the hypothesis of compression failure of pillars that relates R_p proportionally to F_s where this latter is equal to the ratio of pillar strength to applied compression loads on pillar.

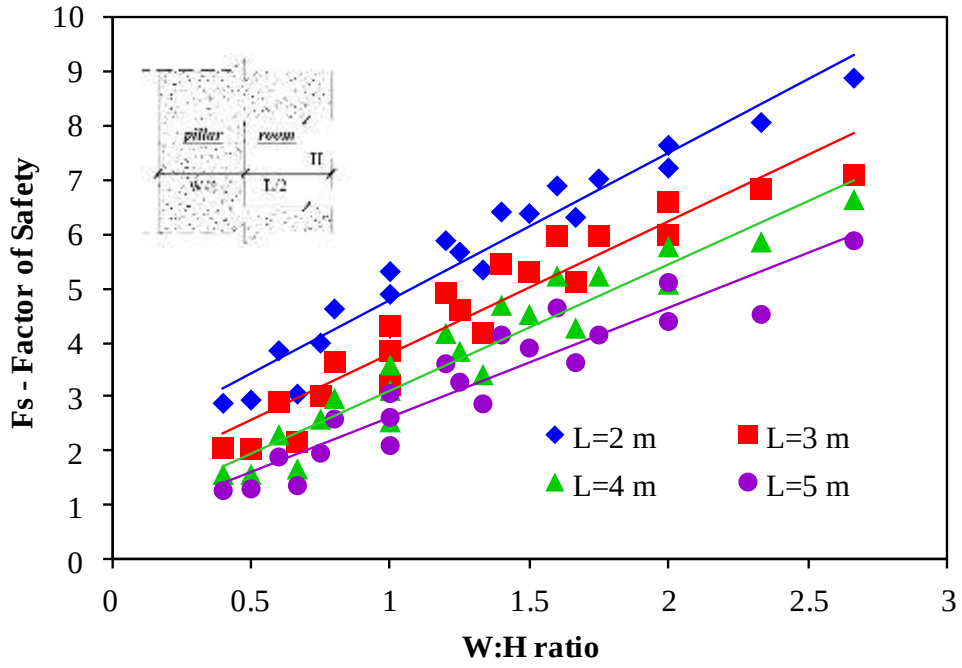

Figure 5.2. Numerical results: Factor of safety with respect to W:H ratios for different L values.

On the other hand, it can be realized that as the span L of the void room increases, F_s decreases. This is due to the fact that larger spans impose greater loads on supporting pillars which consequently results in lower safety factors. More or less, W:H ratios represent the strength of the pillar and the increasing slope in the graph shows that for high ratio of W:H higher F_s is detected which means that the pillar has higher capacity to resist higher loads. Another figure illustrating the effect of L on F_s is provided (Figure 5.3). Concerning the depth of the opening or the height of the overburden h, several models accounting for different h values have been simulated.

However, knowing that the variation of the height of overburden in the zone studied is low and the rigidity of the roof is still considered high for all simulations, F_s is slightly affected. For this reason, the study cases presented correspond to a fixed height of overburden as mentioned before (see Table 5.2).

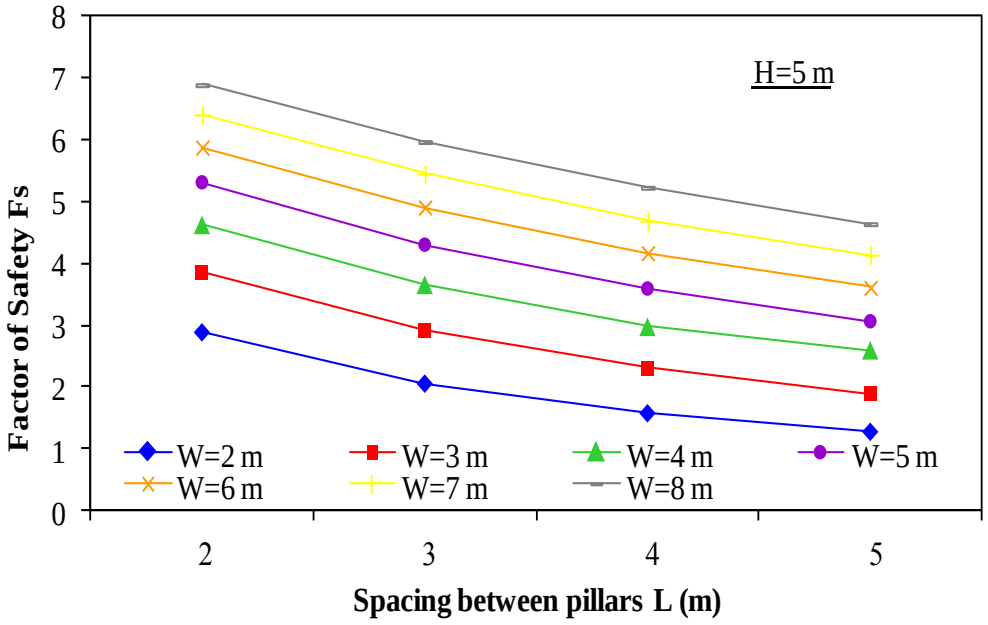

Figure 5.3. Variation of simulated F_s with respect to L values at different W:H ratios.

5.2.2 Resistance of the pillar R_p

In room-and-pillar quarries with a multiple-pillar system, and assuming a compression failure in pillars which represents a majority of collapses investigated in Lille Metropolis (Mikolajczak 1996, Ineris 2007, Courbot et al. 2009, Ville de Lille 2012 and 2013), the overall stability is directly related to that of the system of pillars. In this case, a factor of safety (F_s) which designates the quarry state whether stable or not, can be defined as the ratio of the resistance of the pillar (R_p) to the applied load acting on it (q_p) (Equation 1). This latter represents the imposed loads at the roof and surface. In this study, no external surface loads are applied, and the pillar is expected to support its self-weight next to the weight of the overburden. Besides, R_p depends on the compressive strength of the constituting material of the pillar which is chalk, the pillar

geometry (W & H) and the spacing between adjacent pillars (L). According to the defined relation between F_s and R_p, R_p represents the resistance of the pillar at ultimate conditions; i.e. just before failure happens at the point when F_s is simulated.

$$F_s = \frac{R_p}{q_p} \qquad [5.1]$$

The value of F_s indicates a stable or unstable state of the room-and-pillar system. A limit of F_s between stable and unstable state is when F_s =1 meaning that the applied loads (q_p) are equal to the resistance of the pillar (R_p) associated to the multi-pillar system. Otherwise, if F_s is less than 1, this indicates failure, and if it is greater, then stability is ensured.

The load acting on a pillar q_p is usually evaluated by the tributary area method. Considering the room-and-pillar quarries investigated in Lille and its region where a regular distribution of pillars with square sections supporting the overburden of an average height is observed (Figure 5.4), and applying the tributary area method, the applied load q_p is calculated.

$$q_p = (\rho_{ch} g h_{ch} + \rho_{si} g h_{si})(W + L)^2 + (\rho_{ch} g H_{pi})(W)^2 \qquad [5.2]$$

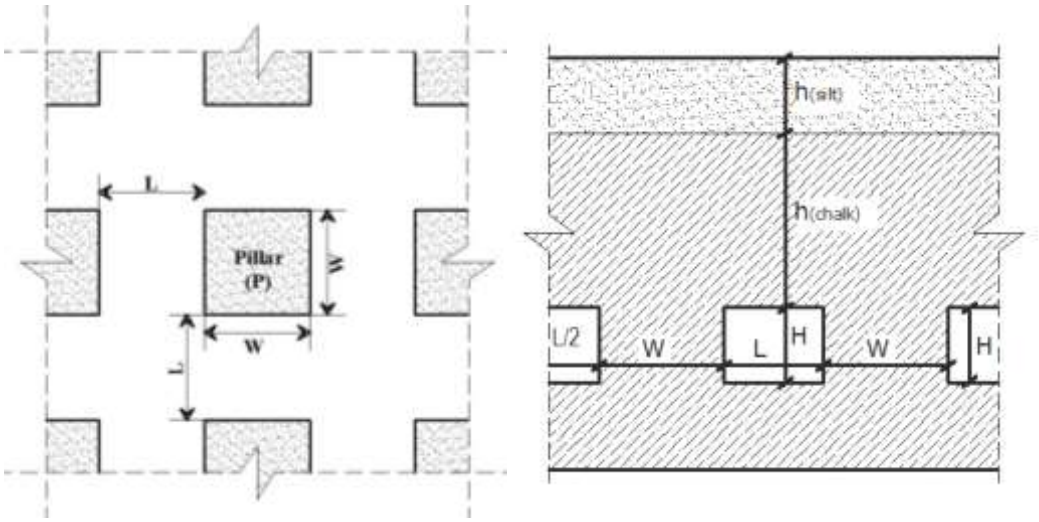

Figure 5.4. Top view and vertical section of the room-and-pillar underground structures.

Using the numerical results of calculated F_s, and the analytical results of calculated q_p, the resistance of the pillar R_p can be determined. R_p values are calculated and plotted with respect to different values of W. The curve that refers to the case of H = L = 3 m is presented (Figure 5.5).

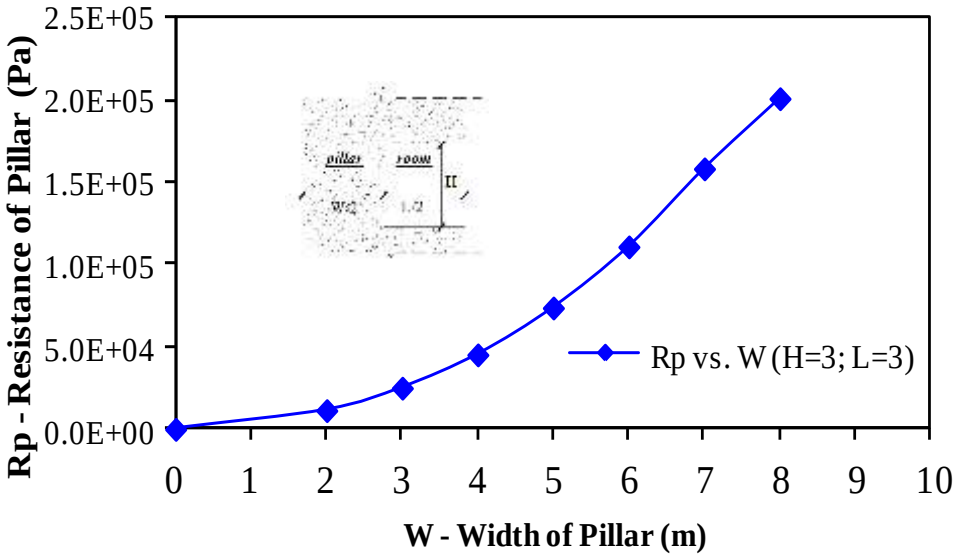

Figure 5.5. Variation of the simulated pillar strength as a function of pillar width.

This is done to demonstrate the influence of geometric characteristic on the stability of pillars and thus reflects the stability state of the room-and-pillar quarries.

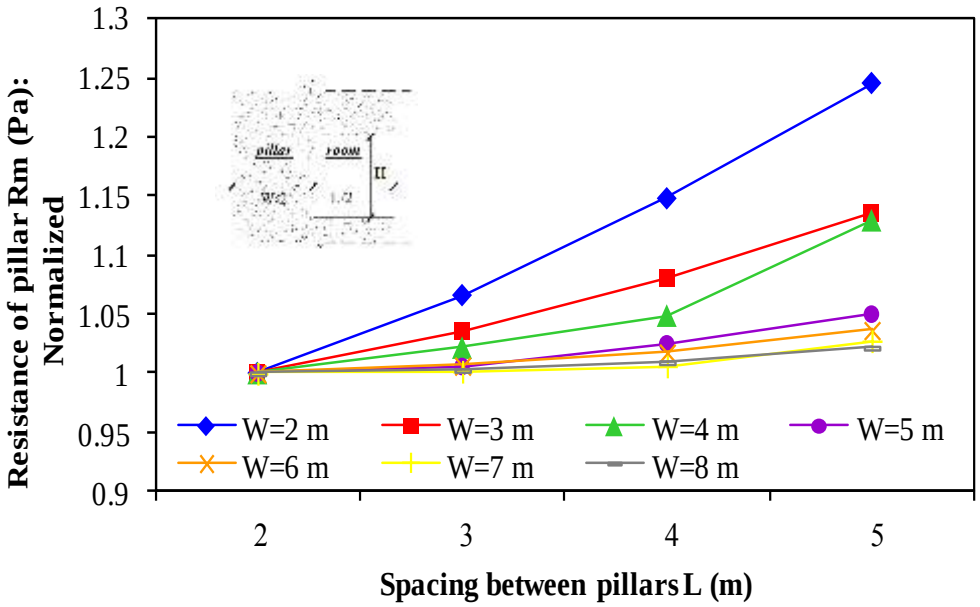

Figure 5.6. Normalized values of R_p with respect to L.

Since it is not an issue of strength of an individual pillar as it is usually illustrated in experimental based studies, however it is the resistance of pillar in a multi pillar system that is being calculated R_p, then it is affected by the spacing between pillars L. This is associated to the failure mechanisms in the room-and-pillar underground structure which are accounted for in the numerical analysis. Normalized values of R_p are plotted with respect to the spacing L at different W:H ratios (H = 5m) in order to clearly illustrate this influence figure (Figure 5.6). It shows that as the spacing between the pillars which represent the supporting elements, increases, the resistance increases so that the underground structure remains in the stable state. The influence of span L on the resistance of the multi-pillar system is greater when the section of the pillar is smaller; i.e. for smaller values of W.

5.3 Extrapolated formulae

According to naturalistic inspections of underground quarries in Lille and its region, the majority of recorded collapses in room-and-pillar quarries is attained due to localized failure in the pillars (Mikolajczak 1996, Ineris 2007, Courbot et al. 2009, Ville de Lille 2012 and 2013), With time, and in the presence of aggravating factors, strength properties of the pillar degrade and the effective section is reduced (Figure 5.7). So, the main failure in the pillar is assumed to be a compression failure.

Figure 5.7. Degraded pillar in the cavity of Don Bosco in Lille on October 2011.

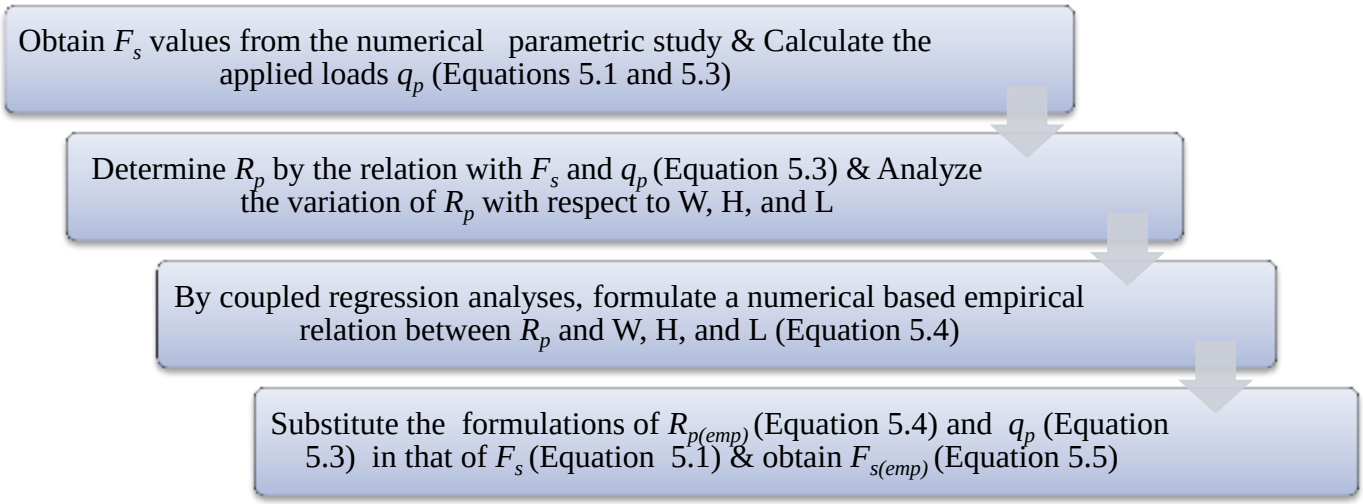

Figure 5.8. Logigram of the approach proposed for the formulation of $F_{s(emp)}$.

Based on the hypothesis of failure by compression, the stability of the quarry which depends on the stability of the system of supporting pillars can be estimated by calculating the safety factor according to the ratio of pillar resistance to the applied compression loads as demonstrated previously (Equation 5.1). Then, by the analysis of the calculated R_p as the product of F_s obtained from the numerical simulations and q_p calculated by the tributary area method, new relations for direct estimation of R_p can be proposed. Consequently, a numerical based empirical formula for F_s can be developed. The approach proposed for the establishment of these formulations is explained in a logigram (Figure 5.8).

For specifications of selected cases of study (see Tables 5.1 & 5.2), the pillar loads are calculated (Equation 5.2) and the following equation is derived:

$$q_p = 21\left[9.572(W+L)^2 + W^2 H\right] \qquad [5.3]$$

In a quarry of multi-pillar system, the pillar strength is directly related to its dimensions (width and height in case of square sections) as well as the spacing between pillars L (which is unified in case of symmetric spans) and the height of the overburden (assuming a 10 m average total height of the overburden). Thus, a series of excavation models that takes into consideration a range of W, H and L values inspired from site inspections performed on quarries of Lille Metropolis is conducted. For each case model, the safety factor F_s(numerical) based on the

conventional c-phi reduction method is calculated. Then, having calculated the pillar pressure q_p by the tributary area method (Equation 5.3), it is possible to determine the pillar resistance R_p for each case of L (room width or spacing between pillars) and W:H (pillar width to height) ratio (Equation 5.1). Afterwards, a coupled regression analysis of the obtained results is performed by which a nonlinear relation between the obtained values of R_p and W:H ratios and L values is constructed. This relation is denoted as a numerical based empirical formula that enables the calculation of the resistance of the pillar in a multi-pillar system R_p(empirical) in terms of W, H and L (Equation 5.4). Then, by the general relation between F_s and R_p (Equation 5.1), F_s(empirical) is derived (Equation 5.5).

$$R_{p(emp)} = 2613.2 \frac{(W)^{\alpha}}{(H)^{\beta}.(L)^{\gamma}} \quad [5.4]$$

$$Fs_{(emp)} = 124.438 \frac{(W)^{\alpha}}{\left[9.572(W+L)^{2} + W^{2}.H\right](H)^{\beta}.(L)^{\gamma}} \quad [5.5]$$

where:

$$\alpha = 2.4797 - 0.0157H - 0.081L - 0.073 H/L \quad [5.6]$$

$$\beta = 0.351 - 0.0157H - 0.012L - 0.073 H/L \quad [5.7]$$

$$\gamma = 0.0572 - 0.069L \quad [5.8]$$

With those equations for α, β, & γ, the correlation shows that it is possible to calculate adequate F_s and R_p as those obtained from numerical simulations, but with the help of these proposed formulations and without the need to regenerate numerical models at every time.

The coupled regression integrated in developing the proposed formulae represents a series of three dependant regression analyses. First regression is done between R_p(numerical) and W:H ratios whereas the second is achieved between coefficients obtained from the first regression and H:L ratios, and the third regression is carried out between coefficients obtained from the second

regression and L values. An example of the fist regression is illustrated and corresponding power functions are presented (Figure 5.9).

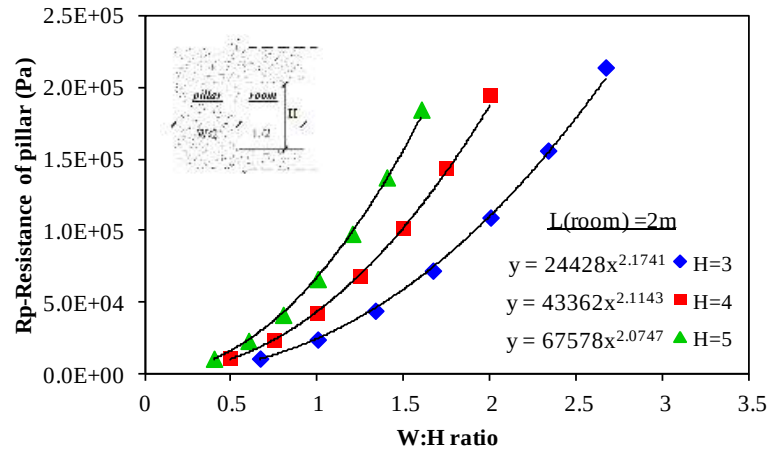

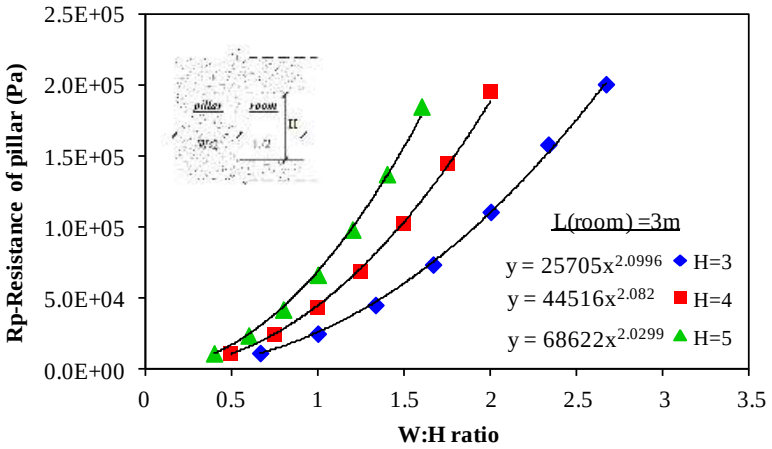

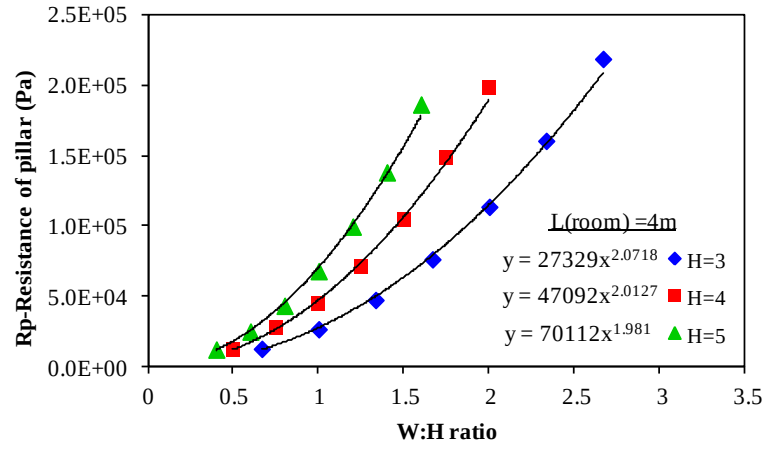

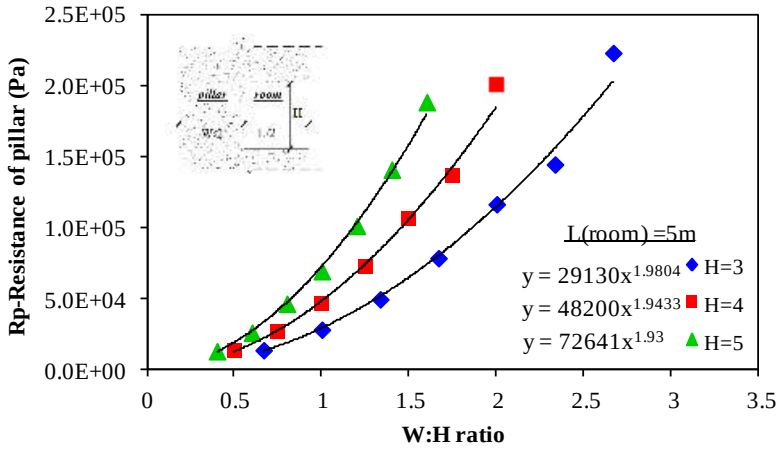

Figure 5.9. Results of the first regression analysis performed between simulated R_p values and W:H ratios.

5.4 Correlation of results of the proposed formulae

To test the error of the obtained regression formulations, a correlation between results obtained by the numerical method and those obtained using the empirical method is calculated for each of the pillar resistance and the safety factor.

High correlations achieved, i.e. 0.998 for R_p and 0.996 for F_s (Figure 5.10a & 5.10b), reflect a negligible error in the proposed approach and show that the developed empirical F_s formulae are capable of estimating R_p and F_s values very close to those calculated by the numerical method. This can help geological and mining engineers easily predict the stability state of the pillar without need to run on complicated numerical models which are considered time consuming.

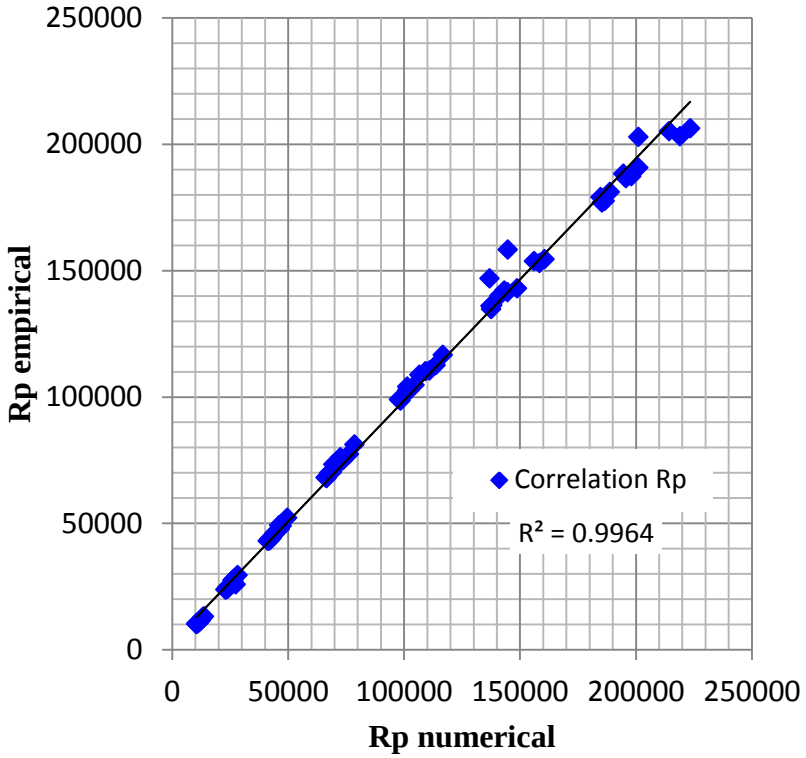

Figure 5.10a. Correlation between numerical and empirical results of R_p calculations.

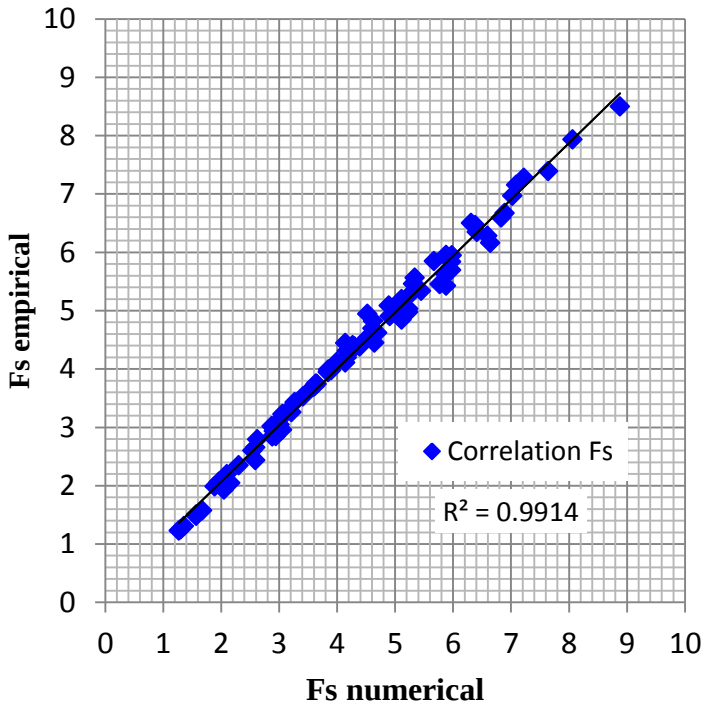

Figure 5.10b. Correlation between numerical and empirical results of F_s calculations.

5.5 Extended Formulae

5.5.1 Critical width

According to the classification given by Lunder and Pakalnis (1997), three categories of stability state are defined according to calculated factors of safety F_s by which F_s less than 1 indicates failure, F_s between 1 and 1.4 means unstable situation or subjected to failure, and F_s greater than 1.4 reflects a stable state. Based on this classification, and in accordance with the empirical formula developed to calculate F_s, a new study is generated to estimate a so called critical width which is the minimum width of a stable pillar capable of resisting failure. So, assuming that 1.4 is the minimum value of F_s for a guaranteed safety (Lunder and Pakalnis 1997, Brady and Brown 2006), replace F_s by the value of 1.4 in the proposed empirical formula (Equation 5.5) and solve for real values of W.

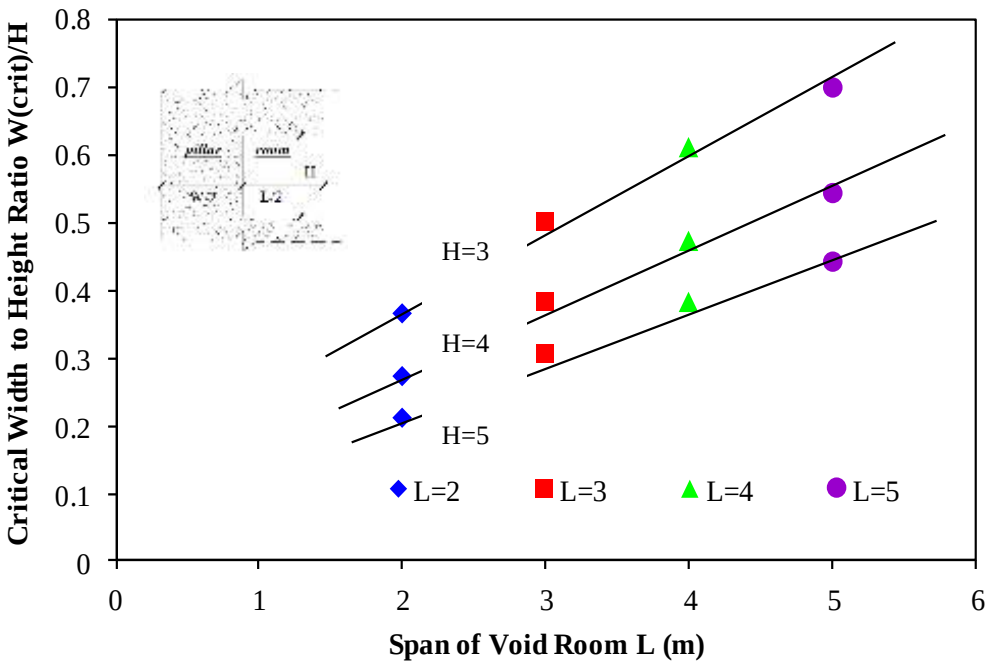

Figure 5.11. Abacus for the estimation of critical width of safety pillars with given height of pillar H and spacing between pillars L.

By applying this inverse method, a set of solutions are determined for all values of H and L in the range of study. The values are traced and a simplified abacus which aims to allow guessing the critical pillar width to height ratio and thus the critical pillar width for each case of study knowing only values of H (pillar height) and L (room span) is proposed (Figure 5.11). This facilitates the preliminary estimation of minimum widths of safety pillars and thus quarry investigators can now directly estimate the stability of the pillar by measuring its dimensions and fitting or comparing them to the abacus.

5.5.2 Admissible scaling

Due to time and the intervention of several aggravating factors the effective width of the pillar is reduced and this is a frequent phenomenon known as scaling of pillars in abandoned underground cavities such as those in Lille and its region (Figure 5.12).

Consequently, a scaling parameter x, relative to the difference between the initial width and the current width is defined. Then, and based on the previous calculation of the critical width, it is possible to estimate the admissible scaling of the pillar and therefore offer mining and geological engineers a new tool for the preliminary assessment of pillar stability.

The suggested scaling parameter x represents the decrease of the pillar width ($W_{critical} = W_{initial} - x$) which is in turn equal to the increase of the room space ($L_{critical} = L_{initial} + x$). By replacing F_s by 1.4, W by W-x, and L by L+x in the proposed equation of F_s (Equation 5.5), a series of nonlinear equations corresponding to all possible permutations among W, H, and L values and including the variable x is derived. By the help of an advanced mathematical tool, these equations are solved and real solutions for x are determined. Obtained results are fit into a new abacus by which it becomes possible for the user to determine the admissible scaling of the pillar just after knowing the initial dimensions W and L; where H does not show a great influence in this analysis (Figure 5.13).

Figure 5.12. Pillar with reduced section from the cavity of Cavaignac, Lille.

In fact, this analysis can also be extended to a further level by which it becomes possible to estimate the time left for pillars subjected to failure, to fail. By this, a new term like a pillar life can be calculated. However, such a provision recommends a data platform containing informative description of occurred collapses, i.e. the nature of collapse, the time between excavation and collapse, the initial and final effective widths of the pillar, etc. For the lack of such information, this provision is not executed.

5.6 Presence of joints

At shallow depths and low-stress environments existing fractures may control the potential failure modes and the associated extent of failure. This occurs when the low confining pressures are not capable of blocking the fracturing phenomenon which in turn leads to progressive fracturing and thus causes reduction in the loading capacity of the pillar at one hand, and provides less resistance to sliding at the other hand. In this case, shear failure in the pillar may appear and even dominate the compression failure. Investigations of the quarries in North France have shown evidence to the presence of natural embedded joints in the chalk substratum as well as mechanical fractures emerged in weak overstressed zones of the pillars basically (Figure 5.14). Hence, it is quite important to account for the presence of joints or fractures in the stability study of underground cavities

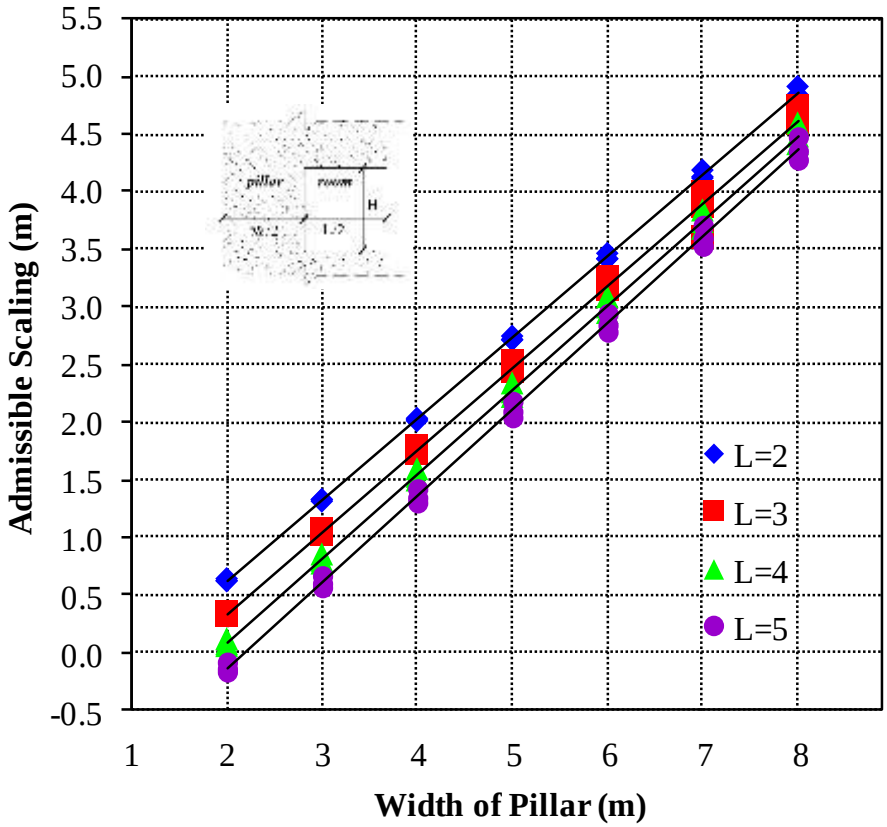

Figure 5.13. Abacus to determine the admissible scaling of the pillar section for any W, H, and L.

Figure 5.14. Fracture at 45° in the pillar of the Cavaignac cavity at Lille in September 2011.

5.6.1 Effect of W:H and L

A numerical approach similar to the one presented before is conducted for the selected range of study cases (Table 5.1) taking into consideration the presence of a single joint set at different inclinations with respect to the vertical axis of the pillar. This latter is achieved using the ubiquitous-joint model implemented in FLAC^{3D} (Itasca 2009). The ubiquitous-joint model is an anisotropic plasticity model that includes weak planes of specific orientation embedded in a Mohr-Coulomb solid (Itasca 2009). In this study, the chalk continuum consists of the chalk matrix and the joints defined as weak planes with reduced shear strength properties (joints cohesion is set equal to 50% that of the matrix).

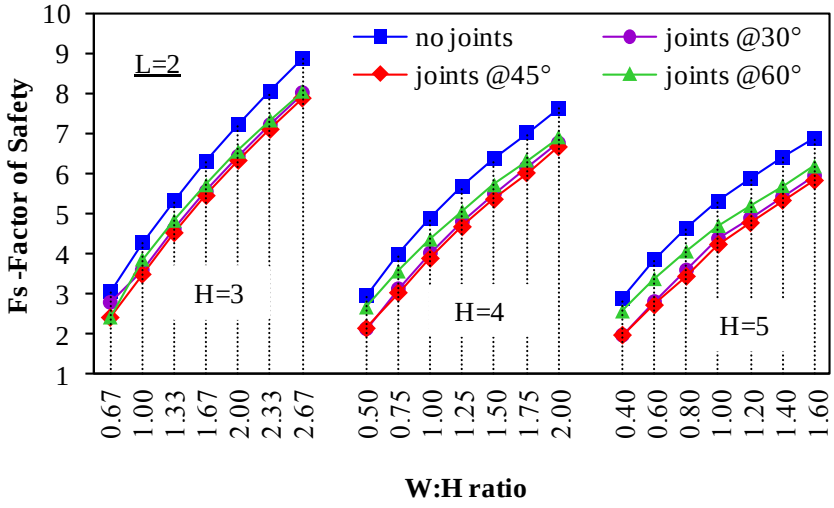

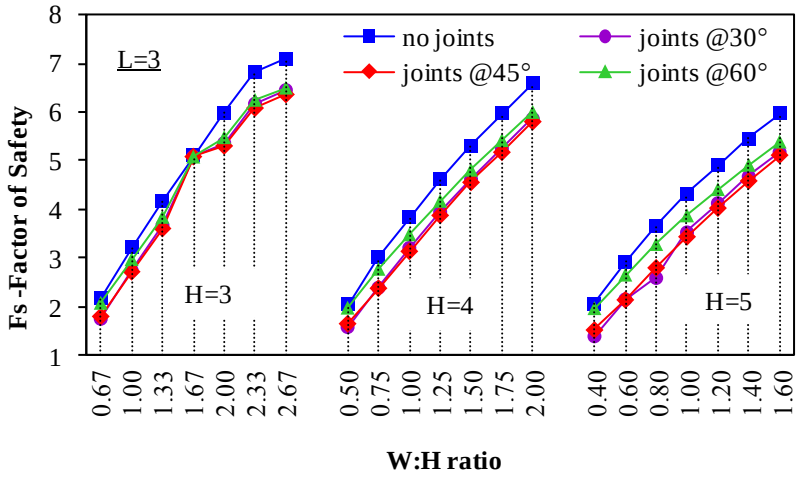

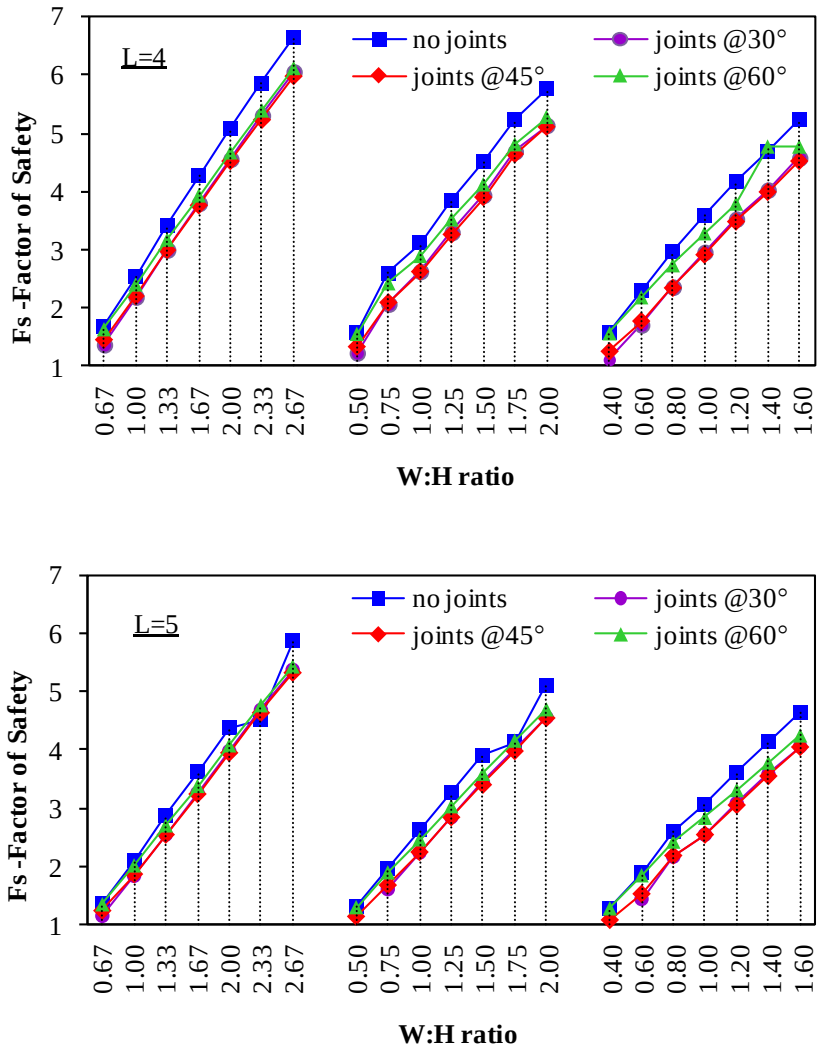

Figure.5.15. Simulated safety factors with respect to all possible permutations of dimensions and joint inclinations

Factors of safety are then simulated according to the conventional shear strength reduction technique (Itasca 2009) applied on both the matrix and the joints in an identical manner. Results corresponding to three selected cases of joint inclinations (30°, 45°, and 60°) are plotted and compared with previous results obtained when no joints were defined (Figure 5.15).

5.6.2 Estimation of the safety factor in the presence of joints

In order to account for the effect of joints at different inclinations on the estimation of F_s, a comparison between the numerical values of F_s in the presence of joints and empirical results of F_s in case of absence of joints is realized. Using a simplified regression approach, three linear

relations or extended empirical formulae corresponding to the three selected cases of joint inclinations are established (Figure 5.16).

The extended empirical formulae to calculate F_s for jointed quarries are proposed as follows:

- Joint set at 30°:

$$F_{s(emp\_j30)} = 1.0394 * F_{s(emp\_nj)} - 0.5771 \quad [5.9]$$

- Joint set at 45°:

$$F_{s(emp\_j45)} = 0.9657 * F_{s(emp\_nj)} - 0.2965 \quad [5.10]$$

- Joint set at 60°:

$$F_{s(emp\_j60)} = 0.9544 * F_{s(emp\_nj)} - 0.0699 \quad [5.11]$$

where $F_{s(emp\_nj)}$ is equal to $F_{s(emp)}$ as defined in the original proposed equation (Equation 5).

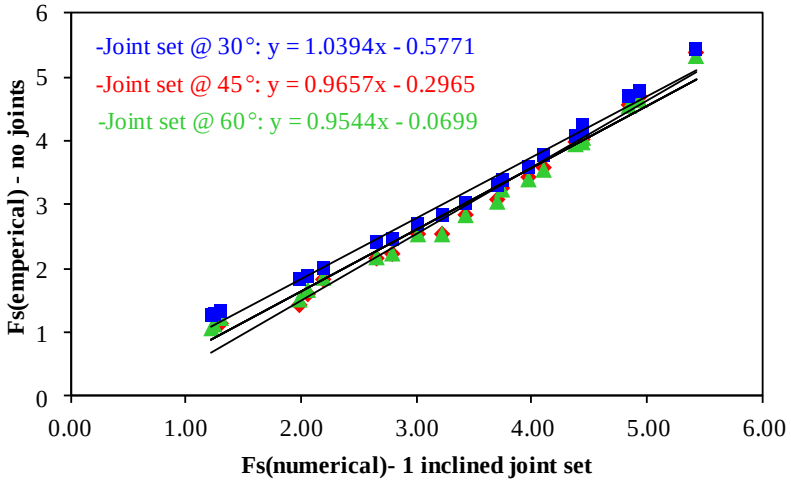

Figure 5.16. Relation between empirical and numerical F_s of cases without and with joints, respectively.

This permits the calculation of F_s for each case of study having known only the dimensions W, H, and L, in addition to the joint set inclination. From these obtained values, and referring to the classification suggested by Lunder and Pakalnis (1997), it is now possible to estimate the stability state of the room-and-pillar jointed cavities and therefore provide a preliminary assessment on whether the studied cavity is stable, subjected to failure, or unstable.

5.7 Conclusions

The phenomenon of unexploited mines and underground quarries reveals a serious problem in terms of stability of the underground strata which eventually provokes damage risks on the surfaces lying on top. This imposes security threats against both people and constructions at one hand, and against urban development at the other hand. North France, and particularly Lille and its region are seriously exposed to such risks since a large number of abandoned quarries are identified. For this reason, the City of Lille has launched the project on risk assessment and control associated to this phenomenon.

In terms of this project, this thesis and particularly this chapter comes to present some of the results of the numerical study performed to test the stability of quarries excavated in chalk layers by the method of room-and-pillar. A parametric study accounting for the wide variation in the dimensions of investigated quarries is conducted. Furthermore, interpretation of these results is performed and formulated to leave efficient tools behind this whole study.

At first sight, this provides a better understanding of the effect of such variations, mainly the width to height ratios of pillars (W:H) and the width of void rooms which represents the spacing between pillars (L), on the overall stability of the quarry. Besides, to facilitate the estimation of the resistance of the pillar in a multi-pillar system R_p and the factor of safety F_s, a coupled regression analysis is affected and accordingly numerical based empirical formulae are developed. Eventually, the presence of joints which is evident in quarries of Lille is considered in a new numerical study. Based on the proposed empirical formulae, new formulae are extended. By this, it is now possible to estimate and provide a preliminary assessment of the stability state of room-and-pillar quarries of Lille Metropolis given only their geometric characteristics (W, H, and L) and an approximate value of the angle of inclination of existing joints. In others words, the originality, if properly described, of this work lies in its efficacy and non-complexity at the same time where, as for first judgement, geo-engineers concerned in this project can tell directly whether the inspected quarry is stable or not based on no more than site investigations and correct usage of the developed formulations and abacuses.

CONCLUSIONS AND PERSPECTIVES

The presence of unexploited mines and underground quarries reveals a serious problem in terms of stability of the underground strata which eventually provokes damage risks on the surfaces on top. This imposes security threats against both people and constructions at one hand, and against urban development at the other hand. North France, and particularly Lille and its region are seriously exposed to such risks since large areas have been undermined since decades ago. Being aware to the volume of the risks encountered by instabilities induced from these cavities, the City of Lille has set up a multi-axial project for the investigation of this hazardous phenomenon. Geological investigations and experimental testing were carried out by geo-engineers involved in the project; however our concern was the numerical study. This thesis aims to present by means of numerical analysis a complementary understanding of the mechanical behaviour and stability state of underground cavities in North France.

According to geological investigations, double symmetric joint sets are stratified in the chalk bed. Induced fractures are also observed at different zones of the quarries which were left unexploited after being excavated decades ago at shallow depths using the method of rooms-and-pillars. Hence, the target in this thesis was to simulate, by numerical methods, a three dimensional model of the room-and-pillar excavation where the effects of both: discontinuities and time are integrated separately and in unison.

To start with, an equivalent continuum model that accounts for anisotropy in chalk by means of embedded joint sets is proposed. This model is achieved by representing implicitly the weak planes with reduced strength properties in the chalk continuum. It is named as the

oriented yield criterion where a new yield surface for each joint set at a different orientation is defined.
The oriented yield criterion is assigned to the chalk continuum and anisotropic behaviour is exhibited. This is verified after the consistency of results with those obtained using existing joint models on the same application.

Afterwards, the joint model developed is integrated in the stability analysis of the underground cavities where stratigraphic joints and induced fractures were observed. A numerical technique based on the shear strength reduction method was implemented to study the stability due to failure in joints. Final reduction factors reflecting the stability of the quarries at maximum weakening of joints are computed. Numerical analysis allows us to understand the impact of joints at different orientations on the behaviour of the room-and-pillar quarry. The effect of joint sets orientation, whether single joint set or double, on the strain mechanisms is analysed. Failure mechanisms are modelled after applying the reduction approach on the strength properties of the joints merely in order to illustrate the influence of the presence of joints in the chalk continuum on the global behaviour of the cavity.

Underground quarries identified in the region of North France have been excavated in the chalk layers decades ago without being exploited. Evidently, the various aggravating factors which are activated with time have caused degradation of the constituent chalk properties and the development of new fractures. Therefore, in the stability study of unexploited quarries, it is essential to account for the time-dependent behaviour assessed by the degradation phenomenon in the presence of fractures or joints. A time dependent degradation approach based on the non-uniform evolution of shear plastic strains is developed. This latter is coupled with the oriented yield criterion that accounts for the presence of joints. The developed phenomenon permits a non-homogeneous degradation distribution on the different zones of the cavity model which is affected by the non-uniform evolution of stresses since physical degradation aspects are considered unlike the conventional stability methods. Numerical analysis of the time-dependent behaviour of the jointed chalk quarries is performed to provide additional elements for a better understanding of the progressive failure and to give an indication about the long term stability of these.

At last, a parametric stability study accounting for the wide variation in the dimensions pillars and roofs of investigated quarries is conducted. At first sight, this provides a better understanding of the effect of confining pressure, which is directly related to the width of the pillars, on the associated failure mechanisms. This is done using the shear strength reduction technique where both cases, with and without joints, are considered. Thereafter, a third order regression analysis is performed and extrapolated formulae that relate the dimensions of the room-and-pillar quarry to its safety factor are determined. Also abacuses for the determination of the minimum pillar width and maximum scaling are obtained. This helps in the preliminary assessment of the stability of investigated quarries having known only few parameters: dimensions and joint inclination.

This thesis is concerned in the numerical modelling performed to investigate the behaviour of unexploited room-and-pillar chalk quarries and thus provide a complementary approach to the geological and experimental investigations.
The work conducted focuses on four major topics which are: (i) modelling the anisotropic behaviour in the chalk continuum induced due to the presence of joints; (ii) modelling the strain and failure mechanisms and calculating the reduction factor to analyse the stability in the presence of joints; (iii) modelling the time-dependent-degradation to assess the long term behaviour of the cavity and likewise the long term stability; and last but not least (iv) modelling a range of existing case studies (parametric study) to provide extrapolated formulae and abacuses that might help in the preliminary analysis of the stability and support the PPR project for the City of Lille.
Eventually, and in correlation with the highlighted topics, new studies can be conducted while alternative methods might be suggested and even additional problem conditions can be considered. Some of these are proposed below:

- Joints can be modelled explicitly using a discontinuum approach such as the one proposed via the distinct element method. Geometric interfaces with prescribed stiffness parameters are then used.

- In our joint model, two joint sets were defined. However, the general case corresponding to ‘n’ joint sets was given. Numerical implementation of the generalized case can be achieved even though it is of high complexity.

- In the time dependent analysis presented in chapter four, the time-degradation model was assigned when one single joint set was defined in the continuum. The time analysis can be maintained in the presence of the two joint sets. The implementation however is considered complicated due to the necessity to perform a five order permutation between the defined yield functions.

- The time-dependent-degradation analysis can be directly related to the water effects. This can be achieved by integrating in the degradation function defined, the water-dependent degradation relation. This relation is to be provided by experimental tests done to study the water effect on the chalk resistance.

- In accordance with the stability analysis, whether on short term or on long term, the influence of different factors that motivate failure (which were mentioned in chapter 1) can be induced. One of these factors is the surcharge imposed by additional static or moving loads applied on the surface. Another one is water;

- The various effects of water can be considered separately in this study. For example, the hydraulic load can be added by considering the non-dry density at the overburden. Pore pressure can also be induced and saturation-desaturation cycles can be accounted for within a suction analysis. Last but not least, the variation of water level inside the galleries according to seasons can be studied by modelling cyclic loads to describe the charging (in rain season) – discharging phenomenon.

- Further analysis on the strain and failure mechanisms can be done to investigate the propagation of instabilities from the galleries to the top surface taking into consideration the rigidity properties of the overburden. I

- inclined quarries or inclined surfaces can provoke mechanisms which might be remarkable if studied.

- A parametric analysis similar to the one conducted in the last chapter of this thesis can be repeated using the developed time-dependent-degradation approach instead of the conventional stability approach. This will allow us to assess the effect of confining pressure on long term and maintain a preliminary estimation on long term behaviour of similar cavities without the need to run dozens of numerical models each time.

BIBLIOGRAPHY

Abdulraheem, A., Zaman, M. & Roegiers, J., 1993. Numerical simulation of a compacting reservoir. *International Journal of Rock Mechanics and Mining Sciences and Geomechanics Abstracts,* pp. 30 (7), 1299-1302.

Agharazi, A. & Martin, C., 2011. Implementation of an equivalent continuum constitutive model for rock masses with systematic joint sets in FLAC3D. *Continuum and Distinct Element Continuum Modeling in Geomechanics.*

Alber, M. & Helland, J., 2001. Investigation of a Limestone Pillar Failure Part 2: Stress History and Application of Fracture Mechanics Approach. *Rock Mechanics and Rock Engineering/ Springer-Verlag.*

Alonso, E., Gens, A. & Josa, A., 1990. A constitutive model for partially saturated soils Geotechnique. Volume 40(3), 405-430.

Amadei, B. & Goodman, R. E., 1981. *A 3D constitutive relation for fractured rock masses.* Ottawa, Canada, International Symposium on the Mechanical Behavior of Structured Media, Ottawa, Canada, Elsevier.

Amitrano, D. & Helmstetter, A., 2006. Brittle creep, damage, and time to failure in rocks. *J. geophys.* , Issue Res., 111, p. 1–17.

Andersen, M. A., Foged, N. & Pedersen, H. F., 1992. *The link between waterflood-induced compaction and rate-sensitive behaviour in weak North Sea chalk.* Deauville, France, s.n.

Auvray, C., Homand, F. & Sorgi, C., 2004. The aging of gypsum in underground mines. *Engineering Geology,* Volume 74 (2004), p. 183–196.

Aydan, O. et al., 2005. *The characteristics of soft rocks and their effect on the long term stability of abandoned room and pillar lignite mines.* Nancy, France, Post-Mining 2005, November 16-17.

Bieniawski, Z. T., 1992 . *A method revisited: coal pillar strength formula based on field investigations.* s.l., Proc. Workshop on coal pillar mechanics and design. US Bureau of Mines IC 9315.

Bieniawski, Z. T., 1992. Ground Control. In: *Chapter in Mining Engineering Handbook, SME.* s.l.:s.n., pp. 897-937.

Bjerrum, L., 1967. Engineering geology of Norwegian normally consolidated marine clays as related to settlements of buildings.. Volume 17 (2), 83-117..

Brady, B. H. G. & Brown, E. T., 2006. dd. *Rock mechanics for underground mining,* Volume Third Edition 10.1007/978-1-4020-2116-9.

Bunting, D., 1991. Chamber Pillars in Deep Anthracite Mines. *Trans. AIME,* Volume 42, pp. 236-245.

Bunting & D, 1991. Chamber Pillars in Deep Anthracite Mines. *Trans. AIME,* Volume vol. 42, pp. 236-245.

Cai, M. & Horii, H., 1993. A constitutive model and FEM analysis of jointed rock masses. *International Journal of Rock Mechanics and Mining Sciences,* 30(4), p. 351-359. .

Calvetti, F., Nova, R. & Castellanza, R., 2004. Modelling the subsidence induced by degradation of abandoned mines. *In Continuous and discontinuous modelling of cohesive frictional materials,* Volume Taylor & Francis Group, p. 137–148.

Canbulat, I. et al., 2002. *Task 6.9.1 The development of techniques to predict and manage the impact of surface subsidence,* s.l.: COALTECH 2020.

Castellanza, R., Nova, R. & Orlandi, G., 2010. Evaluation and remediation of an abandoned gypsum mine. *Journal of geotechnical and geoenvironmental engineering,* Volume 136.4 (2010), pp. 629-639.

Castellanza, R., Nova, R. & Tamagnini, C., 2002. Mechanical effects of chemical degradation of bonded geomaterials in boundary value problems. *Rev. Fran. Génie Civil,* Issue 6, 6, 2002, pp. 1169-1192.

Castro, L., 1996. *Analysis of stress-induced damage initiation around deep openings excavated in a moderately jointed brittle rock mass,* Toronto: PhD thesis. University of Toronto.

Chenga, Y. M., Lansivaarab, T. & Weia, W., 2006. Two-dimensional slope stability analysis by limit equilibrium and strength reduction methods. *Computers and Geotechnics,* 34(3), pp. 137-150.

Collin, F., Cui, Y. J., Schroeder, C. & Charlier, R., 2002. Mechanical behavior of Lixhe chalk partly saturated by oil and water: experiment and modeling. *International Journal for Numerical and Analytical Methods in Geomechanics, ,* Volume 26, pp. 897-924.

Cook, N. & Hood, M., 1978. *The Stability of Underground Coal Mines Workings.* s.l., Proceedings International Symposium on Stanility in Coal Mining, Vancouver, pp. 135-147..

Courbot, T. et al., 2010. *La Prise en Compte des Risques lies aux Cavités Souterraines dans la Métropole Lilloise,* s.l.: Université Lille1.

Cristescu, N., 1989. *Rock Rheology.* Kluver Academic Pub.,336 pages ed. s.l.:s.n.

Cristescu, N. D., 2009. *Time effect in rock mechanics.* Albuquerque New Mexico USA, Proceedings of the SEM Annual Conference June 1-4, 2009.

Cristescu, N. D. & Hunsche, U., 1998. *Time effects in rock mechanics.* s.l.:Wiley-Interscience-Europe; 1998.

Dahou, A., 1995. *Contribution à l'étude du comportement viscoelastoplastique d'une craie poreuse,* s.l.: Ph.D. thesis, Université de Lille 1, France.

Datcheva, M., 2001. *Constitutive Modelling of the Creep Behaviour of Chalk,* s.l.: Laboratory of Geomechanics, University of Liege.

Dawson, E. M., Roth, W. H. & Drescher, A., 1999. Slope stability analysis by strength reduction. *Géotechnique,* Volume 49(6) , pp. 835-840.

Dawson, E., You, K. & Park, Y., 2000. *Strength-Reduction Stability Analysis of Rock Slopes Using the Hoek-Brown Failure Criterion, In Trends in Rock Mechanics.* Denver, Colorado, Geotechnical Speci.

De Gennaro, V., Pereira, J. M., Gutierrez, M. & Hickman, R. J., 2009. On the viscoplastic modelling of porous chalks. *Italian Geotechnical Journal,* Volume 1/2009, p. 44–64.

DeGennaro, V. et al., 2003. Time-dependent behaviour of oil reservoir chalk: a multiphase approach. *Soils and Foundations,* Volume 43(4), pp. 131-147.

Dessene, J. L., 1971. *Etude rhéologique et géotechnique de la craie,* Grenoble: Thèse de doctorat, Université Joseph Fourier Grenoble.

deWaal, J. A., 1986. *On the Rate-Type Compaction Behavior of Sandstone Reservoir Chalk,* s.l.: Ph.D. thesis, Delft Univ. of Technology, The Netherlands.

Diederichs, M. S., 2007. Mechanistic interpretation and practical application of damage and spalling prediction criteria for deep tunnelling. *Canadian Geotechnical Journal,* Volume 44(9), pp. 1082-116.

Duveau, G., Shao, J. F. & Henry, J. P., 1998. Assessment of some failure criteria for strongly anisotropic geomaterials. *Mechanics of Cohesive-Frictional Materials,* Volume 3, pp. 1-26.

Duwicquet, A. & Hulo, Y., 1990. Design of retaining walls in chalk – Determination of chalk mechanical properties – Underground parking example in Lille. *Annales de la Société Géologique du Nord*, pp. 9-13.

El Shayeb, Y., Kounaili, S., Josien, J. P. & Guerniffey, Y., 2001. Towards the determination of surface collapse type over abandoned mines in the Lorraine iron basin. *Rock mechanics—A challenge for society, P. Särkkä and P. Eloranta, eds., Swets & Zeitlinger, Lisse, 819–824.*

Elmo, D. & Stead, D., 2006. An integrated Numerical Modeling-Discrete Fracture Network Approach Applied to the Characterization of Rock Mass Strength of Naturally Fractured Pillars. *Rock Mech Rock Eng,* Volume 43:3-19.

Esterhuizen, G. & Iannacchione, A., 2004. Investigation of Pillar-Roof Contact Failure in Northern Appalachian Stone Mine Workings. *Proceedings of the 23rd International Conference on Ground Control in Mining, Morgantown, WV,* pp. 320-326.

Fang, Z. & Harrison, J., 2002. Application of a local degradation model to the analysis of brittle fracture of laboratory scale rock specimens under triaxial conditions. *International Journal of Rock Mechanics and Mining Sciences,* Volume 39(4), pp. 459-476.

Fasani, G., Bozzano, F., Cardarelli, E. & Cercato, M., 2012. Underground cavity investigation within the city of Rome (Italy): A multi-disciplinary approach combining geological and geophysical data. *Engineering Geology ,* Issue 152 (2013) , p. 109–121.

Fayad, A., 2004. *Etude de stabilité de fontis au toit des carrières souterraines et traitements apportés aux conséquences induites en surface,* France: PhD thesis, l'Institut National Polytechnique de Lorraine.

Fayol, M., 1885. *Sur les movements de terrain provoques par l'exploitation des mines,* s.l.: Bull. Soc. Indust. 14:818..

Ferrero, A. M. & Segalini, A., 2011. Assessment of Stability Conditions of Ancient Underground Quarries using On-Site Monitoring and Numerical Modeling. *International Journal of Geoengineering Case Histories, http://casehistories.geoengineer.org. doi: 10.4417/IJGCH-0,* 2(1), pp. 66-85.

Ferrero, A. M., Segalini, A. & Giani, G. P., 2010. Stability analysis of historic under-ground quarries. *Elsevier, Computers and Geotechnics,* Volume 37 (2010), p. 476–486.

Foged, N. K. A. H. C., Jorgensen, K. Z., Christensen, H. F. & Jepsen, J. E., 1995. *Modeling of stresses and fractures in a reservoir,* s.l.: EFP-93 Final Report to DEA.

Fortsakis, P., Nikas, K. & Marinos, V., 2012. Anisotropic behaviour of stratified rock masses in tunnelling. *Engineering Geology,* Issue 141–142 (2012), p. 74–83.

Fossum, A. F., 1985. Effective elastic properties for randomly jointed rock mass. *International Journal of Rock Mechanics and Mining Sciences,* Volume 22(6), p. 467-470.

Gao, F., 2013. *Simulation of Failure Mechanisms around Underground Coal Mine Openings Using Discrete Element Modelling,* s.l.: Ph.D. thesis, Simon Fraser University, Canada.

G., Canbulat, I. & Jack, B., March 2000. *Coal pillar design procedures,* s.l.: Final Project Report, Safety in Mines Research Advisory Committee, CSIR Mining Technology.

Gens, A. & Nova, R., 1993. *Conceptual bases for a constitutive model for bonded soils and weak rocks.* Balkema: Rotterdam, 1993;485–494, In Geotechnical Engineering of Hard Soils-Soft Rocks, Athens, Greece, Anagnostopoulos et al. (eds).

Gerrard, C., 1982. Elastic models of rock masses having one, two and three sets of joints. *International Journal of Rock Mechanics and Mining Sciences,* Volume 19, pp. 15-23.

Gerrard, C. M., 1982. Elastic models of rock masses having one, two and three sets of joints. *International Journal of Rock Mechanics and Mining Sciences,* Volume 19, pp. 15-23.

Ghabezloo, S. & Pouya, A., 2006. *Numerical modelling of the effect of weathering on the progressive failure of underground limestone mine.* Liège, Belgium, Eurock 2006, Multiphysics Coupling and Long Term Behaviour in Rock Mechanics: Proceedings of the International Symposium of the International Society for Rock Mechanics.

Griffiths, D. V. & Lane, P. A., 1999. Slope stability analysis by finite elements. *Geotechnique,* 49(3), pp. 387-403.

Griffths, D. V., 1980. *Finite element analyses of walls, footings and slopes.* PhD thesis dissertation ed. s.l.:University of Manchester.

Gu, R. & Ozbay, U., 2015. Numerical investigation of unstable rock failure in underground mining condition. *Computers and Geotechnics,* Issue 63 (2015) , p. 171–182.

Gutierrez, M., 1998. *Formulation of a Basic Chalk Constitutive Model,* s.l.: NGI Report no. 541105-2..

Gutierrez, M., 2000. *Formulation of a 3-D stress-strain-time model for chalk,* s.l.: Contract report to Phillips Petroleum Company.

Gutierrez, M. S., 1999. *Modelling of Time-Dependent Chalk Behavior and Chalk-Water Interaction,* s.l.: NGI Report no. 541105-4.

Hajiabdolmajid, V., Kaiser, P. & Martin, C., 2002. Modelling brittle failure of rock. *International Journal of Rock Mechanics and Mining Sciences,* Volume 39(6), pp. 731-41.

Hammah, R., Yacoub, T., Corkum, B. & Curran, J., 2005. *The Shear Strength Reduction Method for the Generalized Hoek-Brown Criterion.* Anchorage, Alaska, In Proceedings of the 40th U.S. Symposium on Rock Mechanics, Alaska Rocks 2005.

Helmut, F. & Schweiger, 2002. Benchmarking in Geotechnics 1. *Computational Geotechnics Group CGG_IR006.*

Hickman, R., 2006. *Formulation and implementation of a constitutive model for soft rock,* s.l.: Ph.D. thesis, Faculty of the Virginia Polytechnic Institute and State University.

Homand, S. & Shao, J. F., 2000. Mechanical behavior of a porous chalk and effect of saturating fluid. *Mechanics of Cohesive-Frictional Materials,* Volume 5, pp. 583-606.

Homand, S., Shao, J. F. & Schroeder, C., 1998. *Plastic modeling of compressible porous chalk and effect of water injection.* s.l., Proceedings of EUROCK '98, Trondheim, Norway, 495-504.

Huang, T. H., Chang, C. S. & Yang, Z. Y., 1995. Elastic moduli for fractured rock mass. *Rock Mechanics and Rock Engineering,* pp. 135-44.

Hunsche, U. & Hampel, A., 1999. Rock salt - the mechanical properties of the host rock material for a radioactive waste repository. *Engineering Geology,* 52(3), pp. 271-291.

Iannacchione, A. T. et al., 1992. *xxx.* s.l., Proceedings, Workshop on Coal Pillar Mechanics and Design. U.S. Department of the Interior, U.S. Bureau of Mines, IC 9315, 302 pp..

Ineris, 2007. *Mise en sécurité des cavités souterraines d'origine anthropique: Surveillance – Traitement, Guide Technique.* , s.l.: Ineris, Rapport d'Etude.

Ineris, 2012. *Carrières souterraines sur le territoire de Lille; Hellemmes; Lomme. Inspection et avis sur l'état géotechnique des carrières souterraines de craie années 2011 et 2012,* s.l.: Rapport d'Etude INERIS DRS-11-123081-10891A PROJET 2, March 2012.

ISRM, 1979. Suggested method for determination of insitu deformability of rock. *International Journal of Rock Mechanics and Mining Sciences,* pp. 143-6.

Itasca, 2009. *FLAC3D– Fast Lagrangian Analysis of Continua in 3 Dimensions, Ver. 4.0 Command Reference Manual.* Minneapolis: Itasca Consulting Co..

Itasca, C. C., 2009. FLAC3D– Fast Lagrangian Analysis of Continua in 3 Dimensions, Ver. 4.0. *Command Reference Manual. Minneapolis: Itasca.* .

Jaeger, J. C., Cook, N. G. W. & Zimmerman, R. W., 2007. *Fundamentals of Rock Mechanics.* 4th edition ed. s.l.:Blackwell.

Kawamoto, T., Ichikawa, Y. & Kyoya, T., 1988. Deformation and fracturing behaviour of discontinuous rock mass and damage mechanics theory. *International Journal for Numerical and Analytical Methods in Geomechanics,* Volume 12, pp. 1-30.

Koiter, W., 1953. Stress-strain relations, uniqueness and variational theorems for elastic- plastic materials with a singular yield surface. In: *Quarterly of Applied Mathematics.* s.l.:s.n., pp. 350-354.

Koiter, W. T., 1960. General theorems for Elastic-Plastic solids.. In: *Progress in Solid Mechanics (Sneddon, I., N., Hill, R., eds.).* North Holland, Amsterdam: s.n., pp. 195-221.

Kortnik, J., 2009. Optimization of the high safety pillars for the underground excavation of natural stone blocks. *Acta Geotechnica Slovenica.*

Lane, P. A. & Griffiths, D. V., 1997. *Finite element slope stability analysis: Why are engineers still drawing circles?,.* Balkema, Rotterdam, In Numerical Models in Geomechanics.

Lavoie, T., 2011. *An Analytical Geomechanical Upscaling Approach for Modeling Jointed Rock Mass Behavior Using Ubiquitous Joints,* s.l.: Master Dissertation, The University of British Columbia.

Lemaitre, J., 1992. *A course of damage mechanics.* 2nd ed. ed. Berlin: s.n.

Liingaard, M., Augustesen, A. & Lade, P. V., 2004. Characterization of Models for Time-Dependent Behaviour of Soils. *The International Journal of Geomechanics,* Issue DOI: 10.1061(ASCE)1532-3641(2004)4:3(157).

Lille, V. d., 2013. *D.I.C.R.I.M. Document d'Information Communal sur les RIsques Majeurs. Lille, Hellemmes, Lomme Les 9 Risques Majeurs.,* s.l.: Document du Ville de Lille - Service Risques Urbains.

Li, X. B. et al., 2005. Constitutive model of rock under static-dynamic coupling loading and experimenta investigation. *Trans. Nonferrous Met. Soc. China,* Volume 16, pp. 714-722.

Lunder, P. J. & Pakalnis, R., 1997. *Determination of the strength of hard-rock mine pillars,* s.l.: Bull Can Inst Min Metall 1997;90:51-5.

Martin, C. & Chandler, N., 1994. The progressive fracture of Lac du Bonnet granite. *International Journal of Rock Mechanics and Mining Sciences & Geomechanics Abstracts,* Volume 31, pp. 643-659.

Martin, C. D. & Maybee, W. G., 2000. The strength of hard-rock pillars. *International Journal of Rock Mechanics & Mining Science,* Volume 37, pp. 1239-1246.

Martin, C. D. & Maybee, W. G., 2000. The strength of hard-rock pillars.

Martin, n.d. Risques d'évolution des anciennes carrières souterraines et solutions envisageables. *Monsieur MARTIN - Chef du service Géothermique, Société ANTEA du groupe BRGM.*

Masson, M., 1973. *Pétrophysique de la craie,* Paris: Bulletin des laboratoires des ponts et chaussées, spécial V, p. 23-48.

Matsui, T. & San, K. C., 1992. Finite element slope stability analysis by shear strength reduction technique. *Soils and Foundations,* Volume 32(1), pp. 59-70.

Maury, V. & Piau, J.-M., 1996. *Subsidence induced by water injection in water-sensitive reservoir rocks: The example of central Ekofisk.* s.l., Proceedings of the 5th North Sea Chalk Symposium, Reims, France, 23 p..

Mikolajczak, A., 1996. *Modélisation du comportement de craies sous sollicitations simples et complexes,* University of Lille, France: PhD thesis dissertation.

Monjoie, A., Schroeder, C. & Da Silva, F., 1985. *Mechanical Behaviour of Chalks.* Stavanger, Norway, Proc. North Sea Chalk Symp..

Monjoie, A., Schroeder, C. & Da Silva, F., 1991. *Testing procedure for time-dependent behaviour of chalk.* Aachen, 7th Int. Conf. on Rock Mechanics 565-567.

Naylor, D. J., 1982. Finite elements and slope stability. *In Numerical Methods in Geomechanics, D.Reidel Publishing Company,* pp. 229-244.

Nguyen, H. D., 2009. *Influence des interactions eau-roche sur le comportement long terme de cavités souterraines dans la craie ,* s.l.: Thèse présenté pour obtenir le diplôme de Docteur de l'Ecole Nationale des Ponts et Chaussées.

Nova, R., 2000. *Modelling the weathering effects on the mechanical behaviour of granite.* Horton, Greece, In Constitutive Modelling of Granular Materials, Horton, Greece, Kolymbas D (eds). Springer: Berlin, 2000; 397–411..

Nova, R. & Castellanza, R., 2001. *Modelling weathering effects on the mechanical behaviour of soft rocks.* Bangalore, India, In International Conference on Civil Engineering. Interline Publishing: Bangalore, India, 2001; 157–167..

Nova, R., Castellanza, R. & Tamagnini, C., 2003. A constitutive model for bonded geomaterials subject to mechanical and/or chemical degradation. *International Journal of Numerical and Analytical Methods in Geomechanics,,* Volume 27(9), pp. 705-732.

Oda, M. et al., 1993. Elastic stress and strain in jointed rock masses by means of crack tensor analysis. *Rock Mechanics and Rock Engineering,* Volume 26(2), p. 89-112.

Omdal, E., 2010. *The Mechanical Behavior of Chalk under Laboratory Conditions Simulating Reservoir Operations,* Stavanger; Norway: Thesis submitted in fulfillment of the requirements for the degree of PhD. University of Stavanger N-4036.

Ou, C. & Do, T., 2014. A study of failure mechanism for deep excavations in soft clay using the finite element method. *Numerical Methods in Geotechnical Engineering - Hicks Brinkgreve & Rohe (Eds). London 978-1-138-00146-6.*

Papamichos, E., Brignoli, M. & Santarelli, F. J., 1997. An experimental and theoretical study of a partially saturated collapsible rock. *Mechanics of Cohesive-Frictional Materials,* Volume 2, pp. 251-278.

PASACHALK, 2004. *Mechanical Behavior of Partially and Multiphase Saturated Chalks FluidSkeleton Interaction: Main Factor of Chalk Oil Reservoirs Compaction and Related Subsidence – Part 2,* s.l.: Final Report, EC Contract no. ENK6-2000-00089.

Pecker, A., 2013. *Overview of Seismic Regulations for French Industrial Facilities.* Paris, Proceedings of the SeDIF Conference.

Perzyna, P., 1966. *Fundamental problems in viscoplasticity.* Adv Application Mech 1966;9:243–377 ed. s.l.:s.n.

Piau, J.-M., Bois, A.-P., Atahan, C. & Maury, V., 1998. *Water/chalk (or collapsible soil) interaction: Part I. Comprehensive evaluation of strain and stress jumps at the waterfront.* s.l., Proceedings of EUROCK '98, Trondheim, Norway, 419-427.

Piau, J.-M. & Maury, V., 1994. *Mechanical effects of water injection on chalk reservoirs.* s.l., Proceedings of EUROCK '94, Delft, The Netherlands, 819-827.

Piau, J.-M. & Maury, V., 1995. *Basic mechanical modelisation of chalk/water interaction.* s.l., Proceedings of the First International Conference on Unsaturated Soils, Paris, 8 p.

Pietruszczak, S., Lydzba, D. & Shao, J. F., 2004. Description of creep in frictional materials in terms of microstructure evolution. *Journal of Engineering Mechanics, ASCE 01/2004; 130:681-690.*.

Plischke, B., 1994. *Finite element analysis of compaction and subsidence - Experience gained from several chalk fields.* s.l., Proceedings of EUROCK '94, Delft, The Netherlands, 795-802.

Plischke, B., 1996. *Some aspects of numerical simulation of water-induced chalk compaction.* s.l., Proceedings of the 5th North Sea Chalk Symposium, Reims, France, 13 p.

Potts, D. M., Jones, M. E. & Berget, O. P., 1988. *Subsidence above the Ekofisk oil reservoirs. Proceedings of BOSS '88, 113-127.* s.l., s.n.

Potts, D. & Zdravkovic, L., 2012. *Using numerical analysis in geotechnical engineering practice.* s.l., Sociedad Mexicana de Ingeniería Geotécnica, A.C. XXVI RNMSeIG, Cancún, Quintana Roo.

Rachez, X., Billaux, D. & Hart, R., 2002. Slope stability analysis with integrated shear strength reduction algorithm,. *In Numerical Methods in Geomechanical Engineering, Presses de I'ENPC/LCPC, Paris,* pp. 731-736.

Rafeh, F., Mroueh, H. & Burlon, S., 2014. *Equivalent continuum model accounting for anisotropy in chalk by means of embedded joint sets.* Kyoto, Japan, In Proceedings of the 14th International Conference of the International Association for Computer Methods and Advances in Geomechanics IACMAG 2014.

Rafeh, F., Mroueh, H. & Burlon, S., 2015. Accounting for joints effect on the failure mechanisms of shallow underground chalk quarries. *Computers and Geotechnics* , Volume 69, pp. 247-261.

Rafeh, F., Mroueh, H. & Burlon, S., 2015. *Numerical analysis of strain mechanisms of cavities excavated in jointed chalk.* Edinburgh, Proceeding of the ECSMGE conference of Geotechnical Engineering for Infrastructure and Development.

Rafeh, F., Mroueh, H. & Burlon, S., 2015. *Numerical creep analysis of chalk cavities accounting for joints degradation.* San Francisco, Proceeding of the 49th US Rock Mechanics/Geomechanics Symposium.

Rhett, D. W., 1994. *The mechanics of time-dependent strain in high-porosity North Sea chalk.* s.l., Proceedings of the EAPG/AAPG Special Conference on Chalk, Copenhagen, Denmark.

Riahi Dehkordi, A. 2., 2009. *3D Finite Element Cosserat Continuum Simulation of Layered Geomaterials,* s.l.: PhD thesis, University of Toronto.

Roosta, R. & Sadaghian, M. H., 2005. Strength reduction technique in stability analysis of jointed rock slopes. *International Journal of Civil Engineering,* Volume Vol.3, Nos 3&4 September & December 2005.

Salamon, M. D. G. & Munro, A. H., 1967. A Study of the Strength of Coal Pillars. *J. S. Afr. Inst. Min. Metall.*

Salamon, M. D. G., Ozbay, M. U. & Madden, B. J., 1998. Life and design of bord-and pillar workings affected by pillar scaling.. *The Journal of The South African Institute of Mining and Metallurgy.*

Salamon, M. D. G., Ozbay, M. U. & Madden, B. J., 1998. Life and design of bord-andpillar workings affected by pillar scaling. *The Journal of The South African Institute of Mining and Metallurgy.*

Samadhiya, N. K., Viladkar, M. N. & Al-Obaydi, M. A., 2008. Numerical implementation of anisotropic continuum model for rock masses. *International Journal of Geomechanics ASCE,* Volume 8(2), p. 157-161.

Schroeder, C., 1995. *Le "Pore Collapse": aspect particulier de l'interaction fluide-squelette dans les craies?.* Belge, Colloque International du Groupement Belge de Mécanique des RochesChalk and Shales.

Schroeder, C. & Shao, J. F., 1996. *Plastic deformation and capillary effects in chalks.* s.l., Proceedings of the 5th North Sea Chalk Symposium, Reims, France, 14 p.

Shao, J. F., Bederiat, M. & Schroeder, C., 1993. A viscoplastic theory for soft rock behaviour and application. *In Anagnostpopoulos et al., editor, Geotecchnical Engineering of Hard Soils-Soft Rocks. Balkema, Rotterdam, 1993.*

Shao, J. F. & Henry, J. P., 1991. Development of an elastoplastic model for porous rock. *International Journal of Plasticity, 7, 1-13.*

Shao, J. F., Zhu, Q. Z. & Su, K., 2003. Modeling of creep in rock materials in terms of material degradation. *Computers and Geotechnics* , Issue 30 (2003), p. 549–555.

Singh, M., 2000. Applicability of a constitutive model to jointed block mass. *Rock Mechanics and Rock Engineering,* Volume 33, pp. 141-7.

Sitharam, T., 2009. Equivalent continuum analyses of jointed rockmass: Some case studies. *Equivalent continuum analyses of jointed rockmass: Some case studies. International Journal of the JCRM Japanese Committee for Rock Mechanics. Volume 5, Number 1, March 2009, pp.39-51.,* 5(1), pp. 39-51.

Sitharam, T. G., 2009. Equivalent continuum analyses of jointed rockmass: Some case studies. *International Journal of the JCRM Japanese Committee for Rock Mechanics,* 5(1), pp. 39-51.

Sitharam, T. G. & Latha, G. M., 2002. Simulation of excavation in jointed rock masses using practical equivalent continuum model. *International Journal of Rock Mechanics and Mining Sciences,* Volume 39, pp. 517-525.

Siwak, J.-M., 1994. *Comportement et modélisation de la craie,* s.l.: Ph.D. thesis, Université de Lille 1, France.

Smith, G. J. & Rosenbaum, M. S., 1993. Recent underground investigations in of abandoned chalk mine workings beneath Norwich City, Norfolk. *Engineering Geology,* Volume 36 (1993), pp. 67-78.

Smith, G. & Rosenbaum, M., 1993. Recent underground investigations in of abandoned chalk mine workings beneath Norwich City, Norfolk. *Engineering Geology,* Issue 36 (1993), pp. 67-78.

Sorgi, C. & De Gennaro, V., 2008. Water-Rock Interaction Mechanisms and Ageing Processes in Chalk.

Suchowerska, A. M., Merifield, R. S., Carter, J. P. & Clausen, J., 2015. Prediction of underground cavity roof collapse using the Hoek–Brown failure criterion. *Computers and Geotechnics,* Issue 44 (2012) , p. 93–103.

Tamagnini, C., Castellanza, R. & Nova, R., 2002. A Generalized Backward Euler algorithm for the numerical integration of an isotropic hardening elastoplastic model for mechanical and chemical degradation of bonded geomaterials. *International Journal for Numerical and Analytical Methods in Geomechanics,* Volume 26, p. 963–1004.

Terzaghi, K., 1946. Rock defects and loads on tunnel support. In: R. V. W. T. e. In: Proctor, ed. *Rock tunneling with steel supports.* Commercial School and Stamping Co, Youngstown: s.n., pp. 15-99.

Tremblay, D., Simon, R. & Aubertin, M., 2007. *A Constitutive model to predict the hydromechanical behavior of rock joints,* Montréal, Québec, Canada Ottawa Geo200: Ecole Polytechnique.

Vinkler, F. & Piguet, J. P., 1999. *Analysis of the long-term stability of an ancient room and abandoned pillar mine - Impact of the water level.* Minneapolis, United States, International FLACS Symposium on Numerical Modeling in Geomechanics, Sep 1999.

Wagner, H., 1980. Pillar design in coal mines.. *J.S. Afr. Min. Metal,* Volume V80, pp. 37- 45.

Wang, J. G., Ichikawa, Y. & Leung, C. F., 2002. A constitutive model for rock interfaces and joints.. *International Journal of Rock Mechanics & Mining Sciences,* Volume 40, pp. 41-53.

Wang, J., Ichikawa, Y. & Leung, C., 2003. A constitutive model for rock interfaces and joints. *International Journal of Rock Mechanics & Mining Sciences,* Volume 40 (2003), p. 41–53.

Wang, T. T. & Huang, T. H., 2009. A constitutive model for deformation of the rock mass containing sets of ubiquitous joints. *International Journal of Rock Mechanics and Mining Sciences,* Volume 46:521-30.

Watelet, J. M., 1996. *Méthode d'analyse et diagnostic des conditions de stabilité des carrières souterraines,* s.l.: Thesis, C.N.A.M, Paris.

Wyllie, D. C., 1992. *Foundations on Rock.* First edition ed. s.l.:Chapman and Hall.

Xie, S., 2005. *Contribution à l'étude du comportement mécanique dune roche poreuse,* s.l.: Thèse présenté pour obtenir le grade de Docteur de l'Université des Sciences et Technologies de Lille.

Yang, J. P., Chen, W. Z., Yang, D. S. & Yuan, J. Q., 2014. Numerical determination of strength and deformability of fractured rock mass by FEM modeling. *Computers and Geotechnics,* Issue 64 (2015), p. 20–31.

Yin, J. H., 1999. Non-linear creep of soils in oedometer tests. *Géotechnique : ,* Volume 49(5), pp. 699- 707.

York, G., Canbulat, I. & Jack, B., 2000. *Coal pillar design procedures,* s.l.: Final Project Report, Safety in Mines Research Advisory Committee, CSIR Mining Technology, COL 337.

Zienkiewicz, O. C., Humpheson, C. & Lewis, R. W., 1975. Associated and non-associated visco-plasticity and plasticity in soil mechanics. *Geotechnique,* Volume 25(4), pp. 671-689.

ANNEX ONE
RESOLUTION OF THE DIFFERENTIAL EQUATION USED IN CHAPTER FOUR

This annex deals with the resolution of the differential equation 4.2 in the main text:

$$\dot{D}(t) = \gamma\left(R_m(t) - D(t)\right)$$

This equation is very common and its resolution is based on the well-known technique of "variation of parameters". The full first-order equation is:

$$\dot{D}(t) + \gamma D(t) = \gamma R_m(t)$$

The corresponding homogeneous equation to find the general solution is:

$$\dot{D}(t) + \gamma D(t) = 0$$

and the general solution is therefore: $D(t) = ke^{-\gamma t}$ where k is a parameter.

Using the method variation of parameters, the particular solution is obtained from the general solution: $D(t) = k(t)e^{-\gamma t}$

By substituting the particular solution into the non-homogeneous equation, k(t) is found:

$$k'(t)e^{-\gamma t} - \gamma k(t)e^{-\gamma t} + \gamma k(t)e^{-\gamma t} = \gamma R_m(t)$$

$$k'(t) = \gamma R_m(t)e^{\gamma t}$$

$$k(t) - k(0) = \int_0^t \gamma R_m(u)e^{\gamma u}du$$

The final solution of the differential equation is:

$$D(t) = \left[\int_0^t \gamma R_m(t)e^{\gamma u}du + k(0)\right]e^{-\gamma t}$$

as: $D(0) = 0 = k(0)$, $D(t) = \left[\int_0^t \gamma R_m(t)e^{\gamma u}du\right]e^{-\gamma t} = \int_0^t \gamma R_m(u)e^{-\gamma(t-u)}du$

ANNEX TWO
ADDITIONAL RESULTS ON THE TIME-DEPENDENT ANALYSIS VIA CHAPTER FOUR

In terms of the analysis of the time-dependent-degradation model simulated in chapter 4, numerous results were obtained. Some of those which were not integrated in the content of chapter four are presented in this Annex. We believe that these results could provide even a better understanding of the time-dependent-behaviour of the modelled underground cavity under different conditions. The figures are numbered after the last figure presented in chapter four.

The first figure for example (Figure 4.20), shows the evolution of the displacements at roof and pillar with respect to the evolution of degradation D. It is clear that the displacements, whether vertical at the roof or horizontal at the pillar, increase which the increase of degradation D. This is obvious since the increase of *D* leads to a decrease in the resistance of the chalk. In addition, at a certain limit when *D* reaches its maximum the displacements keep on increasing at a constant D. This can be a sign of rupture when the displacements keep on increasing and become out of control. On the other hand, the degradation-displacement relation observed in Figure 4.20 can be in accordance with the stress-strain relation attained at creep. In the latter, stains increase with the increase of acting stresses. At a certain point when stresses no more increase, strains keep on growing at a constant stress.

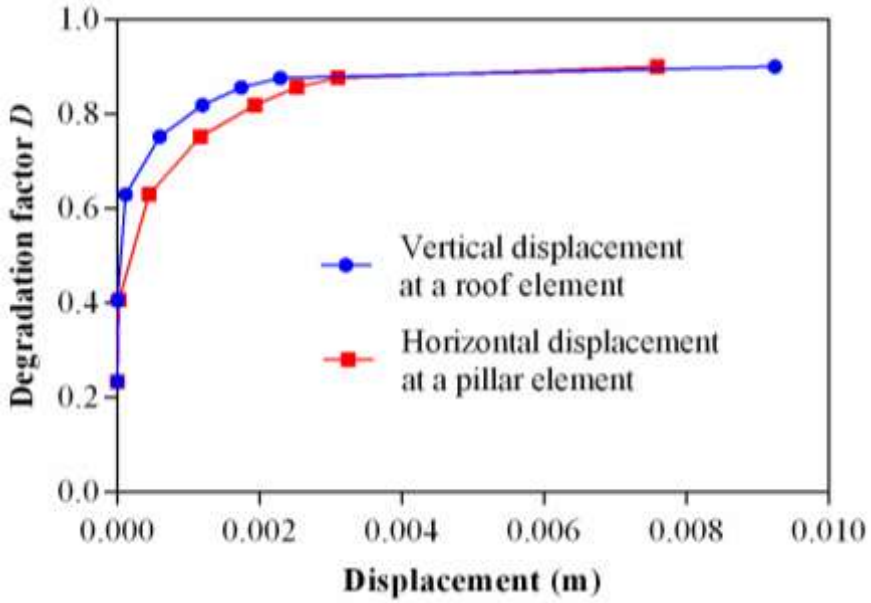

Figure 4.20. Evolution of vertical and horizontal displacements at roof and pillar respectively.

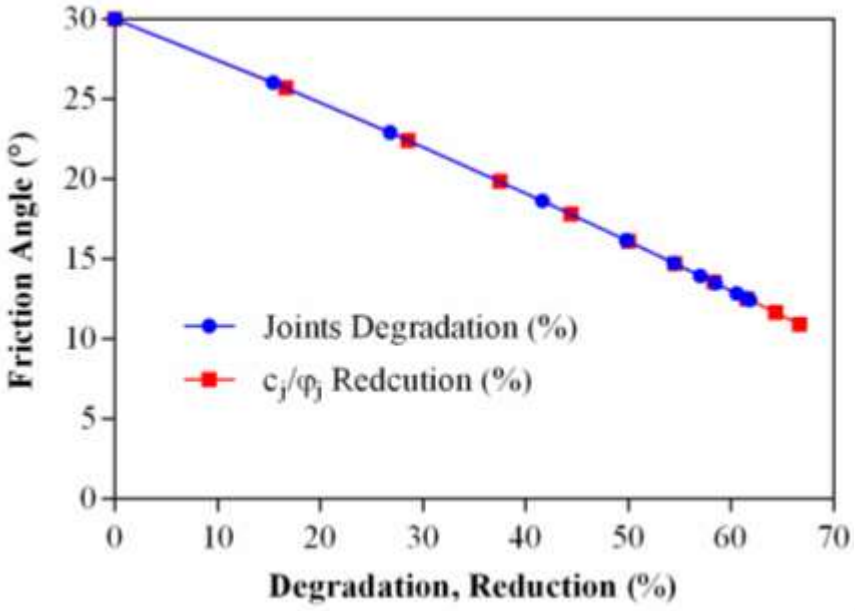

(a)

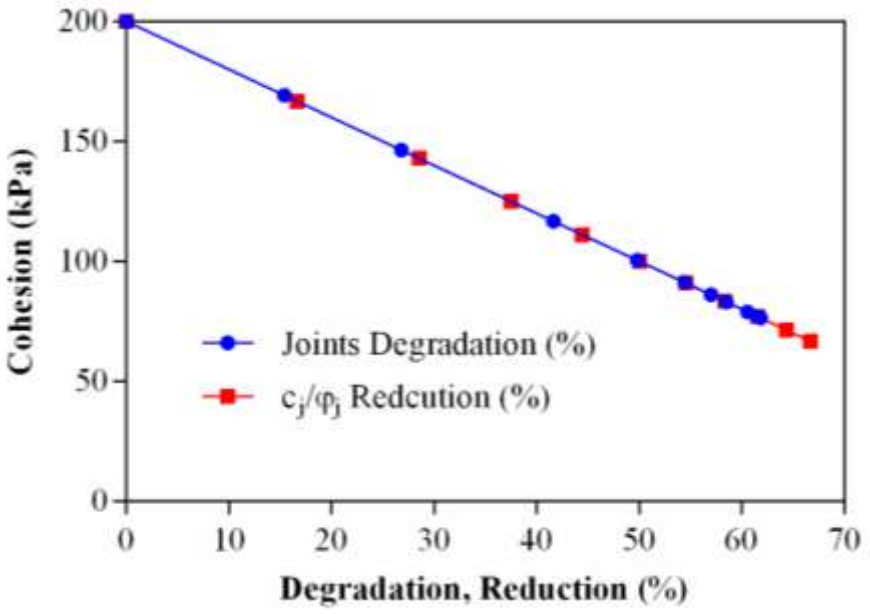

(b)

Figure 4.21. The decrease of strength properties of the joints, **(a)** friction and **(b)** cohesion, imposed by the degradation and reduction approaches used in our analysis.

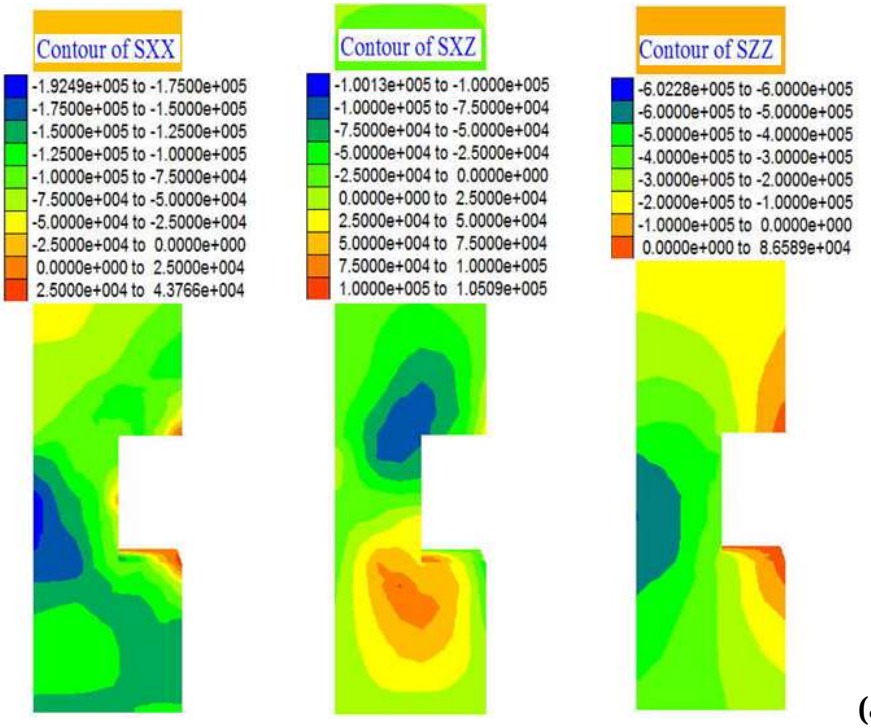

(a)

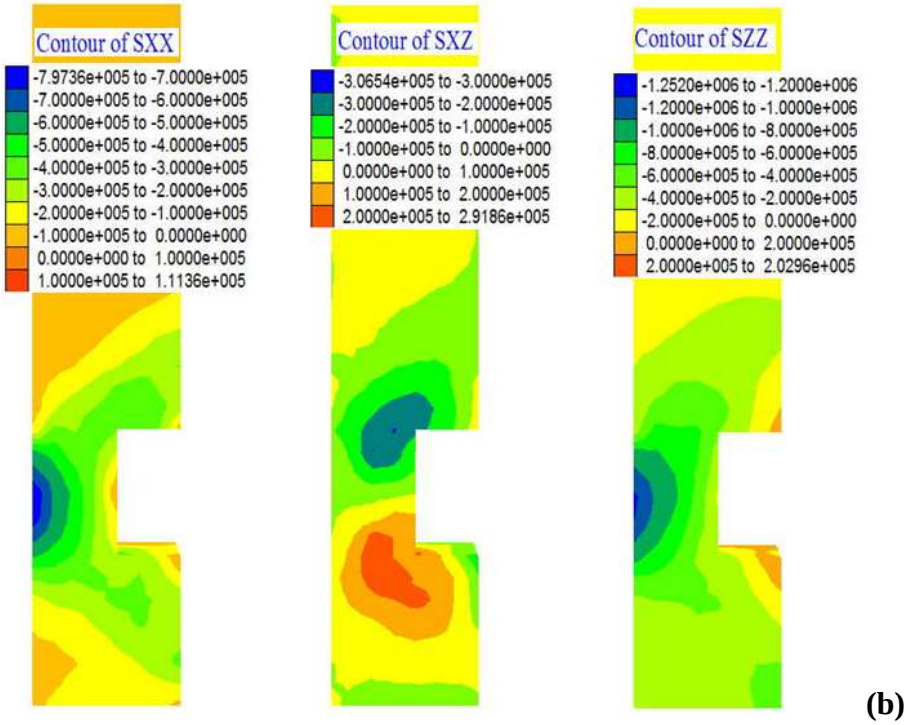

Figure 4.22. Evolution of horizontal, shear, and vertical stresses in the room-and-pillar cavity model.

Case of study:

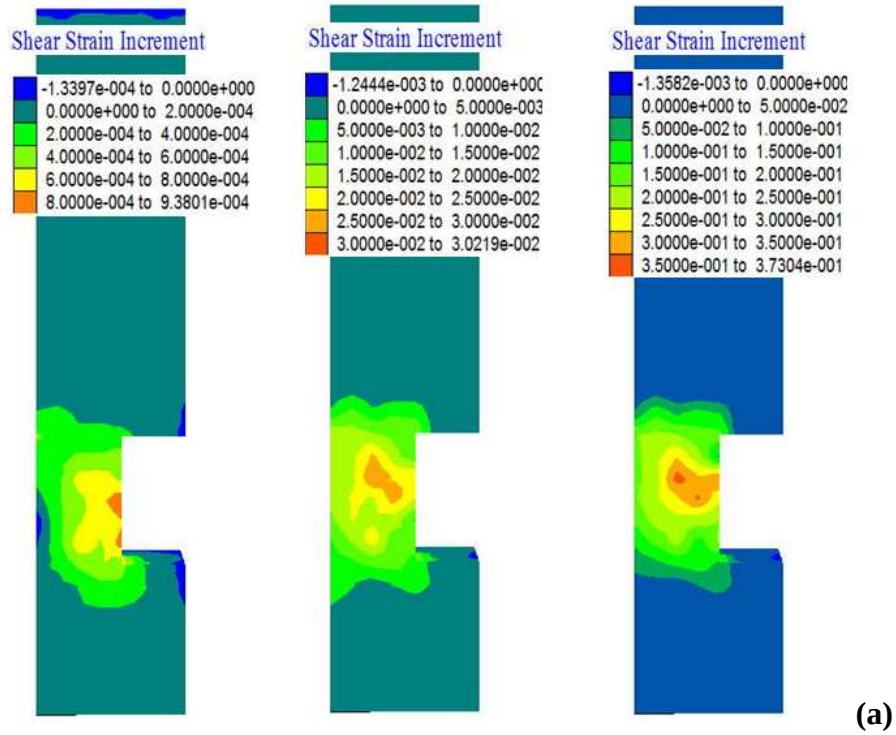

Figure 4.23. Evolution of **(a)** shear and **(b)** volumetric strain at different periods (0.5 years, 10 years, and 100 years from left to right). Case of study: Joint set inclined at 45° from z-axis.

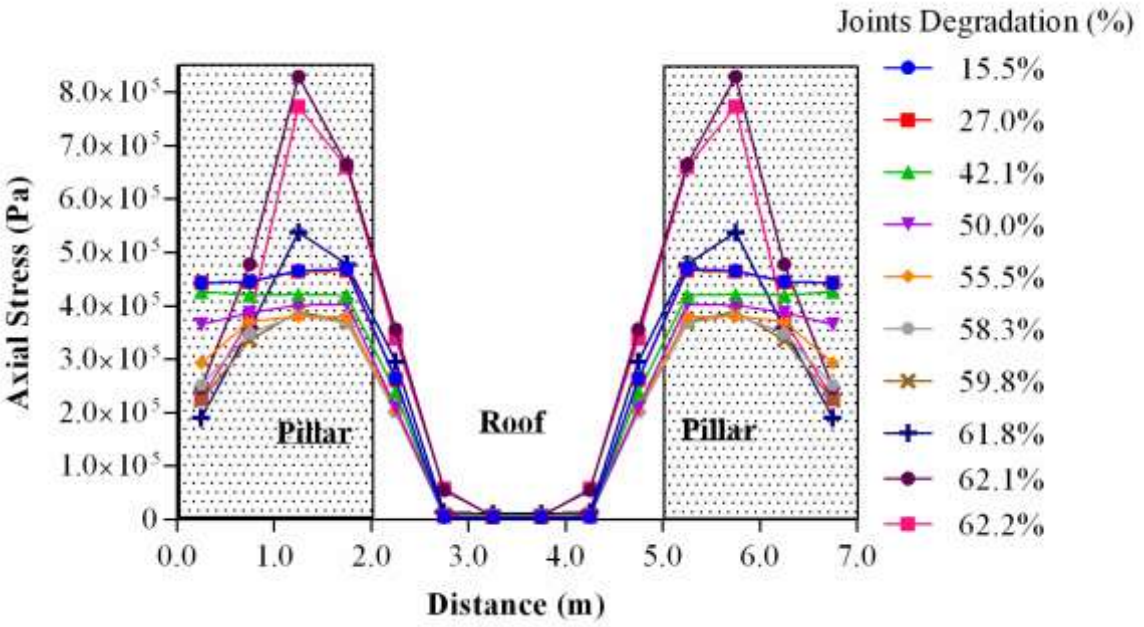

(a)

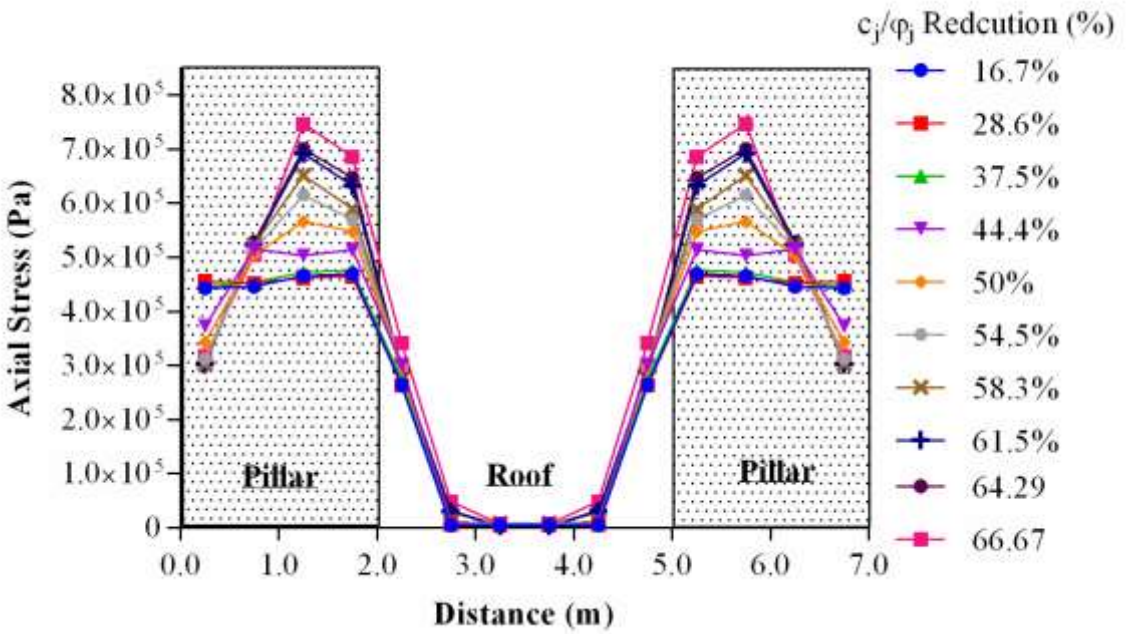

(b)

Figure 4.24. Evolution of axial stresses and strains at roof via both approaches: **(a)** degradation, and **(b)** reduction. Joint set inclined at 45°.

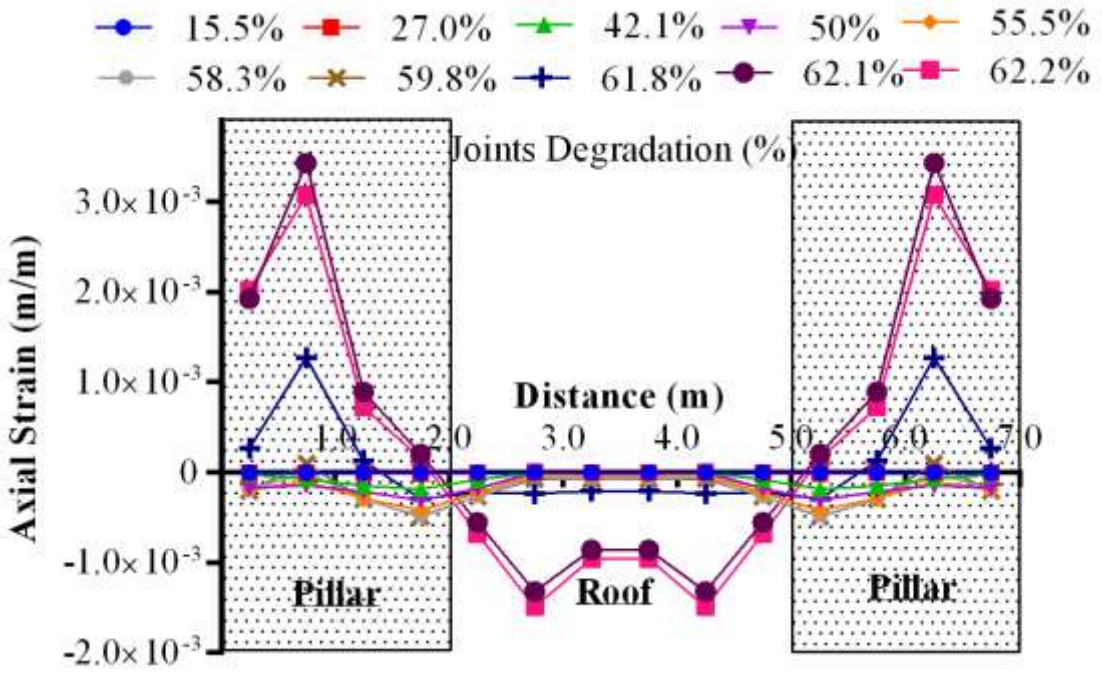

(a)

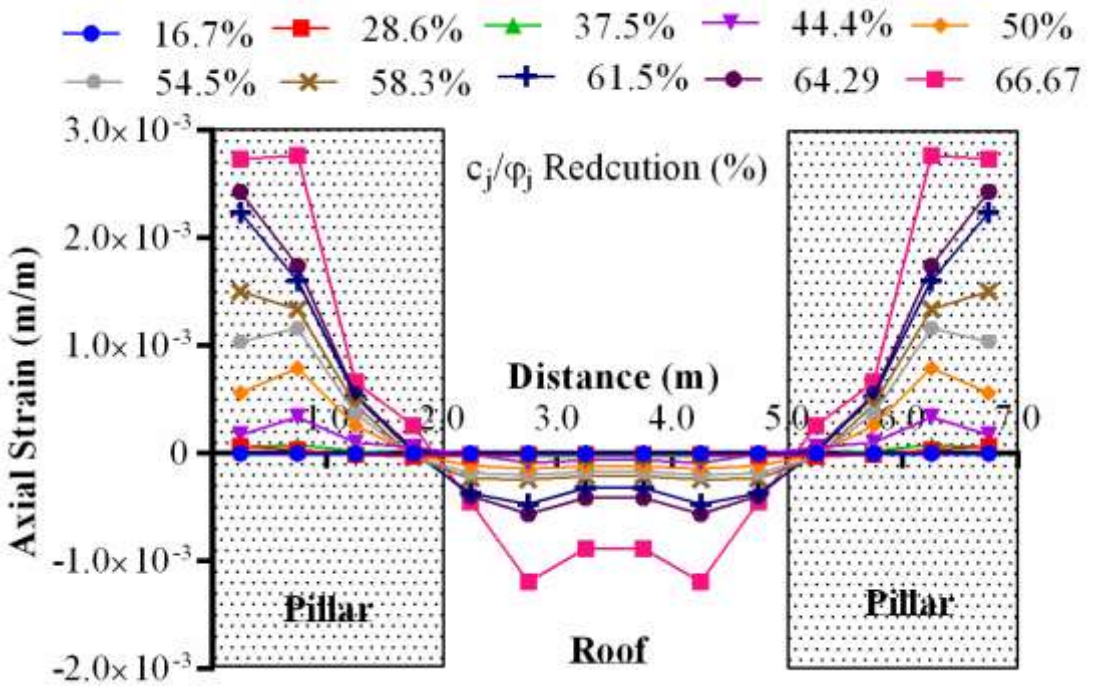

(b)

Figure 4.25. Evolution of axial strain at roof via both approaches: **(a)** degradation, and **(b)** reduction. Joint set inclined at 45°.

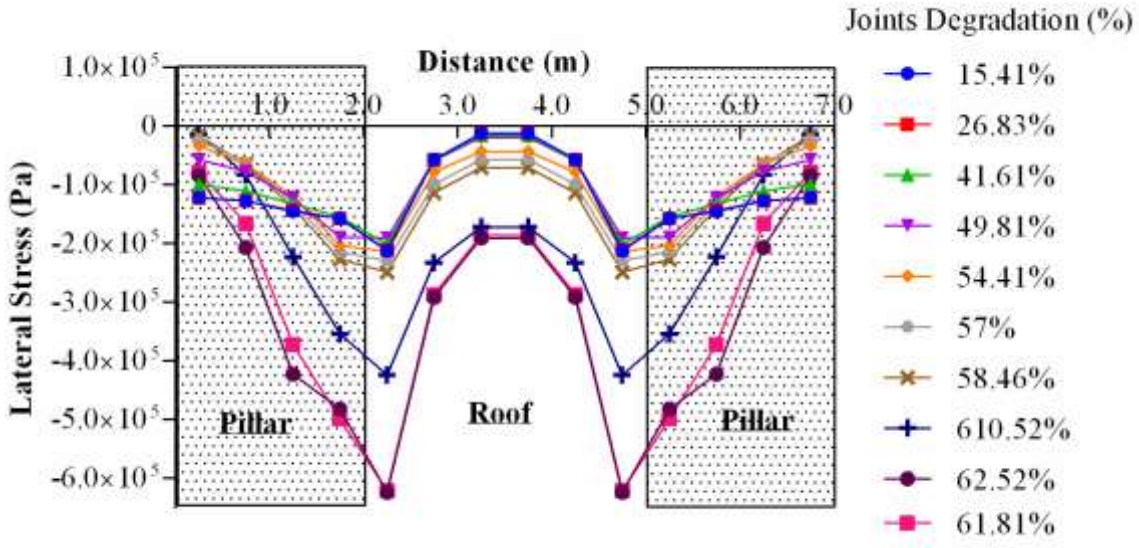

(a)

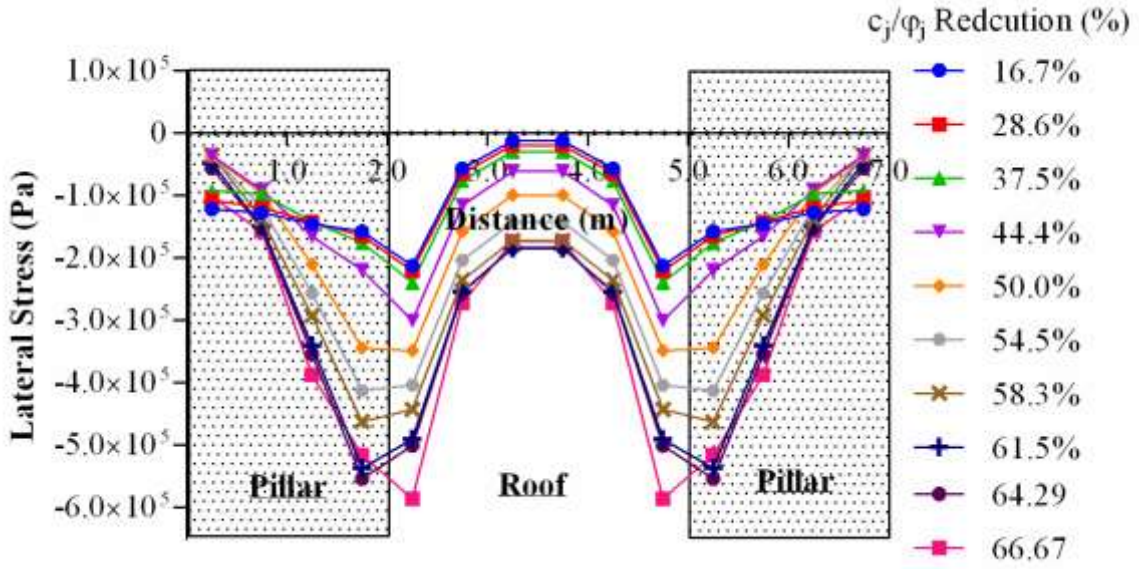

(b)

Figure 4.26. Evolution of lateral stress at roof via both approaches: **(a)** degradation, and **(b)** reduction. Joint set inclined at 45°.

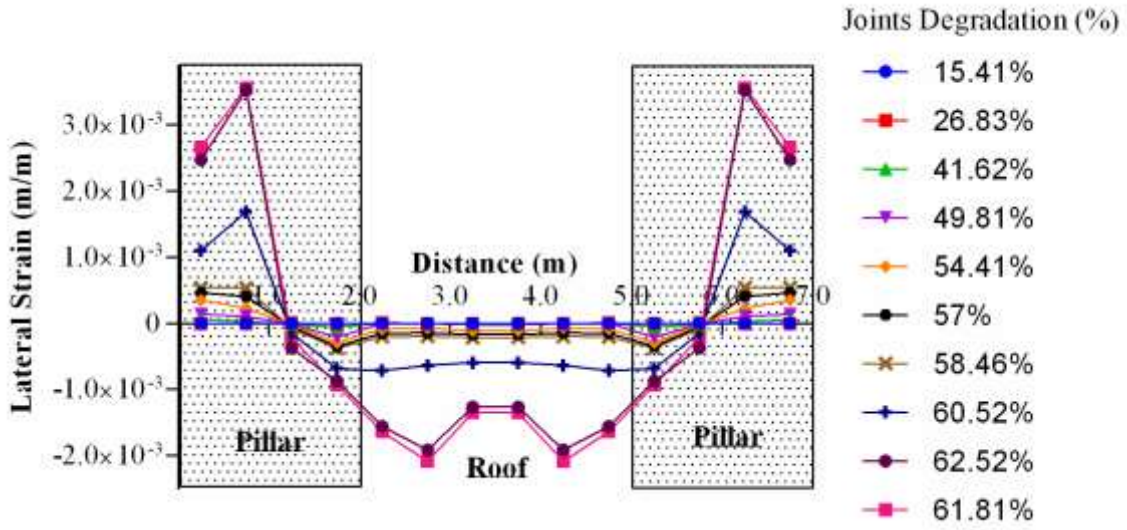

(a)

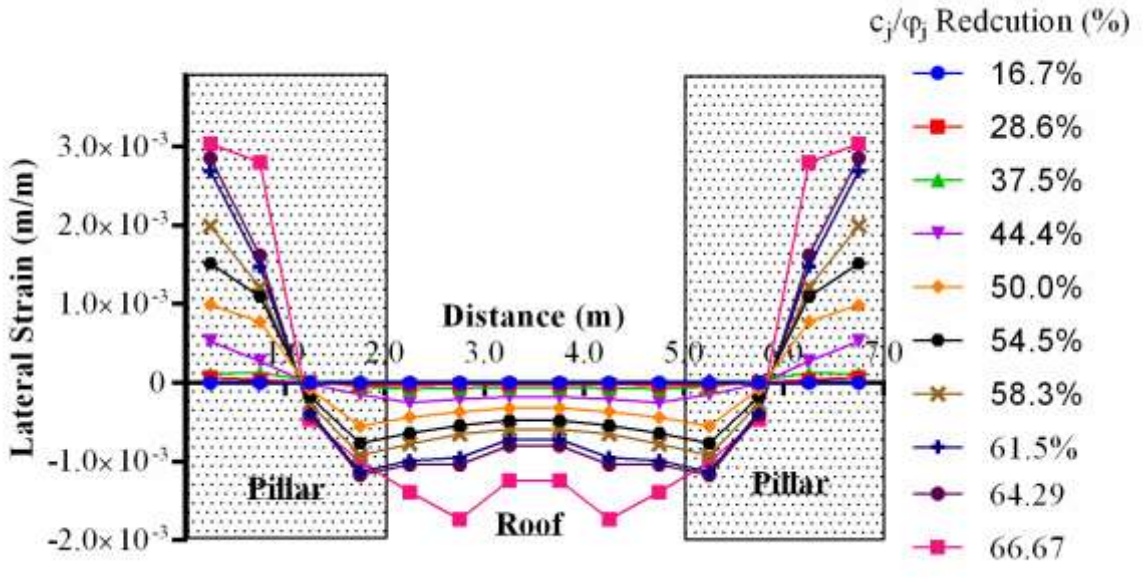

(b)

Figure 4.27. Evolution of lateral strain at roof via both approaches: **(a)** degradation, and **(b)** reduction. Joint set inclined at 45°.

ANNEX THREE
REHABILITATION TECHNIQUES: PASSIVE AND ACTIVE METHODS

As reported by the City of Lille, 15% of the population is nowadays exposed to the risk due to instabilities originated from the underground cavities. To date, more than 364 incidents of collapses, subsidence, and landslides have been recorded. Being aware to the circumstances of this hazardous phenomenon, the Service of Urban and Health Risks of the City of Lille has launched a plan including setting urgent regulations and prerequisites to avoid anticipated risks and control the encountered damage in threatened regions. Basically, measurements concern the protection of people who are directly exposed to the danger of the phenomena of soil instability induced due to the presence of old abandoned underground quarries. Each case of exposure to a risk of collapse necessitates a precise specific treatment method. The final choice of solution adopted inevitably rests on a well identified technical and economic criterion. Some examples of the solutions proposed for this problem are described below based on the review made by the City of Lille and Ineris (Reference).

They are known as rehabilitation technique where three types can be endorsed: (i) active prevention, (ii) passive prevention, (iii) suppression technique.

Rehabilitation Techniques

- Active Prevention:
    1. Cavity Consolidation
        a) Reinforcement of Existing Pillars

            This rehabilitation technique is represented by the following:

            - Combination of shotcrete and bolting

- Shrinking of the pillars by cables or metal bar liner reinforced concrete (chemisage)
- Metal shell filled from the surface by a fluid grout

b) Construction of Masonry Pillars:

Due to the fact that pillars of a building must represent at least 20% of the surface of the building projected, the some rehabilitation work is performed by adding supporting members through constructing masonry pillars for example.

c) Bolting of Roof

Arming the monolithic rock mass at top to make it strong and able to carry the weight of surface resting on pillars or on the sides of the galleries is another effective technique used for the roof strengthening.

d) Implementation of grout or mortar pads from the surface

This method is achieved using pillars sand cement formwork which is a geotextile sock or micro-concrete pillars with wooden formwork or metal. Usually, high angle of repose injected by drilling is plotted.

e) Shotcrete

Shotcrete is almost used when the chalk is subject to alteration or peeling. It is usually of thickness 15cm of shot concrete over an installation of welded mesh.

2. Stabilization by Filling

a) Total filling

- Remove most of the underground void by placing debris, land excavations from large neighboring sites, mining waste, etc.
- Filling material type and method of putting must b based on the expected settlement.

b) Partial filling

- Chalk Pillars are subjected to initiation of brittle collapse at bottom corners.
- Filling at this location helps reduce their slenderness and thus increases their resistance.
- This also prevents uprising of the raft.

c) Injection by drilling

- Suitable for filling inaccessible quarries.

- Passive Prevention:
    1. Strengthening the structure of a building
        - The principle is to make the quasi-monolithic construction of the chaining and foundations strengthened.
        - This solution is normally reserved for cases of small voids whose distribution is unknown.
    2. Realization of deep foundations

- Extending the load below the level quarries through wells or piles.
- This does not prevent the rise in sinkhole.
- Danger on the edge of the building, disorders in basements negative friction, etc.

3. Adaptation of underground networks
    - To avoid water leaks that can accelerate the degradation of a cavity.
    - Either by reinforcement or using flexible and deformable connections.
4. Adaptation of the road
    - The strengthening of the pavement structure of layers of geo-textile reduces deformation and therefore reduces the risk of accident, but does not prevent certain disorders.
    - This method is used when the voids are suspected but not identified and located.

❖ Suppression Techniques

1. Caving
    - The soil is redesigned and the land is not considered buildable.
    - Opportunity of using these cavities for agricultural purposes under certain conditions**.**
2. Excavation of the cavity
    - The technique is to update the cavity by obtaining a filling with compaction.
    - This is a possible solution if the career is shallow.
    - Use as parking.

Note that all figures presented in this Annex were taken during one of the site visits done to the cavities of Lille, North France with the City of Lille- Department of Urban and Sanitary Risks, and to the cavities in Caen, Normandie with Semofi, the engineering company for research and geotechnical works.